<u>Remarks</u>

<u>The Invention</u>

One embodiment of the invention (claims 60, 63, 66, 67, 69-71, and 73-75) provides a bisubstrate inhibitor of a protein kinase. The inhibitor comprises (1) a nucleotide or nucleotide analog moiety, (2) a peptide moiety which is a substrate for said protein kinase, and (3) a tether that comprises a proton donor. The tether is greater than or equal to 4.9 Å as measured from a gamma phosphorus of the nucleotide or nucleotide analog moiety to the proton donor.

Another embodiment of the invention (claims 1-15, 58, 72, and 76) provides a bisubstrate inhibitor of insulin receptor kinase. The inhibitor comprises (1) a nucleotide or nucleotide analog moiety, (2) a peptide moiety which is a substrate for said insulin receptor kinase, and (3) a tether that comprises a proton donor. The tether is greater than or equal to 4.9 Å as measured from a gamma phosphorus of the nucleotide or nucleotide analog moiety to the proton donor.

<u>Claim Amendments</u>

Claim 15 was amended to put it in independent form. Claim 66 was amended to correct the form of the claim only. The claims have not been narrowed in scope.

Claims 1 and 60 were amended to recite that the peptide moiety is a substrate for the recited insulin receptor kinase (claim 1) or the protein kinase (claim 60). Support can be found *inter alia* at page 2, paragraph 08 (emphasis added): "Protein kinases follow ternary complex kinetic mechanisms in which direct transfer of the phosphoryl group from ATP to <u>protein substrate</u> occurs. For such mechanisms, designing covalently linked <u>bisubstrate</u> analogs can be a powerful approach toward potent enzyme inhibitors." See also page 9, paragraph 33 (emphasis added): "This method is generalizable to other protein kinases based on the distinctive <u>peptide substrate</u> sequence selectivities of individual enzymes."

New claims 69-71 recite that the peptide moiety comprises at least 4, 5, or 6 contiguous amino acids of the natural substrate of the protein kinase. Support for the recited number of amino acids can be found at page 7 paragraph 28: "Thus as few as 4, 5,

6, or 7 of the amino acid residues may be sufficient to provide the requisite specificity."
Support for the recited natural substrate can be found at page 7 paragraph 28:
"Bisubstrate inhibitors typically contain a second moiety which is a peptide having
residues similar to that of the natural protein substrates of the particular protein kinase."

New claims 72 and 73 recite that the tether has the following structure:
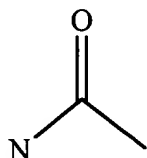
Support can be found in Figure 1a and Figure 4.

New claim 74 recites that the peptide moiety is a natural substrate of the protein
kinase. Support can be found at page 7 paragraph 28: "Bisubstrate inhibitors typically
contain a second moiety which is a peptide having residues similar to that of the natural
protein substrates of the particular protein kinase."

New claim 75 and 76 recite that the nucleotide or nucleotide analog moiety is a
substrate for the protein kinase, and the insulin receptor kinase. Support can be found at
page 7 paragraph 27: "Bisubstrate inhibitors typically contain one moiety which is a
nucleotide or nucleotide analog moiety, which mimics the natural substrate ATP."

No new matter is added by these claim amendments.

The Rejection of Claim 66 Under 35 U.S.C. § 112, Second Paragraph

Claim 66 stands rejected under 35 U.S.C. § 112, second paragraph as indefinite
because the term "the tyrosine" allegedly had no antecedent basis. Claim 66 was
amended to substitute "a tyrosine" for "the tyrosine." Withdrawal of this rejection is
therefore respectfully requested.

The Rejection of Claims 1-14, 58, 60, 63, 66 and 67 Under 35 U.S.C. § 112, First
Paragraph

Claims 1-14, 58, 60, 63, 66 and 67 stand rejected under 35 U.S.C. § 112, first
paragraph as allegedly failing to provide an adequate written description. In particular
the rejection asserts that the application fails to disclose a representative number of
species for the claimed genus of bisubstrate inhibitors of insulin receptor kinase or the

7

claimed genus of bisubstrate inhibitors of protein kinases. Applicants respectfully traverse this rejection.

To satisfy the written description requirement for a claimed genus, the specification may describe a representative number of species (1) by actual reduction to practice, (2) by reduction to drawings, or (3) by disclosure of relevant identifying characteristics sufficient to show the applicant was in possession of the claimed genus. Manual of Patent Examining Procedure § 2163(II)(A)(3)(a)(ii). Relevant identifying characteristics can be, for example, structure or other physical and/or chemical properties, functional characteristics coupled with a known or disclosed correlation between function and structure, or a combination of such identifying characteristics. *Id.* A representative number of species is inversely related to the skill and knowledge in the art. *Id.* The specification need only describe in detail that which is new or not conventional. *Hybritech v. Monoclonal Antibodies*, 802 F.2d 1367, 231 U.S.P.Q. 81 (Fed. Cir. 1986).

Independent claim 1 and dependent claims 2-14 and 58 are directed to bisubstrate inhibitors of insulin receptor kinase. Independent claim 60 and dependent claims 63, 66 and 67 are directed to bisubstrate inhibitors of protein kinases. The bisubstrate inhibitors of insulin receptor kinase and protein kinases comprise (1) a nucleotide or nucleotide analog moiety, (2) a peptide moiety which is a substrate for the insulin receptor kinase or protein kinase, and (3) a tether that is greater than or equal to 4.9 Å when measured from a gamma phosphorus of the nucleotide or nucleotide analog and a proton donor of the tether.

The Office Action asserts that a representative number of species has not been disclosed to support claims 1-14 and 58 to a genus of bisubstrate inhibitors of insulin receptor kinase. However, as detailed below the specification provides a representative number of species of each of the component parts of the bisubstrate inhibitors, in addition to the actual reduction to practice shown in the working examples. These teachings together satisfy the legal requirements for written description of a genus. Applicants provide a working example of a bisubstrate inhibitor of insulin receptor kinase: compound 2. "Kinase assays with compound 2 revealed it to be a potent inhibitor of IRK [insulin receptor kinase]." Page 13, paragraph 47. Compound 2 comprises ATPγ-S as

the nucleotide moiety, a peptide with the sequence of SEQ ID NO:1 as the peptide moiety, and an acetyl group as the tether:

peptide moiety   tether   nucleotide or nucleotide analog moiety
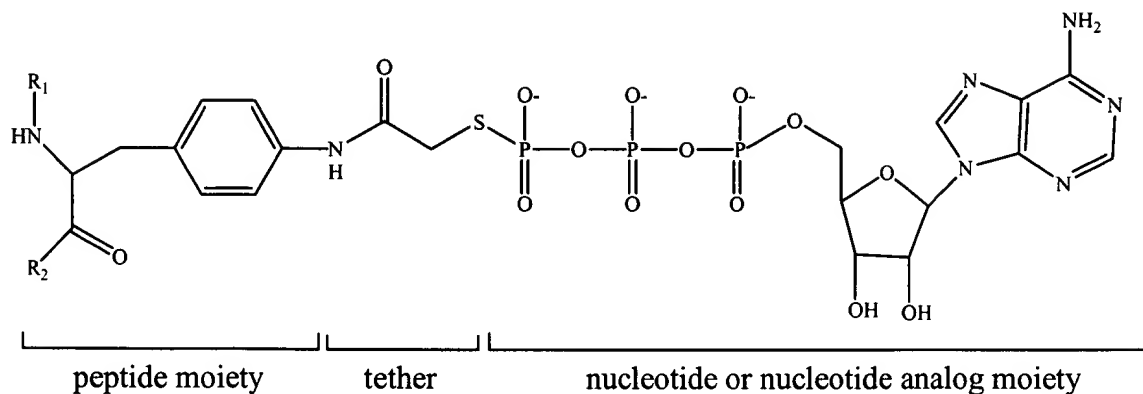
R_1 is AcNH-KKKLPATGD-

R_2 is –MNMSPVGD-CO_2H

The specification provides a representative number of nucleotides or nucleotide analogs. The specification teaches 14 nucleotides or nucleotide analogs that are suitable for use in the bisubstrate inhibitors for insulin receptor kinase. "Suitable moieties include ATP, ATPγ-S, GTP, CTP, TTP, UTP, GTPγ-S, CTPγ-S, TTPγ-S, UTPγ-S, genistein, staurosporine, K252, [and] quercetin." Page 7, paragraph 27. In addition, the specification teaches that one or more of the phosphate groups can be substituted with an uncharged alkyl group. Figure 6 lists 161 examples of possible alkyl substitutions. Thus, specification teaches numerous suitable nucleotide and nucleotide analog moieties. These moieties are a representative number of nucleotide and nucleotide analog moieties.

The specification provides identifying characteristics of the peptide moieties. The specification teaches that the peptide moiety has an amino acid sequence that is similar to the amino acid sequence of the natural protein substrate of the insulin receptor kinase. "Bisubstrate inhibitors typically contain a second moiety which is a peptide having residues similar to that of the natural protein substrates of the particular protein kinase." Page 7, paragraph 28. The specification teaches a peptide (KKKLPATGDYMN-MSPVGD, SEQ ID NO:1) that is useful as a peptide moiety in the bisubstrate inhibitors of insulin receptor kinase. Moreover, other peptides that have amino acid sequences of natural protein substrates of insulin receptor kinase were well known in the prior art. See

9

Table 1. Peptides 1, 5, 7, and 16-19 have amino acid sequences of natural substrates of insulin receptor kinase and have been shown in the prior art to be substrates for insulin receptor kinase. In addition, peptides that have similar amino acid sequences and function as substrates of insulin receptor kinase were well known in the prior art. Peptides 2-4, 6, and 8-15 are substrates of insulin receptor kinase that are similar to natural substrates and have been shown in the prior art to function as substrates for the insulin receptor kinase.

Table 1

	Peptide sequence	Reference	Tab[1]
1	RLEYYENEKK	Shoelson *et al.*, *Proc. Natl. Acad. Sci. USA* 89:2027-2031, 1992.	1
2	KRGEEELSNYICMGGK	Shoelson *et al.*, *Proc. Natl. Acad. Sci. USA* 89:2027-2031, 1992.	1
3	KKVSIEEYTEMMPAK	Shoelson *et al.*, *Proc. Natl. Acad. Sci. USA* 89:2027-2031, 1992.	1
4	KKHTDDGYMPMSPGVA	Shoelson *et al.*, *Proc. Natl. Acad. Sci. USA* 89:2027-2031, 1992.	1
5	RKGNGDGYMPMSPKSV	Shoelson *et al.*, *Proc. Natl. Acad. Sci. USA* 89:2027-2031, 1992.	1
6	KKRVDPNGYMMMSPSGS	Shoelson *et al.*, *Proc. Natl. Acad. Sci. USA* 89:2027-2031, 1992.	1
7	KKKLPATGDYMNMSPVGD	Shoelson *et al.*, *Proc. Natl. Acad. Sci. USA* 89:2027-2031, 1992. Hubbard, *EMBO J* 16:5573-5581, 1997.	1 2
8	KKGSEEYMNMDLGPGR	Shoelson *et al.*, *Proc. Natl. Acad. Sci. USA* 89:2027-2031, 1992.	1
9	KKSRGDYMTMQIG	Shoelson *et al.*, *Proc. Natl. Acad. Sci. USA* 89:2027-2031, 1992.	1

---

[1] Each reference is attached at the indicated tab number.

10

|	Peptide sequence	Reference	Tab[1]
10	KPRNSYVDTSPVAPK	Shoelson *et al.*, *Proc. Natl. Acad. Sci. USA* 89:2027-2031, 1992.	1
11	KKSRGNYMTMQIG	Shoelson *et al.*, *Proc. Natl. Acad. Sci. USA* 89:2027-2031, 1992.	1
12	KKSRGDYITMQIG	Shoelson *et al.*, *Proc. Natl. Acad. Sci. USA* 89:2027-2031, 1992.	1
13	KKSRGDYTTMQIG	Shoelson *et al.*, *Proc. Natl. Acad. Sci. USA* 89:2027-2031, 1992.	1
14	KKSRGDY(Nle[2])TMQIG	Shoelson *et al.*, *Proc. Natl. Acad. Sci. USA* 89:2027-2031, 1992.	1
15	KKSRGDYMTTQIG	Shoelson *et al.*, *Proc. Natl. Acad. Sci. USA* 89:2027-2031, 1992.	1
16	TRDIYETDYYRK	Stadmauer *et al.*, *J Biol. Chem.* 261:10000-10005, 1996.	3
17	LFASSNPEYLSARR	Stadmauer *et al.*, *J Biol. Chem.* 261:10000-10005, 1996.	3
18	KRSYEEHIPYTHMNGGK	Stadmauer *et al.*, *J Biol. Chem.* 261:10000-10005, 1996.	3
19	SRYMEDSTYYKASKG	Baron *et al.*, *J. Biol. Chem.* 273:7162-7168, 1998.	4

Thus, the specification provides identifying characteristics of the peptide moiety and an exemplary peptide moiety. Numerous other peptide moieties that are substrates for the insulin receptor kinase were known to those of skill in the art. Together these provide a representative number of peptide moieties.

The specification provides identifying characteristics of the tether. The specification teaches that the length of the tether "is greater than or equal to 4.9 Å measured from a gamma phosphorus of the nucleotide or nucleotide analog moiety to a

---

[2] Norleucine

11

proton donor." Page 9, paragraph 31. In addition, the specification teaches that "the tether can comprise carbon, hydrogen, and oxygen" Page 8, paragraph 29. An exemplary tether used in compound 2 has the following structure:

$$\text{structure}$$
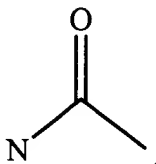
The proton donor of the tether used in compound 2 is nitrogen, and the tether has a length of 5.7 Å. See Figure 1a of the subject application.

Bond lengths of carbon-carbon bonds and carbon-oxygen bonds were well known in the art. A carbon-carbon bond is 1.54 Å and a carbon-oxygen bond is 1.43 Å as measured from the center of one atom to the center of the other atom. CRC Handbook of Chemistry and Physics, Weast (Ed.) The Chemical Rubber Co. Cleveland, OH, 1971, pages F173-F174 (Tab 5). The prior art knowledge of bond lengths combined with the specification's teachings that the tether can comprise carbon, hydrogen, and oxygen, and that it comprises a proton donor would demonstrate to one skilled in the art that applicants had disclosed a representative number of species of the tether.
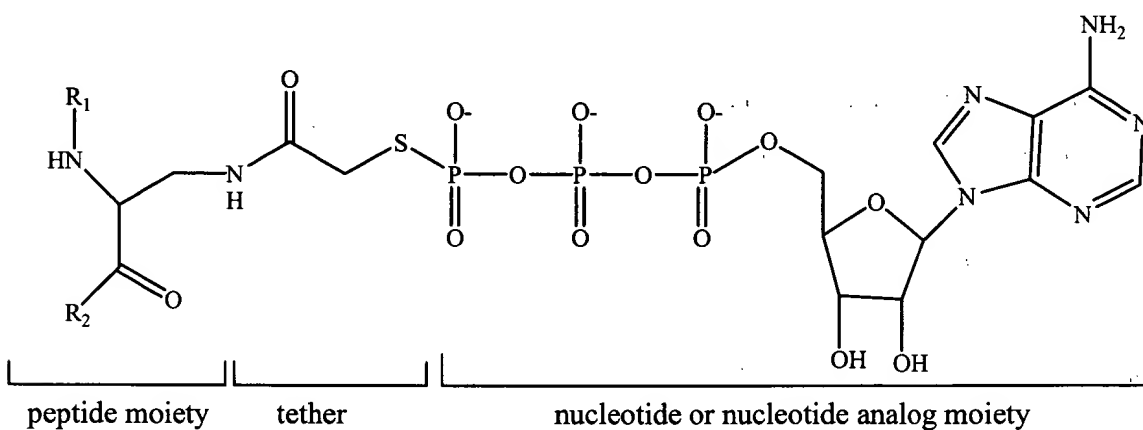
Thus, the specification provides identifying characteristics of the peptide and tether. The specification also teaches numerous examples of nucleotide or nucleotide analog moieties. The art contained numerous examples of suitable peptide moieties. One skilled in the art would reasonably conclude that the applicants had possession of the claimed genus of bisubstrate inhibitors of insulin receptor kinase.

Even if, *arguendo*, the generic claims were not adequately described, claims 2, 3, 5-7, 71, and 72 are adequately described. Claims 2 and 3 recite specific nucleotides or nucleotide analog moieties. Claim 2 specifically recites the nucleotide or nucleotide moiety is ATP. Claim 3 specifically recites the nucleotide or nucleotide analog moiety is ATPγ-S. Thus claim 2 and 3 are clearly supported by an adequate description of the nucleotide. Claims 5 and 6 recite a peptide moiety that is 4 or 5 contiguous amino acids selected from a recited sequence, *i.e.*, SEQ ID NO:1. Claim 7 recites a particular peptide moiety having the sequence shown in SEQ ID NO:1. Thus claims 5, 6, and 7 are clearly

supported by an adequate description of the peptide moiety. Claims 72 and 73 recite a specific tether, an acetyl group. Thus claims 72 and 73 are clearly supported by an adequate description of the tether.

The Office Action similarly asserts that a representative number of species has not been disclosed to support claims 60, 63, 66, and 67 to a genus of bisubstrate inhibitors of protein kinases generically. The specification teaches two bisubstrate inhibitors of protein kinases. Compound 2, discussed above, is a bisubstrate inhibitor of insulin receptor kinase. Compound 4, *i.e.*, kemptide-ATPγ-S conjugate, is a bisubstrate inhibitor of protein kinase A (PKA). "Preliminary assays using the kemptide-ATPγ-S conjugate as a specific inhibitor of protein kinase A (PKA) have been performed and show the conjugate to be inhibitory to PKA." Page 21, paragraph 65. Compound 4 comprises ATPγ-S as the nucleotide moiety, a peptide with the amino acid sequence of SEQ ID NO:4 as the peptide moiety, and an acetyl group as the tether.

Compound 4

R$_1$ is AcNH-LRRA-

R$_2$ is LG-CO$_2$H

As discussed above, the specification teaches numerous suitable nucleotides or nucleotide analogs moieties. In addition, specification provides identifying characteristics of the tether moiety and provides an exemplary tether.

The specification teaches two peptides that are useful as peptide moieties in the bisubstrate inhibitors of protein kinases. A peptide with an amino acid sequence of SEQ

13

ID NO:1 (KKKLPATGDYMNMSPVGD) is a substrate for insulin receptor kinase and is the peptide moiety of compound 2. A peptide with an amino acid sequence of SEQ ID NO:2 (LRRASLG) is a substrate for protein kinase A (PKA) and the peptide moiety of compound 4. Moreover, peptide substrates of protein kinases were well known in the prior art. In addition to the peptide substrates for insulin receptor kinase listed in Table 1, Table 2 lists examples of peptides that were known in the prior art to be substrates for protein kinases. Peptides 36-40, 71, and 96 have amino acid sequences of natural substrates of protein kinases. Peptides 20-35, 41-70, 72-95, and 97-102 are substrates of protein kinases that are similar to natural substrates and have been shown in the prior art to function as substrates.

Table 2

	Peptide sequence	Kinase	Reference	Tab[3]
20	PLSRTLSVSS	PKC[4]	Kwon et al., J. Biol. Chem. 269:4839-4844, 1994.	6
21	PLSRTLSV	PKC	Kwon et al., J. Biol. Chem. 269:4839-4844, 1994.	6
22	PLSRTLS	PKC	Kwon et al., J. Biol. Chem. 269:4839-4844, 1994.	6
23	PLRRTLSVAA	PKC	Kwon et al., J. Biol. Chem. 269:4839-4844, 1994.	6
24	PLSRRLSVAA	PKC	Kwon et al., J. Biol. Chem. 269:4839-4844, 1994.	6
25	KKKKKRFSFKKAFKKLA-GFAFKKNK	PKC	Kwon et al., J. Biol. Chem. 269:4839-4844, 1994.	6
26	DEDADIYDEEDYDL	CK2[5]	Marin et al., J. Biol. Chem. 274:29260-29265, 1999.	7

---

[3] Each reference is attached at the indicated tab number.
[4] Protein Kinase C
[5] Casein kinase-2

	Peptide sequence	Kinase	Reference	Tab[3]
27	DEDADIYDEADYDL	CK2	Marin *et al.*, *J. Biol. Chem.* 274:29260-29265, 1999.	7
28	DEDADIYDAEDYDL	CK2	Marin *et al.*, *J. Biol. Chem.* 274:29260-29265, 1999.	7
29	DEDADIYAEEDYDL	CK2	Marin *et al.*, *J. Biol. Chem.* 274:29260-29265, 1999.	7
30	DEDADDYDEEDYDL	CK2	Marin *et al.*, *J. Biol. Chem.* 274:29260-29265, 1999.	7
31	DEDADISDEEDYDL	CK2	Marin *et al.*, *J. Biol. Chem.* 274:29260-29265, 1999.	7
32	DEDADDSDEEDYDL	CK2	Marin *et al.*, *J. Biol. Chem.* 274:29260-29265, 1999.	7
33	DEDADISAEEDYDL	CK2	Marin *et al.*, *J. Biol. Chem.* 274:29260-29265, 1999.	7
34	DEDADISDEADYDL	CK2	Marin *et al.*, *J. Biol. Chem.* 274:29260-29265, 1999.	7
35	RRREEEESAAA	GRK2[6]	Onorato *et al.*, *J. Biol. Chem.* 270:21346-21353, 1995.	8
36	VSRSGLYRSPSMPENLNRP-RL	Chk1[7]	Hutchins *et al.*, *FEBS Lett.* 466:91-95, 2000.	9
37	LNRSRLYRSPSMPEKLDR-MPL	Chk1	Hutchins *et al.*, *FEBS Lett.* 466:91-95, 2000.	9
38	TPRRTLFRSLSCTVETPLA-NK	Chk1	Hutchins *et al.*, *FEBS Lett.* 466:91-95, 2000.	9
39	YLRPNVSRSRSSGNAPPFL-RS	Chk1	Hutchins *et al.*, *FEBS Lett.* 466:91-95, 2000.	9

[6] G protein coupled receptor kinase
[7] Checkpoint kinase-1

	Peptide sequence	Kinase	Reference	Tab[3]
40	QDTPVVRRTQSMFLNST-RLGL	Chk1	Hutchins *et al.*, *FEBS Lett.* 466:91-95, 2000.	9
41	RLYRSPSMPEKLD	Chk1	Hutchins *et al.*, *FEBS Lett.* 466:91-95, 2000.	9
42	ALYRSPSMPEKLD	Chk1	Hutchins *et al.*, *FEBS Lett.* 466:91-95, 2000.	9
43	RAYRSPSMPEKLD	Chk1	Hutchins *et al.*, *FEBS Lett.* 466:91-95, 2000.	9
44	RLARSPSMPEKLD	Chk1	Hutchins *et al.*, *FEBS Lett.* 466:91-95, 2000.	9
45	RLYASPSMPEKLD	Chk1	Hutchins *et al.*, *FEBS Lett.* 466:91-95, 2000.	9
46	RLYRAPSMPEKLD	Chk1	Hutchins *et al.*, *FEBS Lett.* 466:91-95, 2000.	9
47	RLYRSASMPEKLD	Chk1	Hutchins *et al.*, *FEBS Lett.* 466:91-95, 2000.	9
48	RLYRSPAMPEKLD	Chk1	Hutchins *et al.*, *FEBS Lett.* 466:91-95, 2000.	9
49	RLYRSPSAPEKLD	Chk1	Hutchins *et al.*, *FEBS Lett.* 466:91-95, 2000.	9
50	RLYRSPSMAEKLD	Chk1	Hutchins *et al.*, *FEBS Lett.* 466:91-95, 2000.	9
51	RLYRSPSMPAKLD	Chk1	Hutchins *et al.*, *FEBS Lett.* 466:91-95, 2000.	9
52	RLYRSPSMPEALD	Chk1	Hutchins *et al.*, *FEBS Lett.* 466:91-95, 2000.	9
53	RLYRSPSMPEKAD	Chk1	Hutchins *et al.*, *FEBS Lett.* 466:91-95, 2000.	9

16

	Peptide sequence	Kinase	Reference	Tab[3]
54	RLYRSPSMPEKLA	Chk1	Hutchins et al., FEBS Lett. 466:91-95, 2000.	9
55	RLYRAPSMPEKLDRK	Chk1	Hutchins et al., FEBS Lett. 466:91-95, 2000.	9
56	RLARAASMAAALARK	Chk1	Hutchins et al., FEBS Lett. 466:91-95, 2000.	9
57	RVARAASMAAALARK	Chk1	Hutchins et al., FEBS Lett. 466:91-95, 2000.	9
58	RMARAASMAAALARK	Chk1	Hutchins et al., FEBS Lett. 466:91-95, 2000.	9
59	RRARAASMAAALARK	Chk1	Hutchins et al., FEBS Lett. 466:91-95, 2000.	9
60	RIARAASMAAALARK	Chk1	Hutchins et al., FEBS Lett. 466:91-95, 2000.	9
61	RAARAASMAAALARM	Chk1	Hutchins et al., FEBS Lett. 466:91-95, 2000.	9
62	RLAKAASMAAALARK	Chk1	Hutchins et al., FEBS Lett. 466:91-95, 2000.	9
63	RLAAAASMAAALARK	Chk1	Hutchins et al., FEBS Lett. 466:91-95, 2000.	9
64	RLARAASMAAAAARK	Chk1	Hutchins et al., FEBS Lett. 466:91-95, 2000.	9
65	RLARAASMAAAIARK	Chk1	Hutchins et al., FEBS Lett. 466:91-95, 2000.	9
66	RLARAASMAAAVARK	Chk1	Hutchins et al., FEBS Lett. 466:91-95, 2000.	9
67	RLARAASMAAAALRK	Chk1	Hutchins et al., FEBS Lett. 466:91-95, 2000.	9

	Peptide sequence	Kinase	Reference	Tab[3]
68	RLARAASMAALAARK	Chk1	Hutchins et al., FEBS Lett. 466:91-95, 2000.	9
69	RLARAASAAAAAARK	Chk1	Hutchins et al., FEBS Lett. 466:91-95, 2000.	9
70	RKRLARAASMAAALA	Chk1	Hutchins et al., FEBS Lett. 466:91-95, 2000.	9
71	SAVGFNEMEAPTTAYK	Lyn[8]	Yamanashi et al., Proc. Natl. Acad. Sci. USA 90:3631-3635, 1993.	10
72	KKLIEDAGYAARG	c-Abl[9]	Till et al., J. Biol. Chem. 274:4995-5003, 1999.	11
73	KKLIEDAIYAARG	c-Abl	Till et al., J. Biol. Chem. 274:4995-5003, 1999.	11
74	KKLIEDALYAARG	c-Abl	Till et al., J. Biol. Chem. 274:4995-5003, 1999.	11
75	KKLIEDAHYAARG	c-Abl	Till et al., J. Biol. Chem. 274:4995-5003, 1999.	11
76	KKLIEDAAYAARG	c-Abl	Till et al., J. Biol. Chem. 274:4995-5003, 1999.	11
77	KKLIEDAKYAARG	c-Abl	Till et al., J. Biol. Chem. 274:4995-5003, 1999.	11
78	KKLIEDAQYAARG	c-Abl	Till et al., J. Biol. Chem. 274:4995-5003, 1999.	11
79	KKSRGDYMTMQIG	c-Abl, v-Abl[10], v-Src[11]	Till et al., J. Biol. Chem. 274:4995-5003, 1999; Garcia et al., J. Biol. Chem.	11 12

[8] Cellular Lyn protein kinase
[9] Cellular Abl protein kinase
[10] Viral Abl protein kinase
[11] Viral Src protein kinase

	Peptide sequence	Kinase	Reference	Tab[3]
			268:25146-25151, 1993.	
80	KKSRGDYITMQIG	c-Abl, v-Abl, v-Src	Till *et al.*, *J. Biol. Chem.* 274:4995-5003, 1999;	11
			Garcia *et al.*, *J. Biol. Chem.* 268:25146-25151, 1993.	12
81	KKSRGDY(Nle)[12]TMQIG	c-Abl, v-Abl, v-Src	Till *et al.*, *J. Biol. Chem.* 274:4995-5003, 1999;	11
			Garcia *et al.*, *J. Biol. Chem.* 268:25146-25151, 1993.	12
82	KKSRGDYATMQIG	c-Abl	Till *et al.*, *J. Biol. Chem.* 274:4995-5003, 1999.	11
83	KKSRGDYETMQIG	c-Abl	Till *et al.*, *J. Biol. Chem.* 274:4995-5003, 1999.	11
84	KKSRGDYMTPQIG	c-Abl	Till *et al.*, *J. Biol. Chem.* 274:4995-5003, 1999.	11
85	KKSRGDYMTTQIG	c-Abl, v-Abl, v-Src	Till *et al.*, *J. Biol. Chem.* 274:4995-5003, 1999;	11
			Garcia *et al.*, *J. Biol. Chem.* 268:25146-25151, 1993.	12
86	KKSRGDYMTAQIG	c-Abl	Till *et al.*, *J. Biol. Chem.* 274:4995-5003, 1999.	11
87	KKSRGDYMTEQIG	c-Abl	Till *et al.*, *J. Biol. Chem.* 274:4995-5003, 1999.	11
88	KKHTDDGYMPMSPGVA	v-Src, v-Abl	Garcia *et al.*, *J. Biol. Chem.* 268:25146-25151, 1993.	12
89	RKGNGDGYMPMSPKSV	v-Src, v-Abl	Garcia *et al.*, *J. Biol. Chem.* 268:25146-25151, 1993.	12

---

[12] Norleucine

19

	Peptide sequence	Kinase	Reference	Tab[3]
90	KKRVDPNGYMMMSPSGS	v-Src, v-Abl	Garcia *et al., J. Biol. Chem.* 268:25146-25151, 1993.	12
91	KKKLPATGDYMNMSP-VGD	v-Src, v-Abl	Garcia *et al., J. Biol. Chem.* 268:25146-25151, 1993.	12
92	KKGSEEYMNMDLGPGR	v-Src, v-Abl	Garcia *et al., J. Biol. Chem.* 268:25146-25151, 1993.	12
93	KKKEEEEEYMPMEDL	v-Src, v-Abl	Garcia *et al., J. Biol. Chem.* 268:25146-25151, 1993.	12
94	KKSRGNYMTMQIG	v-Src, v-Abl	Garcia *et al., J. Biol. Chem.* 268:25146-25151, 1993.	12
95	KKSRGDYTTMQIG	v-Src, v-Abl	Garcia *et al., J. Biol. Chem.* 268:25146-25151, 1993.	12
96	ADFGLARLIEDNEYTARG	c-Src[13], Hck[14]	Silicia *et al., J. Biol. Chem.* 273:16756-16763, 1998.	13
97	AEEEIYGEFEAKKKK	c-Src, Hck	Silicia *et al., J. Biol. Chem.* 273:16756-16763, 1998.	13
98	AEEEAYGEAEAKKKK	c-Src, Hck	Silicia *et al., J. Biol. Chem.* 273:16756-16763, 1998.	13
99	AEVIYAAPFAKKKK	c-Src, Hck	Silicia *et al., J. Biol. Chem.* 273:16756-16763, 1998.	13
100	KVEKIGEGTYGVVYK	c-Src, Hck	Silicia *et al., J. Biol. Chem.* 273:16756-16763, 1998.	13

---

[13] Cellular Src protein kinase
[14] Src-like protein kinase

	Peptide sequence	Kinase	Reference	Tab[3]
101	KVEKIGEGTYGVVKK	c-Src, Hck	Silicia *et al.*, *J. Biol. Chem.* 273:16756-16763, 1998.	13
102	KVEKIGVGSYGVVKK	c-Src, Hck	Silicia *et al.*, *J. Biol. Chem.* 273:16756-16763, 1998.	13

Thus, the specification provides identifying characteristics of the peptide moiety and suitable exemplary peptide moieties. Moreover, numerous other peptide moieties which are substrates for protein kinases were well known in the prior art. Together these provide a representative number of peptide moieties that are substrates for protein kinases.

Thus, the specification teaches identifying characteristics of the peptide and tether of the bisubstrate inhibitor for protein kinases. The specification also teaches numerous suitable nucleotide or nucleotide analog moieties. Given the knowledge in the art, the specification's teachings of identifying characteristics of the peptide and tether, and the specification's teaching of numerous suitable nucleotide or nucleotide analog moieties of the bisubstrate inhibitors of protein kinases, one skilled in the art would reasonably conclude that the applicants had possession of the claimed genus of bisubstrate inhibitors of protein kinases when they filed the application. Withdrawal of this rejection is respectfully requested.

The Rejection of Claims 1-14, 58, 60, 63, 66 and 67 Under 35 U.S.C. § 112, First Paragraph

Claims 1-14, 58, 60, 63, 66 and 67 stand rejected under 35 U.S.C. § 112, first paragraph as allegedly failing to enable the genus of bisubstrate inhibitors of insulin receptor kinase or protein kinases generically. Applicants respectfully traverse this rejection.

An analysis of whether a claim is enabled by the specification requires a determination of whether the specification contains sufficient information, together with knowledge in the prior art, to enable one skilled in the art to make and use the claimed

21

invention without undue experimentation. "The test of enablement is whether one reasonably skilled in the art could make or use the invention from the disclosures in the patent coupled with information known in the art without undue experimentation." *United States v. Telectronics, Inc.*, 857 F.2d 778, 8 U.S.P.Q.2d 1217 (Fed. Cir. 1988). Factors that may be considered in determining whether experimentation is undue include: (1) the breadth of the claims, (2) the nature of the invention, (3) the state of the prior art, (4) the level of one of ordinary skill, (5) the level of predictability in the art, (6) the amount of direction provided by the inventor, (7) the existence of working examples, and (8) the quantity of experimentation needed to make or use the invention based on the content of the disclosure. *In re Wands* 858 F.2d 731, 8 U.S.P.Q.2d 1400 (Fed. Cir. 1988). The specification need only describe in detail that which is new or not conventional. *Hybritech v. Monoclonal Antibodies*, 802 F.2d 1367, 231 U.S.P.Q. 81 (Fed. Cir. 1986).

The Nature of the Invention

The invention employs three components: a peptide, a nucleotide or nucleotide analog, and a tether. Each component was known in the art. See, *e.g.*, Rossé *et al.*, *Helvetica Chimica Acta* 80:653-670, 1997 (Tab 14). Rossé teaches design and synthesis of bisubstrate inhibitors of epidermal growth factor receptor tyrosine kinase. The Rossé bisubstrate inhibitors contain a peptide, a triphosphate mimic or spacer, and a nucleotide. "[W]e designed [a] series of bisubstrate inhibitors consisting of a tri- or tetrapeptide as the peptide substrate, a 4-sulfonylbenzoyl (1), a 2-hydroxy-4-sulfonylbenzoyl (2), a benzene-1,4-disulfonyl (3), or an adipoyl moiety (4) as the triphosphate mimic or spacer and adenosine." Page 654, first full paragraph. See also Loog *et al.*, *Bioorg. Med. Chem. Lett.* 9:1447-1452, 1999 (Tab 15). Loog teaches bisubstrate inhibitors of protein kinases that contain a peptide, a nucleotide, and a linker that connects the peptide to the 5' carbon of the nucleotide. "A new class of protein kinase bisubstrate-analog inhibitors was designed on the basis of adenosine-5'-carboxylic acid derivatives, where a short peptide was attached to the 5'-carbon atom of the adenosine sugar moiety via a linker chain." Abstract. Applicants' contribution is in specifying a dimension of the tether which represents the dissociative transition state:

> It is a discovery of the present invention that design and manipulation of the dimensions of bisubstrate inhibitors of protein kinases can dramatically improve their inhibitory properties. In particular, the

inventors have designed the distance between the two substrate-like moieties to mimic the dimensions of a dissociative transition state, *i.e.*, a dimension of greater than 4.9 Å measured from a gamma phosphorous of the nucleotide or nucleotide analog moiety to the proton donor in the peptide moiety.

Page 6, paragraph 26. Thus the nature of the invention is that it is an improvement of bisubstrate inhibitors already known in the art.

State of the Prior Art

The state of the prior art was advanced at the time applicants filed their patent application. Peptide substrates of protein kinases generically and insulin receptor kinase in particular, were well known in the art as of the filing date. As discussed above, a host of both natural and non-natural peptide substrates were known in the art. See Tables 1 and 2. In addition, sequence motifs for protein kinase substrates were well known in the art. For example, Shoelson *et al.*, *Proc. Natl. Acad. Sci. USA* 89:2027-2031, 1992 (Tab 1) teaches an amino acid sequence motif for substrates of insulin receptor kinase. The motif contains the sequence YMXM, where X can be proline, methionine, asparagine, or threonine. Table 1 page 2028. Sharma *et al.*, *J. Biol. Chem.* 274:9600-9606, 1999 (Tab 16) teaches a peptide motif for a different protein kinase, cyclin-dependent kinase 5 (CDK5) protein kinase. The motif for the CDK5 protein kinase is S/TPXK/R. Page 9600, abstract. Sharma also teaches that the motif for protein kinase A (PKA) is RRXS/A. Page 9604, column 2, paragraph 2. Clearly the state of the art was advanced and rich.

The Level of One of Ordinary Skill

The level of one of ordinary skill was high at the time applicants filed their application. The skilled worker, a protein chemist and/or an X-ray crystallographer, would have knowledge of bond lengths, protein kinase substrate motifs, and substrate specificity of protein kinases.

Level of Predictability

Because the state of the prior art and the level of the skilled artisan were high, the level of predictability was also high. The numerous studies in the prior art of protein kinase substrates provide a rich data source of peptide moieties which can function in a bisubstrate inhibitor. The knowledge of organic chemistry to make tethers of carbon,

hydrogen, and oxygen having a suitable length was again extremely rich. The nucleotide moieties and analogs known in the art were also many. Putting these components together by standard techniques of organic chemistry was highly predictable. No reasons have been put forward why these components could not have been readily joined. No reasons have been put forward why such joined components should not function in the intended manner.

The Amount of Guidance Provided

The invention employs known components. It specifies, however, that a tether of at least 4.9 Å be used. Applicants are very specific in guiding those of skill in the art to tethers of the proper length. This tether length is all that those in the art would need to practice the invention based on the state of the prior art and the skill level in the art.

Existence of Working Examples

The applicants provide two working examples: compounds 2 and 4. "Kinase assays with compound 2 revealed it to be a potent inhibitor of IRK." Page 13, paragraph 47. "Preliminary assays using the kemptide-ATPγ-S conjugate as a specific inhibitor of protein kinase A (PKA) have been performed and show the conjugate to be inhibitory to PKA." Page 21, paragraph 65. The existence of these working examples weighs in favor of a finding of enablement.

Quantity of Experimentation Needed

Given the content of the disclosure, one of ordinary skill in the art could readily have practiced the invention without a great deal of experimentation. All component parts of the claimed bisubstrate inhibitors were known. One of ordinary skill would merely need to assemble the parts. These parts had been similarly assembled in the prior art. Such assembly would not require undue experimentation.
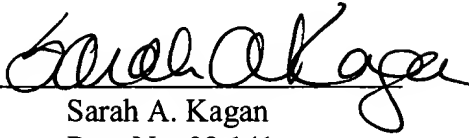
Conclusion

A consideration of the *Wands* factors leads to a conclusion that the invention can be practiced by those of skill in the art without recourse to undue experimentation. Withdrawal of this rejection is respectfully requested.

Respectfully submitted,

BANNER & WITCOFF, LTD.

Dated: 3-17-04

By: _Sarah A. Kagan_____

Sarah A. Kagan
Reg. No. 32,141

Banner & Witcoff Ltd.
Customer No. 22907

YMXM motifs of IRS-1 define substrate specificity of the insulin receptor kinase

(signal transduction/phosphatidylinositol 3'-kinase/oncogene/tyrosine kinase/*src* homology domain 2)

STEVEN E. SHOELSON[†], SWATI CHATTERJEE, MANAS CHAUDHURI, AND MORRIS F. WHITE

Research Division, Joslin Diabetes Center, Departments of Medicine, Brigham and Women's Hospital and Harvard Medical School, Boston, MA 02215

ABSTRACT Of 34 tyrosine residues in insulin receptor substrate 1 (IRS-1), 14 are adjacent to acidic residues, suggesting that they might be phosphorylation sites. Synthetic peptides corresponding to sequences surrounding these tyrosines were used as substrates of the insulin receptor kinase. Surprisingly six of these, each within YMXM motifs, were phosphorylated with greatest efficiency (K_m, 24–92 μM; k_{cat}/K_m, 0.6–2.1 × 10^4 M^{-1}·sec^{-1}). Substituted YMXM peptides revealed a strong preference of the insulin receptor kinase for methionine at Y + 1 and Y + 3 positions. When phosphorylated, related YMXM sequences are recognition motifs for binding to proteins with *src*-homology (SH2) domains. The combined hydrophobic and flexible nature of methionine side chains adjacent to the targeted tyrosines provides a versatile contact for recognition by diverse proteins involved in signal transduction.

Insulin binding to the extracellular α subunits of the insulin receptor activates tyrosine kinase activity intrinsic to the intracellular β subunits (1–4). This finding sparked a search for cellular substrates that could link the insulin receptor to postreceptor signaling events. The first identified endogenous substrate of the insulin receptor was pp185, a cytoplasmic phosphoprotein of 165–185 kDa (5). Recently, a cDNA corresponding to a component of the pp185 band was sequenced to provide the deduced primary structure of insulin receptor substrate 1 (IRS-1) (6, 7). As IRS-1 has little extended sequence homology with other known proteins, an intrinsic function for it has not been assigned. IRS-1 is phosphorylated on tyrosine residues after insulin stimulation (7), although the exact sites of phosphorylation have yet to be determined. Of a total of 34 tyrosines, 14 are preceded by acidic amino acids, suggesting that they might be targets of the insulin receptor kinase. Surprisingly, 6 of these are in YMXM motifs and two more are in YXXM motifs.

The platelet-derived growth factor (PDGF) receptor and polyoma virus middle-sized tumor antigen (middle T antigen) contain similar YMXM and homologous YVXM motifs, which are phosphorylated and thought to be essential for binding to phosphatidylinositol 3'-kinase (PI 3-kinase) (8, 9). The 85-kDa regulatory subunit of PI 3-kinase contains two SH2 domains (10, 11), which are thought to mediate its interactions with the PDGF receptor, the pp60$^{c\text{-}src}$/middle T antigen complex, and other proteins involved in cellular signaling (8). In fact, immunoprecipitation studies suggest that PI 3-kinase activity is closely associated with IRS-1 after insulin stimulation of intact cells (7, 12, 13). Thus, phosphorylated IRS-1 might act as a "docking protein" to bind and regulate PI 3-kinase and additional signal-transducing proteins containing SH2 domains as well.

In this study, we show that peptides corresponding to IRS-1 YMXM motifs are excellent substrates of the insulin receptor kinase. In fact, within a given sequence the presence of methionine residues at Y + 1 and Y + 3 positions is even more important than acidic residues N-terminal to tyrosine for catalytic efficiency. These findings suggest that in addition to being recognition elements for interactions with SH2 domain-containing proteins, residues within YMXM sequences form a recognition motif for insulin receptor-catalyzed phosphorylation. These studies define structural requisites for efficient phosphorylation of a cellular substrate of the insulin receptor and may extrapolate directly to other members of the family of tyrosine kinases and their interactions with additional elements of signaling cascades.

EXPERIMENTAL PROCEDURES

Peptide Synthesis. Solid-phase syntheses were performed on an Applied Biosystems model 430A synthesizer using standard dicyclohexylcarbodiimide-mediated preformed symmetrical anhydride coupling protocols. Amino acids with standard butoxycarbonyl/benzyl protecting groups were purchased from Applied Biosystems; additional solvents and reagents were the highest purity available. Peptide products were cleaved from the resin, side-chain protecting groups were removed, and methionine sulfoxide was reduced during "low-high" cleavages with trifluoromethanesulfonic acid (14). Peptides were typically quite pure; those having ≤95% purity by analytical reversed-phase HPLC were purified further by preparative HPLC (Waters Prep 4000) on a Dynamax-300A 12-μm C8 column (41.4 × 250 mm) equipped with a matched guard column. Peptides were eluted with a mobile phase composed of acetonitrile in 0.05% aqueous trifluoroacetic acid (80 ml/min). Amino acid analyses of all peptides used for kinetic analyses were as predicted.

Insulin Receptor Preparation. Chinese hamster ovary (CHO) cells, transfected with human insulin receptor constructs and expressing 10^6 receptors per cell (15), were grown in suspension in a 10-liter spinner flask in modified McCoy's 5A medium (GIBCO) containing 0.0345 mg of L-proline per ml and no CaCl$_2$ (16, 17). Cells were solubilized in 1.0% Triton X-100 and receptors were partially purified on wheat germ agglutinin (WGA)/agarose as described (17, 18). WGA-purified protein was stored at −70°C until needed. Identical aliquots of receptor were used for all assays.

Substrate Phosphorylation Experiments. WGA-purified insulin receptor (600 μl; 1.5 pmol) was incubated sequentially with 1 μM insulin (1 h at 4°C) and 50 μM ATP/5 mM MnCl$_2$ (1 h at 22°C) for maximal phosphorylation. The peptides were diluted appropriately in a mixture of 50 μM [γ-^{32}P]ATP/5 mM MnCl$_2$ in 50 mM Hepes containing 0.1% Triton X-100. Substrate phosphorylation reactions were initiated by the

Abbreviations: IRS-1, insulin receptor substrate 1; PDGF, platelet-derived growth factor; middle T antigen, polyoma virus middle-sized tumor antigen; PI 3-kinase, phosphatidylinositol 3'-kinase; SH2 and SH3, *src* homology domains 2 and 3; WGA, wheat germ agglutinin.
[†]To whom reprint requests should be addressed.

addition of 13 μl (32 fmol) of activated (insulin stimulated and ATP phosphorylated) insulin receptor, allowed to proceed at 22°C for 5 min (final vol, 40 μl), and terminated by addition of 65 μl of 5% trichloroacetic acid. Incorporated phosphate was determined by a modification of the phosphocellulose adsorption method (19). High molecular weight species were removed by precipitation after incubation in the presence of 0.16% bovine serum albumin for 30 min at 4°C. Portions of each supernatant solution containing phosphorylated peptides were spotted onto 2-cm^2 pieces of P81 phosphocellulose paper (Whatman) and washed four times for 30 min each in 1.0 liter of 0.075 M phosphoric acid. The papers were rinsed in acetone and allowed to air dry; incorporated phosphate was determined by Cerenkov counting.

Kinetic Analyses. Values for ^{32}P incorporation into the peptide substrates (cpm) were converted to pmol/min rates (V) to facilitate direct comparisons between peptides; dividing each pmol/min value by 1.3×10^{-5} mg (the amount of WGA-purified protein) converts it to the corresponding pmol per min per mg of protein value. K_m and V_{max} values and the corresponding standard errors were determined with the assistance of the ENZYME program (20), which follows algorithms for appropriate weighting of data described by Cleland (21); each peptide was analyzed in two to five separate experiments (see Table 2). The amount of insulin receptor in the WGA-purified protein isolated from human insulin receptor construct-transfected CHO cells, estimated by [^{125}I]insulin binding and Scatchard analyses using the LIGAND program (22), was 25 nmol/mg (range, 10–40 nmol/mg), which corresponds to 1% of the lectin-bound protein. This value was used to determine turnover rates (k_{cat}) and catalytic efficiency (k_{cat}/K_m).

RESULTS

Peptide Design. Peptides corresponding to sequences of IRS-1 surrounding tyrosine residues were synthesized. All consensus sites for tyrosine phosphorylation within YMXM motifs were prepared, as were additional consensus sequences not found in YMXM motifs (Table 1). Each peptide was designed to include (*i*) the specificity residue Y, (*ii*) acidic residues N-terminal to Y, (*iii*) residues at Y + 1 to Y + 5 positions, including the entire YMXMSP sequence, when appropriate, and (*iv*) as many native basic residues as possible, up to a total of three. If sufficient basic residues were not present within the native sequence, lysine residues were added at the C or N termini to a total of three to guarantee adsorption to the phosphocellulose paper used in the phosphopeptide assay (23). Therefore, peptides varied in length (10–18 residues) and position of the tyrosine residue.

Each peptide contains only one tyrosine with the exception of Y46,‡ which contains two side-by-side tyrosines flanked by glutamic acid residues (Table 1). Peptides Y460 and Y546 contain YXXM motifs in which the Y + 1 position is isoleucine or threonine, respectively, with acidic residues at appropriate positions relative to Y (Table 1). Peptides Y608, Y628, Y658, Y727, Y939, and Y987 each contain complete YMXM motifs with at least one acidic residue N-terminal to Y (Table 1). A final peptide, Y998, contains a single tyrosine residue that is neither in a YMXM motif nor adjacent to an N-terminal acidic residue; like four of the YMXM peptides, however, it does contain a serine and proline at the Y + 4 and Y + 5 positions (Table 1).

---

‡Peptides are named according to the position of tyrosine in the sequence of IRS-1 (e.g., a peptide corresponding to the sequence surrounding Y^{987} is called Y987); an analogue of Y^{987} in which methionine at the +1 position is mutated to threonine is called Y987(M988T). Peptide sequences are listed in Table 1.

Table 1. Synthetic peptides corresponding to native and modified sequences of IRS-1

Position/name	Sequence
Double tyrosine	
Y46	RLE**YY**ENEKK
YXXM motifs	
Y460	*KK*GEEELSN**YIC**M*GGK*
Y546	*KK*VSIEE**YTE**M*MPAK*
YMXM motifs	
Y608	*KK*HTDDG**YMPM**SPGV*A*
Y628	R*K*GNGDG**YMPM**SPKSV
Y658	*KK*RVDPNG**YMMM**SPSGS
Y727	*KKK*LPATGD**YMMM**SPVGD
Y939	*KK*GSEE**YMNM**DLGPGR
Y987	*KK*SRGD**YMTM**QIG
Nonspecific sequence	
Y998	*K*PRNS**Y**VDT**SP**VAP*K*
Modified Y987 sequences	
Y987(D986N)	*KK*SRG*N***YMTM**QIG
Y987(M988I)	*KK*SRGD**YITM**QIG
Y987(M988T)	*KK*SRGD**YTTM**QIG
Y987(M988Nle)	*KK*SRGD**Y**†**TM**QIG
Y987(M990T)	*KK*SRGD**YMTT**QIG

Phosphorylated tyrosines are boldface and underlined, as are additional elements of the YMXM specificity motif. Non-native residues are in italics; basic residues were added for assay purposes and there is a cysteine to alanine substitution for peptide Y727. For modified Y987 sequences, substituted positions are italicized. †Norleucine.

Additional analogues of Y987 (a low K_m substrate with a complete YMXM motif) were prepared to test the functional importance of residues surrounding the targeted tyrosine (Table 1). To determine directly the effect of isoleucine or threonine in place of methionine at the Y + 1 position, as occurs naturally in sequences surrounding Y460 and Y546, these residues were substituted into the sequence of Y987. In addition, norleucine, which is isomorphic with methionine, was substituted at the Y + 1 position to further test requirements for side-chain hydrophobicity and flexibility. The function of methionine at the Y + 3 position of Y987 was also tested by analogous substitution to threonine, and the requirement for an acidic residue (aspartic acid at Y − 1) was tested by a conservative substitution to asparagine.

Peptide Phosphorylations and Kinetic Analyses. All peptides (Table 1) were phosphorylated by the insulin-stimulated and autoactivated receptor kinase in a time- and temperature-dependent fashion and displayed saturable kinetics (Fig. 1 *A* and *C*), which yielded linear Lineweaver–Burk plots (Fig. 1 *B* and *D*). In every case, phosphorylation reactions were linear for at least 5 min (data not shown), validating conditions used for determinations of K_m and V_{max} values (Table 2). Rates of peptide phosphorylation (V_{max}) and peptide concentrations required for half-maximal saturation (K_m) varied dramatically between peptides (Fig. 1). The slopes of double reciprocal plots, which are proportional to K_m/V_{max} (the inverse of catalytic efficiency), clustered into two groups (Fig. 1 *B* and *D*). Notably, native sequences having entire YMXM motifs displayed the smallest slopes (Fig. 1*D*) and were therefore phosphorylated most efficiently. By contrast, YXXM peptides and other sequences not containing complete YMXM motifs all displayed steeper slopes (Fig. 1*B*), demonstrating that they were phosphorylated less efficiently.

Calculation of kinetic constants revealed that K_m values for YMXM peptides ranged from 24 to 92 μM, lower than values previously reported for any peptides used as exogenous substrates of the insulin receptor (Table 2). Values for V_{max}, which range from 0.9 to 1.7 pmol/min (69–131 nmol·min^{-1}·mg^{-1}), are difficult to compare to previous studies as
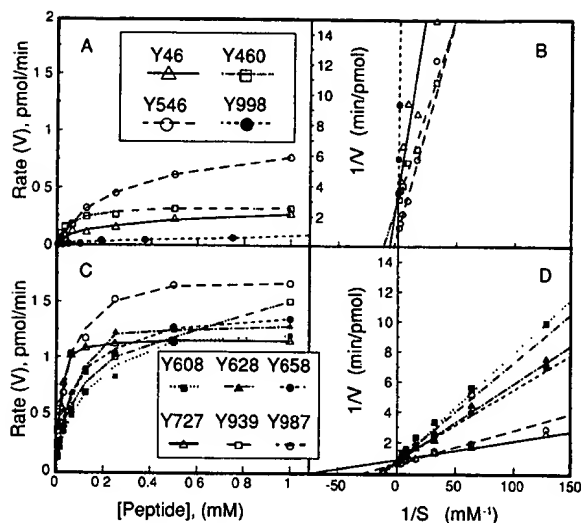
FIG. 1. Phosphorylation of peptides corresponding to native IRS-1 sequences by the insulin receptor kinase. Representative V vs. substrate concentration (A and C) and double reciprocal plots (B and D) are shown for phosphorylation of non-YMXM sequences (A and B) and YMXM sequences (C and D). Peptide sequences are identified in Table 1; methods used for phosphorylation reactions and data handling are described in *Experimental Procedures*.

this number varies with kinase specific activity. Values for k_{cat}/K_m, determined in this study, range from 0.6 to 2.1 × 10⁴ $M^{-1} \cdot s^{-1}$. Therefore, in terms of substrate binding (estimated by K_m), turnover rates (k_{cat}), and overall catalytic efficiency (k_{cat}/K_m), all of the YMXM peptide sequences are excellent substrates of the insulin receptor kinase.

Similar analyses were performed with YXXM motifs (peptides Y460 and Y546; Table 1). Interestingly, K_m for peptide Y460 phosphorylation (isoleucine at the Y + 1 position) was 73 μM, within the range of values for YMXM peptides; this peptide was a less efficient substrate because V_{max} was 0.30 pmol/min, well below the range for YMXM peptides, which suggests that side-chain flexibility in addition to hydropho-

Table 2. Summary of kinetic constants

Peptide	K_m, μM	V_{max}, pmol/min	k_{cat}, s^{-1}	k_{cat}/K_m, $M^{-1} \cdot s^{-1}$
Double tyrosine				
Y46	140 ± 85	0.3 ± 0.06	0.14	1.0 × 10³
YXXM motifs				
Y460	73 ± 15	0.3 ± 0.03	0.16	2.1 × 10³
Y546	300 ± 30	1.4 ± 0.07	0.73	2.4 × 10³
YMXM motifs				
Y608	90 ± 20	1.1 ± 0.09	0.57	6.2 × 10³
Y628	60 ± 8	1.2 ± 0.06	0.63	1.0 × 10⁴
Y658	86 ± 16	1.6 ± 0.12	0.83	9.7 × 10³
Y727	24 ± 2.9	0.9 ± 0.06	0.47	2.0 × 10⁴
Y939	61 ± 29	1.7 ± 0.3	0.89	1.5 × 10⁴
Y987	34 ± 8.8	1.4 ± 0.11	0.73	2.1 × 10⁴
Nonspecific sequence				
Y998	3200 ± 600	0.4 ± 0.04	0.21	6.5 × 10
Modified Y987 sequences				
Y987(D986N)	250 ± 69	3.9 ± 0.6	2.0	8.1 × 10³
Y987(M988I)	80 ± 15	0.9 ± 0.07	0.47	5.9 × 10³
Y987(M988T)	250 ± 80	2.7 ± 0.44	1.4	5.6 × 10³
Y987(M988Nle)	24 ± 7.1	1.3 ± 0.12	0.68	2.8 × 10⁴
Y987(M990T)	370 ± 110	1.2 ± 0.13	0.63	1.7 × 10³

bicity at the Y + 1 position might be necessary for high turnover and catalytic efficiency. By contrast, the reduced catalytic efficiency of peptide Y546 (threonine at the Y + 1 position) was due to a high K_m for phosphorylation, which at 300 μM was substantially greater than corresponding values for YMXM peptides; in this case V_{max}, at 1.4 pmol/min, was similar to the YMXM peptides. Within a limited context, these results begin to suggest that the unique character of methionine (being flexible and hydrophobic) performs a special function in enhanced catalytic efficiency.

To test this more directly, the Y + 1 position within YMXM peptide Y987 was substituted with isoleucine, threonine, and norleucine (Table 1). In fact, both M988I and M988T substitutions reduced catalytic efficiency (k_{cat}/K_m) nearly 4-fold (Fig. 2B, compare slopes); the reasons for reduced efficiency were different for the two peptides, however. The M988I substitution increased K_m 2- to 3-fold and reduced V_{max} nearly 2-fold (Table 2). By contrast, the M988T substitution increased both K_m (7- to 8-fold) and V_{max} (2-fold). Thus, in a single, defined YMXM sequence M988I and M988T substitutions have the same general effect as observed for the YXXM peptides (Y460 and Y546). Substitution of methionine with norleucine, whose side chain mimics that of methionine regarding both hydrophobicity and flexibility, had no observable effect on K_m, V_{max}, and k_{cat}/K_m (Fig. 2B; Table 2).

For further comparison, we substituted the Y + 3 methionine of peptide Y987 and the acidic residue N-terminal to tyrosine (Y − 1). Surprisingly, the M991T substitution had an effect even greater than the related Y + 1 substitutions (Fig. 2D), with a 12-fold reduction in catalytic efficiency (k_{cat}/K_m) resulting exclusively from an increase in K_m (Table 2). Therefore, methionine residues at Y + 1 and Y + 3 positions play a very special role in directing efficient catalysis by the insulin receptor kinase. Acidic residues, which exist near autophosphorylated tyrosines in the insulin receptor and other protein tyrosine kinases, are presumed to be important for intermolecular substrate recognition as well (23–27). The only acidic residue in the Y987 sequence was substituted with
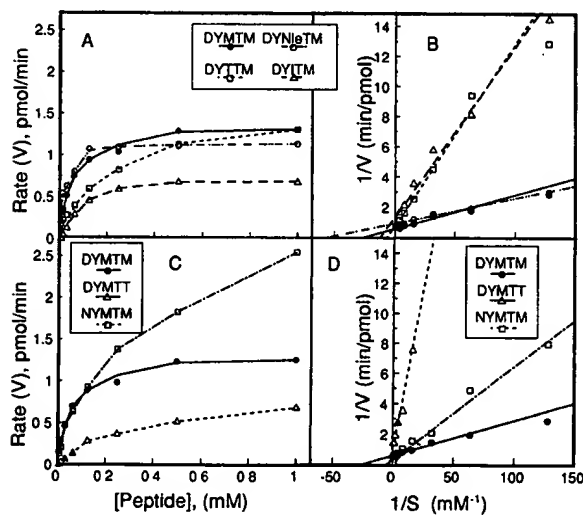

FIG. 2. Insulin receptor-catalyzed phosphorylation of substituted peptides corresponding to the IRS-1 sequence surrounding Y987. Representative V vs. substrate concentration (A and C) and double reciprocal plots (B and D) are shown for phosphorylation of peptides substituted at the Y + 1 position (A and B) or Y − 1 and Y + 3 positions (C and D). Peptide sequences are identified in Table 1; methods used for phosphorylation reactions and data handling are described in *Experimental Procedures*.

asparagine to assess the isolated effect of having no negative charge N-terminal to tyrosine (Fig. 2D). K_m was increased 8-fold while V_{max} was increased nearly 3-fold. These changes caused a net 2.5-fold reduction in catalytic efficiency (k_{cat}/K_m). Surprisingly, this is less deleterious than the corresponding effects observed for substituting methionine residues at either Y + 1 or Y + 3 positions (Table 2).

Two additional peptides corresponding to IRS-1 sequences not associated with YXXM or YMXM motifs were studied for comparison. Y46 contains a paired YY sequence flanked by acidic residues (EYYENE), resembling to a degree the major phosphorylation site of the insulin receptor itself (DIYETDYY) (28–30). The K_m for peptide Y46 phosphorylation was 134 μM, higher than that observed for YMXM peptides (Table 2), and V_{max} was 3- to 4-fold lower. Therefore, although Y46 can be considered to be a good substrate of the insulin receptor, it was phosphorylated with lower efficiency (6- to 36-fold) than YMXM peptides. Peptide Y998, which contains serine and proline at the Y + 4 and Y + 5 positions but lacks an acidic residue and methionine altogether, has a K_m for phosphorylation that is markedly elevated (3.2 mM). In addition, V_{max} is reduced (0.4 pmol/min) so k_{cat}/K_m is dramatically reduced (65 $M^{-1} \cdot s^{-1}$), which demonstrates the importance of primary sequence in directing insulin receptor kinase action and suggests that the effects of acidic residues N-terminal to tyrosine and methionine residues at Y + 1 and Y + 3 positions are cumulative.

DISCUSSION

Unlike serine/threonine-protein kinases, whose substrate recognition sequences are well defined by basic residues neighboring the phosphate acceptor (31–33), recognition sequences for substrates of protein tyrosine kinases are not well characterized. Autophosphorylated tyrosines within protein tyrosine kinase sequences are frequently located near acidic residues, which has led most investigators to focus on these positions as consensus sequences for tyrosine phosphorylation (23–27, 34–37). Synthetic peptides corresponding to autophosphorylation sites are phosphorylated by tyrosine kinases with K_m values typically in the millimolar range, which is considerably higher than values obtained for peptide substrates of serine/threonine kinases (23–27, 31–37). Unrelated peptides such as angiotensin and gastrin analogues are also phosphorylated by protein tyrosine kinases. Angiotensins I and II (both containing the DRVY*IHPF sequence) are phosphorylated with K_m values in the 1–4 mM range (26, 34), while gastrin analogues having five sequential glutamates N-terminal to tyrosine are phosphorylated with K_m values in the 50–200 μM range (35, 36). In fact, of all synthetic peptides studied previously as tyrosine kinase substrates, gastrin had the lowest K_m, a fact supporting the notion that acidic residues are important for tyrosine phosphorylation. However, systematic studies to define substrate specificity showed that when acidic residues of various peptides were replaced by uncharged amino acids, effects on V_{max}/K_m were often relatively small (2- to 4-fold) (23–27, 34–37).

The insulin receptor has tyrosine kinase activity similar to that of the viral transforming proteins, their cellular counterparts, and growth factor receptors. The insulin receptor phosphorylates the src peptide and angiotensin with K_m values in the millimolar range (26) and, in addition, phosphorylates a peptide corresponding to its own major autophosphorylation site (residues 1154–1164) (28–30) with a K_m value of 0.2–0.3 mM (18, 23, 30, 37). While the sequence at residues 1154–1164 might be a preferred substrate sequence, it was the recent identification of an endogenous substrate that allowed us to test sequences that might direct intermolecular substrate recognition. Finding biologically important sites of substrate phosphorylation will facilitate testing the importance of elements of secondary or tertiary structure in

addition to that of primary sequence. For the insulin receptor, IRS-1 may be such a substrate. IRS-1 is a component of pp185 that is immunoprecipitated from insulin-stimulated cells by anti-phosphotyrosine antibodies. IRS-1 is phosphorylated on tyrosine residues in response to insulin (5–7) and appears to link the receptor to other components of the intracellular signaling cascade (e.g., PI 3-kinase; ref. 7).

As yet, we do not know which of the 34 tyrosine residues in IRS-1 are actually phosphorylated, although 14 have acidic residues N-terminal to the tyrosine position, which would categorize them as conventional consensus sequences for tyrosine kinase recognition. Surprisingly, 6 of these are within YMXM motifs and 2 more are in YXXM sequences, which previous studies (8–10, 38) suggest are important for interactions with PI 3-kinase and other proteins having SH2 domains. In this report, we show that synthetic peptides corresponding to IRS-1 YMXM sequences are excellent substrates for the insulin receptor kinase. In fact, calculated values of K_m are lower than has been reported previously for peptides phosphorylated by any tyrosine kinase, with the exception of epidermal growth factor receptor-catalyzed phosphorylation of gastrin (which contains the homologous EEEEEAYGWM sequence; refs. 35 and 36).

Amino acid substitution studies show that different positions within the YMXM motif effect catalytic efficiency. Substitutions of methionine at Y + 1 decrease catalytic efficiency for tyrosine phosphorylation ≈4-fold, estimated by (i) comparisons of k_{cat}/K_m for peptides Y460 and Y546 (YXXM motifs) and the six YMXM peptides, and (ii) direct comparisons between k_{cat}/K_m for the wild-type Y987 sequence and substituted peptides Y987(M988I) and Y987(M988T). Notably, norleucine and methionine at the Y + 1 position are functionally indistinguishable. Substitution of methionine at Y + 3 with threonine has an even greater effect on peptide Y987 phosphorylation, in this case reducing k_{cat}/K_m ≈12-fold due to an effect on K_m. Both of these effects are greater than that produced by substituting aspartic acid with asparagine at Y − 1 of peptide Y987 (≈2.5-fold reduction in k_{cat}/K_m). Sequences having neither N-terminal acidic residues nor methionine at Y + 1 and Y + 3 positions are phosphorylated much less efficiently. We do not know the significance of residues at the Y + 2 position (proline, methionine, asparagine, or threonine in the YMXM sequences studied here). Four of the six YMXM sequences of IRS-1 also have serine and proline at the Y + 4 and Y + 5 positions, although peptides with or without the YMXMSP residues are phosphorylated with equal efficiency. Furthermore, the Y998 sequence contains serine and proline at the Y + 4 and Y + 5 positions but without an acidic residue or methionine phosphorylation was inefficient. The function (if any) served by these residues appears not to be related to phosphorylation.

What, if anything, is special about Y + 1 and Y + 3 positions, and why does methionine at these positions enhance kinetic efficiency? Sequences directly contiguous to and including YMXM are predicted by the Chou–Fasman algorithm (41) to be unstructured, although β-turns are predicted to flank each of the YMXM motifs of IRS-1 (data not shown). Alternatively, it has been proposed that substrates might adopt amphiphilic helical structures at the kinase catalytic surface (42); if so, methionine residues at Y + 1 and Y + 3 positions might be positioned appropriately for direct participation in binding. While we have not yet been able to analyze structure, the unique character of methionine may play a special role here. Isoleucine, leucine, and valine, while also highly hydrophobic, have branched and thus relatively rigid side chains. By contrast, the side chain of methionine is unbranched, providing considerable structural flexibility. In support of this, norleucine, which is equally flexible and hydrophobic compared to methionine, has an identical capacity to direct insulin receptor kinase action. This feature of methionine has recently

Biochemistry: Shoelson *et al.*

Proc. Natl. Acad. Sci. USA 89 (1992) 2031

been proposed to provide a malleable nonpolar surface for signal peptide recognition (43) and plasticity in protein interactions with calmodulin (39), which would allow structurally diverse nonpolar surfaces to conform to the respective recognition surfaces of the proteins to which they bind (40). Such a malleable, nonpolar surface might provide a mechanism to explain how the same IRS-1 YMXM motifs interact with the insulin receptor kinase and PI 3-kinase and, potentially, other tyrosine kinases and proteins with SH2 domains as well. The side chains of residues in the YMXM domain might be sufficiently flexible to provide a nonpolar surface that accommodates itself equally to the surfaces of kinase active sites and SH2 protein binding pockets.

Relationships between IRS-1 and other signal transduction proteins may be quite complex, as IRS-1 contains multiple copies of the YMXM motif that could interact selectively with different tyrosine kinases as well as distinct effector molecules containing various isoforms of the SH2/SH3 domain. Furthermore, other proteins involved in signal transduction contain related sequences. The PDGF receptor phosphorylates itself within YMXM or YVXM motifs (44), the src-associated middle T antigen contains a phosphorylated EEEEEYMPM sequence (8, 45), and similar sequences within the colony-stimulating factor 1 receptor (DTYVEM) and *kit* oncogene (DSTNEYMDM) may be phosphorylated, as well (8). Whether YMXM motifs define a recognition sequence for efficient tyrosine phosphorylation by these and other protein tyrosine kinases remains to be tested. For the src-associated middle T antigen and the PDGF receptor, these sequences are thought to be involved in recognition by PI 3-kinase through interaction with one or the other of its SH2 domains (8, 9, 38, 44). Similarly, studies to block interactions between IRS-1 and PI 3-kinase with synthetic phosphopeptides corresponding to IRS-1 YMXM sequences suggest that these interactions involve SH2 domains as well (unpublished data).

In conclusion, YMXM, a redundant sequence motif identified in IRS-1, is shown to define substrate specificity of the insulin receptor kinase. Methionine residues at the Y + 1 and Y + 3 positions are particularly important for efficient kinase recognition, in addition to acidic residues N-terminal to tyrosine. Knowing a target motif for the action of the insulin receptor kinases, and possibly other tyrosine kinases as well, may enhance our understanding of tyrosine kinase signaling pathways. Furthermore, a tyrosine kinase target motif may facilitate identification of additional known or newly identified proteins that might be involved in related signaling pathways. Certainly, as genomic sequencing efforts progress, it will be increasingly useful to have identified short peptide motifs to help decipher which of these DNA sequences encodes proteins acting as potential targets of tyrosine kinase action.

1. Kasuga, M., Zick, Y., Blithe, D. L., Crettaz, M. & Kahn, C. R. (1982) *Nature (London)* **298**, 667–669.
2. Kasuga, M., Karlsson, F. A. & Kahn, C. R. (1982) *Science* **215**, 185–187.
3. Rosen, O. M., Herrera, R., Olowe, Y., Petruzzelli, L. M. & Cobb, M. H. (1983) *Proc. Natl. Acad. Sci. USA* **80**, 3237–3240.
4. Yu, K. & Czech, M. P. (1984) *J. Biol. Chem.* **259**, 5277–5286.
5. White, M. F., Maron, R. & Kahn, C. R. (1985) *Nature (London)* **318**, 183–186.
6. Rothenberg, P. L., Lane, W. S., Karasik, A., Backer, J. M., White, M. F. & Kahn, C. R. (1991) *J. Biol. Chem.* **266**, 8302–8311.
7. Sun, X. J., Rothenberg, P., Kahn, C. R., Backer, J. M., Araki, E.,

Wilden, P. A., Cahill, D. A., Goldstein, B. J. & White, M. F. (1991) *Nature (London)* **352**, 73–77.
8. Cantley, L. C., Auger, K. R., Carpenter, C., Duckworth, B., Graziani, A., Kapeller, R. & Soltoff, S. (1991) *Cell* **64**, 281–302.
9. Escobedo, J. A., Kaplan, D. R., Kavanaugh, W. M., Turck, C. W. & Williams, L. T. (1991) *Mol. Cell. Biol.* **11**, 1125–1132.
10. Koch, C. A., Anderson, D., Moran, M. F., Ellis, C. & Pawson, T. (1991) *Science* **252**, 668–674.
11. Moran, M. F., Koch, C. A., Anderson, D., Ellis, C., England, L., Martin, G. S. & Pawson, T. (1990) *Proc. Natl. Acad. Sci. USA* **87**, 8622–8626.
12. Ruderman, N. B., Kapeller, R., White, M. F. & Cantley, L. C. (1990) *Proc. Natl. Acad. Sci. USA* **87**, 1411–1415.
13. Edemann, G., Yohezawa, K. & Roth, R. A. (1990) *J. Biol. Chem.* **265**, 396–400.
14. Tam, J. P. & Merrifield, R. B. (1987) in *The Peptides: Analysis, Synthesis, Biology*, eds. Udenfriend, S. & Meienhofer, J. (Academic, New York), pp. 185–248.
15. Ebina, Y., Edery, M., Ellis, L., Beaudoin, J., Roth, R. A. & Rutter, W. J. (1985) *Proc. Natl. Acad. Sci. USA* **82**, 8014–8018.
16. Shymko, R. M., Gonzales, N. S., Backer, J. M., White, M. F. & De Meyts, P. (1989) *Biochem. Biophys. Res. Commun.* **164**, 191–198.
17. Shoelson, S. E., Lu, Z., Parlautan, L., Lynch, C. S. & Weiss, M. A. (1992) *Biochemistry*, in press.
18. Shoelson, S. E., White, M. F. & Kahn, C. R. (1988) *J. Biol. Chem.* **263**, 4852–4860.
19. Glass, D. B., Masaracchia, R. A., Feramisco, J. R. & Kemp, B. E. (1978) *Biochem. J.* **87**, 566–575.
20. Lutz, R. A., Bull, C. & Rodbard, D. (1986) *Enzyme* **36**, 197–206.
21. Cleland, W. W. (1979) *Methods Enzymol.* **63**, 103–138.
22. Munson, P. J. & Rodbard, D. (1980) *Anal. Biochem.* **107**, 220–239.
23. Stadtmauer, L. A. & Rosen, O. M. (1986) *J. Biol. Chem.* **261**, 10000–10005.
24. Hunter, T. (1982) *J. Biol. Chem.* **257**, 4843–4848.
25. Patschinsky, T., Hunter, T., Esch, F. S., Cooper, J. A. & Sefton, B. M. (1982) *Proc. Natl. Acad. Sci. USA* **79**, 973–977.
26. Stadtmauer, L. A. & Rosen, O. M. (1983) *J. Biol. Chem.* **258**, 6682–6685.
27. Geahlen, R. L. & Harrison, M. L. (1989) in *Peptides and Protein Phosphorylation*, ed. Kemp, B. E. (CRC, Boca Raton, FL), pp. 239–250.
28. Ebina, Y., Ellis, L., Jarnagin, K., Edery, M., Graf, L., Clauser, E., Ou, J.-H., Masiarz, F., Kan, Y. W., Goldfine, I. D., Roth, R. A., & Rutter, W. J. (1985) *Cell* **40**, 747–758.
29. Ullrich, A., Bell, J. R., Chen, E. Y., Herrera, R., Petruzzelli, L. M., Dull, T. J., Gray, A., Coussens, L., Liao, Y.-C., Tsubokawa, M., Mason, A., Seeburg, P. H., Grunfeld, C., Rosen, O. M. & Ramachandran, J. (1985) *Nature (London)* **313**, 756–761.
30. White, M. F., Shoelson, S. E., Keutmann, H. & Kahn, C. R. (1988) *J. Biol. Chem.* **263**, 2969–2980.
31. Kemp, B. E. & Pearson, R. B. (1990) *Trends Biochem. Sci.* **15**, 342–346.
32. Kemp, B. E., ed. (1990) *Peptides and Protein Phosphorylation* (CRC, Boca Raton, FL).
33. Kennely, P. J. & Krebs, E. G. (1991) *J. Biol. Chem.* **266**, 15555–15558.
34. Wong, T. W. & Goldberg, A. R. (1983) *J. Biol. Chem.* **258**, 1022–1025.
35. Baldwin, G. S., Burgess, A. W. & Kemp, B. E. (1982) *Biochem. Biophys. Res. Commun.* **109**, 656–662.
36. Baldwin, G. S., Knesel, J. & Monckton, J. M. (1983) *Nature (London)* **301**, 435–438.
37. Shoelson, S. E., White, M. F. & Kahn, C. R. (1989) *J. Biol. Chem.* **264**, 7831–7836.
38. Auger, K. R., Carpenter, C. L., Shoelson, S. E., Piwnica-Worms, H. & Cantley, L. C. (1992) *J. Biol. Chem.*, in press.
39. O'Neil, K. T. & DeGrado, W. F. (1990) *Trends Biochem. Sci.* **15**, 59–64.
40. Gellman, S. H. (1991) *Biochemistry* **30**, 6633–6636.
41. Fasman, G., ed. (1989) *Prediction of Protein Structure and the Principles of Protein Conformation* (Plenum, New York).
42. Radziejewski, C., Miller, W. T., Mobashery, S., Goldberg, A. R. & Kaiser, E. T. (1989) *Biochemistry* **28**, 9047–9052.
43. Bernstein, H. D., Poritz, M. A., Strub, K., Hoben, P. J., Brenner, S. & Walter, P. (1989) *Nature (London)* **340**, 482–486.
44. Escobedo, J. A., Navankasattusas, S., Kavanaugh, W. M., Milfay, D., Fried, V. A. & Williams, L. T. (1991) *Cell* **65**, 75–82.
45. Hunter, T., Hutchinson, M. A. & Eckhart, W. (1984) *EMBO J.* **3**, 73–79.

Crystal structure of the activated insulin receptor tyrosine kinase in complex with peptide substrate and ATP analog

Stevan R.Hubbard

Department of Pharmacology and Skirball Institute of Biomolecular Medicine, 540 First Avenue, New York University Medical Center, New York, NY 10016, USA

e-mail: hubbard@tallis.med.nyu.edu

The crystal structure of the phosphorylated, activated form of the insulin receptor tyrosine kinase in complex with a peptide substrate and an ATP analog has been determined at 1.9 Å resolution. The activation loop (A-loop) of the kinase undergoes a major conformational change upon autophosphorylation of Tyr1158, Tyr1162 and Tyr1163 within the loop, resulting in unrestricted access of ATP and protein substrates to the kinase active site. Phosphorylated Tyr1163 (pTyr1163) is the key phosphotyrosine in stabilizing the conformation of the tris-phosphorylated A-loop, whereas pTyr1158 is completely solvent-exposed, suggesting an availability for interaction with downstream signaling proteins. The YMXM-containing peptide substrate binds as a short anti-parallel β-strand to the C-terminal end of the A-loop, with the methionine side chains occupying two hydrophobic pockets on the C-terminal lobe of the kinase. The structure thus reveals the molecular basis for insulin receptor activation via autophosphorylation, and provides insights into tyrosine kinase substrate specificity and the mechanism of phosphotransfer.

Keywords: autophosphorylation/insulin receptor/protein tyrosine kinase/substrate specificity/ X-ray crystallography

Introduction

Insulin stimulates numerous intracellular signaling pathways that regulate cellular metabolism and growth (White and Kahn, 1994). The physiological effects of insulin are mediated by its cell surface receptor, an $\alpha_2\beta_2$ transmembrane glycoprotein with intrinsic protein tyrosine kinase activity (Ebina et al., 1985; Ullrich et al., 1985). Binding of insulin to the extracellular α-chains results in autophosphorylation of specific tyrosine residues in the cytoplasmic portion of the β-chains: two in the juxtamembrane region, three in the kinase (catalytic) domain, and two in the C-terminal tail (Tornqvist et al., 1987; Tavare et al., 1988; White et al., 1988; Feener et al., 1993; Kohanski, 1993). Autophosphorylation of Tyr1158, Tyr1162 and Tyr1163 in the activation loop (A-loop) of the kinase domain is critical for stimulation of kinase activity and biological function (Rosen et al., 1983; Ellis et al., 1986).

The vast majority of receptor tyrosine kinases contain between one and three tyrosine residues in the kinase A-loop, which comprises subdomains VII and VIII of the protein kinase catalytic core (Hanks et al., 1991). In addition to the insulin receptor, other receptor tyrosine kinases whose biological function has been shown to depend on tyrosine autophosphorylation in the A-loop include insulin-like growth factor 1 (IGF-1) receptor (Kato et al., 1994), fibroblast growth factor (FGF) receptor (Mohammadi et al., 1996a), hepatocyte growth factor receptor (MET) (Longati et al., 1994), nerve growth factor receptor (TRKA) (Mitra, 1991), and brain-derived neurotrophic factor receptor (TRKB) (Middlemas et al., 1994).

The crystal structure of the unphosphorylated, low activity form of the insulin receptor kinase domain (IRK) has been reported previously (Hubbard et al., 1994). This structure suggested an autoinhibitory mechanism whereby Tyr1162 in the A-loop competes with protein substrates for binding in the active site, while residues in the beginning of the A-loop restrict access to ATP such that cis-autophosphorylation of Tyr1162 is prevented. Here, the crystal structure at 1.9 Å resolution of the tris-phosphorylated, activated form of IRK (IRK3P) in complex with a peptide substrate and an ATP analog is presented. The conformational changes that occur upon autophosphorylation provide an understanding at the molecular level of the role of autophosphorylation in the activation of the insulin receptor and presumably other receptor tyrosine kinases. Moreover, the structure reveals the mode of peptide substrate binding to the insulin receptor kinase, and affords insights into the phosphotransfer mechanism.

Results and discussion

Structure determination

A 306-residue fragment of the β-chain of the human insulin receptor which possesses tyrosine kinase activity was produced in a baculovirus/insect cell expression system (Wei et al., 1995). Cytoplasmic residues that are not included in the expressed protein are the first 25 (juxtamembrane region) and the last 72 (C-terminal tail). Addition of MgATP to the purified kinase results in autophosphorylation of Tyr1158, Tyr1162 and Tyr1163 as confirmed by mass spectrometry and microsequencing of tryptic peptides (Wei et al., 1995). Crystals belonging to trigonal space group $P3_221$ were obtained from a ternary complex consisting of IRK3P, an 18-residue peptide substrate and a non-hydrolyzable ATP analog, adenylyl imidodiphosphate (AMP-PNP).

The structure of the ternary complex was solved by molecular replacement using the structure of IRK as a search model, and has been refined at 1.9 Å resolution with a crystallographic R-value of 19.6% (6.0–1.9 Å, $F>2\sigma$). The atomic model includes all but the three N-terminal residues of IRK3P, one AMP-PNP molecule,
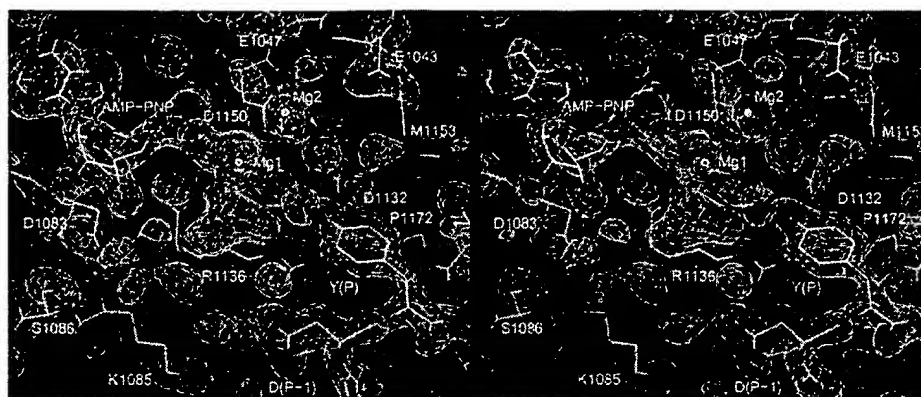
Fig. 1. Electron density map of the active site of IRK3P. Stereo view of a $2F_o-F_c$ map computed at 1.9 Å resolution and contoured at 1.2σ. Superimposed is the refined atomic model. Carbon atoms are yellow, oxygen atoms red, nitrogen atoms blue, phosphate atoms purple, and sulfur atoms green. The red spheres represent water molecules and the white spheres represent Mg^{2+} ions. Figure prepared with SETOR (Evans, 1993).

Table I. Data collection and refinement summary

Data collection					
Resolution (Å)	Observations (N)	Completeness (%)	Redundancy (%)	R_{sym} (%)[a]	Signal $\langle I/\sigma(I)\rangle$
20.0–1.9	93535	98.6 (90.6)[b]	4.1	6.5 (15.3)[b]	12.9

Refinement[c]					
Resolution (Å)	Reflections (N)	R-value (%)[d]	Root-mean-square deviations		
			Bonds (Å)	Angles (°)	B-factors ($Å^2$)[e]
6.0–1.9	25082	19.4 (22.6)[f]	0.008	1.5	1.4

[a]$R_{sym} = 100 \times \Sigma_{hkl}\Sigma_i \mid I_i(hkl)-\langle I(hkl)\rangle \mid /\Sigma_{hkl}\Sigma_i I_i(hkl)$.
[b]Value in parentheses is for the highest resolution shell.
[c]Atomic model includes 303 IRK3P residues, six peptide residues, one AMP-PNP molecule, two Mg^{2+} ions, 202 water molecules (2653 atoms).
[d]R-value = $100 \times \Sigma_{hkl} \mid F_o(hkl)\mid -\mid F_c(hkl)\mid /\Sigma_{hkl}\mid F_o(hkl)\mid$, where F_o and F_c are the observed and calculated structure factors, respectively ($F_o >2\sigma$).
[e]For bonded protein atoms.
[f]Value in parentheses is the free R-value determined from 5% of the data.

two Mg^{2+} ions, six residues of the peptide substrate and 202 water molecules. An electron density map in the vicinity of the active site is shown in Figure 1, data collection and refinement statistics are given in Table I, and a ribbon diagram of ternary IRK3P is shown in Figure 2A.

Activation loop conformation

In the unliganded IRK structure determined previously (Hubbard et al., 1994), the A-loop (residues 1149–1170) traverses the cleft between the N- and C-terminal lobes such that both protein substrate and ATP binding sites are occupied. Tyr1162 in the A-loop is bound in the active site, hydrogen-bonded to the putative catalytic base (Asp1132), and residues of the protein kinase-conserved [1150]DFG sequence in the beginning of the A-loop occupy the ATP binding site. Autophosphorylation of Tyr1158, Tyr1162 and Tyr1163 results in a dramatic change in the conformation of the A-loop (Figures 2B and 4A). Tyr1158, for example, is displaced ~30 Å from its position in the unphosphorylated A-loop. The conformation of the tris-phosphorylated A-loop permits unrestricted access to the binding sites for ATP and protein substrates.

The tris-phosphorylated A-loop is stabilized to various extents by the phosphotyrosine (pTyr) residues (Figure 4B). The phosphate group of pTyr1163 bridges the A-loop via hydrogen bonds to the side chain of Arg1155 on one side of the loop and to the backbone amide nitrogen of Gly1166 on the other side. In addition to the electrostatic interaction with Arg1155, the phenolic ring of pTyr1163 is packed against the aliphatic portion of the Arg1155 side chain. Arg1155 is also hydrogen-bonded to the carbonyl oxygen of the preceding residue. Arginine or lysine is highly conserved in the tyrosine kinase family at this position. The phosphate group of pTyr1162 makes two hydrogen bonds to the side chain of Arg1164. For receptor tyrosine kinases with tandem tyrosine residues corresponding to Tyr1162 and Tyr1163 (e.g. TRK, FGF receptor), an arginine or lysine is often found at the Arg1164 position. The phosphate group of pTyr1158 makes no protein contacts and consequently is the least ordered of the three phosphate groups.

Two short β-strand interactions also serve to stabilize the tris-phosphorylated A-loop. β9 in the A-loop is paired with β6, which precedes the catalytic loop (residues 1130–1137), and β10 in the A-loop is paired with β12 between αEF and αF (Figures 2A and 3). This pairing scheme leaves β11, which in IRK was paired with β10, available
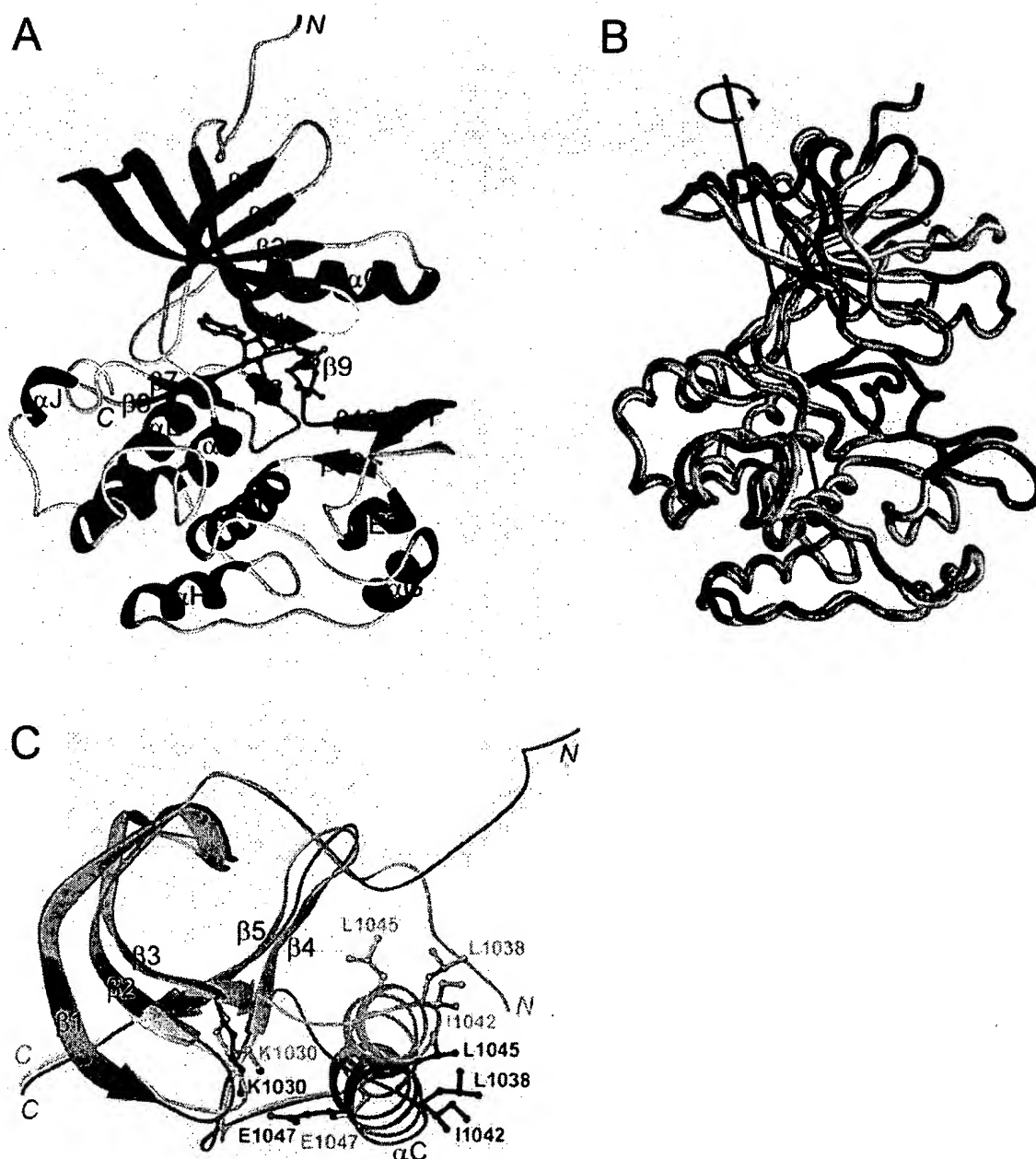
Fig. 2. Overall view of IRK3P and comparison with IRK. (A) Ribbon diagram of the IRK3P structure. The α-helices are shown in red, the β-strands in blue, the nucleotide-binding loop in yellow, the catalytic loop in orange, the activation loop in green, AMP-PNP in black and the peptide substrate in pink. The termini are denoted by N and C. (B) Superposition of the C-terminal lobes of IRK and IRK3P. The backbone representation of IRK/ IRK3P is colored orange/green, with the activation loop colored red/blue. The axis (black) and arrow (blue) specify the rotation required to align the N-terminal β-sheet of IRK with that of IRK3P. (C) Superposition of the β-sheets in the N-terminal lobes of IRK and IRK3P. The backbone representation and carbon atoms of IRK/IRK3P are colored orange/green, oxygen atoms are red and nitrogen atoms are blue. (A) and (C) prepared with RIBBONS (Carson, 1991), (B) with GRASP (Nicholls et al., 1991).

for interaction with a protein substrate. Compared with the unphosphorylated A-loop, which was poorly ordered for residues 1152–1157, the tris-phosphorylated A-loop is relatively well ordered.

The conformation of the tris-phosphorylated A-loop is in general similar to that of the mono-phosphorylated A-loop of cyclic AMP-dependent protein kinase (cAPK) (Knighton et al., 1991), cyclin-dependent kinase 2 (CDK2) (Russo et al., 1996) and the Src-family tyrosine kinase

LCK (Yamaguchi and Hendrickson, 1996). A comparison with these kinase structures reveals that pTyr1163 in the IRK A-loop is structurally related to phosphothreonine (pThr)197 in cAPK, pThr160 in CDK2 and pTyr394 in LCK (Figure 4B–D).

Although pTyr1163 is in a spatial position similar to pThr197/pThr160 in cAPK/CDK2, the number of hydrogen-bonding interactions in which pTyr1163 participates is far fewer than for the pThr residues (Figure 4B
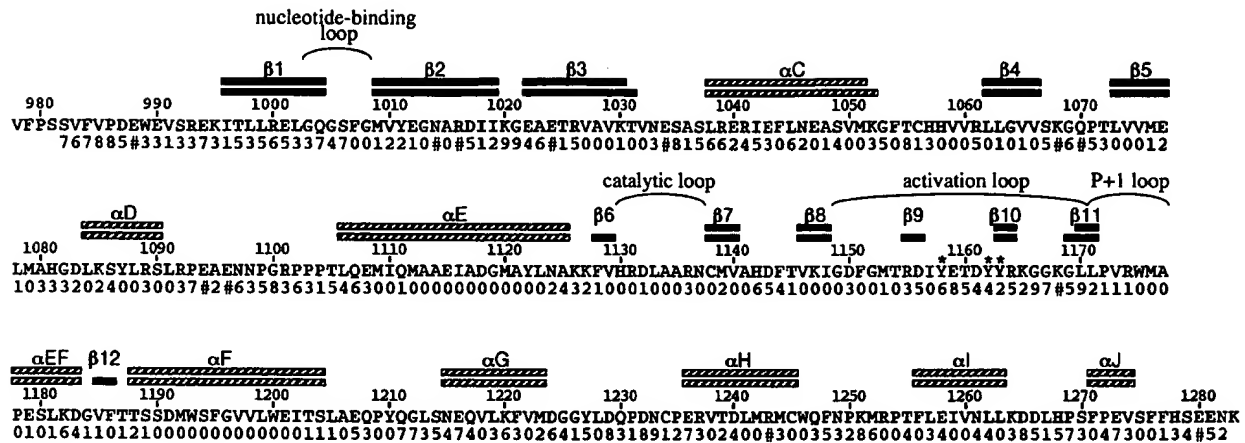
nucleotide-binding loop

β1   β2   β3   αC   β4   β5

980   990   1000   1010   1020   1030   1040   1050   1060   1070

VFPSSVFVPDEWEVSREKITLLRELGQGSFGMVYEGNARDIIKGEAETRVAVKTVNESASLRERIEFLNEASVMKGFTCHHVVRLLGVVSKGQPTLVVME
767885#331337315335653374700122I0#0#5129946#150001003#81566245306201400350813000501010S#6#5300012

catalytic loop   activation loop   P+1 loop

αD   αE   β6   β7   β8   β9   β10   β11

1080   1090   1100   1110   1120   1130   1140   1150   1160   1170

LMAHGDLKSYLRSLRPEAENNPGRPPPTLQEMIQMAAEIADGMAYLNAKKFVHRDLAARNCMVAHDFTVKIGDFGMTRDIYETDYYRKGGKGLLPVRWMA
1033320240030037#2#6358363154630010000000000000024321000100030020065410000300103506854425297#592111000

αEF β12   αF   αG   αH   αI   αJ

1180   1190   1200   1210   1220   1230   1240   1250   1260   1270   1280

PESLKDGVFTTSSDMWSFGVVLWEITSLAEQPYQGLSNEQVLKFVMDGGYLDQPDNCPERVTDLMRMCWQFNPKMRPTFLEIVNLLKDDLHPSFPEVSFFHSEENK
0101641101210000000000000001110530077354740363026415083189127302400#30035328600403400440385157304730013S#52

Fig. 3. Secondary structure comparison of IRK and IRK3P and residue solvent accessibility. The secondary structure assignments for IRK and IRK3P were obtained using PROCHECK (Laskowski et al., 1993). Striped bars delineate α-helices and black bars delineate β-strands. The assignments for IRK appear on top and those for IRK3P on bottom. The three autophosphorylation sites in the activation loop are marked with an asterisk. The numbers under the amino acid sequence represent the fractional solvent accessibility (FSA) of the residue in the IRK3P structure. The FSA is the ratio of the solvent-accessible surface area of a residue in a GXG tri-peptide to that in the IRK3P structure. A value of 0 represents an FSA between 0.00 and 0.09, 1 represents an FSA between 0.10 and 0.19, etc. The higher the FSA, the more solvent-exposed the residue. The FSAs were computed in the absence of MgAMP-PNP, peptide substrate and water molecules. A # in the FSA line indicates that the side chain for that residue is not included in the atomic model due to disorder.

and C). Arg1131, the residue which immediately precedes the putative catalytic base, Asp1132, is highly conserved in both the tyrosine and serine/threonine kinase families. In the cAPK and CDK2 structures (Knighton et al., 1991; Russo et al., 1996), the corresponding arginine is directly hydrogen-bonded to the pThr. Arg1131, however, is not observed to interact directly with pTyr1163. In the LCK structure, pTyr394 is also engaged in relatively few interactions, differing somewhat from those seen for pTyr1163 (Figure 4D), which suggests a susceptibility of these pTyr residues to the action of tyrosine phosphatases (Yamaguchi and Hendrickson, 1996).

A comparison of the phosphorylated A-loops of IRK3P and LCK (one residue shorter) shows that the conformation is similar at the beginning of the loop, which includes the conserved [1150]DFG residues ([382]DFG), but diverges after pTyr1163 (pTyr394) (Figure 4B and D). Residues at the end of the LCK A-loop, including kinase-conserved Pro403 (Pro1172), are displaced further from the active site than the corresponding residues in IRK3P. Interestingly, based on the mode of peptide substrate binding observed in the present structure (discussed below), the C-terminal end of the A-loop in the unliganded LCK structure is not properly positioned for peptide binding.

Lobe closure

The rearrangement of the insulin receptor A-loop upon autophosphorylation facilitates a reorientation of the N- and C-terminal lobes of the kinase, which is necessary for productive ATP binding. In the structure of the unphosphorylated kinase domain of the FGF receptor, the ATP binding site is accessible, yet full engagement of ATP by the kinase does not occur due to interactions that impede lobe rotation (Mohammadi et al., 1996b). In the IRK structure, the lobes are held apart by steric interactions between residues of the nucleotide-binding loop (1003–1008) and the [1150]DFG residues. When the C-terminal lobes of IRK and ternary IRK3P are superimposed, a nearly pure rotation of the N-terminal lobe of IRK by

~21° aligns the five-stranded β-sheets (Figure 2B). The direction of the rotation is both towards the C-terminal lobe and parallel to the long axis of the molecule. Three pivot points in the rotation can be identified: two in the loop between αC and β4 (near Phe1054 and Arg1061) and one near the last residue of β5 (Glu1077), just before the segment connecting the two lobes (between β5 and αD). The protein kinase-conserved glycine in the connecting segment, Gly1082, does not appear to play a role in facilitating lobe movement.

With respect to cAPK, the only other protein kinase for which structures of a ternary complex (with nucleotide and peptide) have been reported (Bossemeyer et al., 1993; Zheng et al., 1993), the lobes of IRK3P are rotated by ~17°. Despite this difference, the actual lobe separation in the IRK3P and cAPK structures is similar as measured by the Cα–Cα distance between Val1010 (Val57) and Met1139 (Leu173), which flank the ATP adenine. This distance is 12.8 Å in ternary IRK3P (15.0 Å in IRK) and 12.9 Å in ternary cAPK. The lobe configuration in unliganded LCK (Yamaguchi and Hendrickson, 1996) is ~8° more open than that in ternary IRK3P, with a corresponding lobe–lobe separation of 13.9 Å.

Upon lobe closure, the β-sheet in the N-terminal lobe of IRK3P moves approximately as a rigid body. However, αC rotates an additional ~35° towards the C-terminal lobe (Figure 2C). This movement of αC places protein kinase-conserved Glu1047 in proximity (4.4 Å) to conserved Lys1030 in the ATP binding site. Three hydrophobic residues which lie along the same face of αC, Leu1038, Ile1042 and Leu1045, are solvent-exposed in the IRK3P structure, whereas the latter two residues are partially buried in the IRK structure (Figure 2C). These hydrophobic residues, which are not conserved in the tyrosine kinase family, are perhaps involved in protein–protein interactions specific to insulin receptor subfamily members.

MgAMP-PNP binding

The entire AMP-PNP molecule is well ordered in the ternary IRK3P structure (Figure 1), indicative of a pro-

S.R.Hubbard
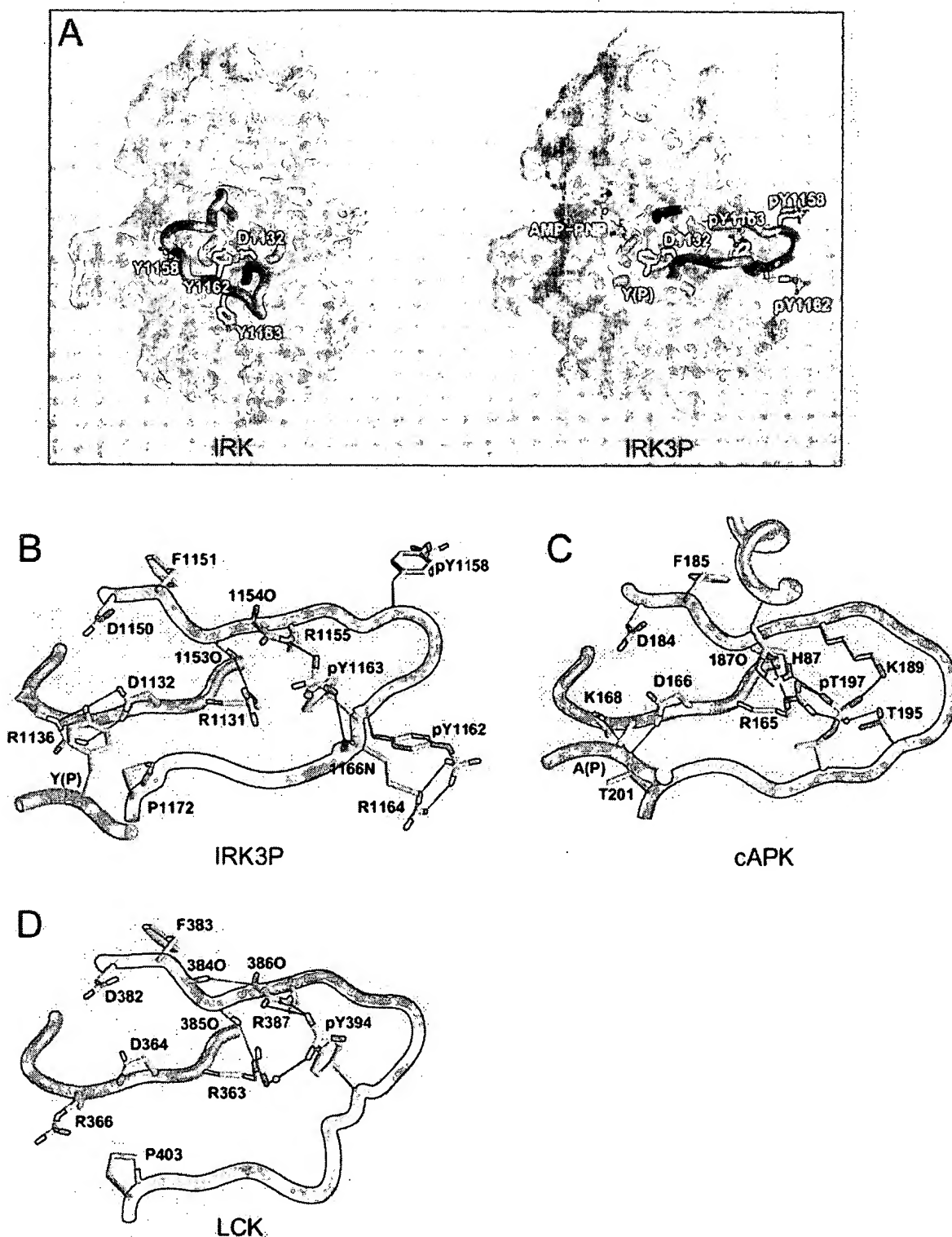
Fig. 4. Conformation of the IRK3P A-loop and comparison with other kinase A-loops. (**A**) Comparison of the A-loop conformations in IRK and IRK3P. The activation loop is colored green, the catalytic loop orange and the peptide substrate pink. The rest of the protein in each case is represented by a semi-transparent molecular surface. Also shown is AMP-PNP, which is partially masked by the N-terminal lobe of IRK3P. Carbon atoms are colored white, nitrogen atoms blue, oxygen atoms red and phosphorus atoms yellow. View is ~90° from that in Figure 2A, from the right side. (**B**) Selected hydrogen-bonding interactions for activation loop residues of IRK3P are shown as black lines. Atom coloring is the same as in (A) except that carbon atoms are gray. Coloring of the backbone representation is the same as in (A). Only a portion of the peptide substrate backbone is shown (P–1 to P+1). (**C**) Selected hydrogen-bonding interactions for activation loop residues of cAPK (Zheng *et al.*, 1993) are shown as black lines. Coloring same as in (B), with other backbone segments colored blue. Only a portion of the peptide inhibitor backbone is shown (P–1 to P+1). (**D**) Selected hydrogen-bonding interactions for activation loop residues of LCK (Yamaguchi and Hendrickson, 1996) are shown as black lines. Coloring same as in (B). Figure prepared with GRASP (Nicholls *et al.*, 1991).
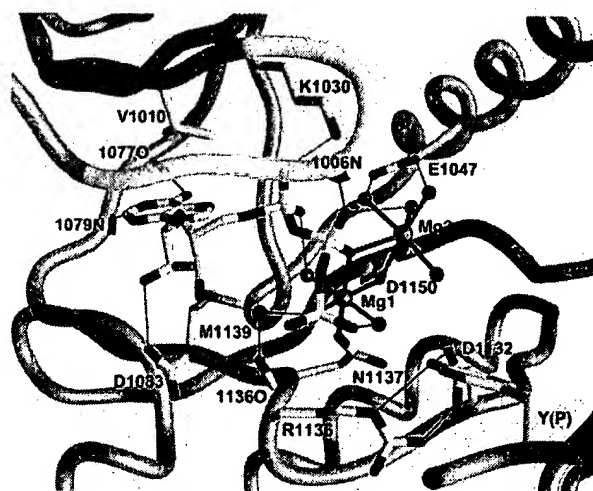
Fig. 5. Interactions of MgAMP-PNP in the ternary IRK3P structure. The coloring of the backbone representation is the same as in Figure 4B, with the nucleotide-binding loop colored yellow. Atom coloring is the same as in Figure 4B, with sulfur atoms colored green and Mg^{2+} ions colored purple. Selected hydrogen bonds are shown as thin black lines and bonds to Mg^{2+} ions are shown as thick black lines. Figure prepared with GRASP (Nicholls *et al.*, 1991).

ductive binding mode. The interactions of AMP-PNP with IRK3P are illustrated in Figure 5. The adenine is situated between Val1010 and Met1139, and hydrogen-bonded to backbone groups of Glu1077 and Met1079. One of the ribose hydroxyl groups (O2′) is hydrogen-bonded to the side chain of Asp1083, and the other (O3′) is hydrogen-bonded via a water molecule to the carbonyl oxygen of Arg1136 in the catalytic loop. The analogous interactions for the adenine and ribose are observed in the ternary cAPK structure (Bossemeyer *et al.*, 1993; Zheng *et al.*, 1993), except that O3′ is hydrogen-bonded directly to the carbonyl oxygen of Glu170 (Arg1136).

The interactions of the nucleotide phosphate groups with IRK3P residues differ from those observed in the ternary cAPK structure. In cAPK, the nucleotide-binding loop is hydrogen-bonded via three backbone groups to the β- and γ-phosphates of ATP (Bossemeyer *et al.*, 1993; Zheng *et al.*, 1993). In IRK3P, only one hydrogen bond is observed, between the backbone amide nitrogen of Ser1006 and the β-phosphate (Figure 5). Moreover, in cAPK, protein kinase-conserved Lys72 is hydrogen-bonded to the α- and β-phosphates, whereas in IRK3P, Lys1030 is hydrogen-bonded to just the α-phosphate.

The greater extension of the nucleotide-binding loop over the phosphates in ternary cAPK is probably due to hydrogen-bonding between the loop and the peptide inhibitor PKI (Bossemeyer *et al.*, 1993). In the ternary IRK3P structure, no interactions are observed between the nucleotide-binding loop and the peptide substrate. Owing to the longer side chain of tyrosine versus serine/threonine, the peptide substrate is positioned significantly further away from the N-terminal lobe in IRK3P than in cAPK (Figure 4B and C). It is likely, therefore, that the lack of interaction with the nucleotide-binding loop is a general feature of protein substrate–tyrosine kinase interactions.

Two well-ordered Mg^{2+} ions have been included in the

atomic model based on the heights of the electron density peaks and the number and distances of coordinating atoms (Figures 1 and 5). Mg1 shows nearly ideal octahedral coordination by six oxygen atoms (Mg⋯O = 2.0–2.2 Å): one from each of the β- and γ-phosphates, one from each of the side chains of protein kinase-conserved Asn1137 (catalytic loop) and Asp1150 (A-loop), and two from well-ordered water molecules (Figure 5). Mg2 has seven oxygen ligands (Mg⋯O = 2.4–2.6 Å): the same β-phosphate oxygen that coordinates Mg1, both carboxylate oxygens of Asp1150, and four water molecules. Mg1 and Mg2 are in positions similar to those of the inhibitory and activating metal ions, respectively, in ternary cAPK (Bossemeyer *et al.*, 1993; Zheng *et al.*, 1993), but the coordination by the phosphate groups differs. Mg1 is coordinated by the β- and γ-phosphates, whereas the inhibitory metal ion in ternary cAPK is coordinated by the α- and γ-phosphates. Mg2 is coordinated by just the β-phosphate, whereas the activating metal ion in ternary cAPK is coordinated by the β- and γ-phosphates. The coordination environment of Mg1 is strikingly similar to that of the Mg^{2+} ion in the structures of GTPases such as Ras (with MgGMP-PNP; Pai *et al.*, 1990) and transducin-α (with MgGTPγS; Noel *et al.*, 1993), wherein the Mg^{2+} ion is octahedrally coordinated by the β- and γ-phosphates, two side-chain oxygens, and two water molecules, in the same spatial configuration as found in the ternary IRK3P structure.

Peptide substrate binding

The 18-residue peptide substrate that was co-crystallized with IRK3P and MgAMP-PNP was derived from a putative insulin receptor phosphorylation site on rat IRS-1, Tyr727 (Sun *et al.*, 1991). This peptide, KKKLPATGDYMN-MSPVGD, has a reported K_m of 24 μM (Shoelson *et al.*, 1992). Of the 18 residues, supporting electron density is seen for only six, from the P–2 to the P+3 residue [GDYMNM; P-residue is the acceptor tyrosine, Tyr(P)]. The residues C-terminal to Tyr(P) form a short β-strand which pairs in an anti-parallel manner with residues of β11 at the end of the A-loop (Figures 2A and 6B). Backbone hydrogen-bonding is observed between Met(P+1) and Leu1171, and between Met(P+3) and Gly1169.

Tyrosine residues in YMXM motifs are efficient substrates of the insulin receptor *in vitro* and *in vivo* (Shoelson *et al.*, 1992; Sun *et al.*, 1993; Songyang *et al.*, 1995). In the ternary IRK3P structure, the methionine side chains of the peptide fit into two adjacent hydrophobic pockets on the surface of the C-terminal lobe, composed of residues from the P+1 loop (1171–1176) and from αEF and αG (Figure 6). The pocket for Met(P+1) comprises Val1173, Leu1219 and the aliphatic portions of the Asn1215 and Glu1216 side chains. The pocket for Met(P+3) comprises Leu1171, Val1173, Met1176, Leu1181 and Leu1219. These pockets appear to be optimized for accommodating long hydrophobic side chains.

The ternary IRK3P structure provides a basis for understanding tyrosine kinase substrate specificity. In a study of substrate specificity using a degenerate peptide library, the cytoplasmic tyrosine kinase Fps was shown to have a strong preference for glutamic acid at the P+1 position of a peptide substrate (Songyang *et al.*, 1995). Of the four insulin receptor residues that form the binding pocket for
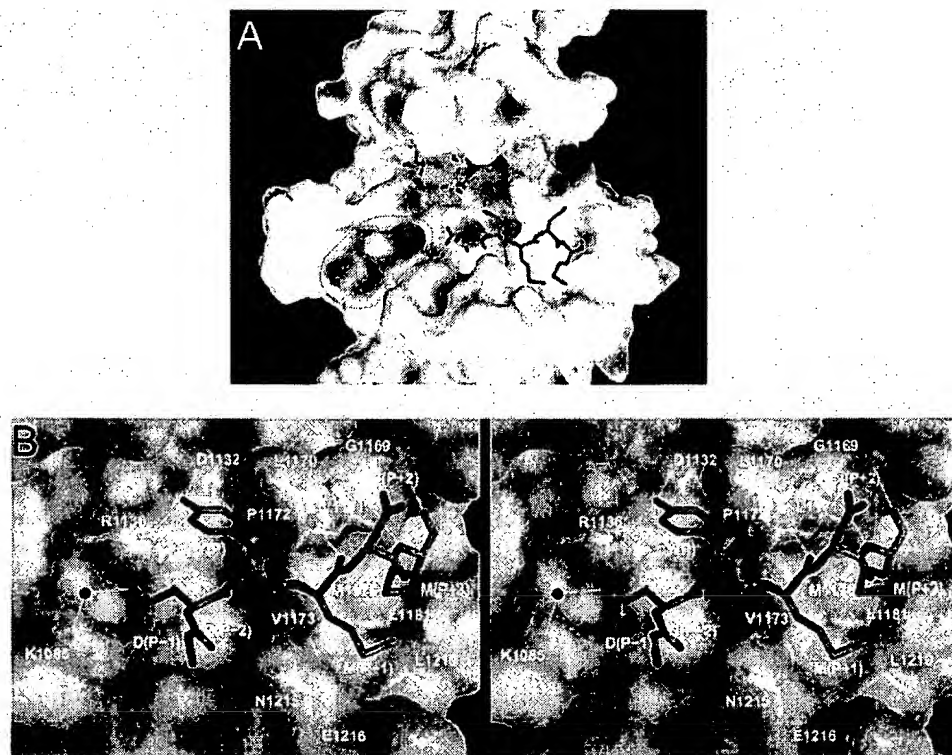
Fig. 6. Mode of peptide substrate binding. (A) Overall view of peptide substrate binding to IRK3P. The molecular surface of IRK3P is colored according to electrostatic potential (calculated in the absence of MgAMP-PNP and peptide). Positive potential is shown in blue, negative potential in red and neutral potential in white. Carbon atoms are green, oxygen atoms are red, nitrogen atoms are blue, sulfur atoms are black and phosphorus atoms are yellow. The dotted line encompasses Lys1085, Arg1089 and Arg1092 of αD. View is approximately the same as in Figure 4A. (B) Stereo view of the interactions between the peptide substrate and IRK3P. Oxygen atoms are red, nitrogen atoms are blue, carbon atoms of IRK3P/peptide are orange/green and sulfur atoms of IRK3P/peptide are green/black. The molecular surface is semi-transparent, and selected hydrogen bonds are shown as white lines. The red sphere represents a water molecule. Figure prepared with GRASP (Nicholls *et al.*, 1991).

Met(P+1), three are identical or similar in Fps, while the fourth, Leu1219, is an arginine in Fps (Arg770). Modeling suggests that an arginine at the Leu1219 position could make a hydrogen bond with a glutamic acid at the P+1 position of a peptide substrate. In the receptor tyrosine kinase RET, the substitution Met918→Thr leads to multiple endocrine neoplasia type 2B (Hofstra *et al.*, 1994), and is thought to alter the substrate specificity of RET (Songyang *et al.*, 1995; Pandit *et al.*, 1996). The corresponding methionine in the insulin receptor, Met1176, is a constituent of the Met(P+3) binding pocket.

Substrates of the insulin receptor and other tyrosine kinases often contain one or more acidic residues N-terminal to the acceptor tyrosine (Hunter, 1982; Stadtmauer and Rosen, 1983; Songyang *et al.*, 1995). The co-crystallized peptide contains an aspartic acid at the P–1 position. In the crystal structure, Asp(P–1) is not directly hydrogen-bonded to residues of the kinase, but instead makes a water-mediated hydrogen bond to Lys1085 (Figure 6B). Two other positively charged residues, Arg1089 and Arg1092, extend from the same face of αD as Lys1085 towards the substrate binding region (Figure 6A). At the position corresponding to Arg1089, a large majority of tyrosine kinases contain a hydrogen-bond donor which is often positively charged. This residue may play a role in the recognition of protein substrates with acidic residues at the P–3 or P–4 position.

Active site

The hydroxyl group of the substrate tyrosine, Tyr(P), is hydrogen-bonded to the carboxylate group of Asp1132 (Oη···Oδ2 = 2.7 Å), and thus appears to be in position for proton abstraction by Asp1132 (Figures 4B and 5). The hydroxyl group is also hydrogen-bonded to tyrosine kinase-conserved Arg1136 in the catalytic loop (Oη···Nε = 3.1 Å). The phenolic ring of Tyr(P) is oriented in part by van der Waals interactions with tyrosine kinase-conserved Pro1172 (P+1 loop), positioned 3.6 Å from the ring (Figures 4B and 6B).

Based on the autoinhibited IRK structure, a difference in the conformation of the P+1 loop near Pro1172 appeared to be a major determinant in conferring specificity for tyrosine versus serine/threonine (Hubbard *et al.*, 1994; Taylor *et al.*, 1995). This is confirmed by the ternary IRK3P structure, in which backbone hydrogen-bonding between the peptide substrate and the P+1 loop of the kinase governs the distance between the peptide backbone and the kinase active site (Figure 6B); the side chain of tyrosine but not of serine/threonine is long enough to reach the active site.

In the ternary IRK3P structure, the γ-phosphorus atom of AMP-PNP is 5.0 Å from the hydroxyl oxygen of Tyr(P) (Figure 5), and is therefore not in position for direct in-line (associative) phosphotransfer, the catalytic mechanism proposed for cAPK (Madhusudan *et al.*, 1994). The use

of AMP-PNP in co-crystallizations (to preclude substrate phosphorylation) could introduce a deviation in γ-phosphate positioning, although no significant differences in nucleotide binding are seen in the structures of cAPK with ATP (Zheng et al., 1993) or with AMP-PNP (Bossemeyer et al., 1993). The present structure is the first to be reported of a complex between a protein kinase, a peptide substrate, and a γ-phosphate-containing nucleotide. Trapping the enzyme with both the non-transferable γ-phosphate and acceptor hydroxyl in position for associative phosphotransfer may be inherently difficult. Alternatively, in view of the difference in the pKa values of tyrosine (~10) and serine/threonine (~13), and the presence in the catalytic loop of an arginine (tyrosine kinases) rather than a lysine (serine/threonine kinases), the structure may suggest a dissociative or mixed associative–dissociative phosphotransfer mechanism (Bramson et al., 1984) for tyrosine kinases.

Functional implications

The crystal structures of IRK and IRK3P afford an understanding at the molecular level of insulin receptor activation via autophosphorylation. The IRK structure, together with mutagenesis data showing that substitution of Tyr1162 with phenylalanine increases basal level kinase activity (Ellis et al., 1986), suggests that residues of the unphosphorylated A-loop compete with ATP and protein substrates for binding at the kinase active site. Upon insulin-triggered trans-autophosphorylation of the tyrosine residues within the A-loop, this peptide segment adopts a markedly different conformation which is stabilized by both pTyr and non-pTyr interactions. For the insulin receptor and presumably other receptor tyrosine kinases, stimulation of kinase activity by autophosphorylation is evidently a consequence of stabilization of an A-loop conformation that (i) allows unhindered access to ATP and protein substrates, and (ii) facilitates the correct positioning of the residues critical for MgATP binding and catalysis.

The bridging interactions of pTyr1163 with other A-loop residues and its similar spatial position to pThr197 in cAPK imply that pTyr1163 is the key pTyr in stabilizing the conformation of the tris-phosphorylated A-loop. Although studies of Tyr→Phe substitutions in the insulin receptor A-loop have not demonstrated a predominant role in kinase activation for a particular tyrosine (Tavare and Siddle, 1993), the tyrosine corresponding to Tyr1163 has been shown to be the critical autophosphorylation site in the FGF receptor (Mohammadi et al., 1996a) and in MET (Longati et al., 1994).

Autophosphorylation mapping experiments have indicated that Tyr1163 is the last of the three A-loop sites to be phosphorylated (Dickens and Tavare, 1992; Wei et al., 1995). This result, together with the mutagenesis data and the structural results presented here, is consistent with a graded activation mechanism in which each autophosphorylation event in the A-loop leads to partial stabilization of the active configuration of the A-loop, with full activation achieved only upon autophosphorylation of pTyr1163. Conceivably, in partially activated (mono- and bis-phosphorylated) states, pTyr1158 and pTyr1162 are engaged in a different set of interactions than those observed in the IRK3P structure. For example, pTyr1162 may substitute

structurally for pTyr1163 in the bis-phosphorylated state, though presumably less effectively.

The lack of engagement of pTyr1158 with other kinase residues and the solvent accessibility of the pTyr1162/ Arg1164 pair suggests that these pTyr residues could potentially serve as docking sites for downstream signaling proteins. Several recent studies have provided evidence that one or more of the A-loop pTyr residues are involved in protein–protein interactions. Yeast two-hybrid experiments have identified an interaction between a region in IRS-2 and the cytoplasmic domain of the insulin receptor, which is dependent on tyrosine phosphorylation in the A-loop but not in the juxtamembrane region or C-terminal tail (He et al., 1996; Sawka-Verhelle et al., 1996). Other yeast two-hybrid experiments together with in vitro binding studies have provided evidence for interactions between the cytoplasmic domain and the Src-homology 2 (SH2) domains of GRB10/IR-SV1 (O'Neill et al., 1996; Frantz et al., 1997) and SHP-2 (Kharitonenkov et al., 1995), which are dependent on phosphorylation of one or more of the A-loop tyrosine residues. The IRK3P structure provides evidence, albeit circumstantial, that one or more pTyr residues of the insulin receptor A-loop may serve as targets for downstream signaling molecules.

Materials and methods

Expression, purification and crystallization of IRK3P

A recombinant baculovirus was engineered to encode residues 978–1283 of the human insulin receptor with the inclusion of two amino acid substitutions: Cys981→Ala and Tyr984→Phe (Wei et al., 1995). Expression and purification of IRK have been described previously (Hubbard et al., 1994). Typically, IRK3P was produced by adding ATP and $MgCl_2$ (10 mM and 25 mM final, respectively) to IRK (~1 mg/ml final) at 4°C. After 20–30 min, the autophosphorylation reaction was terminated by the addition of EDTA (50 mM final). The reaction mixture was passed over a Superdex 75 (Pharmacia) gel filtration column to remove nucleotides, Mg^{2+} and EDTA. The mainly tris-phosphorylated kinase species was separated from the bis-phosphorylated species by Mono Q (Pharmacia) ion exchange chromatography. Purified IRK3P was concentrated to 10–15 mg/ml using a Centricon-10 (Amicon) in 20 mM Tris–HCl, pH 7.5, 200 mM NaCl and 200 μM Na_3VO_4. Solid-phase synthesis of the 18-residue peptide substrate was performed on an Applied Biosystems model 741A synthesizer using Fmoc chemistry, and AMP-PNP was purchased from Boehringer-Mannheim.

Crystals were grown at 4°C by vapor diffusion in hanging drops containing 2.0 μl of protein solution (10 mg/ml IRK3P, 2 mM AMP-PNP, 6 mM $MgCl_2$ and 0.5 mM peptide substrate) and 2.0 μl of reservoir solution [22% polyethylene glycol (PEG) 8000, 100 mM Tris–HCl, pH 7.5, and 2% ethylene glycol]. The crystals belong to trigonal space group $P3_221$ and have unit cell dimensions of $a = b = 66.5$ Å, $c = 139.1$ Å when frozen. There is one molecule in the asymmetric unit and the solvent content is 50% (assuming a partial specific volume of 0.74 cm^3/g).

Data collection, structure determination and analysis

One cryo-cooled crystal was used for data collection. The crystal was transferred into a cryo-protectant containing 25% PEG 8000, 1 mM AMP-PNP, 3 mM $MgCl_2$, 0.25 mM peptide substrate, 100 mM Tris–HCl, pH 7.5 and 15% ethylene glycol. After ~1 min in the cryo-protectant, the crystal was flash-cooled in liquid nitrogen and then transferred to the goniostat, which was bathed in a dry nitrogen stream at –160°C. Data were collected at beamline X4A at the National Synchrotron Light Source, Brookhaven National Laboratory, on Fuji image plates and digitized with a Fuji scanner. All data were processed using DENZO and SCALEPACK (Otwinowski, 1993).

A molecular replacement solution was found with a search molecule consisting of IRK residues 981–1283, excluding 1149–1170 (A-loop), for which the N-terminal lobe (residues 981–1081) was rotated and translated as a rigid body so that the relative orientation of the N- and

C-terminal lobes was similar to that in closed-form cAPK (Zheng *et al.*, 1993). An initial 3.0 Å data set collected on a Rigaku R-AXIS IIC image plate detector was used for molecular replacement (data not shown). With AMoRe (Navaza, 1994), using 80% of the structure factor amplitudes between 15.0 and 3.5 Å, the correlation coefficient for the correct solution in space group $P3_221$ was 0.46 versus 0.34 for the highest incorrect solution in the enantiomeric space group $P3_121$. The AMoRe solution was refined in X-PLOR (Brünger, 1992), first as one rigid-body unit, then as two units each comprising a lobe of the kinase (981–1081, 1082–1283), resulting in a relative rotation of the two lobes of ~13° and an increase of the correlation coefficient from 0.33 to 0.41 (10.0–3.4 Å, F>2σ). Simulated annealing and conjugate-gradient minimization were performed using X-PLOR, and model building was performed using TOM/FRODO (Jones, 1985).

The average atomic B-factors are 18.5 Å² for protein, 15.8 Å² for MgAMP-PNP, 21.9 Å² for peptide and 25.3 Å² for water molecules. Due to poor supporting electron density, residues 978–980 are not included in the atomic model, nor are the side chains indicated in Figure 3. Atomic superpositions were performed with TOSS (Hendrickson, 1979). Per residue solvent accessible surface calculations were done with X-PLOR with a probe radius of 1.4 Å. As defined in PROCHECK (Laskowski *et al.*, 1993), the backbone torsion angles of the protein lie either in most favored regions (93%) or in additional allowed regions (7%).

Acknowledgements

References

Bossemeyer,D., Engh,R.A., Kinzel,V., Ponstingl,H. and Huber,R. (1993) Phosphotransferase and substrate binding mechanism of the cAMP-dependent protein kinase catalytic subunit from porcine heart as deduced from the 2.0 Å structure of the complex with Mn²⁺ adenylyl imidodiphosphate and inhibitor peptide PKI(5–24). *EMBO J.*, **12**, 849–859.

Bramson,H.N., Kaiser,E.T. and Mildvan,A.S. (1984) Mechanistic studies of cAMP-dependent protein kinase action. *CRC Crit. Rev. Biochem.*, **15**, 93–123.

Brünger,A.T. (1992) X-PLOR (Version 3.1) Manual (New Haven, CT: The Howard Hughes Medical Institute and Department of Molecular Biophysics and Biochemistry, Yale University).

Carson,M. (1991) Ribbons 2.0. *J. Appl. Crystallogr.*, **24**, 958–961.

Dickens,M. and Tavare,J.M. (1992) Analysis of the order of autophosphorylation of human insulin receptor tyrosines 1158, 1162 and 1163. *Biochem. Biophys. Res. Commun.*, **186**, 244–250.

Ebina,Y. *et al.* (1985) The human insulin receptor cDNA: the structural basis for hormone-activated transmembrane signalling. *Cell*, **40**, 747–758.

Ellis,L., Clauser,E., Morgan,D.O., Edery,M., Roth,R.A. and Rutter,W.J. (1986) Replacement of insulin receptor tyrosine residues 1162 and 1163 compromises insulin-stimulated kinase activity and uptake of 2-deoxyglucose. *Cell*, **45**, 721–732.

Evans,S.V. (1993) SETOR: hardware lighted three-dimensional solid model representations of macromolecules. *J. Mol. Graphics*, **11**, 134–138.

Feener,E.P., Backer,J.M., King,G.L., Wilden,P.A., Sun,X.J., Kahn,C.R. and White,M.F. (1993) Insulin stimulates serine and tyrosine phosphorylation in the juxtamembrane region of the insulin receptor. *J. Biol. Chem.*, **268**, 11256–11264.

Frantz,J.D., Giorgett-Peraldi,S., Ottinger,E.A. and Shoelson,S.E. (1997) Human GRB-IRβ/GRB10. Splice variants of an insulin and growth factor receptor-binding protein with PH and SH2 domains. *J. Biol. Chem.*, **272**, 2659–2667.

Hanks,S.K., Quinn,A.M. and Hunter,T. (1991) The protein kinase family: conserved features and deduced phylogeny of the catalytic domains. *Science*, **241**, 42–52.

He,W., Craparo,A., Zhu,Y., O'Neill,T.J., Wang,L.-M., Pierce,J. and Gustafson,T.A. (1996) Interaction of insulin receptor substrate-2 (IRS-2) with the insulin and insulin-like growth factor 1 receptors. *J. Biol. Chem.*, **271**, 11641–11645.

Hendrickson,W.A. (1979) Transformations to optimize the superposition of similar structures. *Acta Crystallogr.*, **A35**, 158–163.

Hofstra,R.M. *et al.* (1994) A mutation in the RET proto-oncogene associated with multiple endocrine neoplasia type 2B and sporadic medullary thyroid carcinoma. *Nature*, **367**, 375–376.

Hubbard,S.R., Wei,L., Ellis, L. and Hendrickson,W.A. (1994) Crystal structure of the tyrosine kinase domain of the human insulin receptor. *Nature*, **372**, 746–754.

Hunter,T. (1982) Synthetic peptide substrates for a tyrosine protein kinase. *J. Biol. Chem.*, **257**, 4843–4848.

Jones,T.A. (1985) Diffraction methods for biological macromolecules. Interactive computer graphics: FRODO. *Methods Enzymol.*, **115**, 157–171.

Kato,H., Faria,T.N., Stannard,B., Roberts,C.T. and LeRoith,D. (1994) Essential role of tyrosine residues 1131, 1135, and 1136 of the insulin-like growth factor-I (IGF-I) receptor in IGF-I action. *Mol. Endocrinol.*, **8**, 40–50.

Kharitonenkov,A., Schnekenburger,J., Chen,Z., Knyazev,P., Ali,S., Zwick,E., White,M. and Ullrich,A. (1995) Adapter function of protein-tyrosine phosphatase 1D in insulin receptor/insulin receptor substrate-1 interaction. *J. Biol. Chem.*, **270**, 29189–29193.

Knighton,D.R., Zheng,J., Ten Eyck,L.F., Ashford,V.A., Xuong,N.H., Taylor,S.S. and Sowadski,J.M. (1991) Crystal structure of the catalytic subunit of cyclic adenosine monophosphate-dependent protein kinase. *Science*, **253**, 407–414.

Kohanski,R.A. (1993) Insulin receptor autophosphorylation. II. Determination of autophosphorylation sites by chemical sequence analysis and identification of the juxtamembrane sites. *Biochemistry*, **32**, 5773–5780.

Laskowski,R.A., MacArthur,M.W., Moss,D.S. and Thornton,J.M. (1993) PROCHECK: a program to check the stereochemical quality of protein structures. *J. Appl. Crystallogr.*, **26**, 283–291.

Longati,P., Bardelli,A., Ponzetto,C., Naldini,L. and Comoglio,P.M. (1994) Tyrosines 1234–1235 are critical for activation of the tyrosine kinase encoded by the MET proto-oncogene (HGF receptor). *Oncogene*, **9**, 49–57.

Madhusudan, Trafny,E.A., Xuong,N.H., Adams,J.A., Ten Eyck,L.F., Taylor,S.S. and Sowadski,J.M. (1994) cAMP-dependent protein kinase: crystallographic insights into substrate recognition and phospho-transfer. *Protein Sci.*, **3**, 176–187.

Middlemas,D.S., Meisenhelder,J. and Hunter,T. (1994) Identification of TrkB autophosphorylation sites and evidence that phospholipase C-γ1 is a substrate of the TrkB receptor. *J. Biol. Chem.*, **269**, 5458–5466.

Mitra,G. (1991) Mutational analysis of conserved residues in the tyrosine kinase domain of the human trk oncogene. *Oncogene*, **6**, 2237–2241.

Mohammadi,M., Dikic,I., Sorokin,A., Burgess,W.H., Jaye,M. and Schlessinger,J. (1996a) Identification of six novel autophosphorylation sites on fibroblast growth factor receptor 1 and elucidation of their importance in receptor activation and signal transduction. *Mol. Cell. Biol.*, **16**, 977–989.

Mohammadi,M., Schlessinger,J. and Hubbard,S.R. (1996b) Structure of the FGF receptor tyrosine kinase domain reveals a novel autoinhibitory mechanism. *Cell*, **86**, 577–587.

Navaza,J. (1994) AMoRe: an automated package for molecular replacement. *Acta Crystallogr.*, **A50**, 157–163.

Nicholls,A., Sharp,K.A. and Honig,B. (1991) Protein folding and association: insights from the interfacial and thermodynamic properties of hydrocarbons. *Proteins*, **11**, 281–296.

Noel,J.P., Hamm,H.E. and Sigler,P.B. (1993) The 2.2 Å crystal structure of transducin-α complexed with GTPγS. *Nature*, **366**, 654–663.

O'Neill,T.J., Rose,D.W., Pillay,T.S., Hotta,K., Olefsky,J.M. and Gustafson,T.A. (1996) Interaction of a GRB-IR splice variant (a human GRB10 homolog) with the insulin and insulin-like growth factor 1 receptors. Evidence for a role in mitogenic signaling. *J. Biol. Chem.*, **271**, 22506–22513.

Otwinowski,Z. (1993) Oscillation data reduction program. In Sawyer,L., Isaacs,N. and Bailey,S. (eds), *Proceedings of the CCP4 Study Weekend*. SERC Daresbury Laboratory, Daresbury, UK, pp. 56–62.

Pai,E.F., Krengel,U., Petsko,G.A., Goody,R.S., Kabsch,W. and Wittinghofer,A. (1990) Refined crystal structure of the triphosphate conformation of H-ras p21 at 1.35 Å resolution: implications for the mechanism of GTP hydrolysis. *EMBO J.*, **9**, 2351–2359.

Pandit,S.D., Donis-Keller,H., Iwamoto,T., Tomich,J.M. and Pike,L.J. (1996) The multiple endocrine neoplasia type 2B point mutation alters long-term regulation and enhances the transforming capacity of the epidermal growth factor receptor. *J. Biol. Chem.*, **271**, 5850–5858.

Rosen,O.M., Herrera,R., Olowe,Y., Petruzzelli,L.M. and Cobb,M.H. (1983) Phosphorylation activates the insulin receptor tyrosine protein kinase. *Proc. Natl Acad. Sci. USA*, **80**, 3237–3240.

Russo,A.A., Jeffrey,P.D. and Pavletich,N.P. (1996) Structural basis of cyclin-dependent kinase activation by phosphorylation. *Nature Struct. Biol.*, **3**, 696–700.

Sawka-Verhelle,D., Tartare-Deckert,S., White,M.F. and Van Obberghen,E. (1996) Insulin receptor substrate-2 binds to the insulin receptor through its phosphotyrosine-binding domain and through a newly identified domain comprising amino acids 591–786. *J. Biol. Chem.*, **271**, 5980–5983.

Shoelson,S.E., Chatterjee,S., Chaudhuri,M. and White,M.F. (1992) YMXM motifs of IRS-1 define substrate specificity of the insulin receptor kinase. *Proc. Natl Acad. Sci. USA*, **89**, 2027–2031.

Songyang,Z. *et al.* (1995). Catalytic specificity of protein-tyrosine kinases is critical for selective signalling. *Nature*, **373**, 536–539.

Stadtmauer,L.A. and Rosen,O.M. (1983) Phosphorylation of exogenous substrates by the insulin receptor-associated protein kinase. *J. Biol. Chem.*, **258**, 6682–6685.

Sun,X.J., Rothenberg,P., Kahn,C.R., Backer,J.M., Araki,E., Wilden,P.A., Cahill,D.A., Goldstein,B.J. and White,M.F. (1991) Structure of the insulin receptor substrate IRS-1 defines a unique signal transduction protein. *Nature*, **352**, 73–77.

Sun,X.J., Crimmins,D.L., Myers,M.G., Miralpeix,M. and White,M.F. (1993) Pleiotropic insulin signals are engaged by multisite phosphorylation of IRS-1. *Mol. Cell. Biol.*, **13**, 7418–7428.

Tavare,J.M. and Siddle,K. (1993) Mutational analysis of insulin receptor function: consensus and controversy. *Biochim. Biophys. Acta*, **1178**, 21–39.

Tavare,J.M., O'Brien,R.M., Siddle,K. and Denton,R.M. (1988) Analysis of insulin-receptor phosphorylation sites in intact cells by two-dimensional phosphopeptide mapping. *Biochem. J.*, **253**, 783–788.

Taylor,S.S., Radzio-Andzelm,E. and Hunter,T. (1995) How do protein kinases discriminate between serine/threonine and tyrosine? Structural insights from the insulin receptor protein-tyrosine kinase. *FASEB J.*, **9**, 1255–1266.

Tornqvist,H.E., Pierce,M.W., Frackelton,A.R., Nemenoff,R.A. and Avruch,J. (1987) Identification of insulin receptor tyrosine residues autophosphorylated *in vitro*. *J. Biol. Chem.*, **262**, 10212–10219.

Ullrich,A. *et al.* (1985) Human insulin receptor and its relationship to the tyrosine kinase family of oncogenes. *Nature*, **313**, 756–761.

Wei,L., Hubbard,S.R., Hendrickson,W.A. and Ellis,L. (1995) Expression, characterization and crystallization of the catalytic core of the human insulin receptor protein-tyrosine kinase domain. *J. Biol. Chem.*, **270**, 8122–8130.

White,M.F. and Kahn,C.R. (1994) The insulin signaling system. *J. Biol. Chem.*, **269**, 1–4.

White,M.F., Shoelson,S.E., Keutmann,H. and Kahn,C.R. (1988) A cascade of tyrosine autophosphorylation in the β-subunit activates the phosphotransferase of the insulin receptor. *J. Biol. Chem.*, **263**, 2969–2980.

Yamaguchi,H. and Hendrickson,W.A. (1996) Structural basis for activation of human lymphocyte kinase Lck upon tyrosine phosphorylation. *Nature*, **384**, 484–489.

Zheng,J., Trafny,E.A., Knighton,D.R., Xuong,N.H., Taylor,S.S., Ten Eyck,L.F. and Sowadski,J.M. (1993) 2.2 Å refined crystal structure of the catalytic subunit of cAMP-dependent protein kinase complexed with MnATP and a peptide inhibitor. *Acta Crystallogr.*, **D49**, 362–365.

Phosphorylation of Synthetic Insulin Receptor Peptides by the Insulin Receptor Kinase and Evidence That the Preferred Sequence Containing Tyr-1150 Is Phosphorylated *in Vivo**

Laurel Stadtmauer‡ and Ora M. Rosen§¶

From the ‡Department of Molecular Pharmacology, Albert Einstein College of Medicine, Yeshiva University, Bronx, New York 10461 and the §Program in Molecular Biology, Memorial Sloan-Kettering Institute for Cancer Research, New York, New York 10021

Three peptides were synthesized corresponding to potential autophosphorylation sites of the β subunit of the human insulin receptor. These were peptide 1150 corresponding to amino acids 1142–1153 of the proreceptor, peptide 960 corresponding to amino acids 952–961 of the proreceptor, and peptide 1316 corresponding to amino acids 1313–1329 of the proreceptor. Peptide 1150 served as a better substrate for the insulin receptor tyrosine protein kinase than either of the other peptides or than the Src peptide (corresponding to the sequence surrounding the autophosphorylation site at Tyr-416). Microsequencing of the phosphorylated peptide 1150 indicated that Tyr-1150 rather than Tyr-1146 or Tyr-1151 was phosphorylated in the *in vitro* reaction. The insulin receptor was then isolated from ^{32}P-labeled IM-9 cells that had been exposed to insulin. Tryptic digestion of the β subunit revealed one peptide whose phosphorylation was dependent upon insulin and occurred exclusively on Tyr. This peptide was selectively immunoprecipitated by an antipeptide antibody directed to the Tyr-1150-containing sequence. We conclude that Tyr-1150 is preferentially phosphorylated by the purified receptor kinase and that one of the autophosphorylation reactions elicited by insulin in intact cells occurs in a sequence that contains this residue.

The β subunit of the insulin receptor, like other protein kinases, is a substrate for intramolecular autophosphorylation (1, 2). Phosphorylation of the receptor on tyrosine residues *in vitro* activates the protein kinase of the receptor rendering it insulin-independent (3–6). The receptor isolated from intact cells treated with insulin also appears to be activated when subsequently assayed *in vitro* on exogenous substrates (7). Unlike the situation with some of the well studied protein kinases, such as the cAMP-dependent protein kinase, a preferred amino acid sequence near the modified Tyr has not been well defined for the protein tyrosine kinases. This may be because physiologically relevant substrates for these kinases have yet to be discovered or that protein conformation is an important factor in determining substrate specificity.

Studies of model substrates suggest that acidic amino acids in the immediate vicinity of the modifiable Tyr promote the phosphotransferase reaction (8). Since autophosphorylation sites may reflect the substrate sequences recognized by protein kinases, we synthesized the three peptides corresponding to sequences containing tyrosine residues adjacent to acidic amino acids within the cytoplasmic domain of the β subunit. The amino acid sequences were deduced from the DNA sequence of the proreceptor cDNA (9). When these peptides were tested as substrates *in vitro*, the peptide containing a tyrosine residue that is conserved in growth factor receptor and oncogene tyrosine kinases, Tyr-1150 of the insulin proreceptor, was preferentially phosphorylated. Using an antipeptide antibody elicited to this sequence, we found that one of the autophosphorylation sites in intact cells is also located within this sequence.

MATERIALS AND METHODS

The monoclonal antibody to the human insulin receptor is described in Ref. 10. Porcine insulin was from Lilly and agarose-bound wheat germ agglutinin agarose, from Vector Laboratories (Burlingame, CA). Protein A-agarose and Protein A-Sepharose were obtained from Sigma. TPCK[1]-treated trypsin (241 units/mg) was from Cooper, aprotinin and soybean trypsin inhibitor were from Boehringer Mannheim, [^{32}P]orthophosphate and Na^{125}I were from Amersham, and [γ-^{32}P]ATP (3000 Ci/mmol) was from New England Nuclear. Cellulose thin layer plates were purchased from Analtech. HPLC grade acetonitrile, methylene chloride, and dimethylformamide were from Burdick & Jackson Laboratories and trifluoroacetic acid and phenylisothiocyanate were from Pierce. The Src peptide was from Peninsula Laboratories.

Preparation of Insulin Receptor Tyrosine Kinase—Human placental insulin receptor was purified as described in Ref. 11. The wheat germ agglutinin eluate containing 1 μg of protein/μl and 4–5 fmol of insulin binding activity/μl (measured at 0.3 nM insulin) was immunopurified by adsorption to a monoclonal anti-receptor antibody-Protein A-agarose complex. Insulin receptor monoclonal CII-25 (10) was cross-linked to Protein A-agarose by the procedure described in Ref. 12. The slurry (5 μg of IgG in 30 μl) bound 100 fmol of insulin. The antibody-antigen complex was washed five times with 50 mM Hepes buffer, pH 7.5, 0.15 M NaCl, and 0.1% Triton X-100 and used directly in the protein kinase assays.

Phosphorylation of Peptides with the Insulin-dependent Protein Kinase—Protein kinase assays were performed with the affinity-purified receptor bound to the monoclonal antibody-agarose column; 40–60 fmol of insulin binding activity, (approximately 240 ng of receptor protein) were used per assay. The reaction mixture (40 μl) contained 20 mM Hepes buffer, pH 7.4, 0.1% Triton X-100, 10% (v/

[1] The abbreviations used are: TPCK, L-1-tosylamido-2-phenylethyl chloromethyl ketone; HPLC, high performance liquid chromatography; SDS, sodium dodecyl sulfate; Hepes, 4-(2-hydroxyethyl)-1-piperazineethanesulfonic acid; PTH, phenylthiohydantoin; TFA, trifluoroacetic acid; the term "*in vitro*" is used for reactions catalyzed by the purified receptor kinase.

v) glycerol, 150 mM NaCl, 10 mM $MgCl_2$, 2 mM $MnCl_2$, 20 μM sodium vanadate, and 100 μM ATP (5–7 cpm/fmol). Where indicated, insulin was added to a final concentration of 0.1 μM. Insulin was preincubated with the receptor at 23 °C for 10 min prior to the addition of substrate and [γ-^{32}P]ATP. After 10 min at 23 °C, the reaction was terminated by the addition of 20 μl of 10% trichloroacetic acid, and the phosphocellulose paper assay was performed as described in Ref. 13.

Synthesis and Purification of Peptides—Three peptides were synthesized corresponding to possible autophosphorylation sites of the insulin receptor. "Peptide 960," N-Leu-Phe-Ala-Ser-Ser-Asn-Pro-Glu-Tyr-Leu-Ser-Ala-Arg-Arg-C corresponds to amino acids 952–961 of the insulin proreceptor sequence (9), except that the Tyr at position 953 was changed to Phe and two Args were added at the C terminus to facilitate assays of the phosphopeptide. "Peptide 1150," N-Thr-Arg-Asp-Ile-Tyr-Glu-Thr-Asp-Tyr-Tyr-Arg-Lys-C corresponds to amino acids 1142–1153, and "Peptide 1316," N-Lys-Arg-Ser-Tyr-Glu-Glu-His-Ile-Pro-Tyr-Thr-His-Met-Asn-Gly-Gly-Lys-C corresponds to amino acids 1313–1329 of the proreceptor. These peptides were synthesized according to the solid phase method of Merrifield (14) using a Biosearch synthesizer. The extent of amino acid substitution on the resin was 0.3 mmol/g. Fully protected peptides were synthesized from the resin, cleaved from their support by HF, extracted with ethyl acetate, 1% acetic acid (1:1, v/v), and purified to homogeneity by HPLC using a reverse phase ODS-C18 column (Altex 5 μm 150 × 4.6 mm inside diameter) and a linear gradient of 0.05% TFA/acetonitrile (0–100%). The flow rate was 1.5 ml/min and the peptides eluted between 60% and 80% acetonitrile. The sequence of each peptide was confirmed by amino acid analysis and by sequencing on an Applied Biosystems gas phase sequenator.

Two-dimensional Tryptic Maps and Identification of the Tyr-1150-containing Peptide—^{32}P-labeled IM-9 cells (a cultured line of human lymphoblasts) (7) were treated with or without insulin (0.1 μM) for 5 min. The ^{32}P-labeled β subunit of the receptor was identified by radioautography following immunoprecipitation and SDS-polyacrylamide gel electrophoresis (7). The 95-kDa phosphoprotein was excised from the SDS-polyacrylamide gel, washed for 8 h with 10% methanol, cut into 1-mm squares, dried, and then incubated with shaking for 24 h with 1 ml of 50 mM NH_4HCO_3 buffer, pH 8.3, and 100 μg of TPCK-treated trypsin. This solution was removed and the gel pieces were incubated again for 4 h with 0.5 ml of 50 mM NH_4HCO_3 buffer and 50 μg of trypsin. The two supernatant fluids were combined (recovery of ^{32}P was approximately 80%), dried, washed once with 1 ml of H_2O,

and dried again. The pellet was dissolved in 10 μl of H_2O and spotted on a cellulose thin layer plate (15). Electrophoresis was performed on a flat bed apparatus in formic acid:acetic acid:H_2O (15:15:80) for 35 min at 1000 V. The plates were then dried overnight in a vacuum oven and chromatography was performed in 1-butanol:pyridine:acetic acid:water (34.5:25:5:18).

Antipeptide Antibodies and Immunoprecipitation—Immunoprecipitation with Ab2 (elicited to the amino acid sequence 1142–1162 of the insulin proreceptor) and Ab 4 (elicited to the amino acid sequence 952–967) were performed as in Ref. 16. The procedures used to synthesize the peptides and elicit the antibodies are detailed in Refs. 16 and 17. Each antibody reacted only with the peptide to which it was elicited and was able to immunoprecipitate the phosphorylated, as well as the nonphosphorylated, antigen.

Preparation of ^{32}P-Labeled Peptide 1150 for Amino Acid Sequencing—The peptide sequence was obtained with an Applied Biosystems gas phase sequenator. The 1150 peptide was phosphorylated by the receptor kinase as described above and the reaction was stopped by the addition of trichloroacetic acid to a final concentration of 5% and centrifuged at 10,000 × g for 5 min. The supernatant fluid was collected and 1 ml of 0.05% TFA was added. The solution was applied to a Sep-Pak column (Waters Associates), washed with 10 ml of 0.05% TFA, 5 ml of 10% acetonitrile in 0.05% TFA, and eluted in 2 ml of 50% acetonitrile in 0.05% TFA. The phosphopeptide was purified on an HPLC C18 column with a gradient of 0.05% TFA/0–50% acetonitrile over 25 min at a flow rate of 1 ml/min. The quantity of amino acid recovered in the 1st step of the Edman degradation was 75% and the repetitive yield was 95%.

RESULTS

Phosphorylation of the 1150 Peptide in Vitro—The time course for phosphorylation of the 1150 peptide is depicted in Fig. 1A. Maximal phosphorylation (500 pmol) was obtained at 30 min using 200 μM peptide. Fig. 1B depicts phosphorylation at different concentrations of peptide. The reaction time was 10 min, which is within the linear range of peptide phosphorylation under these conditions. Fig. 2 presents Lineweaver-Burk plots of the *in vitro* phosphorylation of the receptor peptides and the Src peptide. The K_m and V_{max} values calculated from these data are summarized in Table I. The
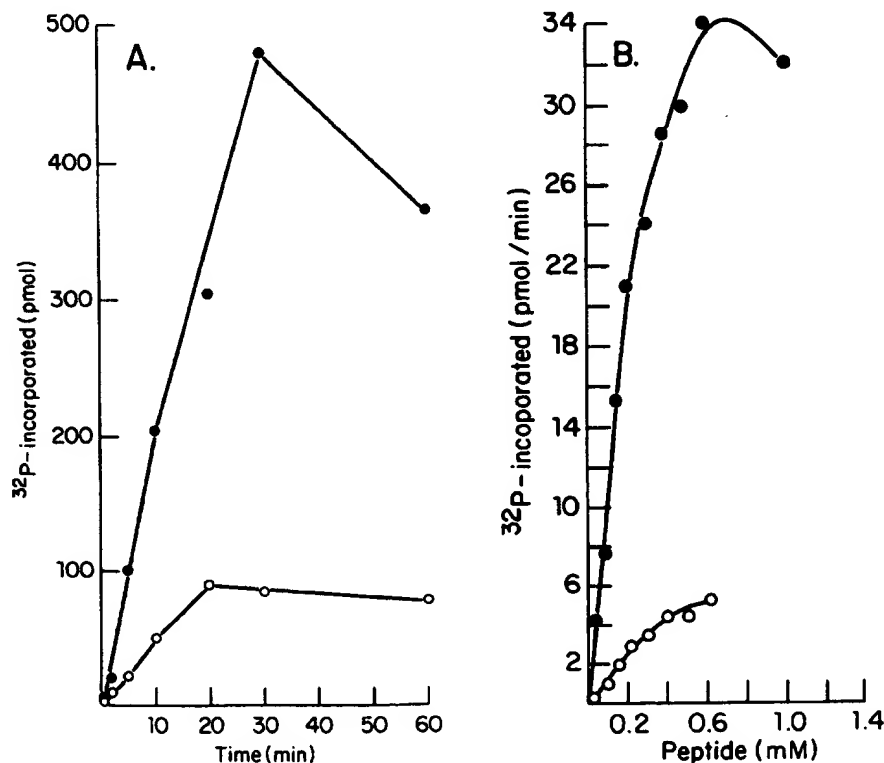
FIG. 1. **Phosphorylation of peptide 1150** *in vitro*. Each reaction mixture contained 40 fmol of insulin-binding activity. In *Panel A*, the concentration of the 1150 peptide was 200 μM. Reactions were initiated by the addition of [γ-^{32}P]ATP (5 cpm/fmol, 100 μM) and incubations were at 23 °C. In *Panel B*, incubations were for 10 min. The data are from a typical experiment. All assays were performed in duplicate. Duplicates differed from each other by less than 5%. The variation between experiments was less than 10%. ●, plus insulin; O, minus insulin.

FIG. 2. **Reciprocal plots of the phosphorylation of insulin receptor peptides and the src peptide *in vitro*.** Assays were performed as described in the legend to Fig. 1, except that 60 fmol of insulin-binding activity were added to each assay and the specific activity of the [γ-³²P]ATP was 7 cpm/fmol. The peptide concentration ranged from 0.05 mM to 2 mM. Assays were for 10 min. Data from two independent experiments were fitted by least squares analyses. The K_m and V_{max} estimates from three independent experiments were within 10% of the reported values. The substrates used were: *Panel A*, Peptide 1150; *Panel B*, Peptide 960; *Panel C*, Peptide 1316; and *Panel D*, Src (see "Materials and Methods" and Table I for peptide sequences).
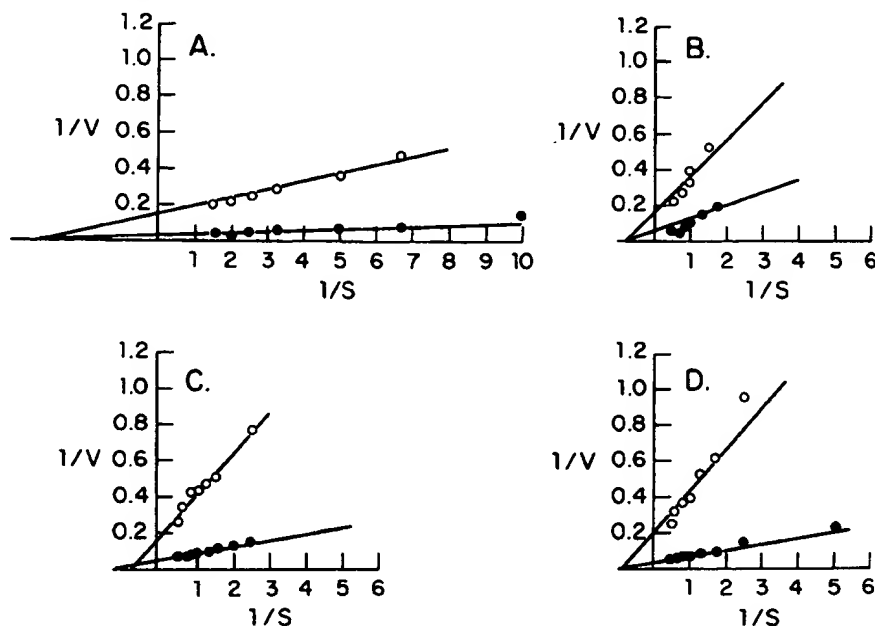
TABLE I

Summary of peptide phosphorylation in vitro

The data from which these values were calculated are presented in Fig. 2.

Peptide	Sequence	V_{max}		K_m	
		+Insulin	−Insulin	+Insulin	−Insulin
		pmol/min		*mM*	
1150	TRDIYETDYYRK	45	7.1	0.24	0.30
960	LFASSNPEYLSARR	25	5.5	1.20	1.33
1316	KRSYEEHIPYTHMNGGK	33	5.0	1.13	1.03
Src	RRLIEDAEYARG	18	6.2	0.96	1.10

best of the substrates is the 1150 peptide; the K_m is 4–5 times lower for this peptide than it is for the other three receptor peptides and the homologous Src peptide and the V_{max} is higher.

Since there are 3 Tyr residues in the 1150 peptide, it was necessary to determine which one(s) was phosphorylated *in vitro*. This was addressed by amino acid sequencing. Table II summarizes the results of one analysis with 400 pmol of phosphopeptide. There were 1.1 pmol of ³²P incorporated per pmol of the HPLC-purified phosphopeptide. Two additional independent analyses gave similar results. Each PTH-derivative was recovered in the expected yield (150–300 pmol), except for PTH-Tyr in cycle 9. Of the 180 pmol of PTH-Tyr predicted for cycle 9, only 35 were recovered. Cycles 5 and 10 contained the predicted amount of PTH-Tyr. Since PTH-pTyr does not co-purify with PTH-Tyr, we conclude that the Tyr in the ninth cycle (Tyr-1150) is the only residue significantly modified by phosphorylation. In the unphosphorylated peptide, the PTH-Tyr in cycle 9 is recovered in theoretical yield (not shown). The radioactivity derived from the phosphopeptide began to appear in cycle 9 and was present in each cycle thereafter (see legend to Table II). When analyzed for [³²P]PTH-pTyr, 70% of the radioactivity in cycle 9 was present in the PTH-derivative. The proportion of radioactivity present in the derivative decreased progressively with each ensuing cycle. Since cycles 5 and 10 contained full complements of PTH-Tyr and all of the ³²P in the original phosphopeptide was on tyrosine, the radioactivity in cycles 9 through

TABLE II

Amino acid sequence of peptide 1150 following phosphorylation in vitro

The 1150 peptide was phosphorylated with 200 fmol of insulin-binding activity in an assay containing 200 μM peptide, 20 mM Hepes buffer, pH 7.4, 0.1% Triton X-100, 10% glycerol, 0.15 M NaCl, 10 mM MgCl₂, 2 mM MnCl₂, 20 μM sodium vanadate, and 0.1 μM insulin. [γ-³²P]ATP (500 cpm/pmol, 100 μM) was added and the assay was performed for 20 min at 23 °C. The reaction was stopped by the addition of trichloracetic acid to a final concentration of 5% and the phosphopeptide was purified by HPLC on an ODS C18 column using a gradient of 0.05% TFA/0–50% acetonitrile at a flow rate of 1 ml/min (see "Materials and Methods"). The phosphopeptide, detected by absorbance at 230 nm, eluted as a single peak coincident with radioactivity at 22.6–23.0 min. The phosphopeptide (400 pmol) was sequenced and each cycle was assayed for PTH-amino acid derivatives, total radioactivity, and [³²P]PTH-pTyr. Fractions which contained radioactivity were analyzed by flat bed thin layer electrophoresis (800 V) in pyridine:acetic acid:H₂O (1:10:189) at pH 3.5. The PTH-derivative of phosphotyrosine was identified by comparison with the PTH-derivative prepared from [³²P]phosphotyrosine (19) and was identified by staining with iodine and autoradiography. The radioactivity present in each cycle was as follows: 0, 0, 0, 16, 46, 204, 116, 100, 1506, 3124, 2511, and 1545 cpm per cycle for cycles 1–12, respectively (determined by Cerenkov counting). The percentage of the total radioactivity identified as [³²P]PTH-pTyr was 73, 52, 33, and 30% for cycles 9–12, respectively.

Cycle	1	2	3	4	5	6	7	8	9	10	11	12
Amino acid	T	R	D	I	Y	E	T	D	Y	Y	R	K
PTH-Tyr (pmol)					222				35	175		

12 must have come predominantly from modification of residue 9. The radioactivity in cycles 10, 11, and 12 is attributed to adsorption of [³²P]PTH-pTyr and other ³²P by-products of the sequencing reactions to the filter with subsequent gradual (and incomplete) elution.

Phosphorylation of the β Subunit in Intact Cells—Since the 1150 peptide appeared to be the best of the substrates tested for insulin-dependent phosphorylation *in vitro*, it was of interest to determine whether this region of the β subunit was also autophosphorylated in intact cells. Two-dimensional tryptic maps of the β subunit were prepared from ³²P-labeled IM-9 cells that had been treated in the absence or presence of insulin. As shown in Fig. 3, there are 3 phosphopeptides visible in the map derived from control cells (*Panel A*). The
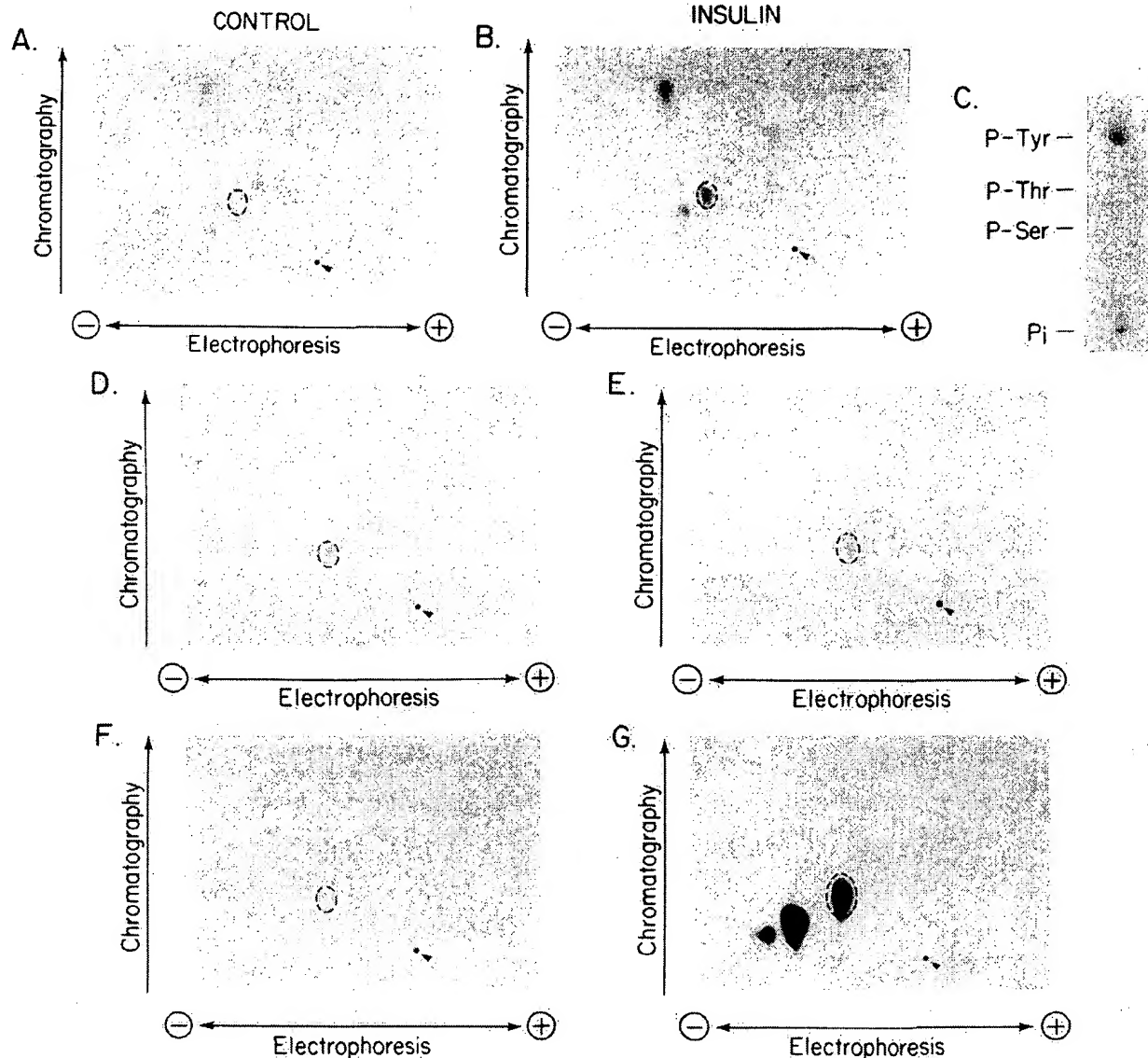
Fig. 3. **Insulin-dependent phosphorylation of the β subunit sequence containing Tyr-1150 in intact cells.** ^{32}P-labeled IM-9 cells were treated with or without insulin and the β subunit of the isolated receptor was resolved by SDS/polyacrylamide gel electrophoresis, excised from the gel, and trypsinized. Thin layer electrophoresis and chromatography were performed as described under "Materials and Methods" and the plates were analyzed for ^{32}P-phosphopeptides by autoradiography. *Panel A,* control cells. *Panel B,* insulin-treated cells. *Panel C,* the insulin-elicited phosphopeptide *circled* in *Panel B* was eluted from the plate with 1 ml of 50% acetonitrile in 0.05% TFA and phosphoamino acid analysis was performed as in Ref. 7. The peptide was hydrolyzed for 50 min in 6 N HCl at 100 °C. Analysis was by one-dimensional thin layer electrophoresis on a cellulose plate (Analtech) in pyridine:acetic acid:H₂O (1:10:189) at 800 V for 75 min. *Panel D,* the insulin-specific ^{32}P-phosphopeptide *outlined* in *Panel B* was eluted from duplicate plates and dissolved in 500 μl of 50 mM NH₄HCO₃ buffer, pH 7.4. Five microliters of either antibody 2 (elicited to the peptide containing Tyr-1150) or antibody 4 (elicited to the peptide containing Tyr-960) were added in the presence of protease inhibitors (1 mM phenylmethylsulfonyl fluoride, 10 μg/ml aprotinin, 20 μg/ml leupeptin, 10 μg/ml soybean trypsin inhibitor, and 20 μM sodium vanadate for 24 h at 4°C. Protein A-Sepharose (100 μl) was then added for 3 h. The immunoprecipitate was sedimented, washed three times with 50 mM NH₄HCO₃ buffer, pH 7.5, 0.1% Triton X-100, 0.15 M NaCl, eluted with 50% acetonitrile in 0.05% TFA, dried, and subjected to the two-dimensional peptide analysis. No radioactivity was immunoprecipitated by Ab 4 (not shown). *Panels E and F,* the β subunit isolated from insulin-treated ^{32}P-labeled IM9 cells was trypsinized with 100 μg of TPCK-treated trypsin as discussed under "Materials and Methods." Soybean trypsin inhibitor (100 μg) was then added and the mixture of peptides was incubated in 500 μl of 50 mM NH₄HCO₃ buffer, pH 7.5, with 5 μl of either antibody 2 (*Panel E*), antibody 4, or antibody 2 plus 1 nmol of peptide 1150 (*Panel F*). Immunoprecipitation was performed as described above. The peptide was eluted from the antibody complex with 50% acetonitrile and 0.05% TFA (1 ml), dried, washed with 1 ml of H₂O, dried again, and subjected to the two-dimensional analysis. There was no radioactivity immunoprecipitated by antibody 4 (not shown). *Panel G,* following phosphorylation of peptide 1150 *in vitro* (as in Fig. 1) the ^{32}P-labeled peptide was purified by HPLC and treated with 100 μg of trypsin for 8 h. The proteolytic products were then subjected to the two-dimensional peptide analysis. The radioactive peptides shown in *Panels D, E,* and *G* had the same relative migration in both dimensions as the peptide *encircled* in *B* and co-migrated with it when mixed (not shown).

tryptic map derived from insulin-treated cells showed an increase in the phosphorylation of these peptides and phosphorylation of several new peptides (*Panel B*). One of the principal new phosphopeptides (encircled in *Panel B*) was isolated following the two-dimensional analysis. Phosphoamino acid analysis revealed that it contained only [^{32}P]phosphotyrosine (*Panel C*). Attempts were then made to identify this peptide immunologically. The isolated ^{32}P-labeled peptide was immunoprecipitable by antibody 2 elicited to the proreceptor sequence 1142–1162 (*Panel D*), but not by antibody 4 elicited to proreceptor sequence 952–967 (not shown). Finally, treatment of the entire tryptic digest derived from the ^{32}P-labeled β subunit of insulin-treated cells with antibody 2 led to immunoprecipitation of the same tryptic peptide shown in *Panel D* (*Panel E*). Immunoprecipitation was abolished by the addition of an excess of unlabeled peptide 1150 (*Panel F*). *In vitro* phosphorylation of peptide 1150 followed by digestion with trypsin led to the formation of two new tryptic ^{32}P-peptides (the peptide on the *left* in *Panel G* is undigested ^{32}P-peptide). One of these peptides co-migrated with the peptide isolated from ^{32}P-labeled cells (*Panel G*). An equally potent antipeptide antibody, directed to the sequence including Tyr-960, immunoprecipitated neither the isolated ^{32}P-labeled tryptic peptide nor any of the other ^{32}P-labeled peptides present in the trypsin hydrolysate. We conclude from this series of experiments that one of the sites of autophosphorylation of the insulin receptor in intact cells occurs on either Tyr-1146, Tyr-1150, or Tyr-1151 since the predicted tryptic peptide would include all three of these tyrosines. Although these experiments do not establish which of these tyrosines is phosphorylated, the experiments with the 1150 peptide *in vitro* suggest that it might be Tyr-1150.

DISCUSSION

Studies employing peptides of the cytoplasmic domain of the β subunit of the insulin receptor that contain tyrosine residues adjacent to acidic amino acid residues as substrates for the insulin-dependent receptor kinase indicate that the peptide containing the conserved Tyr-1150 is better than the other peptides tested, including the peptide that contains the homologous Tyr (Tyr-416) in pp60 src. Perhaps an aromatic amino acid adjacent to the Tyr residue that is phosphorylated, a sequence found only in the human insulin receptor, the *Drosophila* insulin receptor (17), and the oncogene ros kinase (18) is a significant determinant of substrate specificity for the insulin receptor-ros family of tyrosine protein kinases. Sequence analysis of the 1150 peptide phosphorylated *in vitro* indicates that of the three tyrosines recovered in the peptide, only Tyr-1150 is markedly reduced. Since the ^{32}P-labeled phosphotyrosine derivatives adsorb to the filter during sequencing, determination of the amount of radioactivity recovered in each cycle could not be used to discriminate between phosphorylation of adjacent residues. Our conclusion that only Tyr-1150 is modified is based upon three independent analyses of the phosphopeptide in which we failed to recover Tyr-1150, but did recover Tyr-1146 and Tyr-1151 in theoretical yields. Our results with the synthetic peptides are compatible with studies employing the epidermal growth factor receptor tyrosine kinase to phosphorylate synthetic peptides corresponding to those surrounding the *in vitro* phosphorylation site of the epidermal growth factor receptor. Downward *et al.* (20, 21) found peptide P1, a major site for autophosphorylation of the epidermal growth factor receptor *in vivo* and *in vitro* to be the best *in vitro* receptor peptide substrate. It may turn out that, as in the case of the cAMP-dependent protein kinase, the autophosphorylation sites used by the tyrosine protein kinases will provide clues to an un-

derstanding of their substrate specificity.

Since examination of the peptide substrates *in vitro* suggested preference for the 1150 peptide and Tyr-1150 in particular, we used an antipeptide antibody directed to this sequence to determine if this region of the β subunit contained a tyrosine that was autophosphorylated when intact cells were exposed to insulin. The complex pattern depicted in Fig. 3B is consistent with reports that insulin promotes the phosphorylation of more than 1 serine and tyrosine residue in intact cells (22, 23). One of the sites that contains only phosphotyrosine, and may therefore be attributable to autophosphorylation, was selectively and specifically immunoprecipitated by antibody to the sequence containing Tyr-1150. Our results indicate that the amino acid sequence surrounding Tyr-1150 is a good substrate for phosphorylation catalyzed by the insulin receptor *in vitro* and is one of the pTyr-containing receptor peptides that results from exposure of intact cells to insulin. It remains to be determined whether the same Tyr residue that is phosphorylated in the synthetic peptide *in vitro* is phosphorylated in cells and whether Tyr residues other than those present in the 1150 peptide are also autophosphorylated in intact cells. In preliminary experiments, we have isolated two fragments of the β subunit that contain Tyr residues that become autophosphorylated *in vitro*.[2] One of these fragments contains Tyr-1150 and the other contains the C-terminal Tyr-1316. Thus, the sequence in the vicinity of Tyr-1150 appears to be a substrate for autophosphorylation in intact cells and *in vitro*. Although an antipeptide antibody directed to a receptor sequence that includes Tyr-960 inhibits receptor kinase activity (16), there is no evidence, as yet, that it is an autophosphorylation site.

REFERENCES

1. Kasuga, M., Fujita-Yamaguchi, Y., Blithe, D. L., and Kahn, C. R. (1983) *Proc. Natl. Acad. Sci. U. S. A.* **80**, 2137–2141
2. Petruzzelli, L., Herrera, R., and Rosen, O. M. (1984) *Proc. Natl. Acad. Sci. U. S. A.* **81**, 3327–3331
3. Rosen, O. M., Herrera, R., Olowe, Y., Petruzzelli, L. M., and Cobb, M. (1983) *Proc. Natl. Acad. Sci. U. S. A.* **80**, 3237–3240
4. Yu, K.-T., and Czech, M. P. (1984) *J. Biol. Chem.* **259**, 5277–5286
5. Kwok, Y. C., Nemenoff, R. A., Powers, A. C., and Avruch, J. (1986) *Arch. Biochem. Biophys.* **244**, 102–113
6. Kohanski, R. A., and Lane, M. D. (1986) *Biochem. Biophys. Res. Commun.* **134**, 1312–1318
7. Stadtmauer, L., and Rosen, O. M. (1986) *J. Biol. Chem.* **261**, 3402–3407
8. Hunter, T., and Cooper, J. A. (1985) *Annu. Rev. Biochem.* **54**, 897–930
9. Ullrich, A., Bell, J. R., Chen, E.-Y., Herrera, R., Petruzzelli, L. M., Dull, T. J., Gray, A., Coussens, L., Liao, Y.-C., Tsubokawa, M., Mason, A., Seeburg, P. H., Grunfield, C., Rosen, O. M., and Ramachandran, J. (1985) *Nature* **313**, 756–761
10. Ganguly, S., Petruzzelli, L. M., Herrera, R., Stadtmauer, L., and Rosen, O. M. (1985) *Curr. Top. Cell. Regul.* **27**, 83–94
11. Petruzzelli, L. M., Ganguly, S., Smith, C. J., Cobb, M. H., Rubin, C. S., and Rosen, O. M. (1982) *Proc. Natl. Acad. Sci. U. S. A.* **79**, 6792–6796
12. Schneider, C., Newman, R. A., Sutherland, D. R., Asser, U., and Greaves, M. F. (1982) *J. Biol. Chem.* **257**, 10766–10769
13. Stadtmauer, L., and Rosen, O. M. (1983) *J. Biol. Chem.* **258**, 6682–6685
14. Merrifield, R. B. (1963) *J. Am. Chem. Soc.* **85**, 2149–2156
15. Takayama, S., White, M. F., Lauris, V., and Kahn, C. R. (1984) *Proc. Natl. Acad. Sci. U. S. A.* **81**, 7797–7801
16. Herrera, R., Petruzzelli, L. M., Thomas, N., Bramson, H. N.,

[2] R. Herrera and O. M. Rosen, manuscript in preparation.

Kaiser, E. T., and Rosen, O. M. (1985) *Proc. Natl. Acad. Sci. U. S. A.* **82**, 7899–7903

17. Petruzzelli, L. M., Herrera, R., Arenas-Garcia, R., Fernandez, R., Birnbaum, M. J., and Rosen, O. M. (1986) *Proc. Natl. Acad. Sci. U. S. A.*, in press

18. Neckameyer, W. S., and Wang, L.-H. (1985) *J. Virol.* **53**, 879–884

19. Konigsberg, W. (1972) *Methods Enzymol.* **25**, 326–332

20. Downward, J., Parker, P., and Waterfield, M. D. (1984) *Nature* **311**, 483–485

21. Downward, J., Waterfield, M. D., and Parker, P. J. (1985) *J. Biol. Chem.* **260**, 14538–14546

22. White, M. F., Takayama, S., and Kahn, C. R. (1985) *J. Biol. Chem.* **260**, 9470–9478

23. Jacobs, S., and Cuatrecasas, P. (1986) *J. Biol. Chem.* **261**, 934–939

p125^{Fak} Focal Adhesion Kinase Is a Substrate for the Insulin and Insulin-like Growth Factor-I Tyrosine Kinase Receptors*

Véronique Baron‡, Véronique Calléja, Patricia Ferrari, Françoise Alengrin, and Emmanuel Van Obberghen

From INSERM, U145, Faculté de Médecine, Avenue de Valombrose, 06107 Nice Cédex 2, France

The focal adhesion kinase p125^{Fak} is a widely expressed cytosolic tyrosine kinase, which is involved in integrin signaling and in signal transduction of a number of growth factors. In contrast to tyrosine kinase receptors such as the platelet-derived growth factor and the hepatocyte growth factor receptors, which induce p125^{Fak} phosphorylation, insulin has been shown to promote its dephosphorylation. In this study, we compared p125^{Fak} phosphorylation in insulin-stimulated cells maintained in suspension or in an adhesion state. We found that, in nonattached cells, insulin promotes p125^{Fak} phosphorylation, whereas dephosphorylation occurred in attached cells. This was observed in Rat-1 fibroblasts overexpressing the insulin receptor, as well as in Hep G2 hepatocytes and in 3T3-L1 adipocytes expressing more natural levels of insulin receptors. Insulin-induced p125^{Fak} phosphorylation correlated with an increase in paxillin phosphorylation, indicating that p125^{Fak} kinase activity may be stimulated by insulin. Mixing of purified insulin or insulin-like growth factor-I (IGF-I) receptors with p125^{Fak} resulted in an increase in p125^{Fak} phosphorylation. Using a kinase-deficient p125^{Fak} mutant, we found that this protein is a direct substrate of the insulin and IGF-I receptor tyrosine kinases. This view is supported by two additional findings. (i) A peptide corresponding to p125^{Fak} sequence comprising amino acids 568–582, which contains tyrosines 576 and 577 of the kinase domain regulatory loop, is phosphorylated by the insulin receptor; and (ii) p125^{Fak} phosphorylation by the insulin receptor is prevented by addition of this peptide. Finally, we observed that p125^{Fak} phosphorylation by the receptor results in its activation. Our results show that the nature of the cross-talk between the insulin/IGF-I receptors and p125^{Fak} is dependent on the cell architecture, and hence the interaction of the insulin/IGF-I signaling system with the integrin system will vary accordingly.

The focal adhesion kinase p125^{Fak} is a cytosolic tyrosine kinase initially isolated from Src-transformed cells (1, 2). It is localized at focal adhesion plaques of cultured cells and binds to a number of proteins involved in the organization of the cytoskeleton and to signaling molecules, resulting in the formation of multicomponents complexes (reviewed in Refs. 3–6). Tyrosine phosphorylation of p125^{Fak} occurs rapidly in response to integrin clustering or binding to the extracellular matrix, and this correlates with increased kinase activity (2, 7–9).

For most cell types, cooperation of adhesion-mediated and growth factor-mediated signaling pathways is required for appropriate growth control, and it is now widely accepted that p125^{Fak} may be a point of convergence in the actions of integrins and growth factors (10, 11). Indeed, p125^{Fak} is not only activated by integrins, but also by mitogenic neuropeptides (12), thrombin (13), sphingosine (14), the bioactive lipid lysophosphatidic acid (15–17), and by ligands for tyrosine kinase receptors such as platelet-derived growth factor and hepatocyte growth factor (18–20).

In contrast to other tyrosine kinase receptors, which induce tyrosine phosphorylation of p125^{Fak}, it has been reported that in fibroblasts insulin promotes a decrease in p125^{Fak} phosphorylation (21–23).

The insulin receptor is a heterotetrameric oligomer consisting of two extracellular 135-kDa α-subunits and two 95-kDa transmembrane β-subunits containing a tyrosine kinase (24, 25). Insulin binding to the α-subunit stimulates autophosphorylation of the β-subunit cytoplasmic domain on multiple tyrosine residues. This activates the receptor kinase, leading to phosphorylation of several substrates including IRS-1,[1] IRS-2, Shc, and Gab-1 (26–31). IRS-1/2 and Gab-1 carry multiple potential tyrosine phosphorylation sites, which upon phosphorylation become docking sites for SH2 domain-containing proteins. These include the p85 regulatory subunit of phosphatidylinositol 3-kinase, Grb2, and the phosphotyrosine phosphatase SHP-2 (32–34).

IRS-1 is also found to be associated with Csk, the C-terminal Src kinase that is an inhibitor of the Src kinase family. It has been shown recently that the insulin-induced complex of IRS-1 and Csk could be involved in dephosphorylation of p125^{Fak} observed after insulin treatment of fibroblasts (35).

The fact that insulin induces p125^{Fak} dephosphorylation suggests the existence of an antagonistic action of insulin on the integrin signaling pathway. However, examples of cooperation between insulin and integrin signals have been reported. For instance, stimulation of DNA synthesis by insulin is potentiated by engagement of the $\alpha_v\beta_3$ integrin. Moreover, insulin promotes the association of IRS-1 with this integrin, which is indicative of a putative role for IRS-1 in the cooperation between the two signaling pathways (36). Finally, recent studies indicate that conjunction of insulin or IGF-I activation with

[1] The abbreviations used are: IRS, insulin receptor substrate; Fak, focal adhesion kinase; IGF-I, insulin-like growth factor-I; Shc, Src homology collagen; SHP-2, SH2-containing protein-tyrosine phosphatase-2; SH, Src homology; RHIR, Rat-1 human insulin receptor; PAGE, polyacrylamide gel electrophoresis; DMEM, Dulbecco's modified Eagle's medium; FCS, fetal calf serum; BSA, bovine serum albumin; PBS, phosphate-buffered saline; BES, (N,N-bis[2-hydroxyethyl]-2-aminoethane-sulfonic acid).

integrin engagement plays an important role in dissemination of tumor cells (37).

In the present work, we show that the effect of insulin on p125^{Fak} phosphorylation depends on the adhesion status of the cells. Indeed, in nonattached cells insulin stimulates p125^{Fak} phosphorylation, whereas in attached cells it induces its dephosphorylation. In addition, we provide several lines of evidence for the view that p125^{Fak} is a direct substrate of the insulin receptor and the IGF-I receptor tyrosine kinases, and that cross-phosphorylation of p125^{Fak} by a tyrosine kinase receptor results in its activation. This may explain the positive cooperation occurring between integrins and insulin/IGF-I signaling pathways.

EXPERIMENTAL PROCEDURES

Materials—p125^{Fak} cDNA, inserted at the *EcoRI* site into pBluescript (KS$^-$), was a generous gift from Dr. Thomas J. Parsons (University of Virginia, Charlottesville, VA).

Mouse monoclonal anti-p125^{Fak} antibodies (clone 2A7) and anti-phosphotyrosine antibodies (clone AG10) came from Upstate Biotechnology, Inc, (Lake Placid, NY). Rabbit polyclonal antibody to p125^{Fak} (A-17) used in the Western blot experiments was from Santa Cruz Biotechnology (Santa Cruz, CA). Rabbit anti-mouse antibodies were purchased from DAKO (Glostrup, Denmark). Reagents for SDS-PAGE were from Bio-Rad. Hybond-C nitrocellulose was from Millipore, and protein G-Sepharose was from Sigma-France (St. Quentin Fallavier, France). [γ-^{32}P]ATP was purchased from ICN-France. Porcine insulin and recombinant human IGF-I were kindly provided by Novo-Nordisk (Copenhagen, Denmark) and Lilly, respectively.

Cell Lines—Rat-1 embryo fibroblasts transfected with an expression plasmid encoding the human insulin receptor (RHIR) were a gift from Dr. A. Ullrich (Max-Planck-Institut für Biochemie, München, Germany). These cells and Rat-1 cells were grown in Ham's F-12 medium and Dulbeco's modified Eagle's medium (DMEM) (1/1) supplemented with 10% (v/v) fetal calf serum (FCS) and 10 mM glutamine.

NIH 3T3 cells transfected with an expression plasmid encoding the human IGF-I receptor were produced in our laboratory as described previously (38). 293 EBNA cells are human embryo kidney cells, which constitutively express the EBNA-I protein from Epstein-Barr virus, and Hep G2 is a cell line derived from human hepatocyte carcinoma (Invitrogen, San Diego, CA). These cells were grown in DMEM supplemented with 10% (v/v) FCS and 10 mM glutamine. All transfected cells were maintained in 400 μg/ml Geneticin (G418).

3T3-L1 fibroblasts were cultured in DMEM containing 10% (v/v) FCS and 10 mM glutamine and were induced to differentiate into adipocytes as described previously (39).

Cells were seeded into six-well plates or into 100 mm-diameter dishes and grown until confluence. They were starved overnight in DMEM containing 0.2% (w/v) bovine serum albumin (BSA) and 10 mM glutamine before use.

Production of Kinase-deficient p125^{Fak}—Site-directed mutagenesis was performed using the Transformer™ kit from CLONTECH. The two primers (Genset, Paris, France) were CCg CTC TAg AAC TAg Tgg gCC CCC Cgg gCT gC, which changes the *BamHI* site for *ApaI* in the pBKS polylinker, and ggC TgT AgC AAT CAg AAC ATg TAA AAA CTg C, which replaced Lys-454 with Arg in p125^{Fak}. The manufacturer's instructions were followed without modifications. The mutated plasmid was amplified into XL-1Blue *Escherichia coli* strain, and the mutation was checked by sequence analysis. The cDNA was subcloned into pCEP4 expression vector (Invitrogen) by excision at the sites *NheI* and *XhoI* and ligation between the sites *XbaI* and *XhoI* of pCEP4.

Transfection of 293 EBNA Cells—Cells were trypsinized and seeded at 250,000 cells/well of a six-well plate 2 days before use. Transfection was performed by the calcium phosphate precipitation method of Chen and Okayama (40). Plasmid DNA (1 μg/well) was incubated for 30 min at 25 °C with 0.25 M CaCl$_2$ and BES. This solution was added dropwise to the cells, which were incubated overnight at 35 °C under 3% CO$_2$. Cells were starved for 15 h before use in DMEM containing 0.2% BSA (w/v).

p125^{Fak} Phosphorylation in Intact Cells—Insulin was added to the cells at a final concentration of 0.1 μM. After the indicated time periods, insulin was removed by two washes in 50 mM Hepes, pH 7.5, 150 mM NaCl, 10 mM EDTA, 10 mM Na$_4$P$_2$O$_7$, 2 mM sodium orthovanadate, 100 mM NaF (stop buffer). Cells were solubilized for 30 min on ice in the above buffer containing 1% (v/v) Triton X-100 and protease inhibitors (20 μM leupeptin, 100 units/ml aprotinin, 1 mM phenylmethylsulfonyl

fluoride). Lysates were then clarified by centrifugation at 13,000 × g for 20 min at 4 °C before being added for 4 h at 4 °C to antibodies to p125^{Fak} (1 μg/500 μg of protein) preadsorbed on protein G-Sepharose. Pellets were washed three times in 50 mM Hepes, pH 7.5, 150 mM NaCl, 0.1% (v/v) Triton X-100, and were resuspended in Laemmli sample buffer containing 3% (w/v) SDS and 5% (v/v) 2-mercaptoethanol. Proteins were analyzed by SDS-PAGE using a 7.5% resolving gel before Western blot analysis.

In some experiments, we performed immunoprecipitation using antibodies to p125^{Fak} and antibodies to paxillin mixed on protein G-Sepharose (1 and 1.5 μg/500 μg of protein, respectively).

p125^{Fak} Phosphorylation in Detached Cells—Cells were washed twice with phosphate-buffered saline (PBS) containing 1 mM EDTA, and detached gently from the dishes using a rubber policeman. They were washed once in PBS. Cells were maintained in suspension in PBS for 30 min at 37 °C before the addition of insulin (0.1 μM) for the indicated time periods. Cells were dipped into ice, centrifuged at 3,000 × g for 3 min at 4 °C, and washed twice with stop buffer. Cell solubilization and immunoprecipitation of lysates were performed as described above using antibodies to p125^{Fak} mixed or not with antibodies to paxillin.

p125^{Fak} Phosphorylation by Insulin and IGF-I Receptors in Vitro—We used 293 EBNA cells transiently transfected with the plasmids encoding wild-type or kinase-deficient p125^{Fak} (p125^{Fak}/K454R).

Cells were washed twice and solubilized in lysis buffer for 30 min on ice. Cleared lysates were incubated for 4 h at 4 °C with antibodies to p125^{Fak} (1 μg/200 μg of protein) preadsorbed on protein G-Sepharose. Pellets were washed three times in 50 mM Hepes, pH 7.5, 150 mM NaCl, 0.1% (v/v) Triton X-100, and resuspended into this buffer.

Insulin or IGF-I receptors, partially purified by chromatography on wheat germ agglutinin, were stimulated by insulin or IGF-I (0.1 μM) for 30 and 15 min, respectively. Where indicated, insulin and IGF-I receptors were purified by immunoprecipitation using specific antibodies. The receptors were mixed with pellets containing the immunoprecipitated p125^{Fak}. Phosphorylation mix was added to each sample (50 mM MgCl$_2$, 60 μM [γ-^{32}P]ATP (2.5 mCi/mmol) for 15 min at 22 °C. In some experiments, the reaction was stopped by addition of 4-fold concentrated Laemmli sample buffer. In other experiments, the reaction was stopped by addition of ice-cold buffer (50 mM Hepes, pH 7.5, 150 mM NaCl, 0.1% (v/v) Triton X-100), and pellets were washed twice in this buffer before SDS-PAGE analysis.

Western Blot Analysis—Samples were submitted to one-dimensional SDS-PAGE and were then transferred to polyvinylidene difluoride membrane following the method of Towbin *et al.* (41). The membrane was blocked with saline buffer (10 mM Tris, pH 7.4, 140 mM NaCl) containing 5% (w/v) BSA for 4 h at 22 °C. Antibodies to phosphotyrosine (1 μg/ml) were added in blocking buffer for 15 h at 4 °C. Several washes were performed using the saline buffer containing 0.5% (v/v) Tween 20. Rabbit anti-mouse antibodies (1 μg/ml) were added for 1 h at 22 °C in blocking buffer, followed by several washes. The membrane was then incubated with ^{125}I-protein A (250,000 cpm/ml) for 1 h at 22 °C. After several washes, the membrane was autoradiographed.

Phosphorylation of Fak Peptide (Amino Acids 568–582)—The peptide corresponding to p125^{Fak} amino acids 568–582 (SRYMEDSTYYKASKG) was synthesized by Eurogentec (Belgium). The insulin receptor kinase activity toward this peptide was measured as follows. Partially purified insulin receptors were incubated without or with insulin (0.1 μM) for 60 min at 22 °C in a final volume of 40 μl containing 50 mM Hepes, pH 7.5, 150 mM NaCl, 0.1% (v/v) Triton X-100. Increasing peptide concentrations were added to the receptors. Phosphorylation was initiated by addition of 15 μM [γ-^{32}P]ATP (2.5 mCi/mmol), 8 mM MgCl$_2$, 4 mM MnCl$_2$. The reaction was stopped by spotting a constant volume of each sample onto phosphocellulose papers, which were dipped into 1% (v/v) orthophosphoric acid. Papers were washed extensively, and ^{32}P incorporation into the peptide was quantified by Cerenkov counting. The reaction was found to be linear for at least 2 h.

RESULTS

We wished to investigate whether the effect of insulin on p125^{Fak} phosphorylation depends on cellular adhesion. To test this, we compared attached RHIR (Rat-1 fibroblasts overexpressing the insulin receptor) with RHIR in suspension, a condition that causes disassembly of focal adhesion plaques and p125^{Fak} dephosphorylation. Tyrosine phosphorylation of p125^{Fak} was revealed by immunoprecipitation using antibodies to p125^{Fak}, followed by immunoblotting with antibodies to phosphotyrosine.

INSULIN (min): 0 2 5 15 30 60 90

p125Fak →   RHIR cells

INSULIN (min): 0 5 10 15 30

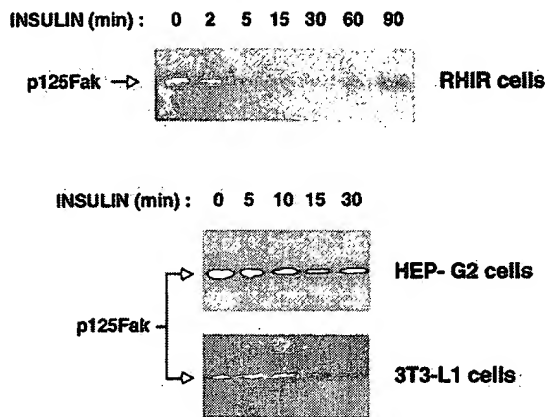p125Fak ⟨   HEP- G2 cells

            3T3-L1 cells

FIG. 1. **Insulin induces the dephosphorylation of p125^{Fak} in attached cells.** Cells were stimulated by insulin (0.1 μM) for different periods and solubilized. Lysates were submitted to immunoprecipitation using anti-p125^{Fak} antibodies. Tyrosine-phosphorylated proteins were revealed by anti-phosphotyrosine immunoblotting. Representative experiments are shown. *Top panel* shows results from RHIR cells, whereas *middle* and *bottom panels* represent Hep G2 hepatocytes and 3T3-L1 adipocytes, respectively.

In attached RHIR cells (Fig. 1, *top panel*), insulin induced rapid dephosphorylation of p125^{Fak}. These data are in accordance with previous studies reporting p125^{Fak} dephosphorylation in response to insulin in quiescent cultures of fibroblasts or CHO cells (21–23, 42). No effect could be seen in parental cells, or in cells expressing kinase-deficient insulin receptors, indicating that p125^{Fak} dephosphorylation is due to overexpression of a functional insulin receptor (data not shown). To determine if the effect of insulin on p125^{Fak} phosphorylation is also observed in cells that express physiological levels of endogenous insulin receptors, we performed similar experiments in 3T3-L1 adipocytes and in Hep G2 hepatocytes (Fig. 1, *middle* and *bottom panels*). As shown, insulin stimulation of Hep G2 hepatocytes and 3T3-L1 adipocytes also resulted in dephosphorylation of p125^{Fak}.

Fig. 2 shows experiments in which cells were gently detached, maintained in suspension for 30 min, and subsequently stimulated with insulin. In these conditions, we observed only a weak phosphorylation of p125^{Fak} in unstimulated cells. Interestingly, insulin induced an increase in tyrosine phosphorylation of p125^{Fak}, both in RHIR and in Hep G2 hepatocytes. Phosphorylation of p125^{Fak} was undetectable in nonattached 3T3-L1 adipocytes, although this could be due to low levels of protein expression (data not shown).

Quantification of p125^{Fak} phosphorylation was performed to compare the time-courses (Fig. 3). Dephosphorylation of p125^{Fak} in attached RHIR cells was maximal at 15 min and returned to initial phosphorylation level within 2 h. The decrease in p125^{Fak} phosphorylation reached 67.5 ± 5% of control after 15 min of insulin treatment. The time dependence shown here is consistent with previously published results (21). No major difference was observed between the three cell lines (see Fig. 1). In contrast, the time course of p125^{Fak} phosphorylation in detached cells was different in RHIR and Hep G2 cells. Indeed, stimulation was observed within 2 min and was maximal between 5 and 10 min in RHIR cells. At 5 min, we measured a 4-fold induction of p125^{Fak} phosphorylation. Phosphorylation decreased rapidly and returned to basal levels within 30 min. In Hep G2 hepatocytes, p125^{Fak} phosphorylation reached its maximal level after 30 min (6-fold induction), but fully persisted until at least 60 min.

As a whole, our data indicate that the effect of insulin on the phosphorylation of p125^{Fak} is regulated by integrin engage-
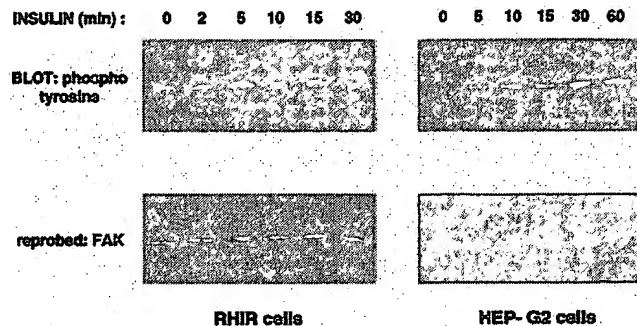
INSULIN (min): 0 2 5 10 15 30   0 5 10 15 30 60

BLOT: phospho tyrosine

reprobed: FAK

RHIR cells   HEP- G2 cells

FIG. 2. **Insulin stimulates p125^{Fak} tyrosine phosphorylation in nonattached RHIR cells and Hep G2 hepatocytes.** Cells were gently detached from the culture dishes and maintained in suspension for 30 min before addition of insulin (0.1 μM) for the indicated periods. Cells were dipped into ice and washed twice with ice-cold buffer before solubilization. Lysates were submitted to immunoprecipitation using anti-p125^{Fak} antibodies. Tyrosine phosphorylation of p125^{Fak} was visualized by anti-phosphotyrosine immunoblotting. The amount of immunoprecipitated p125^{Fak} was checked by reprobing the membranes with antibodies to p125^{Fak}. Representative experiments are shown.
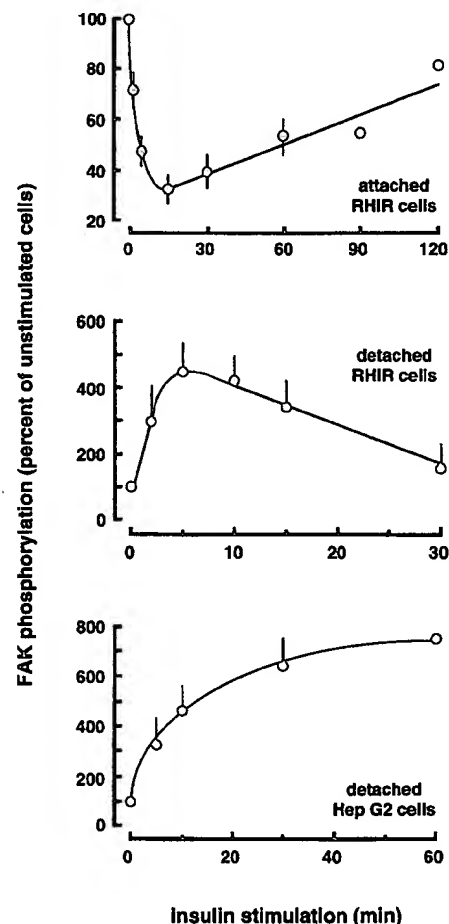

Insulin stimulation (min)

FIG. 3. **The effect of insulin on p125^{Fak} phosphorylation depends on cell adhesion.** Results were quantified using the Molecular Imager system from Bio-Rad. Values are the mean ± S.E. of several independent experiments and are expressed as percent of p125^{Fak} phosphorylation in absence of insulin.

ment. Interestingly, insulin has opposite effects compared with other growth factors such as bombesin, which induces p125^{Fak} phosphorylation in attached cells but not in cells maintained in suspension (43).

It should be noted that stimulation of p125^{Fak} phosphorylation was also observed in detached NIH 3T3 cells overexpress-

FIG. 4. **The insulin receptor and IGF-I receptor stimulate** $p125^{Fak}$ **phosphorylation** *in vitro.* $p125^{Fak}$ was immunoprecipitated from unstimulated fibroblasts. Concomitantly, insulin or IGF-I receptors were immunoprecipitated using specific antibodies and incubated or not with insulin or IGF-I (0.1 μM). After several washes, pellets containing $p125^{Fak}$ were mixed with pellets containing one receptor. Phosphorylation was initiated by addition of 15 μM [γ-^{32}P]ATP, 4 mM MnCl$_2$, 8 mM MgCl$_2$ for 15 min at 22 °C when using the insulin receptor. The phosphorylation mixture consisted in 60 μM ATP and 50 mM MgCl$_2$ when using the IGF-I receptor. The reaction was stopped by addition of Laemmli sample buffer. The samples were analyzed by SDS-PAGE and autoradiographed. Standard molecular weights are indicated on the *right*.
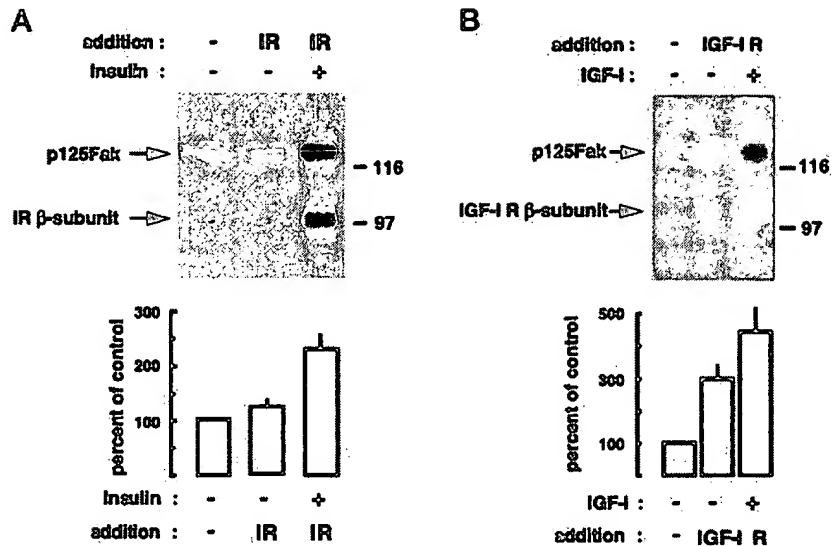

ing IGF-I receptors, whereas dephosphorylation was observed in attached cells, indicating that insulin and IGF-I have similar effects (data not shown).

We were then interested to approach the mechanism of $p125^{Fak}$ phosphorylation seen in cells exposed to insulin or IGF-I. The simplest explanation could be that, in these cells, $p125^{Fak}$ is directly activated by insulin or IGF-I receptors, leading to its autophosphorylation. To test this, $p125^{Fak}$ was immunoprecipitated from unstimulated cells. Concomitantly, immunopurified insulin or IGF-I receptors were activated or not by their respective ligand. The receptors and $p125^{Fak}$ were then mixed together, and [γ-^{32}P]ATP was added to the samples. As shown in Fig. 4A, autophosphorylation of $p125^{Fak}$ in the absence of insulin receptor was detected (*first lane*). The unstimulated receptor did not modify $p125^{Fak}$ phosphorylation (*second lane*). By contrast, addition of insulin-activated receptor induced a 2.3-fold increase in the level of p125-Fak phosphorylation (*third lane*). When unstimulated IGF-I receptors were used, an increase in $p125^{Fak}$ phosphorylation was observed (Fig. 4B, *second lane* compared with *first lane*). This is due to the high basal kinase activity and autophosphorylation levels of the IGF-I receptor *in vitro* that we have described previously (38). IGF-I addition to the receptor further increased $p125^{Fak}$ phosphorylation (4.4-fold stimulation compared with control). We noticed that the intrinsic kinase activity of $p125^{Fak}$ was lower using the phosphorylation mixture suitable for the IGF-I receptor (*i.e.* containing 50 mM MgCl$_2$). Therefore, further experiments using either the insulin or the IGF-I receptors were performed in these conditions.

In summary, incubation of $p125^{Fak}$ with insulin receptor or IGF-I receptor results in an enhancement of $p125^{Fak}$ phosphorylation *in vitro.* In these experiments, the proteins were immunopurified, and therefore this process is unlikely to be due to an intermediate kinase. We can probably rule out the possibility that $p125^{Fak}$ coimmunoprecipitates with Src, since it has been shown that $p125^{Fak}$ and Src are not associated in resting cells.

To determine whether this augmentation in $p125^{Fak}$ phosphorylation is due to direct phosphorylation of the protein by the receptors or to activation of $p125^{Fak}$, we constructed a kinase-deficient mutant of $p125^{Fak}$ by substitution of Lys-454 to Arg (44). We first compared the expression level and kinase activity of the mutant and wild-type proteins in transfected 293 EBNA cells. Protein expression was checked by immunoprecipitation with antibodies to $p125^{Fak}$ followed by $p125^{Fak}$ im-
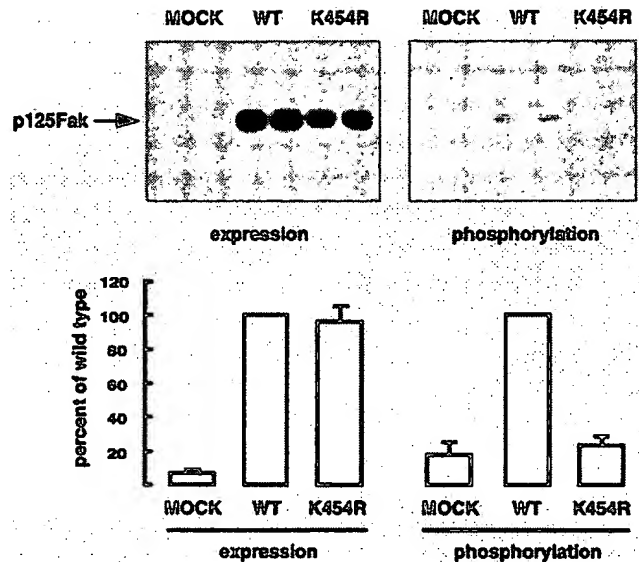
FIG. 5. **Expression and kinase activity of wild-type and kinase-deficient** $p125^{Fak}$. 293 EBNA cells were transfected 2 days before use. Cells were solubilized, and $p125^{Fak}$ was immunoprecipitated using specific antibodies. The level of protein expression was visualized by immunoblotting with antibodies to $p125^{Fak}$ (*left panel*). Autophosphorylation was measured in presence of 4 μM [γ-^{32}P]ATP and 10 mM MnCl$_2$ (*right panel*). The reaction was stopped by addition of Laemmli sample buffer for SDS-PAGE analysis.

munoblotting with antibodies to $p125^{Fak}$ (Fig. 5, *left panel*). The mock-transfected cells express low levels of endogenous $p125^{Fak}$ compared with both the wild-type and mutant-transfected cells. To measure $p125^{Fak}$ kinase activity, the proteins immunoprecipitated from transfected cells were submitted to autophosphorylation (Fig. 5, *right panel*). As expected, the wild-type protein was markedly phosphorylated, whereas the mutant protein did not show detectable kinase activity. Next, we looked for direct phosphorylation of the mutant $p125^{Fak}$ by the two tyrosine kinase receptors. The kinase-deficient $p125^{Fak}$ was overexpressed in 293 cells and immunoprecipitated with antibodies to $p125^{Fak}$. Insulin receptors or IGF-I receptors, stimulated or not, were added to the $p125^{Fak}$-containing pellets. Phosphorylation was performed using [γ-^{32}P]ATP. After extensive washes, the proteins were analyzed by SDS-PAGE (Fig. 6). Since this $p125^{Fak}$ is kinase-deficient, no phosphoryl-
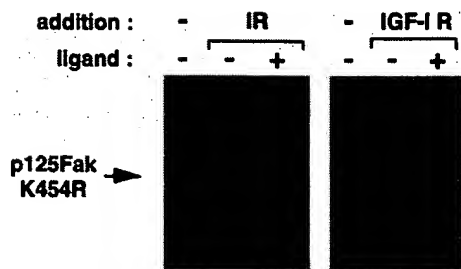
FIG. 6. **Kinase-deficient p125^{Fak}(K454R) is an *in vitro* substrate of the insulin receptor and the IGF-I receptor kinases.** 293 EBNA cells were transfected with the plasmid encoding p125^{Fak} mutated at lysine 454 (K454R). After 2 days, cells were lysed and p125^{Fak}/K454R was immunoprecipitated using antibodies to p125^{Fak}. Insulin or IGF-I receptors, stimulated or not by their respective ligand, were added to the washed pellets containing p125^{Fak}. Phosphorylation was initiated by addition of 60 μM [γ-^{32}P]ATP and 50 mM $MgCl_2$. The reaction was stopped by addition of ice-cold buffer and the pellets were washed twice. Samples were analyzed by SDS-PAGE.

FIG. 7. **A peptide corresponding to p125^{Fak} sequence amino acids 568–582 is phosphorylated by the insulin receptor.** Insulin receptors were incubated without (O) or with (●) insulin (0.1 μM). The following peptide concentrations were added to the receptors: 20, 40, 60, 80, 160, and 320 μM. Phosphorylation was performed in the presence of [γ-^{32}P]ATP. Samples were analyzed using a filter paper assay.

FIG. 8. **p125^{Fak} phosphorylation by the insulin receptor is inhibited by addition of the peptide corresponding to p125^{Fak} sequence amino acids 568–582.** p125^{Fak} was immunoprecipitated from transfected 293 cells and mixed with the insulin receptor in the absence or in the presence of increasing peptide concentrations for 90 min at 4 °C. Insulin (0.1 μM) was then added and phosphorylation was performed in the presence of 60 μM [γ-^{32}P]ATP, 50 mM $MgCl_2$. The reaction was stopped by addition of ice-cold buffer, and the pellets were washed twice. Phosphorylation of p125^{Fak} was detected by Western blotting with antibodies to phosphotyrosine. We show a representative experiment of four experiments, each run in duplicate.

ation was detected in absence of receptors, or in presence of unstimulated receptors. However, phosphorylation of the kinase-dead protein occurred upon addition of ligand-stimulated receptors. Our results indicate that p125^{Fak} is a direct substrate for the insulin and IGF-I receptors, at least *in vitro*. In some experiments, partially purified receptors were used, whereas in others, receptors were immunoprecipitated using specific antibodies. No difference concerning the extent of p125^{Fak} phosphorylation was observed between these procedures.

That p125^{Fak} is a direct substrate for insulin and IGF-I receptors is further supported by the observation that a synthetic peptide corresponding to p125^{Fak} sequence can be phosphorylated by the insulin receptor. The sequence of p125^{Fak} contains two twin tyrosine residues, Tyr-576 and Tyr-577, which are localized in the regulatory loop of its kinase domain and are phosphorylated by the Src kinase both *in vitro* and *in vivo* (45). The peptide corresponding to p125^{Fak} amino acids 568–582, containing tyrosines 570, 576, and 577, was synthesized and used in an *in vitro* kinase assay with the insulin receptor. As shown in Fig. 7, the peptide was heavily phosphorylated by the insulin-stimulated receptor. For each experiment, a Lineweaver-Burk plot was obtained using a computer program for calculation of the best fit of the points. We calculated a K_m = 184 ± 4 μM in the presence of insulin. For comparison, we previously obtained a K_m = 120 μM using a common substrate of the insulin receptor, *i.e.* a synthetic peptide corresponding to the receptor sequence 1142–1158, which also contains three tyrosine residues (46). Another peptide corresponding to p125^{Fak} amino acids 369–406, which contains p125^{Fak} major autophosphorylation site Tyr-397, was tested in a similar kinase assay. However, we did not detect phosphorylation of this peptide by the insulin receptor (data not shown), suggesting that phosphorylation of p125^{Fak} peptide 568–582 by the receptor is specific.

We hypothesized that incubation of this peptide with the insulin receptor would block p125^{Fak} phosphorylation by the receptor. Thus, immunopurified p125^{Fak} from overexpressing cells was incubated with or without the insulin receptor, in the presence of increasing peptide concentrations. Phosphorylation was measured by Western blotting with anti-phosphotyrosine antibodies. Fig. 8 shows that p125^{Fak} peptide (568–582) inhibits p125^{Fak} phosphorylation by the insulin receptor. Inhibition was nearly complete (almost 80%) at 250 μM peptide. We conclude from these experiments that the peptide competes with p125^{Fak} for phosphorylation by the insulin receptor.

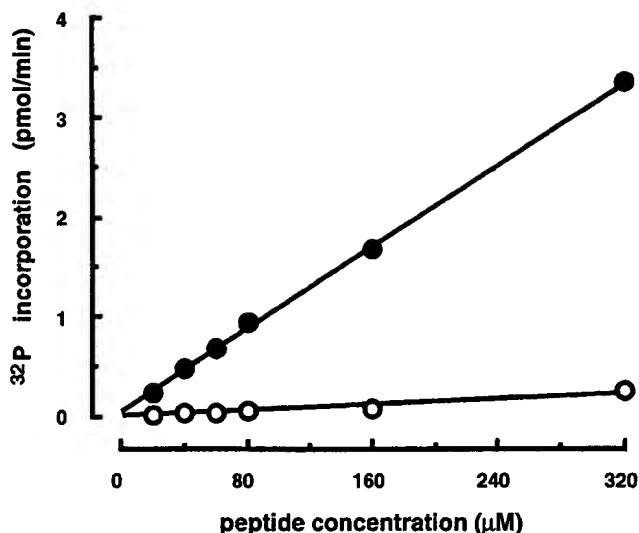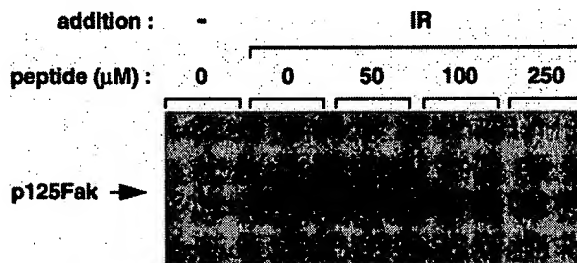Phosphorylation of p125^{Fak} on tyrosines 576 and 577 by the

Src kinase has been shown to activate p125^{Fak} enzymatic activity (45). Therefore, we tested the possibility that p125^{Fak} phosphorylation by the insulin receptor could result in its activation. Overexpressed wild-type p125^{Fak} was immunoprecipitated from 293 cells before being incubated without or with receptors, activated or not. Phosphorylation was performed using nonradioactive ATP. The p125^{Fak}-containing pellets were washed extensively to remove the receptors, and the kinase activity of the protein was measured in the presence of [γ-^{32}P]ATP. The intrinsic kinase activity of p125^{Fak} (determined in the absence of the receptor) is shown in Fig. 9. Addition of unstimulated receptor did not alter p125^{Fak} kinase activity. However, phosphorylation by the ligand-stimulated receptor resulted in an increase in p125^{Fak} activity. We conclude therefore that p125^{Fak} is phosphorylated by the insulin receptor, and that this phosphorylation results, *in vitro*, in activation of its protein kinase.

To determine if, in intact cells, insulin-induced phosphorylation of p125^{Fak} results in the activation of its kinase activity, we measured in parallel the phosphorylation of p125^{Fak} and paxillin, which is thought to be a physiological substrate of

p125^{Fak} kinase. In these experiments, dual immunoprecipitation was performed using antibodies to p125^{Fak} mixed with antibodies to paxillin. In Table I, we show that phosphorylation of paxillin varied similarly to that of p125^{Fak}. Indeed, insulin induced dephosphorylation of both p125^{Fak} and paxillin in attached Hep G2 hepatocytes, whereas in suspended Hep G2 cells p125^{Fak} and paxillin phosphorylation was enhanced. We conclude, therefore, that in intact hepatocytes insulin may induce both p125^{Fak} dephosphorylation and deactivation, or p125^{Fak} phosphorylation and activation, depending on integrin engagement.

DISCUSSION

The cytosolic tyrosine kinase p125^{Fak} is thought to coordinate integrins and growth factors signaling pathways. Thus, tyrosine phosphorylation of p125^{Fak} is modulated both by cell adhesion and by growth factor treatment.

Cross-talk between integrin and insulin signalings is suggested by the finding that insulin stimulation of DNA synthesis is modulated by engagement of $\alpha_v\beta_3$ integrin. Moreover, in this system, insulin promotes association of IRS-1 with the integrin (36). Finally, tyrosine-phosphorylated insulin receptors rapidly associate integrins at focal adhesion contacts (47).

In this paper, we present evidence that cell adhesion regulates the effect of insulin on p125^{Fak} phosphorylation. This was observed in Rat-1 fibroblasts expressing high levels of insulin receptors, but also in Hep G2 hepatocytes and 3T3-L1 adipocytes, which are insulin-sensitive cells. Moreover, we show that insulin regulates the phosphorylation of both p125^{Fak} and paxillin. Since paxillin is thought to be a physiological substrate of p125^{Fak} tyrosine kinase, our results would indicate that p125^{Fak} is activated by insulin. Paxillin may also be phosphorylated by c-Src, which becomes activated by p125^{Fak} upon association to the autophosphorylated form of p125^{Fak}. In this case, insulin-induced phosphorylation of paxillin could reflect the activation of the p125^{Fak}-dependent signaling pathway.

Our present data, together with previously published ones, point to a complex interaction between signaling pathways of p125^{Fak} and the insulin/IGF-I receptors. A recent study has

shown that IRS-I phosphorylation by the activated insulin receptor induces its association with Csk (35). This protein is an inhibitor of c-Src, and could therefore abolish the input provided by Src. Another report indicates that SHP-2 is required for p125^{Fak} dephosphorylation (48). SHP-2 is a phosphotyrosine phosphatase, which is stimulated by insulin through its association with phosphorylated IRS-1. Thus, inhibition of Src and activation of SHP-2 could cooperate to promote p125^{Fak} dephosphorylation.

Alternatively, we show that p125^{Fak} can also be a substrate for the insulin/IGF-I receptor kinases. Indeed, we found that (i) kinase-deficient p125^{Fak} is directly phosphorylated by insulin and IGF-I receptors *in vitro*, and (ii) a peptide corresponding to p125^{Fak} sequence amino acids 568–582 is phosphorylated by the insulin receptor. Moreover, this peptide inhibits phosphorylation of p125^{Fak} by the insulin receptor. p125^{Fak} sequence amino acids 568–582 is localized in the kinase domain regulatory loop, which corresponds to the subdomain VII highly conserved among tyrosine kinases (49). It contains the kinases' consensus motif VXXXDFG, and two twin tyrosines, 576 and 577. Tyrosine 576 corresponds to tyrosine 416 of the Src kinase, which is involved in regulation of Src catalytic activity (50, 51). The two tyrosine residues present in this subdomain are also found in one group of tyrosine kinase receptors, including the insulin and IGF-I receptors, Met, and Trk. Interestingly, these twin tyrosines are involved in regulation of the receptors' enzymatic activity. Autophosphorylation on these sites is correlated with increased kinase activity, and their mutation severely impairs this kinase activity (52–61). Tyrosines 576 and 577 of p125^{Fak} are phosphorylated by the Src kinase, both *in vivo* and *in vitro*, a phosphorylation event that is associated with activation of p125^{Fak} kinase activity (45). Similarly, phosphorylation by the Src kinase of tyrosines 1135 and 1136 in the kinase domain regulatory loop of the IGF-I receptor correlates with receptor activation (57). Our study provides further evidence for the existence of such cross-phosphorylation resulting in activation of a protein-tyrosine kinase, since we show that p125^{Fak} is phosphorylated and stimulated by the insulin receptor.

The tyrosine kinase receptors Met and Trk both contain a kinase regulatory loop similar to that of the insulin receptor and p125^{Fak}. Met is a potent activator of p125^{Fak} in carcinoma cells, and this correlates with its effects on cellular migration (19). Hence, we suggest that transactivation of p125^{Fak} may represent a common capability of this family of tyrosine kinase receptors.

IGF-I/insulin-induced dephosphorylation of p125^{Fak} depends on integrin engagement, since it does not occur in cells that are not in an adhesion state. It is not clear which integrin(s) mediate(s) this response, but we hypothesize that, depending on which integrins are engaged, IGF-I/insulin-induced dephosphorylation of p125^{Fak} may or may not occur. In contrast, phosphorylation of p125^{Fak} in response to insulin or IGF-I is independent of integrin engagement. In our study, cell adhesion was disrupted by maintaining cells in suspension. Although this might correspond to an artificial system, it is a
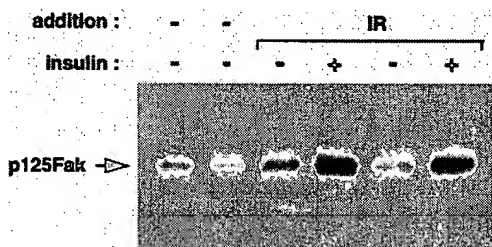

addition :   –   –   IR

insulin :   –   –   –   +   –   +

p125Fak →

FIG. 9. **p125^{Fak} phosphorylation by the insulin receptor stimulates its kinase.** Wild-type p125^{Fak} was immunoprecipitated from transfected 293 cells and mixed with the insulin receptor. Phosphorylation was performed in the presence of 60 μM nonradioactive ATP and 50 mM MgCl$_2$. Pellets were washed six times to remove the receptor. p125^{Fak} kinase activity was then measured in presence of 4 μM [γ-^{32}P]ATP and 10 mM MnCl$_2$. The reaction was stopped by addition of Laemmli sample buffer before SDS-PAGE analysis.

TABLE I
Paxillin phosphorylation correlates with p125^{Fak} phosphorylation in intact cells

Hep G2 hepatocytes were left attached or were detached before insulin stimulation for various times and solubilization. Immunoprecipitation was performed using antibodies to p125^{Fak} and antibodies to paxillin mixed on protein G-Sepharose. Tyrosine-phosphorylated proteins were revealed by immunoblotting using antibodies to phosphotyrosine. Two independent experiments were quantified by the Molecular Imager System.

Hep G2	Phosphorylation in attached cells stimulated with insulin for:					Phosphorylation in detached cells stimulated with insulin for:				
	0 min	5 min	10 min	15 min	30 min	0 min	5 min	10 min	15 min	30 min
p125Fak	100	85.9	55.7	40.4	54.5	100	252	814	768	1721
Paxillin	100	111.6	74.5	51.2	71.3	100	224	418	356	676

powerful way to study a particular cell response without interference of adhesion-mediated signals. Although complete suspension is unlikely to occur in most cells, adhesion-dependent responses will vary depending on which cell type is considered, which integrins are expressed, and which panel of integrins are engaged on a particular extracellular matrix. The integrin system is highly complex, and it will be necessary to decipher all signals transmitted by each integrin to obtain a comprehensive picture of the possible cooperations with hormone and growth factors signals.

We propose that, under particular cellular circumstances, the integrins, which control IGF-I- or insulin-induced dephosphorylation of Fak, will not be expressed or activated. In this case, only phosphorylation will occur, since this signal is independent from integrin engagement. This hypothesis is supported by recent work of Leventhal *et al.* (62), who reported IGF-I stimulation of p125^{Fak} phosphorylation in SH-SY5Y neuronal cells associated with IGF-I-induced morphological changes and cell motility. Although this is in contrast with our observation of p125^{Fak} dephosphorylation in attached fibroblasts overexpressing IGF-I receptors, it supports the idea that IGF-I is also able to stimulate p125^{Fak} phosphorylation depending on the cellular context. This apparent difference may be due to the type of cell system used, or to the specific integrin involved in the motility of SH-SY5Y neuronal cells. Another type of modified cell situation is found in transformed cells, which migrate to different locations and metastasize. Interestingly, insulin or IGF-I treatment also appears to play an active role in dissemination of certain tumor cells, in combination with $\alpha_v\beta_5$ integrin (37).

To conclude, our data provide evidence that, in intact cells, insulin and IGF-I are able to induce p125^{Fak} phosphorylation and activation, a result that would be compatible with a situation of positive cooperation between insulin/IGF-I and integrin signaling pathways. Moreover, cell adhesion appears to control the effect of insulin and IGF-I on p125^{Fak}-dependent signaling pathways. We propose therefore that hormone/growth factor responses should be considered in a global cellular context, which has to take into account other cooperating sytems such as adhesion-dependent signaling systems.
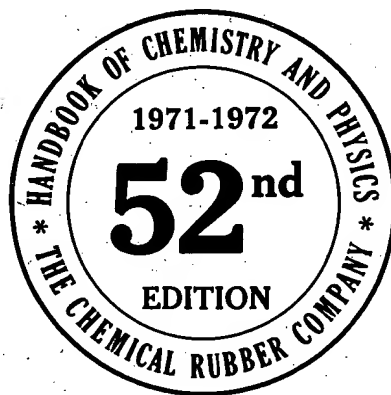
REFERENCES

1. Schaller, M. D., Borgman, C. A., Cobb, B. S., Vines, R. R., Reynolds, A. B., and Parsons, J. T. (1992) *Proc. Natl. Acad. Sci. U. S. A.* **89,** 5192–5196
2. Hanks, S. K., Calalb, M. B., Harper, M. C., and Patel, S. K. (1992) *Proc. Natl. Acad. Sci. U. S. A.* **89,** 8487–8491
3. Richardson, A., and Parsons, J. T. (1995) *BioEssays* **17,** 229–236
4. Craig, S. W., and Johnson, R. P. (1996) *Curr. Opin. Cell Biol.* **8,** 74–85
5. Parsons, J. T. (1996) *Curr. Opin. Cell Biol.* **8,** 146–152
6. Yamada, K. M., and Miyamoto, S. (1995) *Curr. Opin. Cell Biol.* **7,** 681–689
7. Burridge, K., Turner, C. E., and Romer, L. H. (1992) *J. Cell Biol.* **119,** 893–903
8. Guan, J.-L., and Shalloway, D. (1992) *Nature* **358,** 690–692
9. Kornberg, L., Earp, H. S., Parsons, T. J., Schaller, M., and Juliano, R. L. (1992) *J. Biol. Chem.* **267,** 23439–23442
10. Clark, E. A., and Brugge, J. S. (1995) *Science* **268,** 233–239
11. Zachary, I., and Rozengurt, E. (1992) *Cell* **71,** 891–894
12. Zachary, I., Sinnet-Smith, J., and Rozengurt, E. (1992) *J. Biol. Chem.* **267,** 19031–19034
13. Lipfert, L., Haimovich, B., Shaller, M. D., Cobb, B. S., Parsons, T. J., and Brugge, J. S. (1992) *J. Cell Biol.* **119,** 905–912
14. Seufferlein, T., and Rozengurt, E. (1994) *J. Biol. Chem.* **269,** 27610–27617
15. Kumagai, N., Mori, N., Fujisawa, K., Yoshimasa, T., Nakao, K., and Narumiya, S. (1993) *FEBS Lett.* **329,** 273–276
16. Hordijk, P. L., Verlaan, I., van Corven, E. J., and Moolenaar, W. H. (1994) *J. Biol. Chem.* **269,** 645–651
17. Seufferlein, T., and Rozengurt, E. (1994) *J. Biol. Chem.* **269,** 9345–9351
18. Chen, H.-C., and Guan, J.-L. (1994) *J. Biol. Chem.* **269,** 31229–31233
19. Matsumoto, K., Matsumoto, K., Nakamura, T., and Kramer, R. H. (1994) *J. Biol. Chem.* **269,** 31807–31813
20. Rankin, S., and Rozengurt, E. (1994) *J. Biol. Chem.* **269,** 704–710
21. Knight, J. B., Yamauchi, K., and Pessin, J. E. (1995) *J. Biol. Chem.* **270,** 10199–10203
22. Pillay, T. S., Sasaoka, T., and Olefsky, J. M. (1995) *J. Biol. Chem.* **270,** 991–994
23. Konstantopoulos, N., and Clark, S. (1996) *Biochem. J.* **314,** 387–390
24. Ebina, Y., Ellis, L., Jarnagin, K., Edery, M., Graf, L., Clauser, E., Ou, J.-H., Masiarz, F., Kan, Y. W., Goldfine, I. D., Roth, R., and Rutter, W. J. (1985) *Cell* **40,** 747–758
25. Ullrich, A., Bell, J. R., Chen, E. Y., Herrera, R., Petruzzelli, L. M., Dull, T. J., Gray, A., Coussens, L., Liao, Y.-C., Tsubokawa, M., Mason, A., Seeburg, P. H., Grunfeld, C., Rosen, O. M., and Ramachandran, J. (1985) *Nature* **313,** 756–761
26. White, M. F., Maron, R., and Kahn, C. R. (1985) *Nature* **318,** 183–186
27. Sun, X. J., Rothenberg, P., Kahn, C. R., Backer, J. M., Araki, E., Wilden, P. A., Cahill, D. A., Goldstein, B. J., and White, M. F. (1991) *Nature* **352,** 73–77
28. Pelicci, G., Lanfrancone, L., Grignani, F., McGlade, J., Cavallo, F., Forni, G., Nicoletti, I., Grignani, F., Pawson, T., and Pelicci, P. G. (1992) *Cell* **70,** 93–104
29. Pronk, G. J., McGlade, J., Pelicci, G., Pawson, T., and Bos, J. L. (1993) *J. Biol. Chem.* **268,** 5748–5753
30. Sun, X. J., Wang, L.-M., Zhang, Y., Yenush, L., Myers, M. J. J., Glashenn, E., and White, M. F. (1995) *Nature* **377,** 173–177
31. Holgado-Madruga, M., Emlet, D. R., Moscatello, D. K., Godwin, A. K., and Wong, A. J. (1996) *Nature* **379,** 560–564
32. White, M. F., and Kahn, C. R. (1994) *J. Biol. Chem.* **269,** 1–4
33. Myers, M. G. J., Sun, S. J., and White, M. F. (1994) *Trends Biochem. Sci.* **19,** 289–293
34. Keller, S. R., and Lienhard, G. E. (1994) *Trends Cell. Biol.* **4,** 115–119
35. Tobe, K., Sabe, H., Yamamoto, T., Yamauchi, T., Asai, S., Kaburagi, Y., Tamemoto, T., Ueki, K., Kimura, H., Akanuma, Y., Yazaki, Y., Hanafusa, H., and Kadowaki, T. (1996) *Mol. Cell. Biol.* **16,** 4765–4772
36. Vuori, K., and Ruoslahti, E. (1994) *Science* **266,** 1576–1578
37. Brooks, P. C., Klemke, R. L., Schön, S., Lewis, J. M., Schwartz, M. A., and Cheresh, D. A. (1997) *J. Clin. Invest.* **99,** 1390–1398
38. Tartare, S., Mothe, I., Kowalski-Chauvel, A., Breittmayer, J.-P., Ballotti, R., and Van Obberghen, E. (1994) *J. Biol. Chem.* **269,** 11449–11455
39. Student, A. K., Hsu, R. Y., and Lane, M. D. (1980) *J. Biol. Chem.* **255,** 4745–50
40. Chen, C., and Okayama, H. (1987) *Mol. Cell. Biol.* **7,** 2745–2752
41. Towbin, H., Staehelin, T., and Gordon, J. (1979) *Proc. Natl. Acad. Sci. U. S. A.* **76,** 4350–4354
42. Yamauchi, K., Milarski, K. L., Saltiel, A. R., and Pessin, J. E. (1995) *Proc. Natl. Acad. Sci. U. S. A.* **92,** 664–668
43. Rodriguez-Fernandez, J. L., and Rozengurt, E. (1996) *J. Biol. Chem.* **271,** 27895–27901
44. Hildebrand, J. D., Schaller, M. D., and Parsons, T. J. (1993) *J. Cell Biol.* **123,** 993–1005
45. Calalb, M. B., Polte, T. R., and Hanks, S. K. (1995) *Mol. Cell. Biol.* **15,** 954–963
46. Baron, V., Kaliman, P., Alengrin, F., and Van Obberghen, E. (1995) *Eur. J. Biochem.* **229,** 27–34
47. Schneller, M., Vuori, K., and Ruoslahti, E. (1997) *EMBO J.* **16,** 5600–5607
48. Ouwens, D. M., Mikkers, H. M. M., Van Der Zon, G. C. M., Stein-Gerlach, M., Ullrich, A., and Maasen, J. A. (1996) *Biochem. J.* **318,** 609–614
49. Hanks, S. K., Quinn, A.-M., and Hunter, T. (1988) *Science* **241,** 42–51
50. Kmiecik, T. E., and Shalloway, D. (1987) *Cell.* **49,** 69–73
51. Piwnica-Worms, H., Saunders, K. B., Roberts, T. M., Smith, A. E., and Cheng, S. H. (1987) *Cell* **49,** 75–82
52. Ellis, L., Clauser, E., Morgan, D. O., Edery, M., Roth, R. A., and Rutter, R. A. (1986) *Cell* **45,** 721–732
53. Wilden, P. A., Kahn, C. R., Siddle, K., and White, M. F. (1992) *J. Biol. Chem.* **267,** 16660–16668
54. Wilden, P. A., Siddle, K., Haring, E., Backer, J. M., White, M. F., and Kahn, C. R. (1992) *J. Biol. Chem.* **267,** 13719–13727
55. Gronborg, M., Wulff, B. S., Rasmussen, J. S., Kjeldsen, T., and Gammeltoft, S. (1993) *J. Biol. Chem.* **268,** 23435–23440
56. Kato, H., Faria, T. N., Stannard, B., Roberts, C. T. J., and LeRoith, D. (1994) *Mol. Endocrinol.* **8,** 40–50
57. Peterson, J. E., Kulik, G., Jelinek, T., Reuter, C. W. M., Shannon, J. A., and Weber, M. J. (1996) *J. Biol. Chem.* **271,** 31562–31571
58. Naldini, L., Vigna, E., Ferracini, R., Longati, P., Gandino, L., Prat, M., and Comoglio, P. M. (1991) *Mol. Cell. Biol.* **11,** 1793–1803
59. Mitra, G. (1991) *Oncogene* **6,** 2237–2241
60. Middlemas, D. S., Meisenhelder, J., and Hunter, T. (1994) *J. Biol. Chem.* **269,** 5458–5466
61. Cunningham, M. E., Stephens, R. M., Kaplan, D. R., and Greene, L. A. (1997) *J. Biol. Chem.* **272,** 10957–10967
62. Leventhal, P. S., Shelden, E. A., Kim, B., and Feldman, E. L. (1997) *J. Biol. Chem.* **272,** 5214–5218

Handbook

OF

Chemistry and Physics

A Ready-Reference Book of Chemical and Physical Data

1971-1972

52nd

EDITION

HANDBOOK OF CHEMISTRY AND PHYSICS

THE CHEMICAL RUBBER COMPANY

BOND LENGTHS BETWEEN CARBON AND OTHER ELEMENTS

Prepared by Olga Kennard.

The tables are based on bond distance determinations, by experimental methods, mainly X-ray and electron diffraction, and include values published up to January 1, 1956. In the present tables, for the sake of completeness individual values of bond distances of lower accuracy are quoted with limits of error indicated where possible. Values for tungsten and bismuth should be treated with particular caution.

According to the statistical theory of errors if an average quantity $\bar{\mu}$ and a standard deviation σ can be evaluated there is a 95% probability that the true value lies within the interval $\bar{\mu} \pm 2\sigma$. Too much reliance should, however, not be placed on σ values in bond distance determinations since the derivation of these certain sources of error may have been neglected.

Values are given in Ångstrom units and limits of error quoted in units in the last place thus: $2.07 \pm = 2.07 \pm 0.01$.

Reproduced by permission from International Tables for X-ray Crystallography.

BOND LENGTHS BETWEEN CARBON AND OTHER ELEMENTS
Reference: HCP and "Tables of interatomic distances" Chem. Soc. of London, 1958

Group	Bond type	Element						
I	All types	H** 1.056 — 1.115						
II		Be 1.93	Hg 2.07 ± 0.01					
III		B 1.56 ± 0.01	Al 2.24 ± 0.04	In 2.16 ± 0.04				
IV	All types Alkyls (CH₃XH₃) Aryl (C₆H₅XH₃) Neg. Subst. (CH₃XCl₃)	C** 1.54 — 1.20	Ge 1.98 ± 0.03	Si 1.865 ± 0.008 1.84 ± 0.01 1.88 ± 0.01	Sn 2.143 ± 0.008 2.18 ± 0.02	Pb 2.29 ± 0.05		
V	All types Paraffinic (CH₃)₃X	N** 1.47 — 1.1	P 1.87 ± 0.02	As 1.98 ± 0.02	Sb 2.202 ± 0.016	Bi 2.30*		
VI		O** 1.43 — 1.15	S** 1.81 — 1.55	Cr 1.92 ± 0.04	Se 1.98 — 1.71	Te 2.05 ± 0.14	Mo 2.08 ± 0.04	W 2.06 ± 0.01*
VII	Paraffinic (monosubstituted) (CH₃X) Paraffinic (disubstituted) (CH₂X₂) Olefinic (CH₂:CHX) Aromatic (C₆H₅X) Acetylenic (HC:CX)	F 1.381 ± 0.005 1.334 ± 0.004 1.32_5 ± 0.1 1.30 ± 0.01	Cl 1.767 ± 0.002 1.767 ± 0.002 1.72 ± 0.01 1.70 ± 0.01 1.635 ± 0.004	Br 1.937 ± 0.003 1.937 ± 0.003 1.89 ± 0.01 1.85 ± 0.01 1.79_5 ± 0.01	I 2.13_5 ± 0.01 2.13_5 ± 0.1 2.092 ± 0.005 2.05 ± 0.01 1.99 ± 0.02			
VIII		Fe 1.84 ± 0.02	Co 1.83 ± 0.02	Ni 1.82 ± 0.03	Pd 2.27 ± 0.04			

* Error uncertain.
** See following individual tables.

CARBON-CARBON

Single Bond

Paraffinic	1.541	± 0.003
In diamond (18°C)	1.54452	± 0.00014

Partial Double Bond

(1) Shortening of single bond in presence of carbon carbon double bond, e.g. $(CH_3)_2$C:CH₂; or of aromatic ring e.g. C₆H₅.-CH₃ — 1.53 ± 0.01
(2) Shortening in presence of a carbon oxygen double bond e.g. CH₃CHO — 1.516 ± 0.005
(3) Shortening in presence of two carbon-oxygen double bonds, e.g. (CO₂H)₂ — 1.49 ± 0.01
(4) Shortening in presence of one carbon-carbon triple bond, e.g. CH₃.C:CH — 1.460 ± 0.003
(5) In compounds with tendency to dipole formation, e.g. C:C.C:N — 1.44 ± 0.01
(6) In graphite (at 15°C) — 1.4210 ± 0.0001
(7) In aromatic compounds — 1.395 ± 0.003
(8) In presence of two carbon carbon triple bonds, e.g. HC:C.C:CH — 1.373 ± 0.004

Double Bond

(1) Simple — 1.337 ± 0.006
(2) Partial triple bond, e.g. CH₂:C:CH₂ — 1.309 ± 0.005

Triple Bond

(1) Simple, e.g. C₂H₂ — 1.204 ± 0.002
(2) Conjugated, e.g. CH₃.(C:C)₂.H — 1.206 ± 0.004

CARBON-HYDROGEN

(1) Paraffinic (a) in methane — 1.091
    (b) in monosubstituted carbon — 1.101 ± 0.003
    (c) in disubstituted carbon — 1.073 ± 0.004
    (d) in trisubstituted carbon — 1.070 ± 0.007
(2) Olefinic, e.g. CH₂:CH₂ — 1.07 ± 0.01
(3) Aromatic in C₆H₆ — 1.084 ± 0.006
(4) Acetylenic, e.g. CH:C.X — 1.056 ± 0.003
(5) Shortening in presence of a carbon triple bond, e.g. CH₃CN — 1.115 ± 0.004
(6) In small rings, e.g. (CH₂)₂S — 1.081 ± 0.007

CARBON-NITROGEN

Single Bond

(1) Paraffinic (a) 4 co-valent nitrogen   1.479 ± 0.005
         (b) 3 co-valent nitrogen   1.472 ± 0.005
(2) In C—N= e.g. CH_3NO_2 1.475 ± 0.010
(3) Aromatic in $C_6H_5NHCOCH_3$ 1.426 ± 0.012
(4) Snortened (partial double bond) in heterocyclic systems, e.g. C_5H_5N 1.352 ± 0.005
(5) Shortened (partial double bond) in N—C=O e.g. $HCONH_2$ 1.322 ± 0.003

Triple Bond

(1) In R.C:N   1.158 ± 0.002

CARBON-OXYGEN

Single Bond

(1) Paraffinic   1.43 ± 0.01
(2) Strained e.g. epoxides   1.47 ± 0.01
(3) Shortened (partial double bond) as in carboxylic acids or through influence of aromatic ring, e.g. salicylic acid   1.36 ± 0.01

Double Bond

(1) In aldehydes, ketones, carboxylic acids, esters   1.23 ± 0.01
(2) In zwitterion forms, e.g. DL serine   1.26 ± 0.01
(3) Shortened (partial triple bond) as in conjugated systems   1.207 ± 0.006
(4) Partial triple bond as in acyl halides or isocyanates   1.17 ± 0.01

CARBON-SULPHUR

Single Bond

(1) Paraffinic, e.g. CH_3SH 1.81(5) ± 0.01
(2) Lengthened in presence of fluorine, e.g. $(CF_3)_2S$ 1.83(5) ± 0.01
(3) Shortened (partial double bond) as in heterocyclic systems, e.g. C_4H_4S 1.73 ± 0.01

Double Bond

(1) In ethylene thiourea   1.71 ± 0.02
(2) Shortened (partial triple bond) in presence of second carbon double bond, e.g. COS   1.558 ± 0.003

BOND LENGTHS OF ELEMENTS

Element	Bond	Å
Ac	Ac—Ac	3.756
Ag (25°C)	Ag—Ag	2.8894
Al (25°C)	Al—Al	2.863
As	As—As	2.49
As₄	As—As	2.44 ± 0.03
Au (25°C)	Au—Au	2.8841
B₂	B—B	1.589
Ba (room temp.)	Ba—Ba	4.347
Be (α-form, 20°C)	Be—Be	2.2260
Bi (25°C)	Bi—Bi	3.09
Br₂	Br—Br	2.290
Ca (α-form, 18°C)	Ca—Ca	3.947 (f.c.c.)
(β-form, 500°C		3.877 (b.c.c.)
Cd (21°C)	Cd—Cd	2.9788
Cl₂	Cl—Cl	1.988
Ce	Ce—Ce	3.650
Co (18°C)	Co—Co	2.5061
Cr (α-form, 20°C)	Cr—Cr	2.4980
(β-form, >1850°C		2.61
Cs (−10°C)	Cs—Cs	5.309
Cu (20°C)	Cu—Cu	2.5560
Dy	Dy—Dy	3.503

Element	Bond	Å
Er	Er—Er	3.468
Eu	Eu—Eu	3.989
F₂	F—F	1.417 ± 0.001
Fe (α-form, 20°C)	Fe—Fe	2.4823 (b.c.c.)
(γ-form, 916°C)		2.578 (f.c.c.)
(δ-form, 1394°C)		2.539 (b.c.c.)
Ga (20°C)	Ga—Ga	2.442
Gd (20°C)	Gd—Gd	3.573
Ge (20°C)	Ge—Ge	2.4498
H₂	H—H in H₂	0.74611
	H—D in HD	0.74136
	D—D in D₂	0.74164
He	He—He in [He₂]⁺	1.08₀
Hf (α-form, 24°C)	Hf—Hf	3.1273 (h.c.p.)
Hg (−46°C)	Hg—Hg	3.005
Ho	Ho—Ho	3.486
I₂	I—I	2.662
In (20°C)	In—In	3.2511
Ir (room temp.)	Ir—Ir	2.714
K (78°K)	K—K	4.544
La (α-form)	La—La	3.739 (h.c.p.)
(β-form)		3.745 (f.c.c.)
Li (20°C)	Li—Li	3.0390
Lu	Lu—Lu	3.435
Mg (25°C)	Mg—Mg	3.1971
Mn (γ-form, 1095°C)	Mn—Mn	2.7311 (f.c.c.)
(δ-form, 1134°C)		2.6679 (b.c.c.)
Mo (20°C)	Mo—Mo	2.7251
N₂	N—N	1.0975₅ ± 0.0001
Na (20°C)	Na—Na	3.7157
Nb (20°C)	Nb—Nb	2.8584
Nd	Nd—Nd	3.628
Ni (18°C)	Ni—Ni	2.4916
Np (α-form, 20°C)	Np—Np	2.60 (orthorhombic)
(β-form, 313°C)		2.76 (tetragon.)
(γ-form, 600°C)		3.05 (b.c.c.)
O₂	O—O	1.208
O₃ angle 116.8 ± 0.5°		1.278 ± 0.003
Os (20°C)	Os—Os	2.6754
P black	P—P	2.18
P₄	P—P	2.21 ± 0.02
Pa	Pa—Pa	3.212
Pb (25°C)	Pb—Pb	3.5003
Pd (25°C)	Pd—Pd	2.7511
Po (α-form, 10°C)	Po—Po	3.345 (cubic)
(β-form, 75°C)		3.359 (rh. hedr.)
Pr (α-form)	Pr—Pr	3.640 (tetrag.)
(β-form)		3.649 (f.c.c.)
Pt (20°C)	Pt—Pt	2.746
Pu (γ-form, 235°C)	Pu—Pu	3.026 (f.c.c.)
(δ-form, 313°C)		3.279 (f.c.c.)
(ε-form, 500°C)		3.150 (b.c.c.)
Rb (20°C)	Rb—Rb	4.95
Re (room temp.)	Re—Re	2.741
Rh (20°C)	Rh—Rh	2.6901
Ru (25°C)	Ru—Ru	2.6502
S₂	S—S	1.887
S₂	S—S	2.07 ± 0.02
Sb (25°C)	Sb—Sb	2.90
Sc (room temp.)	Sc—Sc	3.212
Se (20°C)	Se—Se	2.321
Se₂	Se—Se	2.152 ± 0.003
Se₃	Se—Se	2.32 ± 0.003
Si (20°C)	Si—Si	2.3517
Sn (α-form, 20°C)	Sn—Sn diamond type lattice	2.8099
(β-form, 25°C)		3.022 (tetrag.)
Sr (α-form, 25°C)	Sr—Sr	4.302 (f.c.c.)
(β-form, 248°C)		4.32 (h.c.p.)
(γ-form, 614°C)		4.20 (b.c.c.)
Ta (20°C)	Ta—Ta	2.86
Tb	Tb—Tb	3.525
Tc (room temp.)	Tc—Tc	2.703
Te (25°C)	Te—Te	2.864
Th (α-form, 25°C)	Th—Th	3.595 (f.c.c.)
(β-form, 1450°C)		3.56 (b.c.c.)
Ti (α-form, 25°C)	Ti—Ti	2.8956 (h.c.p.)
(β-form, 900°C)		2.8636 (b.c.c.)
Tl (α-form, 18°C)	Tl—Tl	3.4076 (h.c.p.)
(β-form, 262°C)		3.362 (b.c.c.)
Tm	Tm—Tm	3.447
U (α-form)	U—U	2.77
(β-form, 805°C)		3.058 (b.c.c.)
V (30°C)	V—V	2.6224
W (25°C)	W—W	2.7409
Y	Y—Y	3.551
Yb	Yb—Yb	3.880
Zn (25°C)	Zn—Zn	2.6694
Zr	Zr—Zr	3.179

The Active Site Substrate Specificity of Protein Kinase C*

Young-Guen Kwon, Marianne Mendelow, and David S. Lawrence‡

From the Departments of Chemistry and Medicinal Chemistry, Acheson Hall, State University of New York, Buffalo, New York 14214

The active site substrate specificity of protein kinase C (PKC) has been evaluated. Like the cAMP-dependent protein kinase (PKA), PKC will efficiently phosphorylate achiral residues attached to an active site-directed peptide. In contrast, PKC exhibits behavior that is dramatically different from PKA with respect to the phosphorylation of α-substituted alcohols. Although PKA will only phosphorylate residues that contain the same stereochemistry as that found in L-serine, PKC will phosphorylate α-configurational isomers that correspond to both the L- and D-stereoisomers. The possible structural basis for the "dual specificity" of PKC is explored. In an analogous vein, although β-substituted alcohols that serve as PKA substrates must contain the same stereochemistry as that present in L-threonine, PKC will phosphorylate configurational isomers which correspond to both L-threonine and L-allo-threonine. The implications of these observations with respect to protein kinase inhibitor design are discussed.

Protein kinases typically catalyze phosphoryl transfer from ATP to the serine, threonine, and/or tyrosine residues contained within intact proteins. In many instances, this reaction serves to modulate the activity of the target protein (1), whereas in other cases, the newly generated phosphorylated amino acid acts as a focal point for the formation of protein-protein complexes (2). Due to the large number of protein kinases present in a typical mammalian cell and the relatively general nature of the reaction catalyzed by these enzymes, it is evident that some degree of control is required to ensure that the proper protein target undergoes phosphorylation at the appropriate point in time. In short, individual protein kinases must possess characteristic structural features which allow the catalytic activity of these enzymes to be carefully regulated. Indeed, many protein kinases are themselves substrates for other protein kinases, and consequently the phosphorylated state of the enzyme determines whether or not the protein kinase is active. Furthermore, once activated, many of these enzymes exhibit a special affinity for specific sequences of amino acids which encompass the phosphorylatable residue on the protein substrate (3). Clearly, kinase specificity may be governed by the local secondary or tertiary structure that envelops the target amino acid on the substrate as well. Evidence has also accrued which suggests that protein phosphorylation is regulated by targeting subunits, molecular entities which restrict kinases to specific microenvironments within the cell (4). In addition, there are even clearly defined critical struc-

tural variations in the catalytic core, a region of strong primary sequence homology among protein kinases (5). Key structural permutations in this region have a profound effect on the catalytic behavior of this enzyme family. For example, protein kinases are typically divided into subfamilies, those which specifically phosphorylate serine/threonine residues and those which phosphorylate tyrosine residues. The particular substrate specificity displayed by an individual protein kinase has now been linked to a critical active site residue (6). Apparently, structural variations are present in the highly conserved ATP binding region as well. For example, the staurosporine derivative, Go 6976, serves as a potent inhibitor of the protein kinase C ("PKC")[1] isozymes α and β1. In this capacity, it acts as a competitive inhibitor *versus* ATP. Yet, it fails to exert any effect on the catalytic activity of the δ, ε, and ζ isoforms (7). Observations such as these suggest that even serine/threonine-specific protein kinases may exhibit differences in terms of their active site substrate specificity. We have recently found that the cAMP-dependent protein kinase ("PKA") will phosphorylate, in addition to the standard serine and threonine amino acid moieties, a wide variety of non-amino acid hydroxyl-containing residues (8). Based upon these observations, we have been able to evaluate the general scope of the active site substrate specificity of PKA, including the effect of stereochemistry at the α and β positions of the hydroxyl-bearing residues on substrate recognition. We now report the active site substrate specificity of a second protein kinase, namely PKC. Astonishingly, PKC's active site specificity exhibits some dramatic differences from that which has been previously noted for PKA.

MATERIALS AND METHODS

All chemicals were obtained from Aldrich, except for [γ-³²P]ATP (DuPont NEN), cAMP (Fluka), protected amino acid derivatives (Advanced Chemtech and United States Biochemical Corp.), Liquiscint (National Diagnostics), and phosphatidylserine (Serdary Research Laboratory). Dialysis tubing was purchased from Fisher, CM C-50 Sephadex and GS-100 Superfine Sephadex were obtained from Pharmacia LKB Biotechnology Inc., and Affi-Gel Blue resin was acquired from Bio-Rad. Phosphocellulose P 81 paper disks were purchased from Whatman.

cAMP-dependent Protein Kinase Preparation—The catalytic subunit was purified to homogeneity using a previously described procedure (9). Purity was assessed via SDS-polyacrylamide gel electrophoresis, which displayed a single band at a molecular mass of 41 kDa. Ellman's reagent titrated the cysteine residues to 2.05–2.10 sulfhydryls/molecule of enzyme, which is in excellent agreement with previously reported studies (10) and the known primary structure of the catalytic subunit (11).

Protein Kinase C—Protein kinase C was purchased from Upstate Biotechnology Inc. The enzyme was obtained from rat brain and was purified to greater than 97% using sequential chromatography on DEAE-Sephacel, phenyl-Sepharose, and poly-L-lysine-agarose (12). The protein kinase C employed in this study is a mixture of the α, β, and γ isoforms (13).

[1] The abbreviations used are: PKC, protein kinase C; PKA, protein kinase A; MOPS, 4-morpholinepropanesulfonic acid; Boc, butoxycarbonyl.

Peptide Synthesis—Boc-Leu-Arg-Arg-Arg-Arg-Phe- and Boc-Leu-Arg(tosyl)-Arg(tosyl)-Arg-Arg-Phe-Ser(O-benzyl)- were prepared on Kaiser's oxime resin with *t*-Boc amino acids and subsequently displaced from the resin with a series of amines using previously described protocols (14–18). Leu-Arg(tosyl)-Arg(tosyl)-Arg(tosyl)-Arg(tosyl)-Phe-Ser(O-benzyl)-Gly-amide was prepared from the benzhydrylamine resin. The serine-containing peptides were then deprotected with 90% HF, 10% anisole, and extracted into 10% acetic acid and lyophilized. All of the crude peptides were subsequently partially purified via ion exchange chromatography on SP-sephadex C-25 (0.65–1.2 M NaCl gradient in a 50 mM NaOAc, pH 3.5, buffer, 300 ml total volume). The peptides were then simultaneously desalted and further purified on a preparative high performance liquid chromatography using three Waters radial compression modules (25 × 10 cm) connected in series (gradient (solvent A: 0.1% trifluoroacetic acid in water; solvent B: 0.1% trifluoroacetic acid in acetonitrile): 0–3 min (100% A); a linear gradient from 3 min (100% A) to 30 min (75% A and 25% B); a steep final linear gradient to 90% B for column cleansing purposes). All peptides gave satisfactory fast atom bombardment mass spectral analyses.

cAMP-dependent Protein Kinase Assay—Assays were performed in triplicate at pH 7.1 and thermostatted in a water bath maintained at 30 °C. Final assay volume totalled 50 µl and contained 100 mM MOPS, 150 mM KCl, 12.5 mM $MgCl_2$, 0.125 mg/ml bovine serum albumin, and 1.5 nM catalytic subunit. For the determination of kinetic constants the following concentrations were employed: 100 µM [γ-^{32}P]ATP (300 cpm/pmol) and a substrate concentration of 10–100 µM for Leu-Arg-Arg-Arg-Arg-Phe-(S-benzyl-(D)-cysteinol). Phosphorylation reactions were initiated by addition of 10 µl of catalytic subunit from a stock solution (1.5 mg/ml in 100 mM MOPS, 0 mM KCl, 1 mM dithiothreitol, and 0.125 mg/ml bovine serum albumin at pH 7.1). Reactions were terminated after 5.0 min by spotting 25-µl aliquots onto 2.1-cm diameter phosphocellulose paper disks. After 10 s the disks were immersed in 10% glacial acetic acid and allowed to soak with occasional stirring for at least 1 h. The acetic acid was decanted, and the disks were collectively washed with four volumes of 0.5% H_3PO_4, 1 volume of water, followed by a final acetone rinse. The disks were air-dried and placed in plastic scintillation vials containing 6 ml of liquiscint prior to scintillation counting for radioactivity.

Protein Kinase C Assay—These assays were performed using a slight modification of a previously published method (19). Assays were performed in triplicate at pH 7.5 and thermostatted in a water bath maintained at 30 °C. Final volume totalled 50 µl and contained 62.5 mM HEPES, 0.75 mM $CaCl_2$, 12.5 mM $MgCl_2$, 0.5 mM EGTA, 7.5 µg/ml phosphatidyl serine, and between 2.5 and 7.0 ng of protein kinase C, depending upon the efficacy of the substrate. For the determination of kinetic constants, the following concentrations were employed: 50 µM [γ-^{32}P]ATP (750–3000 cpm/pmol) and a substrate concentration that varied over a 10-fold range around the apparent K_m. Phosphorylation reactions were initiated by the addition of 10 µl of protein kinase C from a stock solution (11.0 µg/ml in 20 mM Tris·HCl, 1 mM dithiothreitol, 1 mM EDTA, and 0.75 mg/ml bovine serum albumin at pH 7.5). Reactions were terminated after 5.0–10.0 min, depending upon the efficacy of the substrate, by spotting 25-µl aliquots onto 2.1-cm diameter phosphocellulose paper disks. After 10 s the disks were immersed in 10% glacial acetic acid and allowed to soak with occasional stirring for at least 1 h. The acetic acid was decanted, and the disks were collectively washed with 4 volumes of 0.5% H_3PO_4, 1 volume of water, followed by a final acetone rinse. The disks were air-dried and placed in plastic scintillation vials containing 6 ml of liquiscint prior to scintillation counting for radioactivity.

Determination of Kinetic Constants—The apparent K_m (±S.D.) and V_{max} (±S.D.) values for all peptides were determined from initial rate experiments. The data from these experiments were plotted using the Lineweaver-Burk procedure and the corresponding plots proved to be linear in all cases.

RESULTS AND DISCUSSION

PKC is a Ca^{2+}- and phospholipid-activated protein kinase that has gained considerable notoriety by serving as the receptor for the tumor-promoting phorbol esters (20–22). Indeed, PKC is recognized to act both as an important component in normal mitogenic signaling pathways, as well as in its constitutively active state, a key factor in tumor promotion and carcinogenesis. Furthermore, researchers have noted that several lipophilic cationic compounds which impair PKC activity *in vitro* also serve to inhibit the growth of tumors *in vivo* (*e.g.* see

TABLE I
K_m and V_{max} values for previously described peptide substrates for protein kinase C

Peptide	K_m	V_{max}	Ref.
	µM	pmol/min·mg	
1) PLSRTLSVSS-amide	32.5	2.0	19
2) PLSRTLSV-amide	36.9	2.2	19
3) PLSRTLS-amide	761	0.9	19
4) PLRRTLSVAA-amide	14	1.4	19
5) PLSRRLSVAA-amide	21	1.3	19
6) KKKKKRFSFKKAFKLAGFAFKKNKK	0.05	0.62	26

Refs. 23 and 24). The proclivity of cationic species for PKC mirrors the the known substrate sequence specificity of the enzyme, which exhibits a special affinity for proteins and peptides containing serine/threonine moieties surrounded by positively charged amino acid residues (25–31). Several previously reported PKC peptide substrates, along with their K_m and V_{max} values, are provided in Table I.

Active site-directed peptides containing a range of structurally diverse alcohol-bearing residues are required in order to thoroughly analyze the active site substrate specificity of PKC. We have noted previously that there are laborious synthetic obstacles associated with the synthesis of peptides containing hypermodified amino acid residues (8). Fortunately, these difficulties can be readily circumvented by attaching the hydroxyl-bearing residue to the peptide after solid phase peptide synthesis (8). However, such an approach requires ready access to a peptide which is efficiently phosphorylated at either the N or the C terminus. While peptide 3 is phosphorylated at the C-terminal serine residue, the K_m exhibited by this substrate is unattractive for our needs. Peptide 4, which contains an Arg dyad at the P – 3/P – 4 position (*i.e.* on the N-terminal side of the serine moiety) exhibits a somewhat lower K_m than peptide 1, which contains only a single Arg residue. Similarly, peptide 5 contains an Arg dyad at the P – 2/P – 3 position and displays a modestly improved K_m versus 1 as well. Consequently, a peptide containing several contiguous basic residues could improve the efficacy of phosphorylation at the C-terminal site. The affinity of peptides for PKC may be further enhanced by the presence of a hydrophobic residue at the P – 1 site. The tertiary structure of PKA reveals that a small hydrophobic pocket (which lies just below a glycine rich loop) is positioned near the side chain of the P – 1 residue (32–36). Consequently, it is likely that the side chains of lipophilic amino acids can be inserted into this region and thereby enhance the overall interaction between substrate and enzyme. If PKC contains an analogous structural feature, then a hydrophobic residue at P – 1 would be expected to amplify the affinity of peptides for PKC as well. Consequently, we prepared the heptapeptide Leu-Arg-Arg-Arg-Arg-Phe-Ser-amide 7. This species serves as a reasonably efficient substrate (K_m of 52.1 µM and a V_{max} of 2.9 µmol/min·mg). With the parent peptide 7 in hand, we examined the active site substrate specificity of PKC. The latter was isolated from rat brain and is actually a mixture of the α, β, and γ isoforms (37). Consequently, the activities described in this paper represent the combined or "bulk" properties of these closely related PKC enzymes.

An Achiral Residue at the Phosphorylation Site Will Serve as an Efficient Substrate—We initially examined the ability of PKC to phosphorylate achiral alcohol-bearing residues. Upon treatment of the Leu-Arg-Arg-Arg-Arg-Phe-oxime resin with ethanolamine, propanolamine, and butanolamine, we obtained the corresponding derivatives 8, 9, and 10, respectively. All of these species are substrates for PKC. The K_m and V_{max} values are provided in Table II, along with the kinetic constants previously obtained for an analogous series of PKA substrates (8).

TABLE II
K_m (μM) and V_{max} ($\mu mol/min\cdot mg$) values for peptides 7–10

Kinetic constants were determined as described under "Materials and Methods." The values are given as the average ± S.D. The K_m and V_{max} values for the PKA substrates have been reported previously (8). The peptide for the PKC substrates is Leu-Arg-Arg-Arg-Arg-Phe-, whereas its counterpart for the PKA substrates is Gly-Arg-Thr-Gly-Arg-Arg-Asn-.
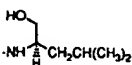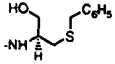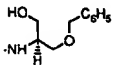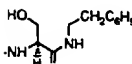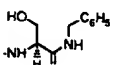
Peptide-amino alcohol	PKC		PKA	
	K_m	V_{max}	K_m	V_{max}
HO–...–NH–...–NH$_2$ (7)	52.1 ± 2.4	2.88 ± 0.10	11.8 ± 1.4	14.5 ± 0.8)
-NH-(CH$_2$)$_2$OH (8)	71.0 ± 3.4	2.07 ± 0.07	114 ± 16	8.29 ± 0.27
-NH-(CH$_2$)$_3$OH (9)	111 ± 3	0.88 ± 0.01	525 ± 37	4.84 ± 0.12
-NH-(CH$_2$)$_4$OH (10)	602 ± 167	0.14 ± 0.01	794 ± 17	0.175 ± .002

TABLE III
K_m (μM) and V_{max} ($\mu mol/min\cdot mg$) values for peptides 11–18

Kinetic constants were determined as described under "Materials and Methods." The values are given as the average ± S.D. The K_m and V_{max} values for the PKA substrates have been reported previously (8). The peptide for the PKC substrates is Leu-Arg-Arg-Arg-Arg-Phe-, whereas its counterpart for the PKA substrates is Gly-Arg-Thr-Gly-Arg-Arg-Asn-.

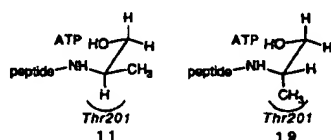| Peptide-amino alcohol	PKC		PKA	
	K_m	V_{max}	K_m	V_{max}
(11) CH$_3$	106 ± 11	2.52 ± 0.14	35.0 ± 7.0	9.73 ± 0.90
(12) CH$_2$CH$_3$	57.0 ± 7.4	1.04 ± 0.05	141 ± 3.0	19.4 ± 0.20
(13) C$_6$H$_5$	80.7 ± 4.0	0.27 ± 0.01	96.0 ± 21	16.2 ± 1.3
(14) CH$_2$CH(CH$_3$)$_2$	129 ± 17	0.072 ± 0.003	74.8 ± 2.9	6.56 ± 0.12
(15) S–C$_6$H$_5$	70.1 ± 5.0	0.58 ± 0.07	7.15 ± 0.75	20.7 ± 0.7
(16) O–C$_6$H$_5$	36.7 ± 1.7	0.90 ± 0.01	Not tested	
(17) NH–CH$_2$C$_6$H$_5$	44.3 ± 2.8	1.00 ± 0.04	Not tested	
(18) NH–C$_6$H$_5$	33.0 ± 5.5	1.91 ± 0.16	Not tested	

FIG. 1. **Proposed unfavorable steric interactions between α-substituents of the substrate and Thr-201 in the active site of the cAMP-dependent protein kinase.** Peptide 11 serves as an efficient substrate, whereas 19 fails to undergo PKA-catalyzed phosphorylation. The latter may be a consequence of disruptive steric interactions between the α-methyl substituent in the latter and the active site Thr-201 residue. Presumably, such an interaction precludes the requisite active site conformation necessary for enzyme-catalyzed phosphoryl transfer. Peptide = Gly-Arg-Thr-Gly-Arg-Arg-Asn-.

It is important to note that the PKA peptide substrates contain a primary sequence (*i.e.* Gly-Arg-Thr-Gly-Arg-Arg-Asn-amino alcohol) that differs from the PKC substrates employed in this study. Consequently, a direct comparison of the kinetic constants obtained for these two peptide series is not particularly meaningful. However, interesting trends are apparent *within* each series. For example, the PKC substrates 7, 8, and 9 exhibit very similar K_m values. In contrast, with the primary sequence employed, PKA is more sensitive to the absence of the C-terminal amide moiety (*cf.* 7 and 8; 10-fold increase in K_m) as well as to an increase in the length of the side chain (*cf.* 7 and 9; 50-fold increase in K_m) than PKC. PKC and PKA do have one property in common, namely the relatively inefficient phosphorylation of the butyl alcohol side chain of 10. However, the most significant feature of the results from Table II is the apparent general ability of protein kinases to catalyze phosphoryl transfer from ATP to an achiral residue. This has implications in terms of inhibitor design, since exceedingly simple derivatives of ethanolamine or propanolamine can now be constructed containing novel and, if necessary, hypersensitive functional groups for enzyme inhibition or inactivation.

TABLE IV

K_m (μM) and V_{max} (μmol/min-mg) values for peptides 19–22

Kinetic constants were determined as described under "Materials and Methods." The values are given as the average ± S.D. The K_m and V_{max} values for the PKA substrates have been reported previously (8). The peptide for the PKC substrates is Leu-Arg-Arg-Arg-Arg-Phe-, whereas its counterpart for the PKA substrates is Gly-Arg-Thr-Gly-Arg-Arg-Asn-.

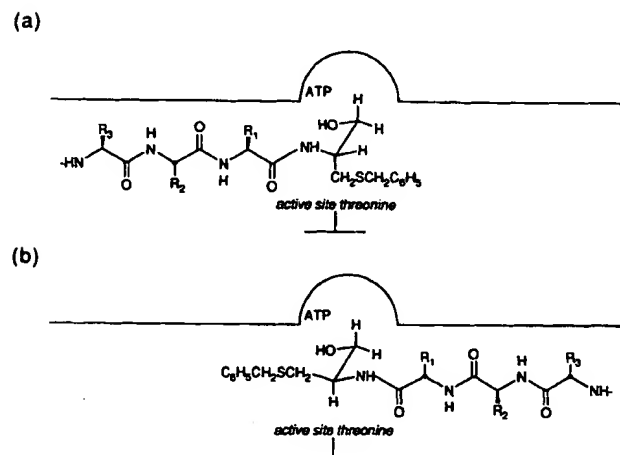| Peptide-amino alcohol	PKC		PKA	
	K_m	V_{max}	K_m	V_{max}
(19)	170 ± 21	0.067 ± 0.003	Not a substrate	
(20)	123 ± 5	0.325 ± 0.003	Not tested	
(21)	100 ± 6	0.209 ± 0.006	Not a substrate	
(22)	87.4 ± 2.9	0.297 ± 0.003	Not a substrate	

(a)

(b)

FIG. 2. **Possible orientations of peptide 22 in the active site of PKC.** *a*, the substrate binds to the enzyme in the "standard" fashion, running from N to C terminus. The active site constraints are such that, in spite of an α-center stereochemistry equivalent to D-serine, the peptide undergoes phosphorylation. *b*, the substrate binds to the enzyme in a "nonstandard" manner, running from C to N terminus. In this conformation, the stereochemistry presented to the enzyme at the α-center of the alcohol-containing residue is analogous to that present in L-serine. However, the α-stereochemistry of the other amino acid residues in the peptide is now inverted.

Substituents at the α-Position Alter the Efficacy of Phosphoryl Transfer—Hydrophobic residues are often present at the P + 1 position in PKC substrates (*e.g.* Table I). Indeed, removal of the C-terminal valine from peptide **2** results in a 20-fold increase in K_m (*cf.* peptides **2** and **3**, Table I). This suggests that hydrophobic substituents at the α-position (Table III) should improve the PKC substrate efficacy of these peptides, if the substituents are of sufficient length to occupy the adjacent P + 1 position. The α-site stereochemistry of the peptides provided in Table III corresponds to that present in L-serine (*cf.* peptide **7**). Interestingly, nearly all the compounds proved to be poorer PKC substrates than the simple unsubstituted ethanolamine derivative **8**. This is especially true of the α-C-benzyl (**13**) and α-C-isobutyl (**14**) derivatives, both of which exhibit dramatically curtailed V_{max} values. The relatively bulky α-substituents on these compounds are positioned to occupy a region in the active site normally held by the peptide amide nitrogen which

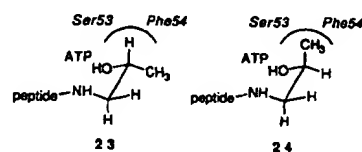FIG. 3. **Proposed unfavorable steric interactions between β-substituents of the substrate and Ser-53/Phe-54 in the active site of the cAMP-dependent protein kinase.** Peptide **23** is phosphorylated by PKA, whereas **24** is not. This may be a consequence of disruptive steric interactions between the β-methyl substituent in the latter and the active site Ser-53/Phe-54 residues. Presumably, such an interaction precludes the requisite active site conformation necessary for enzyme-catalyzed phosphoryl transfer. Peptide = Gly-Arg-Thr-Gly-Arg-Arg-Asn-.

links the P and P + 1 residues. Consequently, it is evident that the enzyme is unable to proficiently incorporate these sterically demanding substituents in this portion of the active site. The S-benzyl derivative **17** also exhibits a relatively low V_{max}. However, both the K_m and the V_{max} improve by 2-fold upon replacement of the sulfur with a smaller oxygen atom (*i.e.* **16**). Further improvement in V_{max} was realized with the benzylamine derivative **18**. Indeed, the best PKC substrates have a decidedly peptide-like structure, with an amide moiety off the α-carbon atom. However, overall the results are somewhat surprising in that even the kinetic constants associated with the phosphorylation of **18** do not represent a significant improvement over those obtained with the parent compound **7**. Indeed, the only structural difference between **7** and **18** is the presence of a hydrophobic N-benzyl moiety in the latter. One possible interpretation is that while hydrophobic substituents at the P + 1 position can improve the effectiveness of a particular substrate (*cf.* **2** and **3**), the impact that such a substituent will have on the kinetics of phosphoryl transfer may ultimately be dependent upon the primary sequence of the peptide.

The Side Chain α- and β-Configuration of the Substrate Is Not a Critical Recognition Element in Protein Kinase C-catalyzed Reactions—We have demonstrated in a series of papers that only peptides containing the proper configuration at the α-center (*i.e.* corresponding to that present in L-serine) serve as substrates for PKA (8, 37, 38). The recently solved tertiary structure of PKA offers some insight into the structural basis for this observed stereospecificity (32–36). When active site-bound, the alcohol-bearing residue on the substrate molecule

TABLE V

K_m (μM) and V_{max} ($\mu mol/min\text{-}mg$) values for peptides 23–24

Kinetic constants were determined as described under "Materials and Methods." The values are given as the average ± S.D. The K_m and V_{max} values for the PKA substrates have been reported previously (8). The peptide for the PKC substrates is Leu-Arg-Arg-Arg-Arg-Phe-, whereas its counterpart for the PKA substrates is Gly-Arg-Thr-Gly-Arg-Arg-Asn-.

Peptide-amino alcohol	PKC		PKA	
	K_m	V_{max}	K_m	V_{max}
HO–CH₃ structure (23)	107 ± 19	0.164 ± 0.007	607 ± 83	1.24 ± 0.10
HO–CH₃ structure (24)	104 ± 3	0.028 ± 0.001	Not a substrate	

lies just above Thr-201, a highly conserved residue present (as either serine or threonine) in all serine/threonine-specific protein kinases (7). In the allowed configuration, the α-hydrogen is directed toward Thr-201. In contrast, in the forbidden configuration, it is the α-alkyl substituent (shown for methyl in Fig. 1) which must be oriented toward this residue. The results suggest that, for PKA, an unfavorable steric interaction may take place in the latter case. This interaction could preclude phosphoryl transfer by interfering with the ability of the hydroxyl moiety to assume the requisite orientation in the active site. Since an active site threonine moiety (corresponding to Thr-201 in PKA) is also present in PKC, we fully expected PKC to exhibit the same pronounced substrate stereospecificity displayed by PKA. However, from Table IV it is clear that this is not the case. Although compounds 19 and 20 are significantly weaker substrates than their stereoisomeric counterparts (11 and 16, respectively), the activities of peptides 21 and 22 approach those exhibited by their corresponding analogs (13 and 15, respectively). We examined this relative lack of stereochemical preference in greater detail with the peptide pair Leu-Arg-Arg-Arg-Arg-Phe-(S-benzyl-D-cysteinol) (15) and Leu-Arg-Arg-Arg-Arg-Phe-(S-benzyl-L-cysteinol) (22). A time-dependent PKC-catalyzed phosphorylation of these compounds was performed, and as expected, alcohol 15 was phosphorylated somewhat more rapidly than its stereoisomeric counterpart (22) (data not shown). This is consistent with the relative K_m and V_{max} values obtained for these substrates. Furthermore, since PKC and PKA are known to exhibit overlapping (but not identical) sequence specificities (39), we examined the ability of Leu-Arg-Arg-Arg-Arg-Phe-(S-benzyl-D-cysteinol) (i.e. 15) to serve as a substrate for the latter. Indeed, this peptide is an excellent PKA substrate (K_m = 19.5 ± 1.6 µM and V_{max} = 5.14 ± 0.04 µmol/min-mg). In contrast, PKA failed to phosphorylate the isomeric L-cysteinol peptide to any significant extent. These results are consistent with our previous observations (8, 37–38) that the cAMP-dependent protein kinase exhibits a strict substrate specificity with respect to the α-center stereochemistry of the alcohol-bearing residue and, furthermore, demonstrates that this facet of active site specificity is dramatically different for PKC. The structural basis for the "dual specificity" of PKC is, at present, unclear. Since the sequence homology is very high among serine/threonine-specific protein kinases within the catalytic core, it has been generally assumed that the corresponding three-dimensional active site architecture would be strongly conserved as well. One obvious interpretation of these results is that there exists some catalytically significant structural differences at or near the active site regions in these enzymes. For example, we previously alluded to the possibility that Thr-201 may be responsible for the unequivocal substrate stereospecificity exhibited by PKA. Although this residue is conserved in PKC as well, it may be that its three-dimensional orientation in the active site has been subtly altered relative to

PKA such that residues containing the inverted α-configuration can bind in the conformation required for phosphoryl transfer (Fig. 2a). An alternative explanation may be related the fact that basic residues, on either the N- or C-terminal side of the site of phosphorylation, will promote the efficacy of PKC substrates. For example, Ferrari et al. (29) have shown that Gly-Ser-Arg-Arg-Arg will act as a substrate for PKC. Consequently, it is possible that the peptides from Table IV are coordinating to the enzyme, not in the expected fashion (Fig. 2a), but rather in the opposite sense (Fig. 2b). In the latter case, the residue at the phosphorylation site is now presented to the enzyme in the "allowed" stereochemical fashion. However, it is important to realize that since the peptide is running from the C to the N terminus in Fig. 2b, the stereochemistry at the α-position of the other residues in the peptide is now oriented in a manner analogous to that present in D-amino acids. Although experiments are currently in progress to address these possibilities, the salient feature is that the results from Table IV imply a novel approach to the selective inactivation of PKC. Since PKC recognizes both configurations at the α-center, whereas PKA can only process the configuration corresponding to that present in L-amino acids, it should be possible to design PKC-selective inhibitors by employing residues containing an α-stereochemistry (i.e. corresponding to D-amino acids) that cannot be accommodated by PKA.

In addition to the effect of the α-configuration on the efficacy of PKC substrates, we also examined what influence, if any, the stereochemistry at the β-center has on phosphoryl transfer. We have previously demonstrated that although PKA will phosphorylate secondary alcohols, the absolute configuration at the β-carbon must correspond to that present in threonine in order for phosphorylation to transpire (8). An analysis of PKA active site structure suggests that an alkyl substituent, positioned on the β carbon in a catalytically inappropriate configuration, may experience deleterious steric interactions with the active site residues Ser-53 and Phe-54 (Fig. 3). The latter residues are conserved in PKC as well (5). In order to address the β-stereocenter preferences of PKC, we prepared the peptides 23 and 24. The former contains the same stereochemistry as that located at the β-position in threonine, whereas the latter possesses the configuration which corresponds to that in allo-threonine. Although the K_m for 23 is not dramatically different from that obtained for 8, there is more than an order of magnitude loss in terms of V_{max} (Table V). With respect to catalytic efficiency (i.e. k_{cat}/K_m), the secondary alcohol-containing species is a 20-fold poorer substrate that its primary alcohol-bearing counterpart. This is not entirely unexpected since Kemp and his colleagues (19) have demonstrated previously that replacement of the serine residue in Pro-Leu-Ser-Arg-Thr-Leu-Ser-Val-Ala-Ala-amide with a threonine moiety reduces the catalytic potency of the peptide substrate. However, in the latter case, it is the K_m which is affected (a 4-fold increase for the threonine substrate),
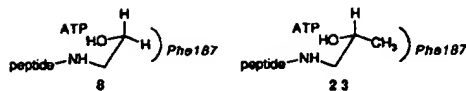
FIG. 4. **Proposed unfavorable steric interactions between β-substituents of the substrate and Phe-187 in the active site of the cAMP-dependent protein kinase.** Peptide 8 serves as an efficient PKA substrate, whereas the k_{cat}/K_m for 23 is 35-fold lower. The latter may be a consequence of disruptive steric interactions between the β-methyl substituent in the latter and the active site Phe-187 residue. Presumably, such an interaction interferes, to some extent, with the requisite active site conformation necessary for enzyme-catalyzed phosphoryl transfer. Peptide = Gly-Arg-Thr-Gly-Arg-Arg-Asn-.

whereas the V_{max} of both peptides are essentially identical. Consequently, it is likely that the ability of PKC to accommodate and subsequently phosphorylate a secondary alcohol is determined by the primary sequence of the peptide substrate. In addition, the position (*i.e.* C terminus *versus* an internal site) of the phosphorylatable residue may also influence the kinetics of phosphorylation. The relatively poor efficacy of secondary alcohols as substrates has also been observed with PKA. For example, 8 exhibits a k_{cat}/K_m 35-fold larger than that displayed by 23 (8). The tertiary structure of PKA suggests that the active site residue, Phe-187, may be the culprit responsible for the less efficient behavior of secondary alcohols (Fig. 4). The amino acid which occupies this position in PKC is methionine. Although it is tempting to ascribe an analogous active site interaction with this residue, the differing active site substrate specificities of PKA and PKC suggests that there are likely to be differences in active site architecture between these two enzymes as well. Consequently, such comparisons between even closely related enzyme species, must be viewed with caution. Finally, unlike PKA, PKC is apparently able to also phosphorylate 24, which contains the inverted stereochemistry at the β-site. However, this compound is processed very slowly, exhibiting a V_{max} of only 28 nmol/min-mg.

In summary, we have evaluated the active site substrate specificity of protein kinase C. From the results of our previous work with the cAMP-dependent protein kinase, it is now clear that the active site specificities of protein kinases are not necessarily identical. Although both enzymes only utilize serine and threonine residues as substrates in proteins, PKA and PKC exhibit differing specificities with respect to non-amino acid residues. Most notable is the ability of PKC to catalyze the phosphorylation of both α-center configurational isomers in the peptide pairs 11/19, 13/21, 15/22, and 16/20. In contrast, the specificity requirements of PKA are limited to substrates that contain the α-configuration corresponding to that present in L-serine. These results are notable for two reasons. First, since the primary sequence homologies are very high in the catalytic core among the members of the protein kinase family, it has been generally assumed that the three-dimensional active site architecture would also be highly conserved. Our results suggest that, although this is still likely to be the case, there may exist some subtle, yet catalytically significant, structural differences at or near the active site regions in these enzymes. Second, PKA and PKC do exhibit some overlapping substrate sequence specificities. Consequently, there is cause for some

anxiety concerning the ability to target peptide-based inhibitors specifically against PKC (however, see Ref. 39). However, it should now be possible to create inhibitors (*e.g.* transition state analogs, mechanism-based inhibitors, etc.) that are not directed against PKA by simply employing residues whose α-configuration is not recognized by this enzyme (*i.e.* the substrates of Table IV). These experiments are in progress.

REFERENCES

1. Krebs, E. G. (1986) *The Enzymes* 17, 3–18
2. Pawson, T., and Gish, G. D. (1992) *Cell* 71, 359–362
3. Kemp, B. E., and Pearson, R. B. (1990) *Trends Biochem. Sci.* 15, 342–346
4. Hubbard, M. J., and Cohen, P. (1993) *Trends Biochem. Sci.* 18, 172–177
5. Hanks, S. K., Quinn, A. M., and Hunter, T. (1988) *Science* 241, 42–52
6. Lindberg, R. A., Quinn, A. M., and Hunter, T. (1992) *Trends Biochem. Sci.* 17, 114–119
7. Martiny-Baron, G., Kazanietz, M. G., Mischak, H., Blumberg, P. M., Kochs, G., Hug, H., Marme, D., and Schachtele, C. (1993) *J. Biol. Chem.* 268, 9194–9197
8. Kwon, Y.-G., Mendelow, M., Srinivasan, J., Lee, T. R., Pluskey, S., Salerno, A., and Lawrence, D. S. (1993) *J. Biol. Chem.* 268, 10713–10716
9. Prorok, M., and Lawrence, D. S. (1989) *J. Biochem. Biophys. Methods* 18, 167–176
10. Armstrong, R. N., and Kaiser, E. T. (1978) *Biochemistry* 17, 2840–2845
11. Shoji, S., Ericsson, L. H., Walsh, K. A., Fischer, E. H., and Titani, K. (1983) *Biochemistry* 22, 3702–3709
12. Allen, B. G., and Katz, S. (1991) *Biochemistry* 30, 4334–4343
13. Huang, K.-P., Nakabayashi, H., and Huang, F. L. (1986) *Proc. Natl. Acad. Sci. U. S. A.* 83, 8535–8539
14. DeGrado, W. F., and Kaiser, E. T. (1980) *J. Org. Chem.* 45, 1295–1300
15. DeGrado, W. F., and Kaiser, E. T. (1982) *J. Org. Chem.* 47, 3258–3261
16. Nakagawa, S. H., and Kaiser, E. T. (1983) *J. Org. Chem.* 48, 678–685
17. Nakagawa, S. H., Lau, H. S. H., Kezdy, F. J., and Kaiser, E. T. (1985) *J. Am. Chem. Soc.* 107, 7087–7092
18. Kaiser, E. T. (1989) *Accts. Chem. Res.* 22, 47–54
19. House, C., Wettenhall, R. E. H., and Kemp, B. E. (1987) *J. Biol. Chem.* 262, 772–777
20. Nishizuka, Y. (1992) *Science* 258, 607–614
21. Rotenberg, S. A., and Weinstein, I. B. (1991) *Biochem. Mol. Aspects Sel. Cancers* 1, 25–73
22. Lester, D. S., and Epand, R. M. (eds) (1992) *Protein Kinase C. Current Concepts and Future Perspectives*, Ellis Horwood, New York
23. Rotenberg, S. A., Smiley, S., Ueffing, M., Krauss, R. S., Chen, L. B., Weinstein, I. B. (1990) *Cancer Res.* 50, 677–685
24. Weiss, M. J., Wong, J. R., Ha, C. S., Bleday, R., Salem, R. R., Steele, G. D. Jr., and Chen, L. B. (1987) *Proc. Natl. Acad. Sci. U. S. A.* 84, 5444–5448
25. O'Brian, C. A., Lawrence, D. S., Kaiser, E. T., and Weinstein, I. B. (1984) *Biochem. Biophys. Res. Commun.* 124, 296–302
26. Graff, J. M., Rajan, R. R., Randall, R. R., Narin, A. C., and Blackshear, P. J. (1991) *J. Biol. Chem.* 266, 14390–14398
27. Turner, R. S., Kemp, B. E., Su, H., and Kuo, J. F. (1985) *J. Biol. Chem.* 260, 11503–11507
28. Woodgett, J. R., Gould, K. L., and Hunter, T. (1986) *Eur. J. Biochem.* 161, 177–184
29. Ferrari, S., Marchiori, F., Borin, G., and Pinna, L. A. (1985) *FEBS Lett.* 184, 72–77
30. Eller, M., Jarv, J., Toomik, R., Ragnarsson, U., Ekman, P., and Engstrom, L. (1992) *Biochem. Int.* 27, 625–631
31. Hunter, T., Ling, N., and Cooper, J. A. (1984) *Nature* 311, 480–483
32. Knighton, D. R., Zheng, J., Eyck, L. F. T., Ashford, V. A., Xuong, N.-G., Taylor, S. S., and Sowadski, J. M. (1991) *Science* 253, 407–414
33. Knighton, D. R., Zheng, J., Eyck, L. F. T., Xuong, N.-G., Taylor, S. S., and Sowadski, J. M. (1991) *Science* 253, 414–420
34. Zheng, J., Knighton, D. R., Eyck, L. F. T., Karlsson, R., Xuong, N.-H., Taylor, S. S., and Sowadski, J. M. (1993) *Acta Crystallogr.* D49, 362–365
35. Zheng, J., Knighton, D. R., Eyck, L. F. T., Karlsson, R., Xuong, N.-H., Taylor, S. S., and Sowadski, J. M. (1993) *Biochemistry* 32, 2154–2161
36. Bossemeyer, D., Engh, R. A., Kinzel, V., Postingl, H., and Huber, R. (1993) *EMBO J.* 12, 849–859
37. Kwon, Y.-G., Srinivasan, J., Mendelow, M., Pluskey, S., and Lawrence, D. S. (1993) *J. Biol. Chem.* 268, 16725–16729
38. Kwon, Y.-G., Srinivasan, J., Mendelow, M., Pluskey, S., and Lawrence, D. S. (1993) *J. Am. Chem. Soc.* 115, 7527–7528
39. Yasuda, I., Kishimoto, A., Tanaka, S., Tominaga, M., Sakurai, A., and Nishizuka, Y. (1990) *Biochem. Biophys. Res. Commun.* 166, 1220–1227

Tyrosine *Versus* Serine/Threonine Phosphorylation by Protein Kinase Casein Kinase-2

A STUDY WITH PEPTIDE SUBSTRATES DERIVED FROM IMMUNOPHILIN Fpr3*

Oriano Marin, Flavio Meggio, Stefania Sarno, Luca Cesaro, Mario A. Pagano, and Lorenzo A. Pinna‡

From the Dipartimento di Chimica Biologica and Centro di Studio delle Biomembrane del C.N.R., Università di Padova, viale G. Colombo 3, 35121 Padova, Italy

Protein kinase casein kinase-2 (CK2) is a spontaneously active, ubiquitous, and pleiotropic enzyme that phosphorylates seryl/threonyl residues specified by multiple negatively charged side chains, the one at position $n + 3$ being of crucial importance (minimum consensus S/T-x-x-E/D/S(P)/T(P). Recently CK2 has been reported to catalyze phosphorylation of the yeast nucleolar immunophilin Fpr3 at a tyrosyl residue (Tyr[184]) fulfilling the consensus sequence of Ser/Thr substrates (Wilson, L.K., Dhillon, N., Thorner, J., and Martin, G.S. (1997) *J. Biol. Chem.* 272, 12961–12967). Here we show that, by contrast to other tyrosyl peptides fulfilling the consensus sequence for CK2, a peptide reproducing the sequence around Fpr3 Tyr[184] (DEDADIY[184]DEEDYDL) is phosphorylated by CK2, albeit with much higher K_m (384 *versus* 4.3 μM) and lower V_{max} (8.4 *versus* 1,132 nmol·min^{-1}·mg^{-1}) than its derivative with Tyr[184] replaced by serine. The replacement of Asp at position $n + 1$ with alanine and, to a lesser extent, of Ile at $n - 1$ with Asp are especially detrimental to tyrosine phosphorylation as compared with serine phosphorylation, which is actually stimulated by the Ile to Asp modification. In contrast the replacement of Glu at $n + 3$ with alanine almost suppresses serine phosphorylation but not tyrosine phosphorylation. It can be concluded that CK2 is capable to phosphorylate, under special circumstances, tyrosyl residues, which are specified by structural features partially different from those that optimize Ser/Thr phosphorylation.

Protein kinase CK2[1] (also termed "casein kinase-2 or II") is a ubiquitous Ser/Thr-specific protein kinase, essential for cell viability, independent of second messengers or phosphorylation for activation, generally composed of two catalytic (α and/or α') and two noncatalytic β subunits and implicated in cell proliferation and transformation (for review, see Refs. 1–5). The

[1] The abbreviations used are: CK2, casein kinase 2; Fmoc, *N*-(9-fluorenyl)methoxycarbonyl; HPLC, high-performance liquid chromatography; PKA, protein kinase A.

elucidation of the crystal structure of CK2 α subunit from *Zea mays*, 70% identical to its human counterpart (6), has disclosed the structural features that account for some unusual properties of this kinase, notably high basal activity and ability to use GTP, besides ATP as phosphate donor.

Another striking feature of CK2 is its terrific pleiotropy. The list of its substrates includes more than 160 proteins, many of which are implicated in signal transduction, gene expression, protein synthesis, and cell division and proliferation. Consistent with this wide spectrum of physiological targets is the subcellular localization of CK2, which is found in nearly all the subcellular compartments, including the outer side of the plasma membrane (7) and with the possible exception of the Golgi apparatus (8), although it is especially abundant in nuclei (9) and in the soluble cytosol (2). A common denominator of CK2 substrates is the presence of highly acidic phosphoacceptor sites in them, almost invariably fulfilling the consensus S/T-x-x-E/D, but generally including several additional negatively charged side chains (either carboxylic or phosphorylated residues) in addition to or, in few instances, instead of the crucial one at position $n + 3$ (10). The requirement of these acidic clusters for optimal phosphorylation efficiency has been clearly outlined by systematic studies with peptide substrates (11–14), and a number of unique basic residues responsible for the binding of individual specificity determinants (with special reference to those at positions $n + 3$ and $n + 1$) have been identified by site-directed mutagenesis of CK2α (15–17). In the course of these studies on CK2 specificity, some clues were provided that tyrosyl residues might bind to the active site instead of serine and threonine; thus random polymers including tyrosine and glutamic acid are much more powerful inhibitors than just poly-Glu (18) and pseudosubstrate peptides in which tyrosine has been replaced for serine inhibit CK2 more efficiently than their counterparts where serine had been replaced by alanine (1). Consequently the peptide EEEEEY-EEEEEEE is a powerful inhibitor (19) whose binding to CK2 is closely reminiscent to that of a canonical substrate (20). Neither in the case of this peptide nor in that of poly(Glu$_4$Tyr), however, could any significant phosphorylation of tyrosine be detected, supporting the view that CK2 is a *bona fide* Ser/Thr-specific protein kinase unable to catalyze phosphate transfer to tyrosyl resides once these are bound in its active site.

Recently, however, a yeast nucleolar protein, immunophilin Fpr3, has been found to be tyrosine-phosphorylated (21), although in *Saccharomyces cerevisiae bona fide* tyrosine kinases are lacking (22); the kinase responsible for this event was shown to be CK2 (23). The tyrosyl residue phosphorylated in Fpr3 either *in vivo* or *in vitro* by CK2 (Tyr[184]) is embedded in a very acidic cluster (DEDEDADIYDSEDYD) and fulfills the optimal sequence for CK2 phosphorylation for including in

addition to the crucial acidic determinant at $n + 3$ several other acidic residues nearby. Consequently a peptide substrate reproducing this sequence was also phosphorylated by CK2 at Tyr^{184}. Such a phosphorylation was improved by previous phosphorylation of the seryl residue at position $n + 2$ or by its replacement with a glutamic acid, suggesting that in this special case the determinant at position $n + 2$ might play a relevant role. The relevance of the other residues nearby, however, was not assessed nor was the phosphorylation of the tyrosyl peptide compared with that of canonical seryl peptide substrates of CK2. Here we show that the phosphorylation efficiency of the Fpr3 tyrosyl peptide is very low compared with that of its seryl counterpart, both in terms of V_{max} and K_m and depending on structural features that are partially distinct from those determining the phosphorylation of canonical substrates.

EXPERIMENTAL PROCEDURES

Materials—DEAE-cellulose filters (NA45) were from Schleicher & Schuell. P81 phosphocellulose papers were from Whatman. $[\gamma^{-32}P]ATP$ (3,000 Ci/mmol) was purchased from Amersham Pharmacia Biotech. All other reagents were from Sigma. Native CK2 was purified from rat liver cytosol as described previously (24). Recombinant forms of CK2 either wild type or its mutants defective in substrate recognition were obtained as described elsewhere (16).

Synthetic Peptides—The tyrosyl peptides DEDADIYDEEDYDL, DEDADIYDS(p)EDYDL, DEDADIYAEEDYDL, DEDADIYDAEDYDL, DEDADIYDEADYDL, DEDADDYDEEDYDL, DEDADIFDEEDYDL, and RRRADDYDDDDD as well as their seryl analogues DEDADISDEEDYDL, DEDADISAEEDYDL, DEDADISDEADYDL, and DEDADDSDEEDYDL were synthesized by an automated peptide synthesizer ABI 431-A (Applied Biosystems) on 4-hydroxymethyl-phenoxymethylcopolystirene-1% divinylbenzene resin (1.04 mmol/g). The synthesis of the peptides EEEEEYEEEEEEE and PEGDYEEELE was described previously (19, 25). The synthesizer was equipped for using Fmoc chemistry (26) and 2-(1H-benzotriazole-1-yl)-1,1,1,3,3 tetramethyluronium hexafluorophosphate/N-hydroxybenzotriazole protocol (27) in a 0.05 mmol scale.

The incorporation of phosphate into the Ser residue has been performed according to a building block approach using Fmoc-Ser(PO(benzyl))OH (from Novabiochem) during the synthesis.

Cleavage of peptides from the resin and side chain deprotection was carried out by treatment of the peptidyl resin with trifluoroacetic acid/anisole/ethanedithiol/ethylmethylsulfide (95:3:1:1). In the presence of the benzyl protecting group on phosphoserine a mixture of trifluoroacetic acid /triisopropylsilane/water (95:2.5:2.5) was preferred.

The crude peptides were purified by high-performance liquid chromatography (HPLC) on a preparative reverse phase column Prep Nova-Pak HR C18, 6 μm, 25 × 10 mm (Waters). The analytical HPLC and matrix-assisted laser desorption ionization/time of flight mass spectrometry analysis of the purified peptides showed a correct sequence and a ≥95% purity.

Phosphorylation Assay—Synthetic peptide substrates (0.5 mM) were phosphorylated by incubation in a medium (25 μl final volume) containing 50 mM Tris-HCl buffer, pH 7.5, 10 mM $MgCl_2$, 50 mM KCl, and 100 μM $[\gamma^{-32}P]ATP$ (specific radioactivity 500–1,000 cpm/pmol) unless otherwise indicated. The reaction was started with the addition of the enzyme (0.23 μg of either native or recombinant CK2) and stopped by the addition of 10 μl of 0.25 M EDTA and cooling in ice. Phosphorylation of Fpr3-derived synthetic peptides was evaluated according to the procedure described by Wilson *et al.* (23) by using DEAE-cellulose filters. Phosphorylation of RRRADDSDDDDD and of its tyrosyl derivative was quantitated by the phosphocellulose paper procedure (28). Control experiments were also performed with both types of peptides by determining phosphate incorporation after conversion of $[\gamma^{-32}P]ATP$ into P_i and phosphomolybdic complex extraction as described previously (29).

HPLC Separation of Tyrosine-phosphorylated Fpr3 Peptide—The peptide DEDADIYDEEDYDL, previously phosphorylated by CK2 as described above, was loaded onto a SuperPac Pep-S (Amersham Pharmacia Biotech) C2/18 (5 μm) column (4.6 × 250 mm). Elution was carried out at a flow rate of 1 ml/min with a gradient of acetonitrile in 0.08% trifluoroacetic acid from 0 to 40% for 30 min and then from 40 to 100% for 10 min. The effluent was monitored by absorbance measurements at 220 nm. The radioactivity of the fractions collected (1 ml) was determined by counting in a liquid scintillation apparatus (Canberra-Packard).
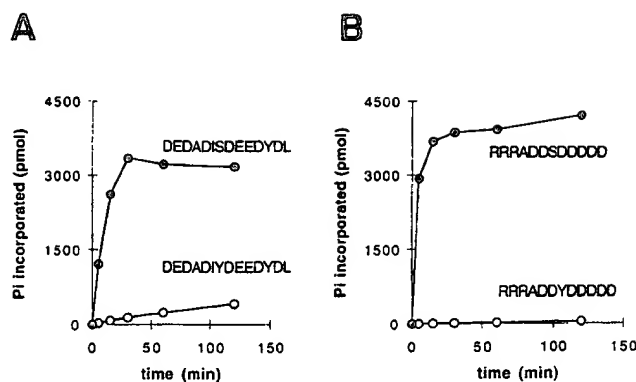

FIG. 1. **Time course phosphorylation of seryl peptides and their tyrosyl counterparts by CK2.** Phosphorylation was performed for the times indicated and evaluated as described under "Experimental Procedures." The concentrations of ATP and of peptide substrates were 0.2 mM and 0.5 mM, respectively.

Molecular Modeling—Calculations were made on an Indy R4000 (Silicon Graphics) workstation. For human CK2α subunit modeling, the crystal structure of *Zea mays* CK2α was used (Protein Data Bank number 1A6O). The two sequences were aligned using the Insight II package (Molecular Simulation Inc.) with the protein homology tools. For elaboration of the model of human CK2α, the program Modeler (30) was used. Five structures were obtained from Modeler, and the one with the highest structural homology with respect to maize CK2α was used further. The backbone of the central part of the Fpr3 peptide (DIYDEE) has been shaped using as a template the equivalent sequence of protein kinase inhibitor bound to the catalytic subunit of PKA (Protein Data Bank number 1atp). The peptide was manually placed in CK2α catalytic pocket avoiding physical interference with residues of the kinase. The obtained structure was minimized using the Discover module of Insight II package until the energy reached a minimum.

RESULTS

The time courses for CK2-catalyzed phosphorylation of the Fpr3 peptide with Glu at position $n + 2$ relative to Tyr^{184} instead of serine and of its derivative where Tyr^{184} was replaced by serine are compared in Fig. 1A. It can be seen that the phosphorylation of the tyrosyl peptide is negligible as compared with that of its seryl counterpart, especially after short incubation times. By prolonging incubation the phosphorylation of the seryl peptide reaches a plateau when ATP is nearly exhausted, whereas the phosphorylation of the tyrosyl peptide slowly increases up to 2 h of incubation. By increasing ATP concentration (1 mM) over that of the peptides (0.5 mM) a stoichiometric phosphorylation of the seryl peptide was attained after 30 min of incubation, whereas the phosphorylation of the tyrosyl peptide was still far from stoichiometric (around 0.03 mol/mol) after 2 h (not shown). Albeit slow, the phosphorylation of the Fpr3 tyrosyl peptide was quite significant especially if compared with that of another tyrosyl peptide featured after the optimal peptide substrate routinely used for assaying CK2 (Fig. 1B). In this case, no detectable phosphorylation of the tyrosyl peptide could be observed, although that of its seryl counterpart was even faster than that of the seryl derivative of the Fpr3 peptide. The stoichiometry of the Fpr3 tyrosyl peptide phosphorylation was confirmed by HPLC where the phosphoderivative can be resolved from the nonphosphorylated peptide (Fig. 2), thus allowing their relative quantitation (~3% *versus* 97%).

The suspicion that tyrosine phosphorylation in the Fpr3 peptide might rely on structural features different from those determining serine phosphorylation was corroborated by the finding that two other tyrosyl peptides, in addition to RRRADDYDDDDD, namely EEEEEYEEEEEEE and PEGDYEEELE, are totally unaffected by CK2 despite the fact that they fulfill optimal conditions for Ser/Thr phosphorylation (see Table I).

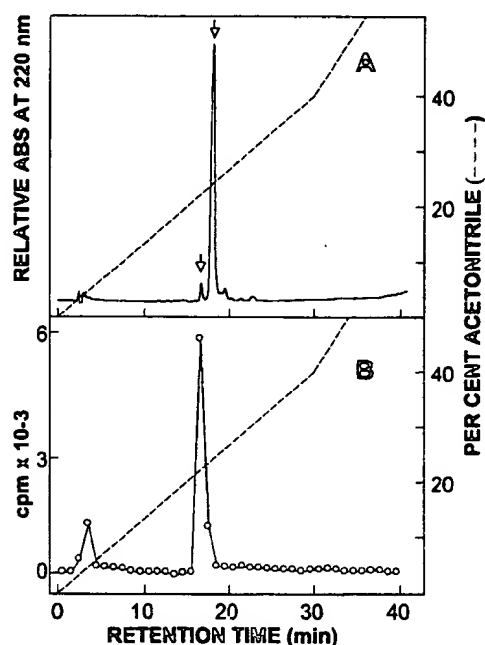To shed light on the uncommon phosphorylation of tyrosine

FIG. 2. **HPLC separation of tyrosine-phosphorylated and unphosphorylated forms of the Fpr3-derived peptide DEDADIY-DEEDYDL.** The peptide was phosphorylated by CK2 for 90 min as described under "Experimental Procedures" and directly subjected to HPLC analysis. The absorbance at 220 nm (*A*) and the radioactivity incorporated (*B*) are shown. The *arrows* denote the position of the phosphorylated (*left*) and unphosphorylated (*right*) peptide, respectively.

TABLE I
*Kinetic constants for the phosphorylation of tyrosyl and
seryl peptides by CK2*

Phosphorylation conditions and evaluation of phosphate incorporated are described under "Experimental Procedures." The data are the mean of at least three independent experiments with standard errors not exceeding 10%. Substituted residues relative to the reference peptide are in bold type. The residue phosphorylated is underlined.

Peptide	V_{max}	K_M	V_{max}/K_M
	nmol/min/mg	*μM*	
DEDADIYDEEDYDL	8.4	384	0.0218
DEDADIYDSpEDYDL	20.7	370	0.0559
DEDADIYDEADYDL	8.4	729	0.0115
DEDADIYDAEDYDL	8.4	740	0.0113
DEDADIYAEEDYDL	0.5	787	0.0006
DEDADDYDEEDYDL	2.1	166	0.0126
DEDADIFDEEDYDL	ND[a]	ND	
EEEEEYEEEEEEE	ND	ND	
PEGDYEEELE	ND	ND	
DEDADISDEEDYDL	1132	4.3	263.2558
DEDADDSDEEDYDL	1311	4.0	327.7500
DEDADISAEEDYDL	586	66.0	8.8787
DEDADISDEADYDL	394	125.0	3.1520

[a] ND = not determined due to undetectable phosphorylation.

in the Frp3 peptide a number of derivatives with individual substitutions were synthesized and compared with the parent peptide. This latter includes a glutamic acid at position $n + 3$, which is the main determinant for CK2 recognition (13) and an aspartic acid at position $n + 1$ where also an acidic residue is very important (17). Position $n + 2$ is occupied in the wild type peptide by a serine, whose primary phosphorylation by CK2 is believed to improve subsequent phosphorylation of tyrosine, because its replacement by alanine, but not by glutamic acid, was detrimental (23); thus it appeared that a negatively charged side chain at $n + 2$, a position rather unimportant for serine phosphorylation (13), might be crucial for tyrosine phoshorylation. In contrast, position $n - 1$ in the Fpr3 site is
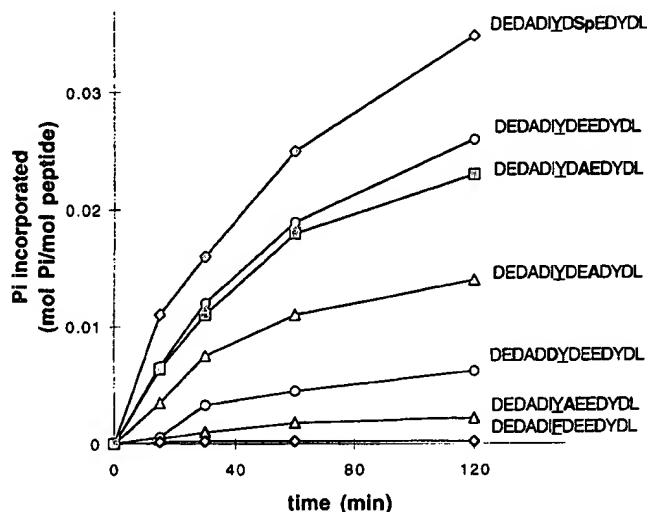

FIG. 3. **Effect of amino acid substitutions on the phosphorylation of the Fpr3 tyrosyl peptide by CK2.** All peptides tested were 0.5 mM. Phosphorylation conditions and evaluation of the phosphate incorporated were performed as described under "Experimental Procedures." Substitutions relative to the reference peptide (DEDADIY-DEEDYDL) are *bold type*. The phosphorylated tyrosine is underlined.

occupied by isoleucine, a rare feature in CK2 sites, where an acidic residue was shown to be preferred and is actually found in about 50% of the natural substrates (10). We therefore decided to check how much the substitution of this Ile by Asp, of Asp (+1) by Ala, of Glu (+2) by Ala or phosphoserine, and of Glu (+3) by Ala might affect phosphorylation by CK2. As shown by the time courses in Fig. 3, the most detrimental substitution (a part of Tyr[184], confirming that this one and not the other tyrosine, Tyr[189] undergoes phosphorylation) is that of alanine instead of glutamic acid at $n + 1$, followed by aspartic acid instead of isoleucine at $n - 1$, whereas the replacement of the most important acidic determinant in canonical CK2 substrates, *i.e.* Glu at $n + 3$, by alanine is in this case much better tolerated. In contrast to a previous report (23), the replacement of Glu at $n + 2$ by alanine has no effect, whereas a phosphoserine in this position significantly improves phosphorylation (Fig. 3). As shown in Table I, the differences in phosphorylation outlined by the time courses of Fig. 3 are variably accounted for by changes in V_{max} and/or K_m. Especially remarkable is the drop in phosphorylation efficiency due to both a dramatic decrease of V_{max} and an increase of K_m promoted by the Ala for Asp substitution at $n + 1$. In comparison, the effect of a similar substitution at the "crucial" $n + 3$ position, due to just a 2-fold increase in K_m, is negligible. The detrimental effect of replacing Ile at $n - 1$ with Asp (see Fig. 3), appears to be be exclusively due to a drop in V_{max} (Table I).

Table I also highlights the striking superiority of the seryl derivative of the Fpr3 peptide over the tyrosyl peptide both in terms of V_{max} (>130-fold higher) and of K_m (almost 90-fold lower), and it corroborates the view that the specificity determinants are different with the two peptides. In fact the replacement of Ile at $n - 1$ by Asp, far from being detrimental, is actually improving the phosphorylation efficiency of the seryl derivative and the replacement at position $n + 3$ is more detrimental than that at $n + 1$.

The particularly crucial role of the acidic determinant at position $n + 1$ as opposed to that at position $n + 3$ in determining tyrosine phosphorylation was also confirmed by experiments with CK2 mutants, which are defective in the recognition of individual determinants. As shown in Fig. 4, mutant K198A with reduced ability to bind the determinant at position +1 (17) is much more defective toward the tyrosyl peptide than
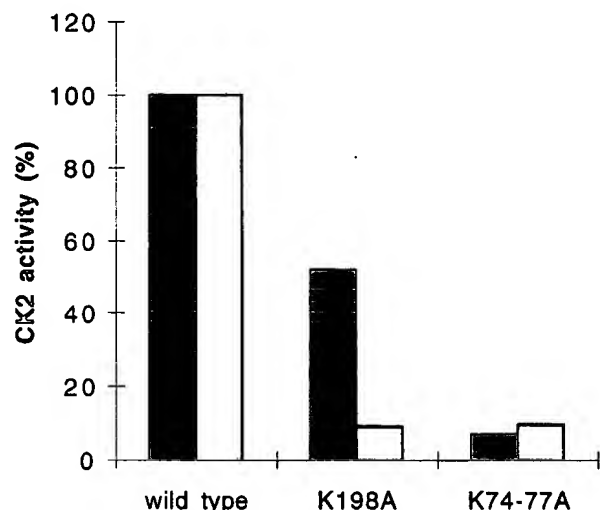
FIG. 4. **Phosphorylation of tyrosyl *versus* seryl Fpr3-derived peptides by wild type CK2 and CK2 mutants defective in substrate recognition.** 0.23 μg of either wild type or mutated CK2 were incubated at 37 °C in the presence of 0.12 mM DEDADISDEEDYDL (*solid bars*) or 1.2 mM DEDADIYDEEDYDL (*empty bars*) Fpr3 derivatives for 5 and 40 min, respectively, and ^{32}P incorporated was determined as described under "Experimental Procedures." CK2 activity is expressed as percentage of the activity measured with CK2 wild type, which was 271 and 38 pmol for the seryl and the tyrosyl peptide, respectively.

it is toward its seryl derivative. The opposite applies to another mutant, K74A/K77A, which is unable to recognize the determinant at $n + 3$ (16).

To gain further information about the mode of binding of Tyr^{184}-containing peptides to CK2 active site a modelization analysis has been performed using as a template a structure of human CK2α derived from 70% identical maize CK2α crystallized in the absence of phosphoacceptor substrate (6). The central part of the parent Fpr3 peptide (-DIY^{184}DEE-) shaped after the pseudo-substrate peptide bound to the catalytic subunit of PKA (31) has been placed into the active site of CK2α. After energy minimization, a model was obtained (Fig. 5) that is largely consistent with experimental observations. It should be noted in particular that the tyrosyl residue protrudes into the active site with its hydroxyl group in the proximity of two crucial elements of catalysis, namely the catalytic base Asp^{156} (homologous to PKA Asp^{166}) and Lys^{158}, homologous to PKA Lys^{168} believed to bridge the phosphate to the peptide during the catalytic event (32). The distances between the phosphoacceptor hydroxyl group of tyrosine and either Asp^{156} (2.67 Å) or Lys^{158} (2.89 Å) are comparable with those found in the complex between PKA and a seryl peptide substrate (2.7 and 3.0 Å, respectively) (32). The only evident interaction with peptide substrate side chains is the one between the carboxylate of aspartate at position $n + 1$ and positively charged groups in the loop p + 1 (Lys^{195} and Lys^{198}). In contrast, the side chain of glutamate at position $n + 3$ is far away from the 74–77 basic cluster, which is responsible for tight interaction with the $n + 3$ determinant of seryl peptides (17). This is also in agreement with the relatively modest effect of replacing Glu ($n + 3$) as compared with the dramatic drop of efficiency promoted by Asp ($n + 1$) substitution (see Table I). In our model, the side chain of Ile ($n - 1$) protrudes outside the surface of the kinase. This, however, is likely to be an artifact of modelization where the water surrounding CK2α, expected to repel the hydrophobic side chain of isoleucine, is not considered.

It should be finally outlined that the Tyr *versus* Ser/Thr specificity of CK2 appears not to be affected by a number of effectors and/or experimental conditions, which are known to

impinge on CK2 activity. In particular CK2 catalytic activity toward the Frp3 tyrosyl and seryl peptides is equally stimulated by association with the β subunit (about 3-fold) and by addition of 336 nM polylysine to the holoenzyme (about 2-fold) and displays similar activation curves by either Mg^{2+} or Mn^{2+}. With both peptides, GTP can replace ATP as phosphate donor and the K_m with respect to ATP (33 μM) is not modified by replacing one peptide with the other (data not shown).

DISCUSSION

Nearly all members of the huge eukaryotic protein kinase family fall into two categories, Ser/Thr- and Tyr-specific enzymes, respectively (33). In most instances the borderline between these two groups, empirically drawn using substrates of the two sorts, is quite sharp and clear-cut, being also based on differences in primary structure motifs (34). In a few instances, however, protein kinases may display a dual specificity in that they are able to phosphorylate both Ser/Thr and Tyr residues (35). The only known *sensu stricto* dual specificity protein kinases are probably those of the mitogen-activated protein kinase kinase family, which are highly dedicated kinases that catalyze the simultaneous phosphorylation of both Thr and Tyr in a conserved sequence, T-x-Y present in the activation loop of mitogen-activated protein kinases. In several instances, however, *bona fide* Ser/Thr protein kinases have been reported to display tyrosine kinase activity as well under certain circumstances, detectable either as autophosphorylation or toward trans substrates. In general the latter is negligible compared with that observed toward canonical Ser/Thr sites. The list of these Ser/Thr kinases exhibiting low Tyr kinase activity as well includes among others phosphorylase kinase (36), calcium-calmodulin-dependent protein kinase II and Spk1 (37), CK1 (38, 39), CK2 (40), and even PKA (37). Conversely it should be noted that also a classical tyrosine kinase like Src can phosphorylate aliphatic as well as aromatic alcohols in a stretch of peptide (41). It is likely therefore that in several instances this hardly detectable "dual" specificity of *bona fide* Ser/Thr protein kinases is a mechanistic curiosity devoid of practical consequences. That this may not always be the case, however, is supported by the observation that in lower eukaryotes, like yeast, where *bona fide* tyrosine kinases are absent, tyrosine-specific protein phosphatases are nevertheless present (22), and tyrosine phosphorylation of proteins other than kinases of the mitogen-activated protein kinase family has been reported to take place. It is tempting therefore to assume that tyrosine phosphorylation by *bona fide* Ser/Thr kinases is a physiologically relevant event in these cases.

A notable example of this situation is provided by immunophilin Fpr3, an abundant nucleolar protein, a member of the FK506-binding subfamily of immunophilins (42), which is a substrate of *S. cerevisiae* protein-tyrosine phosphatase Ptp1. Phosphotyrosine dephosphorylation by Ptp1 prevents nucleolar accumulation of Fpr3 *in vivo* (21). The tyrosyl residue phosphorylated in Fpr3 was identified as Tyr^{184}, residing in a highly acidic sequence fulfilling optimal conditions for CK2 catalyzed phosphorylation, and indeed CK2 was shown to be responsible for Tyr phosphorylation of Fpr3 and to be able to phosphorylate *in vitro* a tyrosyl peptide reproducing the sequence around Tyr^{184} (23). This observation would include CK2 in the growing list of *sensu lato* dual specificity protein kinases, despite the previous failure to demonstrate any activity of CK2 toward tyrosyl peptides fulfilling its consensus sequence. This prompted us to undertake a study of the structural features underlying tyrosine phosphorylation by CK2 and to compare this activity with that toward canonical Ser/Thr substrates. The main outcomes of this investigation are the following.

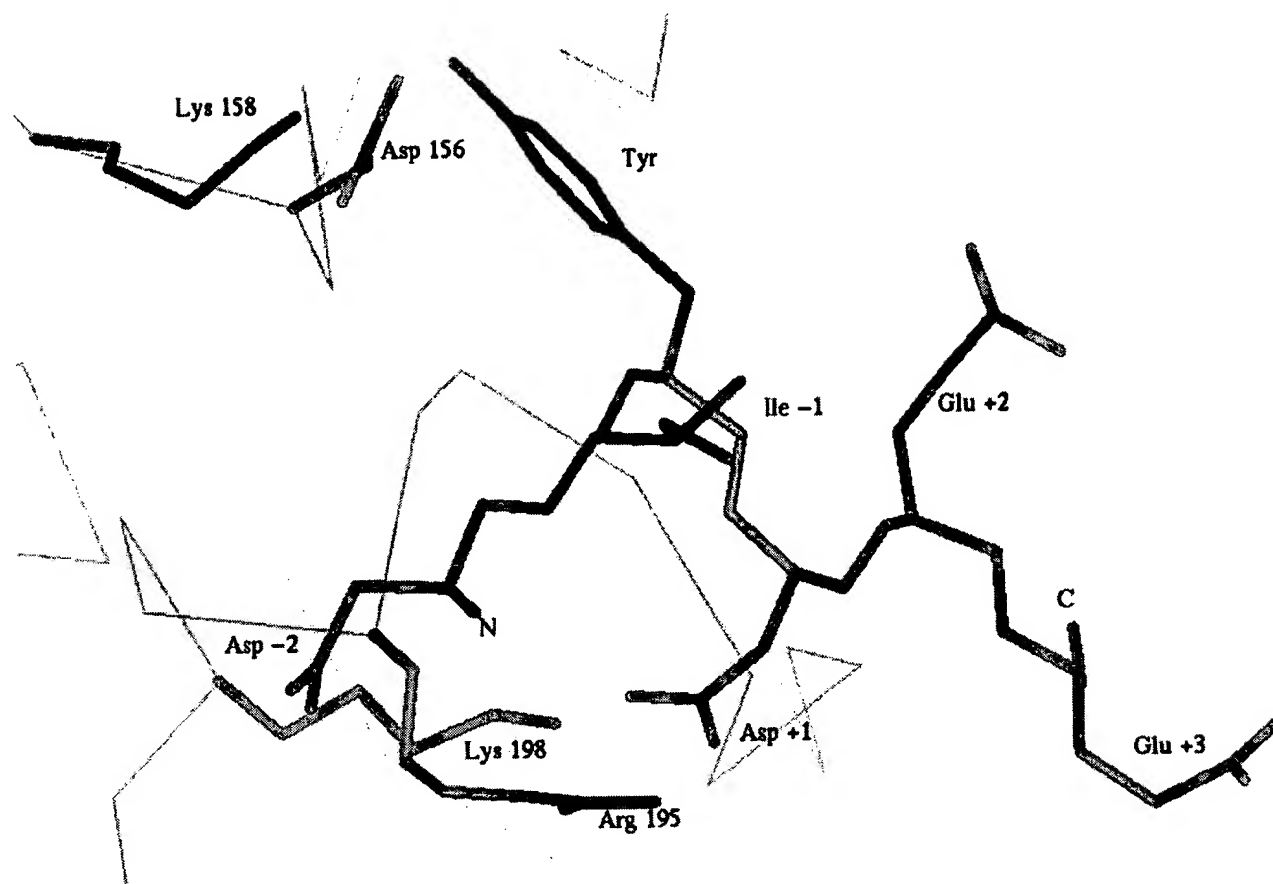1) The phosphorylation of Fpr3-derived tyrosyl peptide, al-

FIG. 5. **Modelization of Fpr3-derived 181–188 tyrosyl peptide bound to the catalytic site of human CK2α.** Drawn from human CK2α modeling based on the crystal structure of maize CK2α (see "Experimental Procedures"). The peptide is shown in *green,* and the CK2α elements in *light blue.* The peptide residues are indicated according to their position relative to the phosphorylatable tyrosine (Tyr[184] of Fpr3). Distances between key residues at active site and peptide residues were as follows: Asp[156] to substrate Tyr-OH, 2.67 Å; Lys[158] to substrate Tyr-OH, 2.89 Å; Lys[198] to side chain carboxylate of substrate Asp (n + 1), 4.11 Å; Arg[195] to side chain carboxylate of substrate Asp (n + 1), 2.46 Å.

beit quite significant, is negligible compared with that of an identical peptide where tyrosine is replaced by serine. This shows that even in this case serine is by far preferred over tyrosine by CK2. The superiority of the seryl peptide is due to both much lower K_m and much higher V_{max}. The low V_{max} of the tyrosyl peptide suggests that its phosphorylated product leaves the active site of the kinase very slowly, a situation that could give rise to remarkable product inhibition. Also, consistent with this interpretation would be the low phosphorylation stoichiometry of the tyrosyl peptide (<5%). It is possible that *in vivo* the kinetics of Tyr[184] phosphorylation are improved either by features intrinsic to the full-length Fpr3 protein conformation or by the fast translocation of phospho-Fpr3 to separate compartment(s). In this respect a comparison between the kinetic constants of Tyr[184] peptides and those of full-length Fpr3 would be misleading since Tyr[184] is just a minor Fpr3 phosphoacceptor site (23); consequently the parameters calculated with Fpr3 would mainly reflect the phosphorylation of residues other than Tyr[184]. It is worth noting, however, that a significant phosphorylation of Tyr[184] by CK2 is observable under conditions where GST-Fpr3 is about 1 μM (23), although at this concentration the phosphorylation of the best peptide substrate, whose K_m is 370 μM, would be flatly undetectable. It is likely therefore that indeed the phosphorylation efficiency of Tyr[184] is improved by features that are lacking in the peptides used in our study. On the other hand the reason for the discrepancy between our data and that reported by Wilson *et al.*

(23) where a 1 to 1 phosphorylation stoichiometry of the same peptide is reported to occur after less than 2 h of incubation with recombinant human CK2, is not clear. It should be noted, however, that the stoichiometry reported in that paper is not consistent with the experimental conditions used, where ATP and the peptide are 100 and 580 μM, respectively, allowing at best a 20% phosphorylation stoichiometry.

2) CK2 activity ratio toward the tyrosyl *versus* the seryl derivative of the Fpr3 peptide is not significantly affected by either the subunit composition of CK2 (catalytic subunit *versus* holoenzyme), or the addition of polycationic stimulators, or the nature of the phosphate donor (GTP *versus* ATP) and of the activatory cation (Mn^{2+} *versus* Mg^{2+}). This last outcome is worth noting, because in the case of phosphorylase kinase, Mn^{2+} instead of Mg^{2+} is required to see tyrosine-phosphorylating activity (36).

3) Ability to phosphorylate tyrosine is not a general feature of CK2 toward any kind of substrate fulfilling its consensus sequence, because the replacement of serine (or threonine) by tyrosine in several outstanding peptide substrates of CK2 different from the Fpr3-derived peptide rendered their phosphorylation undetectable.

4) Among the local structural determinants favoring tyrosine *versus* serine phosphorylation, the isoleucine at position $n - 1$ and the acidic residue at position $n + 1$ appear to play a prominent role. Interestingly, hydrophobic residues are only sporadically found in CK2 substrates at position $n - 1$, where

instead acidic residues are quite frequent (10). Consequently the replacement of Ile by Asp at this position in the seryl derivative of the Fpr3 peptide increases its phosphorylation efficiency, but it is detrimental in the tyrosyl peptide. The molecular basis for such an opposite behavior is presently unclear. The favorable effect of an acidic residue at position $n + 1$, on the other hand, is a well known feature of all CK2 phosphoacceptor sites, including Ser/Thr (10, 12). In the latter case, however, the $n + 1$ acidic determinant is generally less important than the one at $n + 3$ (10, 12), whereas the opposite applies to the Fpr3 tyrosyl peptide where the replacement of the $n + 3$ Glu by alanine is exceptionally well tolerated. Computer-aided modelization (Fig. 5) corroborates the concept that in the case of Fpr3-derived tyrosyl peptide the acidic determinant at $n + 1$ is much more important than the one at $n + 3$ in making contacts with the enzyme. The replacement of glutamate at $n + 2$ with phosphoserine improves 2–3-fold the V_{max} and phosphorylation efficiency of the peptide, consistent with the knowledge that phosphoserine is a better determinant than Glu especially at positions $n + 1$ and $n + 2$ (14); it is quite possible therefore that, as suggested by others (23), the phosphorylation of Fpr3 *in vivo* is enhanced by a hierarchical effect where previous phosphorylation of Ser[186] will improve subsequent phosphorylation of Tyr[184]. The replacement of Glu at $n + 2$ with Ala, however, has only a modest effect, similar to that caused by the same substitution in canonical seryl peptide substrates of CK2 (12). therefore, it seems unlikely that the phosphorylation of Tyr[184] in the Fpr3 peptide is entirely dependent on the presence of a negatively charged side chain at $n + 2$, as suggested by others (23). The reasons why the same peptide, DEDADIYDAEDYDL, which in our hands is nearly as good as the parent peptide with Glu instead of the underlined Ala (see Fig. 3 and Table I), was not phosphorylated at all (23) is unclear to us.

5) The different mode of binding of tyrosyl *versus* seryl peptide substrates was also corroborated by experiments with CK2 mutants with a reduced ability to recognize individual determinants. Especially remarkable is the behavior of the mutant K198A, which is much more defective toward the Fpr3 tyrosyl peptide as compared with its seryl derivative.

In conclusion, CK2 can be legitimately included in the list of *sensu lato* dual specificity protein kinases. Clearly, however, its ability to phosphorylate tyrosine in peptide substrates is very modest as compared with its canonical Ser/Thr kinase activity and, more important, it depends on structural features that are partially different from those determining Ser phosphorylation. Among these the most striking are the absolute requirement for the acidic determinant at position $n + 1$ as opposed to the tolerance toward the replacement of the one at position $n + 3$, and the preference for a hydrophobic over an acidic residue at position $n - 1$.

REFERENCES

1. Pinna, L. A. (1990) *Biochim. Biophys. Acta* **1054**, 267–284
2. Issinger, O.-G. (1993) *Pharmacol. Ther.* **59**, 1–30
3. Allende, J. E., and Allende, C. C. (1995) *FASEB J.* **9**, 313–323
4. Pinna, L. A., and Meggio, F. (1997) *Prog. Cell Cycle Res.* **3**, 77–79
5. Guerra, B., and Issinger, O.-G. (1999) *Electrophoresis* **20**, 391–408
6. Niefind, K., Guerra, B., Pinna, L. A., Issinger, O.-G., and Schomburg, D. (1998) *EMBO J.* **17**, 2451–2462
7. Walter, J., Schnolzer, M., Pyerin, W., Kinzel, V., and Kübler, D. (1996) *J. Biol. Chem.* **271**, 111–119
8. Lasa, M., Marin, O., and Pinna, L. A. (1997) *Eur. J. Biochem.* **243**, 719–725
9. Krek, W., Maridor, G., and Nigg, E. A. (1992) *J. Cell Biol.* **116**, 43–55
10. Meggio, F., Marin, O., and Pinna, L. A. (1994) *Cell. Mol. Biol. Res.* **40**, 401–409
11. Meggio, F., Marchiori, F., Borin, G., Chessa, G., and Pinna, L. A. (1984) *J. Biol. Chem.* **259**, 14576–14579
12. Marin, O., Meggio, F., Marchiori, F., Borin, G., and Pinna, L. A. (1986) *Eur. J. Biochem.* **160**, 239–244
13. Marchiori, F., Meggio, F., Marin, O., Borin, G., Calderan, A., Ruzza, P., and Pinna, L. A. (1988) *Biochim. Biophys. Acta* **971**, 332–338
14. Perich, J. W., Meggio, F., Reynolds, E. C., Marin, O., and Pinna, L. A. (1992) *Biochemistry* **31**, 5893–5897
15. Sarno, S., Boldyreff, B., Marin, O., Guerra, B., Meggio, F., Issinger, O.-G., and Pinna, L. A. (1995) *Biochem. Biophys. Res. Commun.* **206**, 171–179
16. Sarno, S., Vaglio, P., Meggio, F., Issinger, O.-G., and Pinna, L. A. (1996) *J. Biol. Chem.* **271**, 10595–10601
17. Sarno, S., Vaglio, P., Marin, O., Issinger, O.-G., Ruffato, K., and Pinna, L. A. (1997) *Biochemistry* **36**, 11717–11724
18. Meggio, F., and Pinna, L. A. (1989) *Biochim. Biophys. Acta* **1010**, 128–130
19. Vaglio, P., Sarno, S., Marin, O., Meggio, F., Issinger, O.-G., and Pinna, L. A. (1996) *FEBS Lett.* **380**, 25–28
20. Sarno, S., Vaglio, P., Cesaro, L., Marin, O., and Pinna, L. A. (1999) *Mol. Cell. Biochem.* **191**, 13–19
21. Wilson, L. K., Benton, B. M., Zhou, S., Thorner, J., and Martin, G. S. (1995) *J. Biol. Chem.* **270**, 25185–25193
22. Hunter, T., and Plowman, G. D. (1997) *Trends Biochem. Sci.* **22**, 18–22
23. Wilson, L. K., Dhillon, N., Thorner, J., and Martin, G. S. (1997) *J. Biol. Chem.* **272**, 12961–12967
24. Meggio, F., Donella Deana, A., and Pinna, L. A. (1981) *J. Biol. Chem.* **256**, 11958–11961
25. Brunati, A. M., Donella-Deana, A., Ruzzene, M., Marin, O., and Pinna, L. A. (1995) *FEBS Lett.* **367**, 149–152
26. Fields, G. B., and Noble, R. L. (1990) *Int. J. Pept. Protein Res.* **35**, 161–214
27. Marin, O., Meggio, F., Sarno, S., and Pinna, L. A. (1997) *Biochemistry* **36**, 7192–7198
28. Glass, D. B., Masaracchia, R. A., Feramisco, J. R., and Kemp, B. E. (1978) *Anal. Biochem.* **87**, 566–575
29. Meggio, F. Donella, A., and Pinna, L. A. (1976) *Anal. Biochem.* **71**, 583–587
30. Sali, A., and Blundell, T. L. (1993) *J. Mol. Biol.* **234**, 779–815
31. Knighton, D. R., Zheng, J., Ten Eyck, L. F., Xuong, N.-h., Taylor, S. S., and Sowadski, J. M. (1991) *Science* **253**, 414–420
32. Madhusudan, Trafny, E. A., Xuong, N.-h., Adams, J. A., Ten Eyck, L. F., Taylor, S. S., and Sowadski, J. M. (1994) *Protein Sci.* **3**, 176–187
33. Hanks, S. K., and Hunter, T. (1995) *FASEB J.* **9**, 576–596
34. Hanks, S. K., Quinn, A. M., and Hunter, T. (1988) *Science* **241**, 42–52
35. Lindberg, L. A., Quinn, A. M., and Hunter, T. (1992) *Trends Biochem. Sci.* **17**, 114–119
36. Yuan, C.-J., Huang, C.-Y. F., and Graves, D. J. (1993) *J. Biol. Chem.* **268**, 17683–17686
37. Stern, D. F., Zheng, P., Beidler, D. R., and Zerillo, C. (1991) *Mol. Cell. Biol.* **11**, 987–1001
38. Hoekstra, M. E., Dhillon, N., Carmel, G., DeMaggio, A. J., Lindberg, R. A., Hunter, T., and Kuret, J. (1994) *Mol. Biol. Cell* **5**, 877–886
39. Pulgar, V., Tapia, C., Vignolo, P., Santos, J., Sunkel, C. E., Allende, C. C., and Allende, J. E. (1996) *Eur. J. Biochem.* **242**, 519–528
40. Chardot, T., Shen, H., and Meunier, J. C. (1995) *C. R. Acad. Sci. (Paris)* **318**, 937–942
41. Lee, T. R., Niu, J., and Lawrence, D. S. (1995) *J. Biol. Chem.* **270**, 5375–5380
42. Benton, B., Zang, J.-H., and Thorner, J. (1994) *J. Cell Biol.* **127**, 623–629

The β-Adrenergic Receptor Kinase (GRK2) Is Regulated by Phospholipids*

James J. Onorato‡§, Mary E. Gillis‡, Yu Liu¶, Jeffrey L. Benovic‖, and Arnold E. Ruoho¶

From the ‡Department of Medicine, University of Wisconsin, Madison, Wisconsin 53706, the ‖Department of Pharmacology, Jefferson Cancer Center, Thomas Jefferson University, Philadelphia, Pennsylvania 19107, and the ¶Department of Pharmacology, University of Wisconsin, Madison, Wisconsin 53706

The β-adrenergic receptor kinase (βARK) is a member of growing family of G protein coupled receptor kinases (GRKs). βARK and other members of the GRK family play a role in the mechanism of agonist-specific desensitization by virtue of their ability to phosphorylate G protein-coupled receptors in an agonist-dependent manner. βARK activation is known to occur following the interaction of the kinase with the agonist-occupied form of the receptor substrate and heterotrimeric G protein βγ subunits. Recently, lipid regulation of GRK2, GRK3, and GRK5 have also been described. Using a mixed micelle assay, GRK2 (βARK1) was found to require phospholipid in order to phosphorylate the β_2-adrenergic receptor. As determined with a nonreceptor peptide substrate of βARK, catalytic activity of the kinase increased in the presence of phospholipid without a change in the K_m for the peptide. Data obtained with the heterobifunctional cross-linking agent N-3-[^{125}I]iodo-4-azidophenylpropionamido-S-(2-thiopyridyl)-cysteine ([^{125}I]ACTP) suggests that the activation by phospholipid was associated with a conformational change in the kinase. [^{125}I]ACTP incorporation increased 2-fold in the presence of crude phosphatidylcholine, and this increase in [^{125}I]ACTP labeling is completely blocked by the addition of MgATP. Furthermore, proteolytic mapping was consistent with the modification of a distinct site when GRK2 was labeled in the presence of phospholipid. While an acidic phospholipid specificity was demonstrated using the mixed micelle phosphorylation assay, a notable exception was observed with PIP$_2$. In the presence of PIP$_2$, kinase activity as well as [^{125}I]ACTP labeling was inhibited. These data demonstrate the direct regulation of GRK2 activity by phospholipids and supports the hypothesis that this effect is the result of a conformational change within the kinase.

The molecular mechanisms involved in signal transduction of G protein-coupled receptors are best understood in the visual system where rhodopsin serves as the "receptor" for light (1) and the β-adrenergic pathway in which the β-adrenergic receptor (βAR)[1] binds catecholamines (2, 3). A feature common to both model systems as well as many other G protein receptors is the diminished responsiveness with time to a signal of equal intensity. This phenomenon is known as desensitization (4) and exhibits both an agonist-specific and nonspecific pattern. Rapid, agonist-specific desensitization of rhodopsin and the β_2-adrenergic receptor (β_2AR) occurs in response to the phosphorylation of the receptor by the enzymes rhodopsin kinase and the β-adrenergic receptor kinase (βARK) (5). Rhodopsin kinase and βARK are members of a family known as G protein-coupled receptor kinases (GRKs). A common feature to the GRK family of kinases is multi-site phosphorylation of receptor substrates in response to agonist occupancy (6). The relationship between agonist occupancy and receptor phosphorylation by GRKs is key to the specificity of the desensitization process, while other kinases such as protein kinase A and C play a role in nonspecific or heterologous desensitization. Two possible mechanisms could explain the enhanced phosphorylation of the activated form of the receptor by kinases of the GRK family. First, receptor occupancy may induce a conformational change exposing potential phosphorylation sites previously sequestered from the kinase. Alternatively, interaction of the kinase with the agonist-bound form of the receptor could result in enhanced catalytic activity of the kinase. The bulk of the experimental evidence supports the latter hypothesis (7–9). In addition to the enhanced catalytic activity of GRKs in the presence of agonist-occupied receptor, GRK2 and GRK3 activity is also increased by heterotrimeric G protein βγ subunits (10–13). The potential for finely controlled desensitization by the interplay of receptors and βγ subunits is an exciting possibility given the evidence for dual regulation of GRK2 and GRK3 by these proteins (14).

While G protein-coupled receptors serve as substrates for the kinase after reconstitution into phospholipid vesicles, only recently has specific lipid requirements for GRKs been described. GRK5 was reported to require phospholipid for maximal catalytic activity (15). In this case, phospholipid-stimulated autophosphorylation of GRK5 was necessary for phosphorylation of the β_2AR and rhodopsin. In addition, GRK2 and GRK3 were regulated by phospholipids via the interaction with the carboxyl-terminal portion of the kinase known as the pleckstrin homology domain (16, 17). In the initial report, the incorporation of negatively charged lipids into phospholipid vesicles resulted in a physical interaction of GRK2 or GRK3 with the vesicle. With the exception of PIP$_2$, this resulted in enhance phosphorylation of the human m2 muscarinic acetylcholine receptor. The addition of PIP$_2$ resulted in inhibition of phosphorylation of the receptor in a competitive manner with respect to other phospholipids. Purified heterotrimeric G protein βγ subunits

[1] The abbreviations used are: β-adrenergic receptor; βARK, β-adrenergic receptor kinase; G protein, guanine nucleotide-binding protein; GRK, G protein-coupled receptor kinase; [^{125}I]ACTP, N-3-[^{125}I]iodo-4-azidophenylpropionamido-S-(2-thiopyridyl)cysteine; PIP$_2$, phosphatidylinositol 4,5-bisphosphate; PAGE, polyacrylamide gel electrophoresis.

were able to reverse this inhibition. Furthermore, the lack of additivity suggested a common site of interaction on the kinase for the lipids and G protein $\beta\gamma$ subunits. This hypothesis was further supported by the finding that two previously characterized G protein $\beta\gamma$ subunit binding proteins, phosducin and glutathione S-transferase-βARK (466–689) fusion protein, prevented the effects of the phospholipids. In a subsequent report, similar effects in terms of PIP_2-enhanced binding of GRK2 to phospholipid vesicles was described. In contrast to the previous manuscript, data are presented that demonstrate increased GRK2 activity when coincubated with both PIP_2 and G protein $\beta\gamma$ subunits. Additionally, the remaining lipids previously reported to increase kinase activity in the absence of $\beta\gamma$ subunits in this case required the addition of G protein $\beta\gamma$ subunits to enhance GRK2 activity. The interpretation by these authors was that effective membrane localization of βARK, which enhanced both the rate and extent of phosphorylation of receptor substrates, required the simultaneous presence of two pleckstrin homology domain ligands.

In this manuscript, we provide evidence of an acidic phospholipid requirement of GRK2 based on the phosphorylation of dodecyl maltoside-solubilized receptors and the direct activation of the kinase toward peptide substrates by the addition of various phospholipids. Additionally, lipids that failed to enhance kinase activity did not increase labeling of GRK2 with the the heterobifunctional reagent [125I]ACTP. Finally, data obtained in the absence of G protein $\beta\gamma$ subunits agree with the original report in which PIP_2 promotes kinase binding to phospholipid vesicles but inhibits enzymatic activity (16). Thus, we provide evidence for catalytic activation as well as a conformational change in GRK2 following the interaction of the kinase and phospholipid. These data raise the possibility of a third level of regulation of GRK2 activity within the cell and suggest that the mechanism of phospholipid is more complex than simply targeting of the kinase to the plasma membrane.

EXPERIMENTAL PROCEDURES

Materials—Isoproterenol, alprenolol, and all phospholipids were purchased from Sigma. Western blot detection reagents including donkey anti-rabbit horseradish peroxidase-conjugated secondary antibody was obtained from Amersham Corp. The peptide substrate (RRREEEEESAAA) was synthesized using t-butoxycarbonyl chemistry with an Applied Biosystems 430A peptide synthesizer. Prior to use, the synthetic peptide was purified by reverse phase high performance liquid chromatography using a C-18 column and a 0–50% acetonitrile gradient in 0.1% trifluoroacetic acid/water. [γ-32P]ATP, Na125I, and [125I]iodocyanopindolol were obtained from DuPont NEN. All other reagents were of the the highest commercial grade available.

Preparation of βARK—βARK (GRK2) was overexpressed and purified from Sf9 cells using the baculovirus expression system as previously detailed (18). Briefly, cells were harvested 48 h after infection by low speed centrifugation. Following homogenization in 20 mM Hepes, pH 7.2, 250 mM NaCl, 5 mM EDTA, 3 mM phenylmethylsulfonyl fluoride, and 3 mM benzamidine, a high speed supernatant was prepared. The soluble fraction was diluted and applied to a SP-Sepharose column, which was washed and eluted in a 50–300 mM NaCl linear gradient. Peak activity fractions were pooled, diluted, and loaded on a heparin-Sepharose column. The βARK was eluted from the heparin column using a 100–600 mM NaCl gradient. The peak activity was pooled and made 0.02% final in Triton X-100 and stored at 4 °C. Protein concentration was determined by the method of Bradford (19) using purified bovine serum albumin as a standard. Purity of the βARK preparation was determined by SDS-polyacrylamide gel electrophoresis and was routinely >95%.

Preparation of β_2AR—The hamster β_2AR was expressed in Sf9 cells using the baculovirus system and purified on an alprenolol-Sepharose column using a modification of previously described techniques (20, 21). n-Dodecyl β-D-maltoside (10 mM) in 100 mM NaCl, 10 mM Tris-HCl, pH 7.4, 5 mM EDTA, 10 μg/ml each of leupeptin, benzamidine, pepstatin A, and soybean trypsin inhibitor, along with 1 mM phenylmethylsulfonyl fluoride was used to effect solubilization of the receptor from the Sf9 cell pellet. Following a high and low salt wash of the alprenolol Sepharose

column, the β_2AR was eluted into 50 ml of 1 mM dodecyl maltoside, 100 mM NaCl, 10 mM Tris-HCl, pH 7.4, 5 mM EDTA containing 100 μM (−)-alprenolol. The receptor was concentrated to ~2 ml by ultrafiltration on a YM-30 or YM-100 membrane (Amicon) and stored at −80 °C.

For reconstitution studies, the purified receptor was reinserted into phosphatidylcholine vesicles, pelleted by centrifugation, and resuspended in 20 mM Tris-HCl, pH 7.4, 2 mM EDTA as described previously (22). The concentration of receptor was determined using the β-adrenergic receptor antagonist [125I]iodocyanopindolol.

For studies in mixed detergent-lipid micelles, the purified receptor was diluted in 1 mM dodecyl maltoside, 100 mM NaCl, 10 mM Tris-HCl, pH 7.4, 5 mM EDTA and concentrated on a YM-100 membrane using a centricon device (Amicon). Alternatively, receptor purified in digitonin underwent detergent exchange on a G-50 column equilibrated in 0.5 mM dodecyl maltoside, 100 mM NaCl, 10 mM Tris-HCl, pH 7.4, 5 mM EDTA and concentrated on a YM-100 membrane using a centricon device. Crude phosphatidylcholine vesicles were produced using a tip sonicator with three 1-min bursts on ice. The desired amount of β_2AR was added to various amounts of phospholipid in 20 mM Tris-HCl, pH 7.4, 2 mM EDTA. Other phospholipids, stored as stock solutions in chloroform, were first dried under a stream of N_2. The desired amount of phospholipid was mixed with dodecyl maltoside-solubilized β_2AR, from which alprenolol had been removed as described above, prior to use in the phosphorylation assay.

Phosphorylation of the β_2AR—Reconstituted β_2AR (0.03–0.5 pmol) was incubated with GRK2 in a total volume of 25–50 μl containing 20 mM Tris-HCl, pH 7.4, 2 mM EDTA, 7.5 mM $MgCl_2$, 0.1 mM [γ-32P]ATP (200–1,000 cpm/pmol) at 30 °C. When indicated, (−)-isoproterenol was included at a final concentration of 10–50 μM. The reaction was stopped by the addition of 50 μl of SDS-PAGE stop solution and the receptor resolved on 9 or 12% polyacrylamide gels (23). Phosphorylated β_2AR was visualized by autoradiography, and the corresponding bands were excised and counted to determine the extent of phosphate incorporation. Unlike some previous studies with reconstituted receptor, no correction factor for the stoichiometry of receptor phosphorylation was used in these studies.

Phosphorylation of dodecyl maltoside-solubilized β_2AR was performed in the presence or absence of crude phosphatidylcholine or various purified phospholipids in a buffer of 20 mM Tris-HCl, pH 7.4, 2 mM EDTA, 7.5 mM $MgCl_2$, 0.1 mM [γ-32P]ATP (200–1,000 cpm/pmol). The final volume was 50 μl, and the phosphorylation reaction was carried out at 30 °C for various times as indicated. The reaction was stopped, and the phosphate incorporation was determined as detailed above.

Phosphorylation of Synthetic Peptides—A stock solution of purified synthetic peptides was prepared, and the pH was adjusted to 7.4 by the addition of Tris base. The peptides were incubated with GRK2 (~80 ng/assay tube) in a buffer containing 20 mM Tris-HCl, pH 7.4, 2 mM EDTA, 0.1 mM [γ-32P]ATP (200–1,000 cpm/pmol), 7.5 mM $MgCl_2$ in a final volume of 25 μl at 30 °C. The reaction was stopped by transferring the entire reaction mixture to a 2 × 2-cm square of P-81 paper followed by six washes in 75 mM phosphoric acid (10 ml/square). GRK2 activity was defined as the difference in phosphate incorporation in the presence and absence of peptide. Similar results are obtained if the kinase activity was determined in the presence or absence of GRK2. As phosphorylation reactions exhibited a higher blank when performed in the presence of added phospholipid, separate blanks were determined for assays in the absence or presence of additional phospholipid. A nonlinear regression program (Enzfitter, Elsevier-Biosoft, Cambridge, UK) was used to estimate the kinetic parameters.

[125I]ACTP Labeling—[125I]ACTP was synthesized as described previously by Dhanasekaran *et al.* (24). GRK2 (8 μg or 0.1 nmol) is reacted with an excess (1–200-fold) of [125I]ACTP in dimethylformamide (final concentration of DMF is <10%). After a 120-min incubation in the dark at 4 °C, the reaction was stopped by the addition of SDS (2% final) and 40 mM N-ethylmaleimide. The labeled kinase band was resolved by SDS-PAGE under nonreducing conditions. The GRK2 band was localized by autoradiography, excised, and counted. The stoichiometry was calculated after determining the specific activity of the [125I]ACTP preparation (typically 1 Ci/mmol).

Immunodetection of GRK2—Polyacrylamide gels were transferred overnight to nitrocellulose membranes. Immunodetection of GRK2 was performed using a rabbit antisera raised to purified βARK1 at a 1:4,000 dilution. Detection of the GRK2 using horseradish peroxidase conjugated donkey anti-rabbit antibody was as described by the manufacturer (Amersham Corp.).
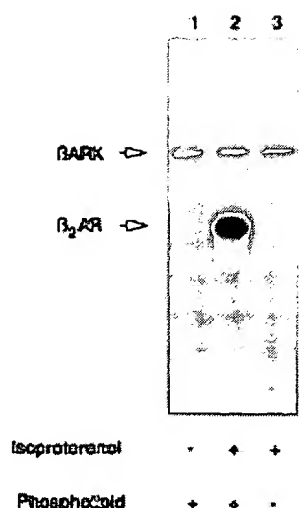
GRK2 Is Regulated by Phospholipids

FIG. 1. **Phosphorylation of detergent-solubilized β_2-adrenergic receptor by GRK2.** β_2AR is expressed in Sf9 cells, solubilized in dodecyl maltoside, and purified by affinity chromatography using an alprenolol-Sepharose column. Alprenolol is removed by size-exclusion chromatography on a G-50 column in 100 mM NaCl, 10 mM Tris-HCl, pH 7.4, and 1 mM dodecyl maltoside. The receptor is then concentrated using a Centricon-100 ultrafiltration device prior to phosphorylation. Receptor phosphorylation is carried out as described in the text, and the reaction is quenched by the addition of SDS sample buffer. The receptor is resolved by 9% SDS-polyacrylamide gel electrophoresis followed by autoradiography. The phosphorylation reaction is performed in the presence (*lanes 1* and *2*) or absence (*lane 3*) of crude phosphatidylcholine (50 µg). Isoproterenol (50 µM) is added (*lanes 2* and *3*) to demonstrate the agonist dependent nature of receptor phosphorylation by GRK2. The stoichiometry of phosphorylation is determined by excising the receptor band, quantitating the ^{32}P and expressing the data as mol of phosphate/mol of β_2AR.

RESULTS

A unique feature of the GRK family is the ability to phosphorylate the agonist-occupied form of a variety of G protein-coupled receptors. In order for a receptor to serve as a substrate for βARK, the protein is typically purified and reinserted into phospholipid vesicles. If phosphorylation of the receptor in detergent is attempted, no significant incorporation of phosphate is observed. Based on binding data, the receptor exhibits appropriate binding properties and is not degraded. While the possibility exists that detergents inhibit the kinase or reconstitution into bulk lipid provides a conformational structure required for interaction with GRKs, only recently have specific lipid requirement for GRKs been described (15–17). Fig. 1 demonstrates the phosphorylation of the β_2AR in dodecyl maltoside by GRK2. The phosphorylation of the receptor requires the addition of crude phosphatidylcholine and is stimulated by the addition of β-adrenergic agonist. The stoichiometry of phosphorylation is maximal at 4–5 mol of phosphate/mol of receptor. In data not shown, the effect of isoproterenol is blocked by the addition of the β-adrenergic receptor antagonist alprenolol. Also, there is a linear dependence between the amount of β_2AR added to the reaction mixture and the phosphate incorporation observed after resolving the receptor by SDS-PAGE with the maximal stoichiometry remaining ~4 mol phosphate/mol receptor. Finally, the phosphorylated receptor is not pelleted by a 300,000 × g centrifugation step in contrast to reconstituted receptor.

In order to define the phospholipid specificity of the GRK2 phosphorylation reaction, solubilized β_2AR is added to a variety of neutral, acidic, and basic phospholipids. As shown in Fig. 2, only lipids with a net negative charge including cardiolipin, phosphatidylglycerol, phosphatidic acid, phosphatidylserine,

and phosphatidylinositol support the phosphorylation of the β_2AR by GRK2. The addition of crude, but not purified, phosphatidylcholine results in receptor phosphorylation. This suggests that a phospholipid other than phosphatidylcholine is responsible for the activation of GRK2 observed above. Fig. 3 compares the effects of phosphatidylinositol to those of PIP$_2$. While phosphatidylinositol enhanced receptor phosphorylation by GRK2, there is no significant β_2AR phosphorylation in mixed micelles containing PIP$_2$.

To further investigate the effect of phospholipid on GRK2 activity, a nonreceptor peptide substrate (RRREEEEESAAA) previously shown to serve as a βARK1 substrate is used (25). The time course of phosphorylation of the peptide by GRK2 is linear for 2 h in the absence or presence of phospholipid (Fig. 4). However, there is a substantial increase in phosphate incorporation observed with the addition of crude phosphatidylcholine to the reaction mixture. The effect of phosphatidylcholine is not due to protection of the kinase from degradation or other nonspecific effects as Western blotting reveals equal amounts of the 80,000 M_r kinase band without evidence of proteolytic cleavage (data not shown).

The kinetic parameters of phosphorylation are determined in the presence of varying amounts of the peptide substrate. As shown in Table I, the effect of phospholipid is to increase the V_{max} of the phosphorylation reaction approximately 3-fold (8.7–25.4 nmol/min·mg of βARK) without a change in the K_m for the peptide substrate. In data shown in Table II, phosphatidylinositol increased phosphorylation of the peptide substrate 6-fold while PIP$_2$ decreased GRK2 activity to 30% of the control level.

As GRK5, a member of the GRK family related to βARK, has been shown to undergo phospholipid-stimulated autophosphorylation and association with phospholipid vesicles (15), we examine GRK2 to determine if a similar mechanism may be responsible for the phospholipid activation of the kinase. GRK2 does not autophosphorylate to any significant degree in the presence or absence of crude phosphatidylcholine (Fig. 5). At 1 h, the maximal amount of autophosphorylation is observed with a stoichiometry of 0.1 mol phosphate/mol kinase. A Western blot of GRK2 incubated with vesicles prepared from purified lipids demonstrates a significant amount of immunoreactivity associated with the pellet (Fig. 6). 10–20% of the immunoreactive GRK2 did pellet with phosphatidylinositol, and ~5% pelleted with PIP$_2$. These data stand in contrast to that seen with GRK5 (15) and suggest different mechanisms of lipid activation of the two kinases. Moreover, the demonstration of GRK2 association with vesicles containing either phosphatidylinositol or PIP$_2$ is in agreement with the previously published findings (16, 17).

The heterobifunctional cross-linking reagent, N-3-[^{125}I]iodo-4-azidophenylpropionamido-S-(2-thiopyridyl)cysteine has been used to map the molecular structure of transducin's α subunit (24). Under mild, nondenaturing conditions, [^{125}I]ACTP derivatizes reduced sulfhydryls to form a mixed disulfide easily cleaved by the addition of excess reducing agents. When GRK2 is incubated for 2 h in the dark with a 100-fold molar excess of [^{125}I]ACTP relative to kinase, there is incorporation of ~1 mol [^{125}I]ACTP/mol kinase. The addition of phospholipid vesicles to the reaction results in a 2-fold enhancement of incorporation to a stoichiometry of 2 mol of [^{125}I]ACTP/mol of βARK1 (Fig. 7). The additional [^{125}I]ACTP incorporation observed in the presence of phospholipid vesicles is blocked by the addition of MgATP at concentrations identical to those used in the phosphorylation assay. The effect of MgATP was specific for [^{125}I]ACTP in response to phospholipid as there is no effect observed with [^{125}I]ACTP incorporation in the absence of phos-
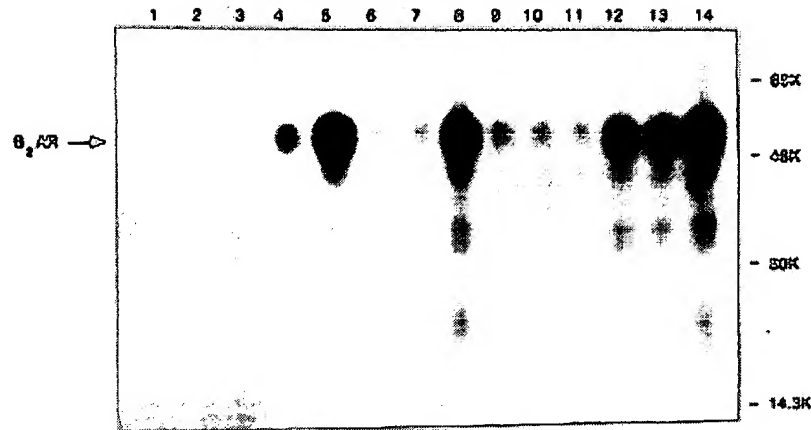
FIG. 2. **Phospholipid specificity of β₂AR phosphorylation by βARK.** 2.5 μl of a phospholipid (10 mg/ml stock in chloroform) is taken to dryness with a stream of nitrogen gas and rehydrated with 10 μl of 20 mM Tris-HCl, pH 7.2, 2 mM EDTA, and 1 mM dodecyl maltoside at 30 °C. Mixed micelles are formed by the addition of Alprenolol-free β₂AR. The final volume of the phosphorylation reaction is 50 μl and contained 2.8 pmol of receptor. The phosphorylation reaction is begun by the addition of kinase and ATP at 30 °C and stopped after 60 min with 10 μl of the SDS-PAGE stop solution. 20-μl aliquots were loaded on a 12% polyacrylamide gel, and the phosphorylated receptor was localized by autoradiography. The samples are as follows: *lane 1*, no lipid (incubation performed in the absence of 10 μM isoproterenol); *lane 2*, no lipid; *lane 3*, crude phosphatidylcholine (incubation performed in the absence of 10 μM isoproterenol); *lane 4*, crude phosphatidylcholine; *lane 5*, cardiolipin; *lane 6*, lysophosphatidylcholine; *lane 7*, palmitic acid; *lane 8*, phosphatidyl-DL-glycerol; *lane 9*, purified phosphatidylcholine; *lane 10*, phosphatidylethanolamine; *lane 11*, sphingomyelin; *lane 12*, phosphatidic acid; *lane 13*, phosphatidyl-L-serine; *lane 14*, phosphatidylinositol.
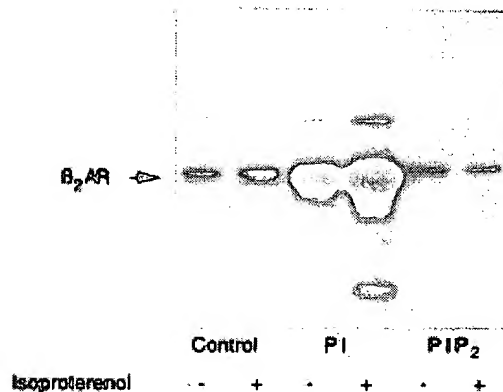

FIG. 3. **Effect of PIP₂ on GRK2 phosphorylation of the β₂AR.** 2.5 μl of phosphatidylinositol, PIP₂ (10 mg/ml stock in chloroform), or chloroform are taken to dryness with a stream of nitrogen gas and rehydrated with 10 μl of 20 mM Tris-HCl, pH 7.2, 2 mM EDTA, and 1 mM dodecyl maltoside at 30 °C. β₂AR phosphorylation by GRK2 in mixed micelles is performed as described above in the presence or absence of 10 μM isoproterenol.

pholipid. In all cases, the [¹²⁵I]ACTP incorporation is sensitive to reducing agents, indicating the presence of a mixed disulfide and not covalent attachment via the azide moiety. When a variety of lipids are examined, only the acidic phospholipids previously shown to enhance GRK2 activity led to an increase in [¹²⁵I]ACTP labeling of the kinase (Fig. 8). Of note is the observation that PIP₂ not only failed to increase the labeling of GRK2, but decreased [¹²⁵I]ACTP incorporation to a level below that seen in the basal state. A preliminary mapping experiment demonstrates that the ¹²⁵I associated with GRK2 resulted in a unique proteolytic map when cleaved with V-8 protease. The appearance of proteolytic bands of 14 and 6 kDa are observed when the kinase is labeled in the presence of the activating lipid phosphatidic acid (Fig. 9). These cleavage products are greatly diminished by co-incubation of lipid and MgATP or with the omission of the phospholipid to the labeling reaction (data not shown).

DISCUSSION

Regulation of G protein-coupled receptor function involves the process of desensitization in which a cell exposed to an
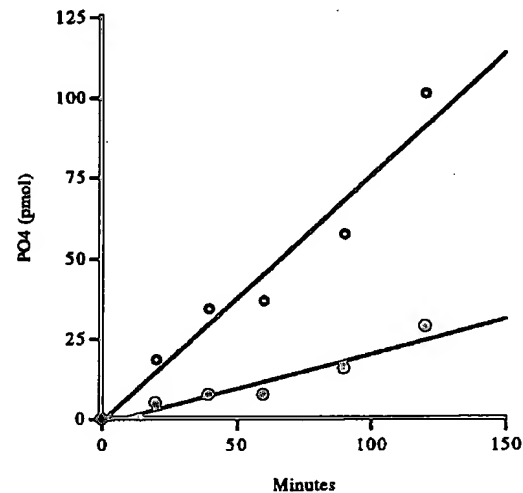
FIG. 4. **Time course of synthetic peptide phosphorylation by GRK2.** The synthetic peptide substrate RRREEEEESAAA (1 mM) is incubated for various times as indicated in the presence (E) or absence (●) of crude phosphatidylcholine (50 μg). The reaction is stopped by spotting the sample on a square of P-81 ion-exchange paper and washing in phosphoric acid as described. Each sample is performed in triplicate, and the results shown are that of a typical experiment.

TABLE I
Kinetics of peptide phosphorylation

Various concentrations of the peptide RRREEEEESAAA (0–5 mM) are incubated with GRK2 (2.4 pmol) in the presence of 100 μM ATP (~1000 cpm/pmol) at 30 °C for 60 min. The reaction is stopped, and phosphorylation of the synthetic peptide was determined as described in the text. The kinetic parameters are determined by a nonlinear regresssion program (Enzfitter) and expressed as the mean ± S.E. with $n = 3$.

Additions	K_m	V_{max}	V_{maxm}
	mM	nmol P_i/(min mg)	
Control	1.34 ± 0.17	8.7 ± 1.5	6.5
Phospholipid	1.37 ± 0.42	25.4 ± 6.2	18.5

agonist becomes less sensitive to subsequent stimulation. In the β₂AR-adenylyl cyclase system, nonselective, and agonist-specific forms of desensitization occur and appear to be related

TABLE II

Effect of PI and PIP₂ on peptide phosphorylation

The peptide RRREEEEESAAA (1 mM) was incubated with GRK2 (1 pmol) in the presence of 100 μM ATP (~1000 cpm/pmol) at 30 °C for 60 min. Phosphorylation of the synthetic peptide is determined as described in the text. Phosphate incorporation (pmol) is expressed as the mean ± S.E. with $n = 4$.

Additions	Phosphate incorporation
Control	4.1 ± 1.5
Phosphatidylinositol	25.5 ± 7.4
PIP₂	1.3 ± 0.2
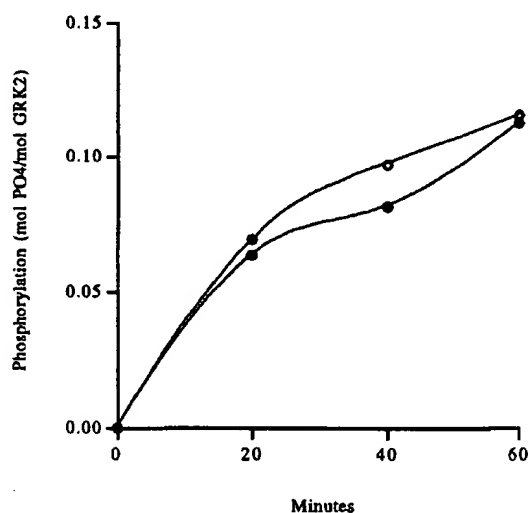
FIG. 5. **Autophosphorylation of GRK2.** Autophosphorylation of GRK2 is determined under conditions identical to receptor phosphorylation studies containing 80 ng (1 pmol) of purified GRK2 with (E) or without (●) added crude phosphatidylcholine (50 μg). The kinase is resolved by SDS-PAGE and localized by autoradiography. The gel slice containing the GRK2 band is excised and counted to determine the stoichiometry of phosphorylation, which is expressed as mol of phosphate/mol of GRK2.

FIG. 6. **Effect of lipids on GRK2 binding to phospholipid vesicles.** Lipids are dried under a stream of nitrogen and resuspended in 20 mM Tris-HCl, pH 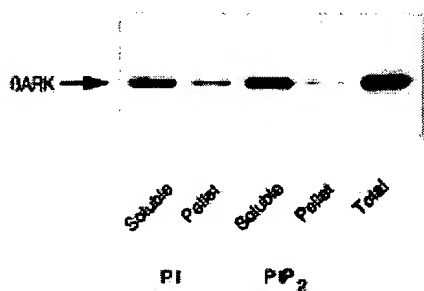7.2, 2 mM EDTA with three bursts of a tip sonicator. GRK2 (1 pmol) is added, and the mixture is incubated on ice for 15 min. The phospholipid vesicles are collected by centrifugation at 15,000 × g for 30 min. The supernatants and corresponding phospholipid pellets analyzed by SDS-PAGE and GRK2 were detected by immunoblotting. GRK2 binding to phosphatidylcholine and PIP₂ vesicles as well as a control lane representing the total amount of kinase used in each incubation is shown.

to phosphorylation of the receptor (26). Kinases of the GRK family are thought to play a role in rapid, agonist-specific desensitization, as these enzymes phosphorylate the receptor in an agonist-dependent fashion. Several lines of evidence support this proposed role of GRKs in the desensitization process. First, cells that express β_2ARs that have had the putative GRK2 phosphorylation sites deleted exhibit delayed desensiti-
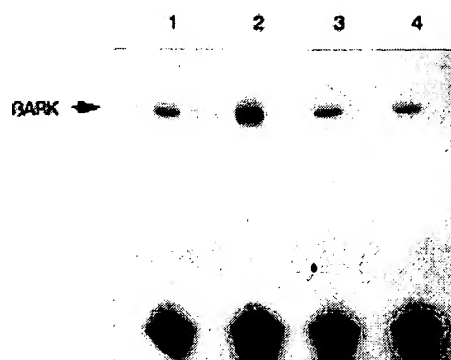
FIG. 7. **[¹²⁵I]ACTP labeling of GRK2.** A 100-fold excess of [¹²⁵I]ACTP relative to kinase is incubated in the dark on ice for 2 h. The labeling is stopped by the addition of 2% SDS and 40 mM *N*-ethylmaleimide (final concentrations). SDS sample buffer without β-mercaptoethanol is added and the GRK2 resolved under nonreducing conditions by SDS-PAGE. Fig. 7 is a autoradiograph under basal (*lane 1*), 50 μg crude phosphatidylcholine (*lane 2*), MgCl₂ (7.5 mM) and ATP (0.1 mM) (*lane 3*), and phosphatidylcholine and MgATP (*lane 4*) conditions. The GRK2 band is excised and [¹²⁵I]ACTP incorporation determined by γ counting. The specific activity of the [¹²⁵I]ACTP varied with each preparation and is determined separately. These results are representative of [¹²⁵I]ACTP labeling performed a minimum of 4 times.
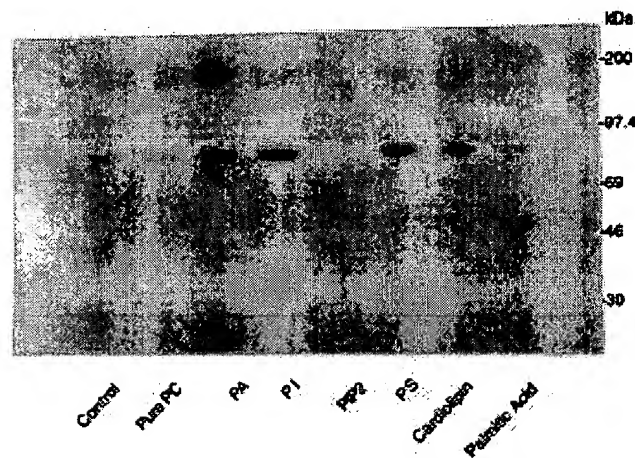
FIG. 8. **Lipid profile of [¹²⁵I]ACTP incorporation into GRK2.** GRK2 is incubated with a 100-fold molar excess of [¹²⁵I]ACTP and the addition of 50 μg of various lipids as described above. The reaction is terminated by the addition of *N*-ethylmaleimide and SDS, and the kinase band is resolved by electrophoresis. An autoradiograph of labeled GRK2 is shown.

zation (27). Second, a permeabilized cell system has been used to demonstrate that heparin, a potent inhibitor of GRK2, blocked both agonist-induced receptor phosphorylation and desensitization (28). Third, type-specific antibodies directed toward GRK3 attenuated odorant-induced desensitization in olfactory cells (29, 30). Fourth, Ishii *et al.* (31) have shown that GRK3 blocks thrombin signaling when the receptor and kinase are coexpressed in *Xenopus* oocytes. Finally, overexpression of a GRK2 dominant negative mutant in airway epithelial cells attenuates desensitization of the β_2AR (32). At this time, these data are consistent with a role of GRK-mediated receptor phosphorylation in the process of agonist-specific desensitization.

The agonist-dependent phosphorylation of receptors by GRK2 and other members of the GRK family is a key feature of this class of enzymes. A conformational change in the receptor could expose potential phosphate acceptor sites to the kinase resulting in agonist-dependent phosphorylation of the receptor. However, this does not appear to be the mechanism involved in receptor-GRK interactions (7). Alternatively, the kinase ap-
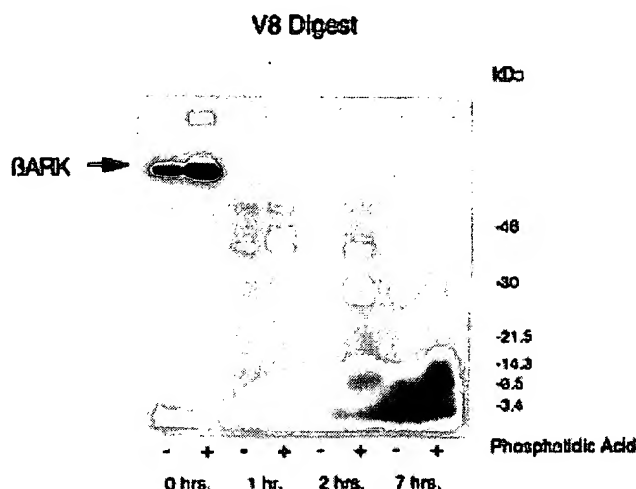
V8 Digest

FIG. 9. **Proteolytic digest of [^{125}I]ACTP labeled GRK2.** GRK2 is labeled is the absence (−) or presence (+) of phosphatidic acid (50 μg) as described above. The reaction is stopped by the addition of *N*-ethylmaleimide (40 mM) and [^{125}I]ACTP-labeled GRK2 digested with V-8 protease (1:10 ratio by weight) for the times indicated at 30 °C. The digest is stopped by the addition of SDS-sample buffer without β-mercaptoethanol. The peptide fragments are resolved on a 10–20% SDS-PAGE gradient. [^{125}I]ACTP-labeled fragments are identified by autoradiography. The majority of unincorporated [^{125}I]ACTP is removed by desalting on a G-50 column in 20 mM Tris-HCl, pH 7.2, 2 mM EDTA, 0.02% Triton X-100 before proteolysis.

pears to interact with the agonist-occupied form of the receptor, which primarily results in an increase in the V_{max} of the enzyme (8, 9). Presumably, a conformational change occurs in GRK2 and other GRKs, which results in enhanced catalytic efficiency. Recently, it has been shown that the peptide mastoparan increases the activity of rhodopsin kinase (8) and a GRK isolated from porcine brain with properties similar to βARK1 (13). Since mastoparan activates G proteins by mimicking a structure similar to agonist-occupied receptors (33), a similar mechanism would seem likely in the stimulation of kinase activity.

In addition to the activation of the kinase following the interaction with agonist-occupied receptors, GRKs also interact with membranes via different mechanisms. Photostimulation of rhodopsin results in the association of rhodopsin kinase with the retinal membrane. The translocation to the membrane requires the farnesylation of rhodopsin kinase, a post-translational modification unique to this member of the GRK family (6). GRK2 (βARK1), GRK3 (βARK2), and a related kinase from porcine brain all exhibit enhanced phosphorylation of agonist-occupied receptors in the presence of βγ-subunits from heterotrimeric G proteins (10–12). The effect of exogenous βγ-subunits is to increase the rate and maximal stoichiometry of phosphorylation (11, 12). This effect is synergistic with the activation of the kinase by agonist-occupied receptor or mastoparan (13). Similarly to rhodopsin kinase, βARK1 activity has been shown to translocate from the cytosol to the plasma membrane following stimulation of the target cell with a wide variety of agonists including isoproterenol, PGE$_1$, somatostatin, and platelet activating factor (34–36). Unlike rhodopsin kinase, GRK2 does not undergo isoprenylation (37, 38). However, the interaction of the kinase with the βγ-subunits appears to target βARK to the membrane (11). Thus, two different molecular mechanisms exist for localizing GRKs to a membrane surface. Most recently, a third member of the GRK family (GRK5) was cloned and found to lack the sequence required for either isoprenylation or interaction with βγ-subunits (15). Consistent with the later is the finding that β$_2$AR or rhodopsin

phosphorylation by GRK5 is not enhanced by the addition of βγ-subunits. However, phospholipid-stimulated autophosphorylation of GRK5 at Ser-484 and Thr-485 increased receptor phosphorylation ~15-fold and represents yet a third mechanism for membrane association of GRKs.

Despite the experimental data, which demonstrate the importance of phospholipid associations between GRKs, a clear effect of phospholipids is only now beginning to emerge. The observation that G protein-coupled receptors serve as substrates of GRKs following reconstitution into phospholipid vesicles or if expressed in high numbers in the plasma membrane of cells such as Sf9 insect cells (39) suggests the importance of lipids in the phosphorylation of receptor substrates. The traditional detergent for the solubilization of β$_2$ARs has been digitonin (20). While biologic activity is preserved, the digitonin is difficult to remove due to its low critical micellar concentration (CMC). Furthermore, digitonin tends to concentrate with most ultrafiltration techniques. We have used dodecyl maltoside to effect solubilization and purification of the β$_2$AR. Dodecyl maltoside has a defined critical micellar concentration and forms micelles of ~50,000 Da. We have taken advantage of these properties to concentrate the purified receptor using a YM-100 membrane. Under these conditions, detergent passes through while detergent-receptor micelles are retained by the membrane. In this manner, we could manipulate the receptor preparation without excessive concentration of the detergent. In addition, enzymatic activity of rhodopsin kinase (40) and βARK1[2] is minimally affected by dodecyl maltoside while other detergents completely inhibit kinase activity despite concentrations below the critical micellar concentration of the detergent.

In the current study, we clearly demonstrate that detergent-solubilized β$_2$AR serves as a substrate for GRK2, provided phospholipid is added to the phosphorylation reaction. Under the conditions used in this study, the receptor resides in a mixed detergent-lipid micelle. The concentration of detergent used would not permit the formation of pure lipid vesicles typical of previous reconstitution experiments. Furthermore, the receptor under these conditions does not pellet following a 300,000 × *g* centrifugation step adding support to the notion that the receptor is present in mixed micelles. This data would suggest that GRK2 has a phospholipid requirement for phosphorylation of receptor substrates. Using a variety of neutral, acidic, and basic phospholipids, we clearly demonstrate that negatively charged phospholipids, including cardiolipin, phosphatidylglycerol, phosphatidic acid, phosphatidylserine, and phosphatidylinositol, were necessary for phosphorylation of the β$_2$AR by GRK2. Previously, purified receptor was first inserted into crude phosphatidylcholine vesicles in order to observe GRK2-dependent phosphorylation. Therefore, we initially performed studies of phospholipid requirements of GRK2 using the same preparation of crude phosphatidylcholine. The fact that crude, but not purified, phosphatidylcholine preparations resulted in kinase activity is consistent with the notion that a phospholipid(s) other than phosphatidylcholine is required by GRK2. Thus, the long recognized requirement for reconstitution of the β$_2$AR into phosphatidylcholine vesicles most likely serves to provide a source of negatively charged phospholipid to the phosphorylation reaction.

As mentioned above, the lipid profile demonstrates that phospholipids with a net negative charge at physiologic pH enhance the phosphorylation of the β$_2$AR when studied in mixed detergent lipid micelles. A notable exception is the effect of PIP$_2$, as receptor phosphorylation is not observed when this

---

[2] J. J. Onorato, unpublished observation.

phospholipid is included in the phosphorylation assay. Similar data has recently been reported when phosphorylation of the m2 muscarinic acetylcholine receptor was studied in reconstituted lipid vesicles (16). In contrast, others reported that PIP_2 enhanced GRK2 phosphorylation of the β_2AR only in the presence of added $\beta\gamma$ subunits of heterotrimeric G proteins (17). While the stoichiometry of phosphorylation is rather low compared with that previously reported using crude phosphatidylcholine, qualitatively similar results were noted for a variety of lipids tested. In contrast to our findings and that of DebBurman *et al.* (16), in which >4 mol of phosphate/mol of receptor was achieved in the absence of $\beta\gamma$ subunits, a recent manuscript (17) indicated the stoichiometry was < 0.5 mol of phosphate/mol of β_2AR without the addition of G protein $\beta\gamma$ subunits.

The initial step in the mechanism of lipid regulation of GRK2 activity must involve the interaction between lipid and the kinase or the receptor. Evidence of a specific lipid-kinase interaction is provided by the finding that GRK2 becomes associated with vesicles provided they contain negatively charged lipids such as phosphatidylserine, phosphatidylinositol, or PIP_2. However, the phosphorylation data presented in this manuscript as well as that previously reported (16) suggests that the effects of lipids are more complex than simply targeting the kinase to the membrane surface. This is evident by the the effect of PIP_2 to cause membrane association in addition to inhibition of receptor phosphorylation.

In order to test the hypothesis that GRK2 activity is increased by phospholipids, we used a previously characterized peptide substrate of βARK (25). The advantage of the peptide substrate was 2-fold. First, the peptide substrate was designed to bind to ion exchange paper in 75 mM phosphoric acid permitting a large number of phosphorylation reactions necessary to obtain kinetic data. Second, the peptide substrate permits the identification of direct effects of phospholipid upon the kinase in the absence of any possible phospholipid-receptor interactions. The catalytic activity increases 3-fold with respect to the peptide substrate without a change in the K_m in the presence of crude phosphatidylcholine. We determined the kinetic parameters using crude phosphatidylcholine as this was the source of lipid that has been used for years in the reconstitution assay. Knowing that the crude preparations were 20% phosphatidylcholine and the results that demonstrate that crude but not purified phosphatidylcholine resulted in receptor phosphorylation in the mixed micelle system, we suspect that other phospholipids were responsible for βARK activity in the reconstitution assay. As further support, we demonstrate that the inclusion of phosphatidylinositol to the peptide assay results in a dramatic enhancement of phosphate incorporation. Moreover, PIP_2 inhibited the ability of GRK2 to phosphorylate the synthetic peptide substrate, consistent with our data and that of others (16), in which receptor phosphorylation was studied. In general, peptides are poor substrates for GRKs when compared with reconstituted receptors based on their low affinity for the kinase; however, they provide valuable data as to the mechanism of GRK activation. In this situation, the simplest explanation of the data is that GRK2 is directly activated following interaction with phospholipid. This observation would explain in part the apparent requirement for G protein-coupled receptors to be reconstituted into phospholipid vesicles in order to serve as GRK2 substrates.

Finally, we have used $[^{125}I]ACTP$ as a probe to assess conformational changes that may occur in the kinase. We have observed that GRK2 will incorporate ~1 mol of ACTP/mol of kinase under basal conditions. In the presence of crude phosphatidylcholine, the stoichiometry of $[^{125}I]ACTP$ labeling dou-

bled. We suggest that this represents a sulfhydryl group exposed following the interaction of GRK2 and phospholipid. This hypothesis is further supported by three observations. First, the increase in $[^{125}I]ACTP$ incorporation secondary to phospholipid exposure is completely blocked in the presence of MgATP. Second, the V-8 proteolytic map of $[^{125}I]ACTP$-labeled GRK2 identifies two unique bands in the presence of phospholipid that are diminished under basal conditions or in the presence of MgATP. Finally, lipids, which have been shown to activate GRK2, also increased the $[^{125}I]ACTP$ incorporation. More importantly, PIP_2, which binds GRK2 but results in an inhibition of catalytic activity completely abolished any $[^{125}I]ACTP$ labeling, including what appears to be the site labeled in the absence of lipids. At this time, our working hypothesis is that the sulfhydryl group(s) exposed following phospholipid interaction with GRK2 is near the ATP binding site and/or catalytic groove of the kinase and protected from ACTP labeling by the binding of MgATP. Furthermore, our ability to label this additional site serves as a probe of a putative conformational change, which occurs as the kinase is activated by regulatory lipids.

Data presented in this manuscript provide the first direct evidence to support the direct regulation of GRK2 by lipid. The effect on catalytic activity, in addition to the membrane localization, which occurs via the interaction between various lipids and the pleckstrin homology domain of GRK2 and GRK3, have clear implications as to the regulation of the kinase. Given the apparent association of several members of the GRK family with phospholipid membranes, it is tempting to speculate that many of the GRKs require phospholipid for maximal catalytic activity. While several different types of interaction between various GRKs and phospholipid membranes have been described, it will prove valuable to test whether a common molecular mechanism exists among this family of kinases. We are currently mapping the sites of ACTP incorporation in GRK2 to permit such a study. Additional studies are ongoing to define specific phospholipid interactions with βARK and extend the current studies to other members of the GRK family.

REFERENCES

1. Yarfitz, S., and Hurley, J. B. (1994) *J. Biol. Chem.* **269**, 14329–14332
2. Dohlman, H. G., Thorner, J., Caron, M. G., and Lefkowitz, R. J. (1991) *Annu. Rev. Biochem.* **60**, 653–688
3. Gomez, J., and Benovic, J. L. (1992) in *Molecular Biology of Receptors and Transporters: Receptors* (Friedlander, M., and Muekler, M., eds) pp. 1–34, Academic Press, New York
4. Sibley, D. R., Benovic, J. L., Caron, M. G., and Lefkowitz, R. J. (1987) *Cell* **48**, 913–922
5. Benovic, J. L., Onorato, J. J., Caron, M. G., and Lefkowitz, R. J. (1990) *Soc. Gen. Physiol.* **45**, 87–103
6. Inglese J., Freedman, N. J., Koch, W. J., and Lefkowitz, R. J. (1993) *J. Biol. Chem.* **268**, 23735–23738
7. Fowles, C., Sharma, R., and Akhtar, M. (1988) *FEBS Lett.* **238**, 56–60
8. Palczewski, K., Buczylko, J., Kaplan, M. W., Polans, A. S., and Crabb, J. W. (1991) *J. Biol. Chem.* **266**, 12949–12955
9. Chen, C. Y., Dion, S. B., Kim, C. M., and Benovic, J. L. (1993) *J. Biol. Chem.* **268**, 7825–7831
10. Haga, K., and Haga, T. (1990) *FEBS Lett.* **268**, 43–47
11. Pitcher, J. A., Inglese, J., Higgins, J. B., Arriza, J. L., Casey, P. J., Kim, C., Benovic, J. L., Kwatra, M. M., Caron, M. G., and Lefkowitz, R. J. (1992) *Science* **257**, 1264–1267
12. Kim, C. M., Dion, S. B., and Benovic, J. L. (1993) *J. Biol. Chem.* **268**, 15412–15418
13. Haga, K., Kameyama, K., and Haga, T. (1994) *J. Biol. Chem.* **269**, 12594–12599
14. Clapham, D. E., and Neer, E. J. (1993) *Nature* **365**, 403–406
15. Kunapuli, P., Gurevich, V. V., and Benovic, J. L. (1994) *J. Biol. Chem.* **269**, 10209–10212
16. DebBurman, S. K., Ptasienski, J., Boetticher, E., Lomasney, J. W., Benovic, J. L., and Hosey, M. M. (1995) *J. Biol. Chem.* **270**, 5742–5747
17. Pitcher, J. A., Touhara, K., Payne, E. S., and Lefkowitz, R. J. (1995) *J. Biol. Chem.* **270**, 11707–11710
18. Kim, C. M., Dion, S. B., Onorato, J. J., and Benovic, J. L. (1993) *Receptor* **3**, 39–55
19. Bradford, M. M. (1976) *Anal. Biochem.* **72**, 248–254
20. Benovic, J. L., Shorr, R. G. L., Caron, M. G., and Lefkowitz, R. J. (1984) *Biochemistry* **23**, 4510–4518
21. Kunapuli, P., Onorato, J. J., Hosey, M. M., and Benovic, J. L. (1994b) *J. Biol. Chem.* **269**, 1099–1105

22. Cerione, R. A., Strulovici, B., Benovic, J. L., Lefkowitz, R. J., and Caron, M. G. (1983) *Nature* **306**, 562–566
23. Laemmli, U. K. (1970) *Nature* **227**, 680–685
24. Dhanasekaran, N., Wessling-Resnick, M., Kelleher, D. J., Johnson, G. L., and Ruoho, A. E. (1988) *J. Biol. Chem.* **263**, 17942–17950
25. Onorato, J. J., Palczewski, K., Regan, J. W., Caron, M. G., Lefkowitz, R. J., and Benovic, J. L. (1991) *Biochemistry* **30**, 5118–5125
26. Hausdorff, W. P., Caron, M. G., and Lefkowitz, R. J. (1990) *FASEB J.* **4**, 2881–2889
27. Bouvier, M., Hausdorff, W. P., DeBlasi, A., O'Dowd, B. F., Kobilka, B. K., Caron, M. G., and Lefkowitz, R. J. (1988) *Nature* **333**, 370–373
28. Lohse, M. J., Lefkowitz, R. J., Caron, M. G., and Benovic, J. L. (1989) *Proc. Natl. Acad. Sci. U. S. A.* **86**, 3011–3015
29. Dawson, T. M., Arriza, J. L., Jaworsky, D. E., Borisy, F. F., Attramadal, H., Lefkowitz, R. J., and Ronnett, G. V. (1993) *Science* **259**, 825–829
30. Schleicher, S., Boekhoff, I., Arriza, J. L., Lefkowitz, R. J., and Breer, H. (1993) *Proc. Natl. Acad. Sci. U. S. A.* **90**, 1420–1424
31. Ishii, K., Chen, J., Ishii, M., Koch, W. J., Freedman, N. J., Lefkowitz, R. J., and Coughlin, S. R. (1994) *J. Biol. Chem.* **269**, 1125–1130
32. Kong, G., Penn, R., and Benovic, J. L. (1994) *J. Biol. Chem.* **269**, 13084–13087
33. Higashijima, T., Uzu, S., Nakajima, T., and Ross, E. M. (1988) *J. Biol. Chem.* **263**, 6491–6494
34. Strasser, R. H., Benovic, J. L., Caron, M. G., and Lefkowitz, R. J. (1986) *Proc. Natl. Acad. Sci. U. S. A.* **83**, 6362–6366
35. Mayor, F., Benovic, J. L., Caron, M. G., and Lefkowitz, R. L. (1987) *J. Biol. Chem.* **262**, 6468–6471
36. Chuang, T. T., Sallese, M., Ambrosini, G., Parruti, G., and DeBlasi, A. (1992) *J. Biol. Chem.* **267**, 6886–6892
37. Lorenz, W., Inglese, J., Palczewski, K., Onorato, J. J., Caron, M. G., and Lefkowitz, R. J. (1991) *Proc. Natl. Acad. Sci. U. S. A.* **88**, 8715–8719
38. Inglese, J., Koch, W. J., Caron, M. G., and Lefkowitz, R. J. (1992) *Nature* **359**, 147–150
39. Pei, G., Tiberi, M., Caron, M. G., and Lefkowitz, R. J. (1994) *Proc. Natl. Acad. Sci. U. S. A.* **91**, 3633–3636
40. Palczewski, K., McDowell, J. H., and Hargrave, P. A. (1988) *Biochemistry* **27**, 2306–2313

Substrate specificity determinants of the checkpoint protein kinase Chk1

James R.A. Hutchins, Mike Hughes, Paul R. Clarke*

Biomedical Research Centre, University of Dundee, Level 5, Ninewells Hospital and Medical School, Dundee DD1 9SY, UK

Abstract The Chk1 protein kinase plays a critical role in a DNA damage checkpoint pathway conserved between fission yeast and animals. We have developed a quantitative assay for Chk1 activity, using a peptide derived from a region of *Xenopus* Cdc25C containing Ser-287, a known target of Chk1. Variants of this peptide were used to determine the residues involved in substrate recognition by Chk1, revealing the phosphorylation motif Φ-X-β-X-X-(S/T)*, where * indicates the phosphorylated residue, Φ is a hydrophobic residue (M > I > L > V), β is a basic residue (R > K) and X is any amino acid. This motif suggests that Chk1 is a member of a group of stress-response protein kinases which phosphorylate target proteins with related specificities.

© 2000 Federation of European Biochemical Societies.

Key words: Cdc25; Chk1; Cell cycle checkpoint; Protein kinase specificity

1. Introduction

Eukaryotic cells possess checkpoint mechanisms which ensure that cell division is restrained in the presence of damaged or unreplicated DNA [1,2]. The Chk1 protein kinase is an essential component of the DNA damage checkpoint pathway conserved from yeast to animals that regulates entry into mitosis [3–5]. Chk1 phosphorylates the Cdc25 protein phosphatase, promoting the binding of a 14-3-3 protein to Cdc25 [6,7] and preventing nuclear translocation of Cdc25 [8–10]. Cdc25 is thus unable to activate the protein kinase Cdc2/cyclin B and the cell cycle is arrested prior to mitosis.

Chk1 may also execute its function through phosphorylation of other substrates. In vitro, Chk1 can phosphorylate *Schizosaccharomyces pombe* Wee1, the protein kinase that maintains inhibitory phosphorylation of Cdc2 [11]. In *Saccharomyces cerevisiae*, Chk1 phosphorylates Pds1, stabilising Pds1 and preventing the onset of anaphase [12]. However, the phosphorylation sites on these proteins have not been identified. It is also likely that other substrates remain to be discovered. In order to predict sites of phosphorylation on known substrates and to identify novel candidate substrates for a protein kinase, it is useful to determine minimal sequence requirements for recognition. The sequence specificity of Chk1 has not been reported, but a comparison of the sequences surrounding the known Chk1 phosphorylation sites in the human, *Xenopus laevis* and *S. pombe* isoforms of Cdc25 reveals conserved basic and hydrophobic residues N-terminal

to the target serine, suggesting that these residues may be important for recognition by the kinase (Fig. 1). Here, we report the substrate specificity of human Chk1 determined using peptides derived from Cdc25C as in vitro substrates. We define a recognition motif that is present in other potential Chk1 substrates. This motif suggests that Chk1 is a member of a group of related kinases with similar substrate specificities that respond to different cellular stresses.

2. Materials and methods

2.1. Expression and purification of GST-hChk1

A human Chk1 cDNA [5] was sub-cloned as a fusion product with the glutathione *S*-transferase (GST) gene into the pFastBac1 vector, and recombinant baculoviruses were produced using the Bac-to-Bac system (Gibco). *Sf21* insect cells in suspension culture were infected with *GST-hChk1* baculoviruses and incubated at 27°C for 96 h. The following steps were carried out at 4°C: cells were harvested by centrifugation, the cell pellet was resuspended in lysis buffer (50 mM Tris–HCl, pH 8.5, 10 mM dithiothreitol (DTT), 1% (v/v) NP-40, 1 μg/ml each of leupeptin and aprotinin, 1 mM each of phenylmethyl-sulphonyl fluoride, pepstatin A, chymostatin and benzamidine), and sonicated four times for 10 s. The sonicate was centrifuged at $14000 \times g$ for 10 min, and the supernatant mixed with 1 ml gluta-thione-Sepharose beads (Pharmacia) for 60 min. After washing with 50 mM Tris–HCl, pH 8.5, 150 mM NaCl, 5 mM DTT, 1%(w/v) NP-40, GST-hChk1 protein was eluted from the beads by successive incubations with 20 mM HEPES-KOH, pH 7.5, 50 mM reduced gluta-thione. Eluates containing GST-hChk1 protein (as judged by SDS-PAGE) were pooled, dialysed against 10 mM HEPES-KOH, pH 7.5, 1 mM DTT, aliquoted, snap-frozen, and stored at −70°C.

2.2. Synthesis of peptides

The *Xenopus* Cdc25 'SPS', 'APS', 'SPA' and 'human Cdc25C' peptides were synthesised and purified by Dr G. Bloomberg, Department of Biochemistry, University of Bristol, UK. All other peptides were synthesised on a 1.0 μmol scale as Cleaved PepSets (Chiron Technologies, Vic., Australia), dissolved in dimethylsulphoxide (DMSO), and stored at −70°C.

2.3. Phosphorylation of peptides by GST-hChk1

Peptides at 200 μM (unless stated otherwise) were phosphorylated in 50 mM HEPES, pH 7.5, 1 mM DTT, 100 μM γ[^{32}P]ATP (approx. 10 kBq/nmol), 10 mM MgCl$_2$ in a 10 μl reaction volume containing approximately 60 ng GST-hChk1. Reactions were carried out for 30 min at 37°C, then stopped by spotting 8 μl onto 15 mm × 15 mm squares of Whatman P81 phosphocellulose cation-exchange paper. Squares were washed three times for 5 min in 500 ml 150 mM H$_3$PO$_4$, rinsed in ethanol, air-dried and Cerenkov counted for 1 min. Reactions were performed in triplicate and the mean rate of phosphorylation calculated.

2.4. Kinetic experiments

For assays in which Chk1 activity was determined at various peptide concentrations, serial dilutions of peptide were made in 50 mM HEPES-KOH (pH 7.5), 25% (v/v) DMSO to give a final concentration of 5%(v/v) DMSO in the kinase reaction, with the exception of the experiment shown in Fig. 2, where no DMSO was present. Reaction velocity and substrate concentration data were fitted to a Michaelis–Menten curve using GraphPad Prism software, which determined the kinetic constants V_{max} and K_M.

*Corresponding author. Fax: (44)-1382-669993.
E-mail: p.clarke@icrf.icnet.uk

3. Results

3.1. A quantitative assay for Chk1 activity

To generate a substrate for in vitro phosphorylation by Chk1, we synthesised the peptide, RLYRSPSMPEKLDRK, derived from residues 281–294 of the *Xenopus* Cdc25C protein and including the Ser-287 site phosphorylated by Chk1 [7]. A C-terminal Lys residue was added to promote binding to phosphocellulose paper. Phosphorylation of this peptide (hereafter referred to as the 'SPS peptide') was catalysed by human Chk1 expressed as a fusion protein with glutathione-*S*-transferase (Fig. 2). In addition to the Ser-287 site, this peptide contains a serine at position 285 (the numbering corresponding to the position in the parent protein), a residue reported to be phosphorylated by cyclin-dependent kinases [13]. A peptide containing a Ser-285 to Ala substitution (the APS peptide) was phosphorylated with similar kinetics to the SPS peptide (Fig. 2), showing that Ser-285 is not required for recognition by Chk1 and is not itself a site of phosphorylation. In contrast, a peptide in which Ser-287 was changed to an alanine residue (the SPA peptide) was not phosphorylated, confirming the site of phosphorylation as Ser-287. Since the kinase used in these studies was the human sequence, we also compared a peptide derived from human Cdc25C which has three amino acid changes compared to the APS peptide. The human-derived sequence was a slightly poorer substrate than the *Xenopus*-derived APS peptide and the latter was therefore used as the parent sequence for subsequent studies. Standard assay conditions were optimised such that the rate of phosphorylation was close to the V_{max} of the enzyme, linear up to 60 min, and proportional to the amount of Chk1 used (data not shown).

3.2. Chk1 can phosphorylate serine or threonine, but not tyrosine residues

All of the phospho-acceptor sites for Chk1 identified thus far are serine residues. To determine whether threonine or tyrosine residues can also be phosphorylated by Chk1, variant APS peptides, in which Ser-287 was substituted for threonine or tyrosine, were tested in the Chk1 assay. The Thr-287 peptide was phosphorylated by Chk1 at a rate (28.6 pmol/min) slightly higher than the Ser-287 peptide (26.2 pmol/min), but the Tyr-287 peptide was not significantly phosphorylated. Chk1 is therefore a protein-serine/threonine kinase, but not a protein-tyrosine kinase.

3.3. Residues at positions −3 and −5 upstream of the target phosphorylation site are important for substrate recognition by Chk1

To determine which residues surrounding the phospho-acceptor site are important for recognition by Chk1, an alanine

Protein	Sequence $\underset{\downarrow \text{ Chk1}}{}$	Site
Human Cdc25C	VSRSGLYRSPSMPENLNRPRL	Ser-216
Xenopus Cdc25C	LNRSRLYRSPSMPEKLDRMPL	Ser-287
S. pombe Cdc25	TPRRTLFRSLSCTVETPLANK	Ser-99
S. pombe Cdc25	YLRPNVSRSRSSGNAPPFLRS	Ser-192
S. pombe Cdc25	QDTPVVRRTQSMFLNSTRLGL	Ser-359

Fig. 1. Amino acid sequence alignment of known Chk1 substrates. Conserved hydrophobic residues are underlined, conserved basic residues are in bold.

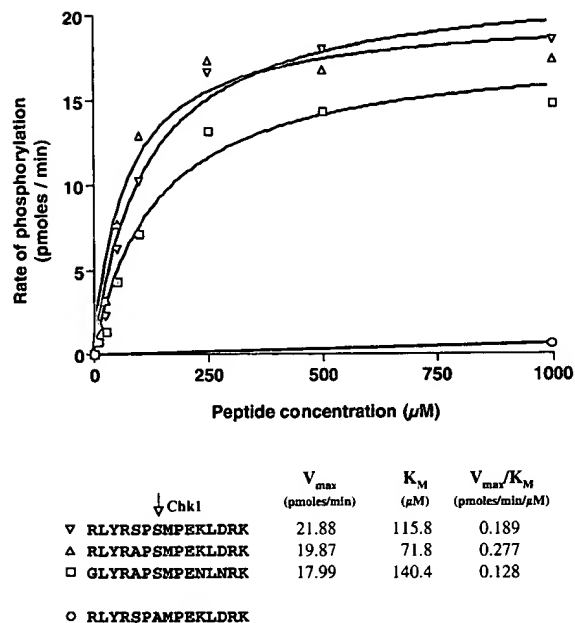|	V_{max} (pmoles/min)	K_M (μM)	V_{max}/K_M (pmoles/min/μM)
▽ RLYRSPSMPEKLDRK	21.88	115.8	0.189
△ RLYRAPSMPEKLDRK	19.87	71.8	0.277
□ GLYRAPSMPENLNRK	17.99	140.4	0.128
○ RLYRSPAMPEKLDRK			

Fig. 2. Comparison of the rate of phosphorylation of Cdc25C peptides by Chk1: (▽) *Xenopus* SPS peptide; (△) *Xenopus* APS peptide; (□) Human Cdc25C peptide; (○) *Xenopus* SPA peptide.

scan analysis of the APS peptide was performed. A panel of 12 APS peptide variants, each with one residue substituted for alanine, were assayed at 200 μM as substrates for Chk1 (Fig. 3A). Under these conditions, the majority of substitutions had little effect on the rate of phosphorylation of the peptide. Apart from the Ser-287 site, the only residues whose substitution to alanine significantly reduced the rate of phosphorylation were Leu-282 and Arg-284, five and three residues upstream of the phosphorylation site, respectively. None of the downstream residues, when substituted for alanine, caused a large reduction in the rate of phosphorylation by Chk1. More detailed kinetic experiments varying the concentration of substrate (Fig. 3B) showed that whereas substitution of Arg-281 or Met-288 to alanine resulted in an approximately two-fold reduction in catalytic efficiency (expressed as V_{max}/K_M), substitution of Leu-282 or Arg-284 to alanine reduced the catalytic efficiency by approximately 20-fold.

3.4. Variations in position and identity of residues surrounding the targeted serine affect the rate of phosphorylation by Chk1.

To investigate in more detail the contribution of the critical residues for recognition by Chk1, we designed a peptide, RLARAASMAAALARK, based on the APS peptide, but with seven of the non-essential residues substituted by alanine. This minimal peptide maintained a high rate of phosphorylation by Chk1 (Fig. 4A). When Leu^{-5} was substituted with Met or Ile, the rate of phosphorylation increased, but with Val or Arg, and particularly Ala substitutions, the rate was decreased. When Arg^{-3} was substituted with Lys, the peptide was phosphorylated at 80% of the rate of the parent peptide, whereas substitution to Ala greatly reduced the rate. Peptides in which Leu^{+5} was substituted or moved relative to the phosphorylated serine residue showed a slight increase in the rate of phosphorylation, the largest being when Leu was moved from the +5 to the +4 position. However, a peptide in which

A

B

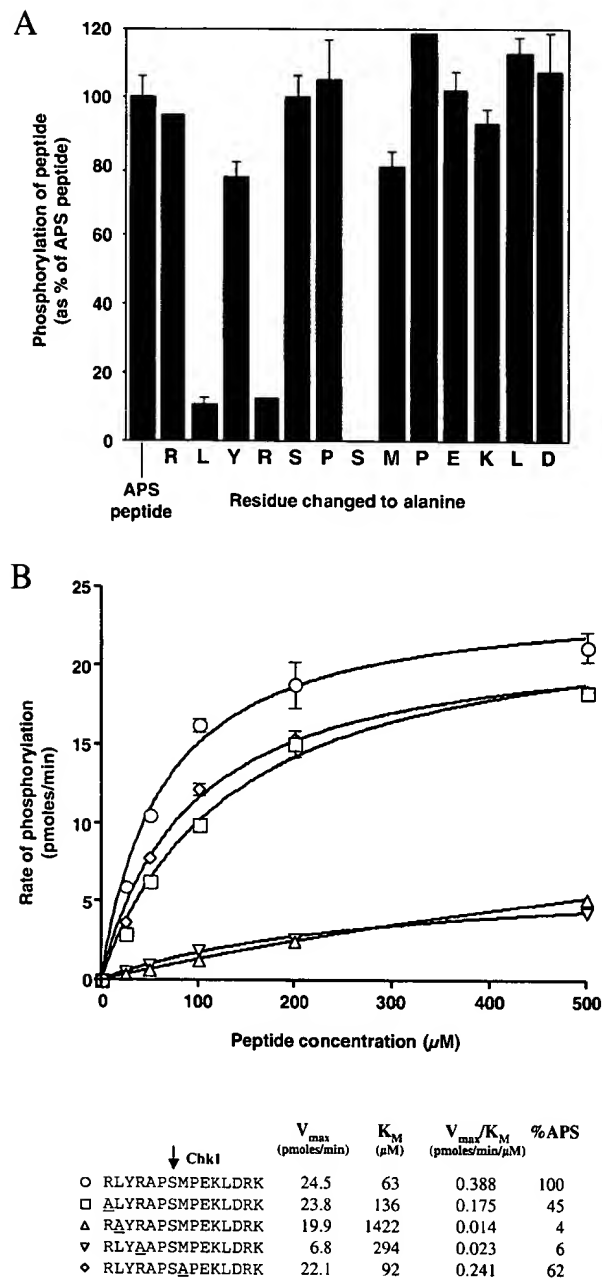| ↓ Chk1	V_{max} (pmoles/min)	K_M (μM)	V_{max}/K_M (pmoles/min/μM)	%APS
O RLYRAPSMPEKLDRK	24.5	63	0.388	100
□ ALYRAPSMPEKLDRK	23.8	136	0.175	45
△ RAYRAPSMPEKLDRK	19.9	1422	0.014	4
▽ RLYAAPSMPEKLDRK	6.8	294	0.023	6
◇ RLYRAPSAPEKLDRK	22.1	92	0.241	62

Fig. 3. Effect of substitution of residues in the *Xenopus* Cdc25C APS peptide on phosphorylation by Chk1. A: Alanine scan analysis. B: Comparison of phosphorylation kinetics.

all of the downstream residues were substituted by alanine was phosphorylated at 89% of the rate of the parent peptide, showing that residues C-terminal to the phospho-acceptor site do not play a strong role in substrate recognition by Chk1. A peptide in which the C-terminal Arg and Lys residues were swapped onto the N-terminal end of the molecule increased the rate of phosphorylation by 52%, indicating that N-terminal basic residues are positive determinants. More detailed kinetic experiments were performed on minimal peptide variants in which the positions of the upstream Leu and Arg residues were altered (Fig. 4B). Whereas movement of Arg^{-3} to the −4 or −2 positions resulted in 63% and 92% of the catalytic efficiency being retained, respectively, move-

ment of Leu^{-5} and Arg^{-3} together relative to the phosphorylated Ser resulted in the reduction of the V_{max}/K_M to less than 35% of that of the minimal peptide. Together these data indicate a minimal consensus for recognition by Chk1 as Φ-X-β-X-X-(S/T)*, where * indicates the phosphorylated residue, Φ is a hydrophobic residue (M > I > L > V), β is a basic residue (R/K) and X is any amino acid.

3.5. Serines 104 and 117 of S. pombe Wee1 are putative sites of phosphorylation by Chk1

S. pombe Wee1 protein kinase is phosphorylated on one or

A

B

↓ Chk1	V_{max} (pmoles/min)	K_M (μM)	V_{max}/K_M (pmoles/min/μM)	% min
O RLARAASMAAALARK	33.54	266.0	0.126	100.0
□ ALARAASMAAALARK	14.04	157.7	0.089	70.6
△ RLAARASMAAALARK	11.49	142.9	0.080	63.5
▽ RLRAAASMAAALARK	13.19	113.2	0.116	92.1
◇ RALARASMAAALARK	2.66	60.8	0.044	34.9
× LARAASMAAALARK	18.15	534.6	0.034	27.0
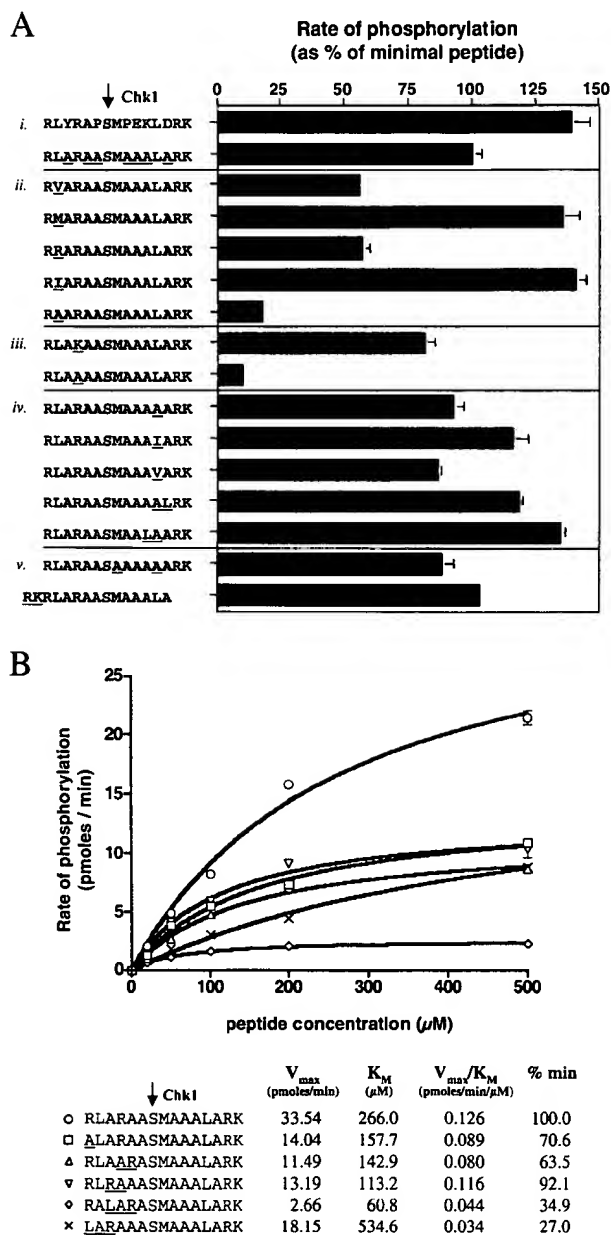
Fig. 4. Comparison of minimal peptides as Chk1 substrates. A: Effect of substituting specific residues (underlined) on rate of phosphorylation: (*i*) APS peptide and minimal parent peptide; (*ii*) varying Leu-282; (*iii*) varying Arg-284; (*iv*) varying Leu-292; (*v*) substitution of residues 288–293 to Ala, and swapping C-terminal RK onto N-terminus. B: Effect of changing the position of upstream residues on the kinetics of phosphorylation.

more serine residues by Chk1 in vitro [11]. Examination of the contexts of all the serine residues present in *S. pombe* Wee1 revealed two sites, Ser-104 and Ser-117, which contained a basic residue at position −3 and a small hydrophobic residue at position −5. We found that two peptides containing these serine residues, PVPRRP$\underline{S}^{104}$LFDRPNRK and LVSR-SS$\underline{S}^{117}$RLGDSPRK were phosphorylated at rates comparable to the APS peptide (Fig. 5). Substitution Ser-104 with Ala completely abolished phosphorylation by Chk1, confirming this residue as the site of phosphorylation. Substitution of Ser-117 with Ala reduced the rate of phosphorylation by 64%, indicating that this residue is a target for Chk1, although other residues in this peptide are also phosphorylated by Chk1.

3.6. Serine 343 of Xenopus Cdc25C is a good in vitro substrate for Chk1

Chk1 phosphorylates *Xenopus* Cdc25C on multiple sites, although only one of these, Ser-287, has been identified [7]. Inspection of the *Xenopus* Cdc25C sequence identified a potential Chk1 phosphorylation site, Ser-343, within the motif L-X-K-X-X-S*. This residue is located in a region of Cdc25C highly conserved between the *Xenopus* and human forms, and is equivalent to Ser-263 of human Cdc25C, shown to be a residue targeted by the kinase C-TAK1 [14]. The *Xenopus* Cdc25C-derived peptide SLKKTL$\underline{S}^{343}$LCDVDIRK was a good substrate for Chk1, with a phosphorylation rate 56% that of the APS peptide (Fig. 5). Phosphorylation of the peptide by Chk1 was abolished when Ser-343 was substituted with Ala, but 92% of the original rate was maintained when both Thr-341 and Ser-337 were substituted with Ala, confirming Ser-343 as the residue targeted by Chk1 in this peptide.

3.7. Chk1 can phosphorylate peptide substrates of related protein kinases

The requirement of Chk1 for upstream hydrophobic and basic residues is similar to that reported for mammalian AMP-activated protein kinase (AMPK), plant 3-hydroxy-3-methylglutaryl-CoA reductase kinase (HRK-A), SNF1 from *S. cerevisiae* and the Ca^{2+}/calmodulin-dependent protein ki-

nase I (CaMKI) [15]. We therefore wished to determine whether Chk1 could phosphorylate two peptides used as substrates for these kinases, the 'SAMS' peptide, HMRSAMS^{79}GLHLVKRR, derived from the sequence surrounding Ser-79 of rat liver acetyl-CoA carboxylase [16], and the 'AMARA' peptide, AMARAA$\underline{S}$AAALARRR, which contains the minimal consensus sequence [15]. The SAMS peptide was phosphorylated at a reasonable rate (33%) compared to the APS peptide (Fig. 5). A peptide with a Ser-79 to Ala substitution was not phosphorylated, confirming this residue as the target of Chk1. The AMARA peptide was a better substrate for Chk1 than the SAMS peptide, being phosphorylated at 92% of the rate of the APS peptide.

4. Discussion

We have determined the substrate specificity of the checkpoint protein kinase Chk1 using a series of synthetic peptides derived from a known substrate, Cdc25C. We show that the most important determinants for substrate recognition by Chk1 are a hydrophobic residue at position −5 (M > I > L > V) and a basic residue (R > K) at position −3 relative to the phospho-acceptor site, which can be a serine or threonine residue. These data allow us to define the minimal consensus motif for phosphorylation by Chk1 phosphorylation as Φ-X-β-X-X-(S/T)*. This motif is consistent with the primary sequence context of known Chk1 sites in Cdc25 from different species (Fig. 1), which all show a conserved basic residue (Arg) in the−3 position, and a small hydrophobic residue (Leu or Val) in the −5 position. It seems likely therefore that the substrate specificity of Chk1 homologues from *S. pombe* to vertebrates is conserved.

Using these substrate specificity data, we have predicted likely additional sites targeted by Chk1 in *Xenopus* Cdc25C and *S. pombe* Wee1, and we have confirmed that peptides derived from these sites are indeed phosphorylated by Chk1. Database searches reveal many other proteins containing potential Chk1 phosphorylation sites. One of these, Pds1, is a protein involved in controlling the timing of anaphase that has been proposed recently to be a Chk1 substrate in *S. cerevisiae* [12]. Examination of the amino acid sequence reveals that Pds1 contains six sites conforming to the Chk1 motif that are putative sites of phosphorylation. Of course, the recognition motif for a protein kinase is only the minimal requirement for phosphorylation. Whether or not a protein is a substrate in cells may depend upon interactions with this motif and localisation to the same sub-cellular compartment as the kinase.

The Ser-343 site of *Xenopus* Cdc25C that we have identified as a putative target for Chk1 lies within a region of this phosphatase highly conserved between frogs and humans. The equivalent residue in human Cdc25C, Ser-263, is phosphorylated by C-TAK1 [14]. This kinase also phosphorylates Ser-216 [14], the major site phosphorylated by Chk1 [5] and Chk2 [17]. In *S. pombe*, Cds1 and Chk1 phosphorylate Cdc25 in an identical manner on three serine residues in vitro [18]. Taken together, these results suggest that the three kinases Chk1, Cds1 and C-TAK1 have very similar phosphorylation motifs.

The catalytic domains of Chk1, Cds1 and C-TAK1 is most closely related in sequence to the Ca^{2+}/calmodulin-dependent protein kinase (CaMK) group [19]. Other members of this

Rate of phosphorylation
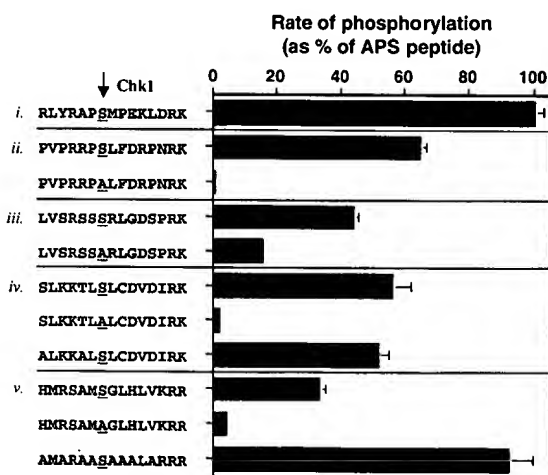**(as % of APS peptide)**

Fig. 5. Rate of phosphorylation of peptides predicted to be substrates of Chk1: (*i*) APS (*Xenopus* Cdc25C Ser-287) peptide; (*ii*) *S. pombe* Wee1 (Ser-104); (*iii*) *S. pombe* Wee1 (Ser-117); (*iv*) *Xenopus* Cdc25C (Ser-343); (*v*) SAMS [16] and AMARA [15] peptides.

group, AMPK, SNF1 and CaMKI, similarly require N-terminal basic and hydrophobic residues, although they have a stronger preference for C-terminal hydrophobic residues than Chk1 [15,20]. Consistent with these related specificities, Chk1 phosphorylates two peptide substrates designed for AMPK. How then can the sequence specificities of these Ser/Thr protein kinases be rationalised, based on their structures? X-ray crystallographic studies of the catalytic domains of several protein kinases have identified residues which form the 'specificity pockets' that determine substrate recognition [21,22]. In the autoinhibited form of CaMKI [23], the active site of the kinase is occupied by a pseudosubstrate region ([297]NFAKSKW*KQAFN[308]) containing the Φ-X-β-X-X-(S/T)*-X-X-X-Φ motif found in substrates of this kinase [24], but with a non-phosphorylatable Trp residue in the phospho-acceptor position. There is an electrostatic interaction between Glu-102 in the catalytic domain and Lys-300 in the pseudosubstrate. A hydrophobic pocket formed by residues Phe-104, Ile-210 and Pro-216 accommodates a hydrophobic residue at position -5 in the pseudosubstrate. Sequence alignment shows that these contact-making residues are conserved in the catalytic domains of kinases which share similar phosphorylation motifs. In an analysis of 24 protein- Ser/Thr kinases, we find that the residue in the position equivalent to Glu-102 in CaMKI is acidic (either Glu or Asp) in kinases (including Chk1) which recognise an upstream basic residue in their substrates. Similarly, all three of the residues Phe-104, Ile-210 and Pro-216 are retained or conservatively substituted in those kinases (including Chk1) which require a hydrophobic residue at the -5 position. Both the Glu-102 equivalent residue and the hydrophobic pocket-forming triplet are also conserved in the kinases C-TAK1, Cds1 and Chk2, further suggesting that they share with Chk1 the Φ-X-β-X-X-S/T* substrate recognition motif.

While this group of protein-serine/threonine kinases have related catalytic domains with similar substrate specificities, they have distinct regulatory domains that respond to different cellular stresses, e.g. ATP depletion (AMPK), glucose starvation (SNF1), elevated cytoplasmic Ca^{2+} concentration (CaMKI), DNA damage (Chk1) or DNA replication arrest (Cds1/Chk2). While it remains to be determined if these kinases have common substrates in vivo, it may be interesting to examine the possible effects of stresses other than DNA damage or DNA replication arrest on the phosphorylation of Cdc25 and the timing of mitotic initiation. It may also be interesting to examine whether Chk1 can phosphorylate known substrates of these related kinases, which include metabolic enzymes and transcription factors [25].

References

[1] Weinert, T.A. and Hartwell, L.H. (1988) Science 241, 317–322.
[2] Hartwell, L.H. and Weinert, T.A. (1989) Science 246, 629–634.
[3] Walworth, N., Davey, S. and Beach, D. (1993) Nature 363, 368–371.
[4] Al-Khodairy, F., Fotou, E., Sheldrick, K.S., Griffiths, D.J.F., Lehmann, A.R. and Carr, A.M. (1994) Mol. Biol. Cell 5, 147–160.
[5] Sanchez, Y., Wong, C., Thoma, R.S., Richman, R., Wu, R.Q., Piwnica-Worms, H. and Elledge, S.J. (1997) Science 277, 1497–1501.
[6] Peng, C.Y., Graves, P.R., Thoma, R.S., Wu, Z.Q., Shaw, A.S. and Piwnica-Worms, H. (1997) Science 277, 1501–1505.
[7] Kumagai, A., Guo, Z.J., Emami, K.H., Wang, S.X. and Dunphy, W.G. (1998) J. Cell Biol. 142, 1559–1569.
[8] Lopez-Girona, A., Furnari, B., Mondesert, O. and Russell, P. (1999) Nature 397, 172–175.
[9] Yang, J., Winkler, K., Yoshida, M. and Kornbluth, S. (1999) EMBO J. 18, 2174–2183.
[10] Kumagai, A. and Dunphy, W.G. (1999) Genes Dev. 13, 1067–1072.
[11] O'Connell, M.J., Raleigh, J.M., Verkade, H.M. and Nurse, P. (1997) EMBO J. 16, 545–554.
[12] Sanchez, Y., Bachant, J., Wang, H., Hu, F., Liu, D., Tetzlaff, M. and Elledge, S.J. (1999) Science 286, 1166–1171.
[13] Izumi, T. and Maller, J.L. (1993) Mol. Biol. Cell 4, 1337–1350.
[14] Peng, C.Y., Graves, P.R., Ogg, S., Thoma, R.S., Byrnes, M.J., Wu, Z., Stephenson, M.T. and Piwnica-Worms, H. (1998) Cell Growth Diff. 9, 197–208.
[15] Dale, S., Wilson, W.A., Edelman, A.M. and Hardie, D.G. (1995) FEBS Lett. 361, 191–195.
[16] Davies, S.P., Carling, D. and Hardie, D.G. (1989) Eur. J. Biochem. 186, 123–128.
[17] Matsuoka, S., Huang, M.X. and Elledge, S.J. (1998) Science 282, 1893–1897.
[18] Zeng, Y., Forbes, K.C., Wu, Z.Q., Moreno, S., Piwnica-Worms, H. and Enoch, T. (1998) Nature 395, 507–510.
[19] Hanks, S.K. and Quinn, A.M. (1990) Methods Enzymol. 200, 38–62.
[20] Weekes, J., Ball, K.L., Caudwell, F.B. and Hardie, D.G. (1993) FEBS Lett. 334, 335–339.
[21] Kemp, B.E., Parker, M.W., Hu, S., Tiganis, T. and House, C. (1994) Trends Biochem. Sci. 19, 440–444.
[22] Songyang, Z., Lu, K.P., Kwon, Y.T., Tsai, L.H., Filhol, O., Cochet, C., Brickey, D.A., Soderling, T.R., Bartleson, C., Graves, D.J., DeMaggio, A.J., Hoekstra, M.F., Blenis, J., Hunter, T. and Cantley, L.C. (1996) Mol. Cell. Biol. 16, 6486–6493.
[23] Goldberg, J., Nairn, A.C. and Kuriyan, J. (1996) Cell 84, 875–887.
[24] Lee, J.C., Kwon, Y.G., Lawrence, D.S. and Edelman, A.M. (1994) Proc. Natl. Acad. Sci. USA 91, 6413–6417.
[25] Hardie, D.G., Carling, D. and Carlson, M. (1998) Annu. Rev. Biochem. 67, 821–855.

Identification of HS1 protein as a major substrate of protein-tyrosine kinase(s) upon B-cell antigen receptor-mediated signaling

(membrane-bound immunoglobulin/tyrosine phosphorylation/Lyn kinase/Src homology 2 domain)

YUJI YAMANASHI*[t], MASATO OKADA[t], TOSHIHIKO SEMBA[§], TAKASHI YAMORI[¶], HISASHI UMEMORI*, SUSUMU TSUNASAWA[‖], KUMAO TOYOSHIMA**, DAISUKE KITAMURA[tt], TAKESHI WATANABE[tt], AND TADASHI YAMAMOTO*

*Department of Oncology, Institute of Medical Science, University of Tokyo, 4-6-1 Shirokanedai, Minato-ku, Tokyo 108, Japan; [t]Division of Protein Metabolism and [‖]Division of Protein Chemistry, Institute for Protein Research, Osaka University, 3-2 Yamadaoka, Suita-shi, Osaka 565, Japan; [§]Applied Biosystems Japan, Inc., 3-3-6 Minamisuna, Koto-ku, Tokyo 136, Japan; [¶]Cancer Chemotherapy Center, Japanese Foundation for Cancer Research, 1-37-1 Kami-Ikebukuro, Toshima-ku, Tokyo 107, Japan; **Department of Oncogene Research, Research Institute for Microbial Diseases, Osaka University, 3-1 Yamadaoka, Suita-shi, Osaka 565, Japan; and [tt]Department of Molecular Immunology, Medical Institute of Bioregulation, Kyushu University, 3-1-1 Maidashi, Higashi-ku, Fukuoka 812, Japan

ABSTRACT   Crosslinking of membrane-bound immunoglobulins, which are B-cell antigen receptors, causes proliferation and differentiation of B cells or inhibition of their growth. The receptor-mediated signaling involves tyrosine phosphorylation of cellular proteins and rapid activation of Src-like kinases. The amino acid sequences of five proteolytic peptides of p75, a major substrate of protein-tyrosine kinase(s) in the signaling, showed that p75 is the human HS1 gene product. The HS1 gene is expressed specifically in hematopoietic cells and encodes p75[HS1], which carries both helix–turn–helix and Src homology 3 motifs. p75[HS1] showed rapid tyrosine phosphorylation and association with a Src-like kinase, Lyn, after crosslinking of membrane-bound IgM. Thus, p75[HS1] may be an important substrate of Lyn and possibly other protein-tyrosine kinases upon B-cell antigen receptor-mediated signaling.

Membrane-bound immunoglobulin (mIg) forms an antigen receptor complex on the plasma membrane of B cells with at least two transmembrane proteins, MB-1 and B29 (1–3). In general, crosslinking of the receptor complex of resting B cells by antigens or antibodies to the immunoglobulins activates B cells to enter the G_1 phase of the cell cycle, in which they become susceptible to proliferative signals provided by helper T cells. These responses are preceded by phosphatidylinositol turnover, activation of phospholipase C, and Ca^{2+} mobilization, which are apparently dependent on the functions of a GTP-binding protein(s), protein-tyrosine kinase(s), and protein-tyrosine-phosphatase(s) (1, 2). The tyrosine phosphorylation of proteins after mIg crosslinking is thought to be an initial intracellular signaling event. As mIg, MB-1, and B29 carry no catalytic domain, the receptor must regulate protein-tyrosine kinase(s) as an intracytoplasmic signal transducer(s) (1–3).

Src-like kinases are intracytoplasmic protein-tyrosine kinases of 55–60 kDa that are thought to be localized on the inner part of the plasma membrane via myristic acid (4, 5). Thus, the physical and functional associations of the Src-like kinases p53/56[lyn], p55[blk], and p59[fyn] with two major B-cell antigen receptors, mIgM and mIgD, strongly suggest that these protein-tyrosine kinases are intracytoplasmic signal transducers of the receptor (6–9). Recent data have suggested that another intracytoplasmic protein-tyrosine kinase, p72[syk], is also such a signaling molecule (10, 11). In addition,

physical association of p56[lck] with mIg has been reported (12).

Several significant substrates for growth control and signal transduction have been identified for growth factor receptors carrying intrinsic protein-tyrosine kinase activity (13). These substrates include intracellular signal transducers, such as phospholipase C-γ, phosphatidylinositol 3-kinase, and Ras-associated GTPase-activating protein. Each of these molecules contains both Src homology 2 (SH2) and Src homology 3 (SH3) motifs, which are homologs to noncatalytic regions of the Src-like kinases (13, 14). The substrates of the receptor-type tyrosine kinases are good candidates for those of protein-tyrosine kinase(s) regulated by mIg. In fact, tyrosine phosphorylations of phospholipase C-γ and phosphatidylinositol 3-kinase have been shown to be involved in mIg-mediated signaling (8, 15–18). Physical association of phosphatidylinositol 3-kinase and Lyn kinase in the signaling has also been reported (8). Studies on these SH2/SH3-containing enzymes may elucidate some aspects of the antigen-induced biological events which are common to growth factor-induced biological events of nonlymphoid cells. Our present study shows that p75[HS1], a 75-kDa protein encoded by a gene (HS1) expressed only in hematopoietic cells, is a major substrate of protein-tyrosine kinase(s) regulated by B-cell antigen receptors and that p75[HS1] associates with the SH2 domain of Lyn kinase upon receptor-mediated signaling.

MATERIALS AND METHODS

Cells. Daudi cells are human B-lymphoblastoid cells and were maintained as described (8). The cells carry mIgM on their surface and behave as normal B cells in terms of initial biochemical events such as phosphatidylinositol turnover, Ca^{2+} mobilization, and tyrosine phosphorylation of proteins after mIgM crosslinking.

Antibodies. Affinity-purified goat polyclonal antibodies to human IgM (μ chain) were purchased from Sigma. Monoclonal antibody 25.2G4 to phosphotyrosine was prepared as described (19). PY20 is another monoclonal antibody to phosphotyrosine, which was purchased from ICN. NU-Lpan is a monoclonal antibody to human CD45, which was purchased from Nichirei (Tokyo, Japan). Lyn-9 is a monoclonal antibody to human Lyn (8). Mouse antiserum to human

Abbreviations: mIg, membrane-bound immunoglobulin; GST, glutathione S-transferase; SH2 or SH3, Src homology 2 or 3.
[t]To whom reprint requests should be addressed.

p75^{HS1} was raised against the full-length sequence of human HS1 expressed in *Escherichia coli* (20).

Purification of Phosphotyrosine-Containing Proteins. Daudi cells (2 × 10^8) in 1.5 ml of RPMI-1640 medium were stimulated at 37°C for 1 min with 70 μg of goat antibody to IgM. Cells were lysed with 10 ml of TNE buffer [1% (vol/vol) Nonidet P-40/50 mM Tris·HCl, pH 8.0/20 mM EDTA/0.2 mM sodium orthovanadate with aprotinin at 10 μg/ml], and the lysate was cleared by centrifugation. Sixteen samples of the cleared lysates were incubated at 4°C for 2.5 hr with 1.5 mg of the 25.2G4 anti-phosphotyrosine monoclonal antibody (19), which was covalently coupled to protein A-Sepharose (Pharmacia) as described (8). The slurry was washed extensively, and phosphotyrosine-containing proteins were eluted with 50 mM phenyl phosphate in 1 mM sodium phosphate/15 mM sodium chloride at pH 7.5 and were collected in 1-ml fractions. The peak fraction containing proteins at the highest concentration was selected by SDS/8.5% polyacrylamide gel electrophoresis (PAGE) followed by Coomassie brilliant blue staining (Fig. 1a), and was subjected to proteolysis and peptide sequencing.

Separation and Sequencing of Proteolytic Peptides. The phosphotyrosine-containing proteins prepared from anti-IgM-stimulated Daudi cells (6.4 × 10^9) were digested with lysyl endopeptidase (Wako Pure Chemicals, Osaka, Japan) and the peptide fragments were separated by HPLC as described (Fig. 1b) (21). Peptide sequence of each fragment was determined by automated gas-phase microsequencing (Fig. 1c) (22).

mIgM Crosslinking and Immunoprecipitation. Daudi cells were stimulated with affinity-purified goat antibody to IgM and lysed with TNE buffer as described (8). The crude lysate from 10^7 cells was cleared by centrifugation and treatment with excess protein A-Sepharose (Pharmacia LKB) as described (8), then incubated with 2–3 μg of Lyn-9 or PY20 or 3 μl of antiserum to human p75^{HS1} at 4°C for 1–1.5 hr. The immune complexes were precipitated with protein A-Sepharose. For immunoblotting, the immunoprecipitate was washed six times with TNE buffer. Ten micrograms of Lyn-9 coupled covalently to protein A-Sepharose (8) was used for
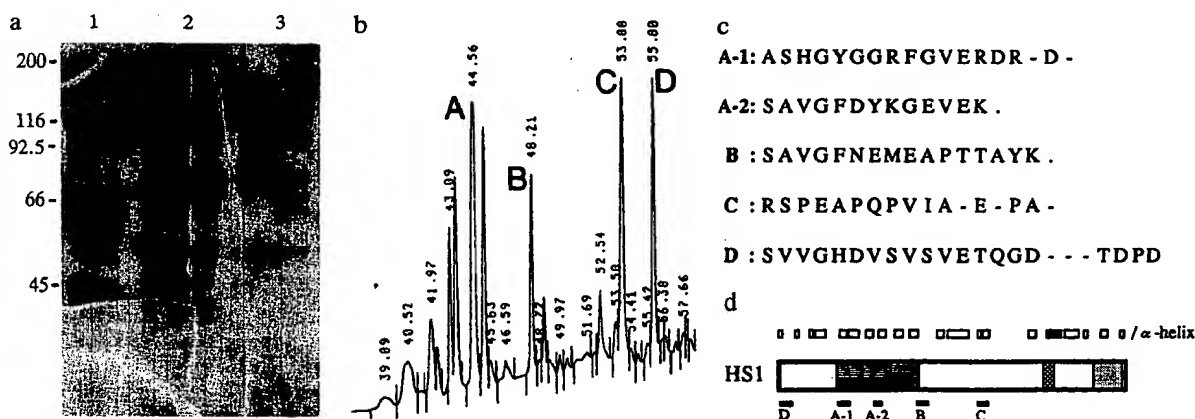
the immunoprecipitation for immunoblotting with antiserum to p75^{HS1}.

In Vitro Phosphorylation of Immunoprecipitate. The immune complexes precipitated with protein A-Sepharose were washed four times with TNE buffer and four times with kinase buffer (20 mM Hepes·NaOH, pH 7.4/10 mM MgCl$_2$). The immunoprecipitate was suspended in 20 μl of kinase buffer with 10 μCi (370 kBq) of [γ-^{32}P]ATP and was incubated at 30°C for 20 min with occasional mixing.

Preparation of Glutathione S-Transferase (GST) Fusion Proteins. The 375-base-pair (nucleotides 654–1028) *lyn* cDNA (23), which encodes 124 amino acid residues (Lys-120 to Pro-243) encompassing the SH2 domain (Trp-129 to Leu-218), was cloned into pGEX-2T (Pharmacia LKB) in the proper orientation to obtain plasmid pGEX-Lyn/SH2. The 610-base-pair (nucleotides 256–865) PTP1C cDNA (24), which encodes 203 amino acid residues (Met-1 to Glu-203) encompassing the two SH2 domains (Trp-6 to Leu-88 and Trp-112 to His-195) of the PTP1C protein-tyrosine-phosphatase, was cloned into pGEX-2T in the proper orientation to obtain plasmid pGEX-PTP1C/SH2. Oligonucleotides were used to adjust the reading frame for each plasmid. The fusion proteins GST-Lyn/SH2 and GST-PTP1C/SH2 were produced in *E. coli* DH5α cells transformed with pGEX-Lyn/SH2 and pGEX-PTP1C/SH2, respectively. The fusion proteins were purified by binding to glutathione-agarose (Sigma) essentially as described (25).

GST Fusion Protein–Binding Assay. The cleared lysate of anti-IgM-stimulated or unstimulated Daudi cells (5 × 10^6) was incubated at 4°C for 2 hr with glutathione-agarose bound to 10–20 μg of GST fusion protein. The slurry was washed six times with TNE buffer and subjected to immunoblotting.

Subcellular Fractionation. Growing Daudi cells (2 × 10^7) were washed twice with RPMI-1640 and suspended in 2 ml of hypotonic buffer (20 mM Hepes·NaOH, pH 7.4/10 mM EDTA/2 mM dithiothreitol with aprotinin at 10 μg/ml). The suspension was left on ice for 15 min, and cells were broken by 50–100 strokes in a Dounce homogenizer with a tight-fitting pestle. The rupture of >98% of the cells and the presence of apparently intact nuclei were confirmed by

A-1: A S H G Y G G R F G V E R D R - D -

A-2: S A V G F D Y K G E V E K .

B : S A V G F N E M E A P T T A Y K .

C : R S P E A P Q P V I A - E - P A -

D : S V V G H D V S V S V E T Q G D - - - T D P D

FIG. 1. Identification of p75^{HS1} as a major phosphotyrosine-containing protein in stimulated B cells. (a) Anti-phosphotyrosine monoclonal antibody (25.2G4)-reactive proteins from 3.2 × 10^9 anti-IgM-stimulated Daudi cells were eluted and collected in 1-ml fractions. Standard protein markers (Bio-Rad; 0.1 μg of each protein) (lane 1), 50 μl of the peak fraction (lane 2), and 50 μl of the second peak fraction (lane 3) were subjected to SDS/8.5% PAGE and Coomassie brilliant blue staining. Positions and sizes (kDa) of standard protein markers are indicated at left. (b) The peak fractions prepared from stimulated Daudi cells (6.4 × 10^9) were digested with lysyl endopeptidase and the proteolytic fragments were separated by HPLC. Values above peaks indicate retention times. Vertical axis represents the relative absorbance at 215 nm. Peaks A–D, whose sequences were determined, are indicated. (c) Peptide sequence of each fragment was determined by automated gas-phase microsequencing. Peak A in b contained two major peptides, which were separated by capillary HPLC (A-1 and A-2). Hyphens indicate undetermined residues. Period indicates absence of amino acid. (d) Predicted structure of p75^{HS1} is schematically represented. The small boxes at the top indicate the α-helices predicted from the amino acid sequence of p75^{HS1} (20, 21). The helix containing an amphipathic region is indicated by a black box. The large box represents the primary structure of p75^{HS1} containing three copies of repeating motifs (striped), the same Glu/Pro stretch as that in adenovirus 2 E1A (crosshatched), and an SH3 motif (shaded). The small bars at the bottom indicate the positions of peptides sequenced in c.

microscopic analysis. Nuclei were separated by centrifugation for 1 min at 800 × g, washed twice with 10 mM sodium phosphate/150 mM sodium chloride, pH 7.5/0.5% Nonidet P-40, and solubilized by boiling in Laemmli SDS/PAGE sample buffer. The postnuclear supernatant was separated by centrifugation at 30,000 × g for 30 min into membrane (pellet) and cytoplasmic (supernatant) fractions. The membrane fraction was washed twice with sodium phosphate buffer and solubilized by boiling in SDS sample buffer. The cytoplasmic fraction was mixed with 3× sample buffer and boiled.

Immunoblotting. Proteins in the cleared lysate, in subcellular fractions, or in Lyn-9, PY20, or anti-HS1 immunoprecipitate, or proteins bound to GST fusion protein were resolved by SDS/8.5% PAGE under reducing conditions and then transferred to polyvinylidene difluoride membrane (Bio-Rad), which was subsequently blocked by incubation with bovine serum albumin (50 mg/ml). Then, the blot was probed with PY20, NU-Lpan, or antiserum to HS1 followed by alkaline phosphatase-coupled antibody to mouse IgG (Promega) as described (6, 8, 20).

RESULTS AND DISCUSSION

Identification of p75HS1 as a Major Phosphotyrosine-Containing Protein in Anti-IgM-Stimulated B Cells. We previously demonstrated that p53/p56lyn (Lyn) are associated with mIgM and activated within 15 sec after mIgM crosslinking (6, 8). We also demonstrated the tyrosine phosphorylation of several unidentified proteins and their association with Lyn within 1 min after mIgM crosslinking. To identify these proteins, using monoclonal antibody to phosphotyrosine, we purified phosphotyrosine-containing proteins from Daudi cells stimulated for 1 min with goat antibody to IgM. The purified fraction contained a major protein of 75 kDa, p75, in an amount >3-fold those of any other proteins in the fraction (Fig. 1a). Digestion of the phosphotyrosine-containing proteins with lysyl endopeptidase generated several major peptide fragments (Fig. 1b). Five independent sequences of the major fragments were identical to those deduced for the product of the human HS1 gene (Fig. 1 c and d) (20). The apparent molecular mass of the human HS1 gene product is 75 kDa on SDS/PAGE. Antiserum to human HS1 protein reacted strongly with a 75-kDa component of the purified phosphotyrosine-containing proteins of anti-IgM-stimulated Daudi cells (data not shown). These data indicate that p75 is the HS1 gene product, p75HS1.

Tyrosine Phosphorylation of p75HS1 in B-Cell Antigen Receptor-Mediated Signaling. The HS1 gene is expressed specifically in cells of hematopoietic lineage (20). The N-terminal moiety of p75HS1 is rich in basic and acidic residues and has three copies of a 37-amino acid repeating motif, each of which contains a helix–turn–helix motif (Fig. 1d). The C-terminal moiety is rich in acidic residues and has the same Glu/Pro stretch as that in adenovirus 2 E1A transcription factor, as well as a potential α-helix containing an amphipathic region (20). In addition, an SH3 motif was present near the C terminus (14, 20). That p75HS1 is the most abundant phosphotyrosine-containing protein in anti-IgM-stimulated B cells strongly suggests that p75HS1 is a major substrate of protein-tyrosine kinase(s) activated by the stimulation. To verify this possibility, we examined whether p75HS1 undergoes tyrosine phosphorylation during signaling. The amount of p75HS1 immunoprecipitated with mouse polyclonal antibody was not affected by mIgM crosslinking of Daudi cells, but the abundance of p75HS1 in immunoprecipitates with monoclonal antibody to phosphotyrosine was greatly increased within 1 min (Fig. 2a). This result suggested that a large fraction of p75HS1 was tyrosine-phosphorylated within 1 min after crosslinking. However, this observation did not exclude the possibility that p75HS1 was associated with some unknown
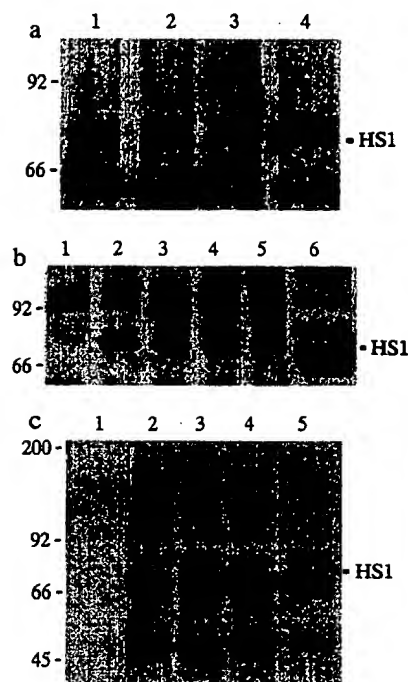
FIG. 2. Tyrosine phosphorylation of p75HS1. Daudi cells (1 × 10^7) were stimulated with affinity-purified goat antibody to IgM for various periods and lysed by addition of 1 ml of cold TNE buffer. The anti-p75HS1 or anti-phosphotyrosine (PY20) immunoprecipitates of the lysates were washed and tested for the presence of p75HS1 or phosphotyrosine by immunoblotting. Positions and sizes (kDa) of standard protein markers are indicated at left. Position of p75HS1 is indicated at right. (a) Lysates were prepared from unstimulated cells (lanes 1 and 3) or cells stimulated for 1 min (lanes 2 and 4). Anti-HS1 immunoprecipitate (lanes 1 and 2) and PY20 immunoprecipitate (lanes 3 and 4) were prepared from lysates of 1 × 10^6 and 4 × 10^6 cells, respectively, and tested for p75HS1. (B) Anti-HS1 immunoprecipitates prepared from lysates of 3 × 10^6 cells stimulated for various times were tested for tyrosine phosphorylation. Lane 1, unstimulated control; lane 2, 1 min; lane 3, 2 min; lane 4, 4 min; lane 5, 10 min; lane 6, whole lysate of 3 × 10^5 cells stimulated for 1 min (the same preparation as for lane 2 in c). (c) Lysates prepared from 3 × 10^5 cells stimulated for various times were examined for phosphotyrosine. Lane 1, unstimulated control; lane 2, 1 min; lane 3, 2 min; lane 4, 4 min; lane 5, 10 min.

protein that was tyrosine-phosphorylated by crosslinking. Therefore, we examined tyrosine phosphorylation of the HS1 immunoprecipitate. The result showed that p75HS1 was, in fact, tyrosine-phosphorylated on stimulation with antibody to IgM and that the phosphorylation was rapid (within 1 min) and decreased after 4 min (Fig. 2b). In addition, the mobility of tyrosine-phosphorylated p75HS1 was the same as that of the protein that reacted most intensely with antibody to phosphotyrosine in a whole lysate of stimulated cells (Fig. 2b). Thus we compared the time courses of tyrosine phosphorylations of these two proteins. The two were parallel, supporting the notion that p75HS1 is a major substrate of the protein tyrosine kinase(s) in B-cell antigen receptor-mediated signaling (Fig. 2 b and c).

Association of p75HS1 with the SH2 Domain of Lyn Kinase by mIgM Crosslinking. As mentioned above, several proteins were tyrosine-phosphorylated and associated with p53/56lyn by mIgM crosslinking. Among these unidentified proteins, a 75-kDa protein was the most intensely phosphorylated after in vitro phosphorylation of Lyn immunoprecipitates (8). To verify that the 75-kDa protein in Lyn immunoprecipitate was p75HS1, we examined the in vitro phosphorylation of Lyn and
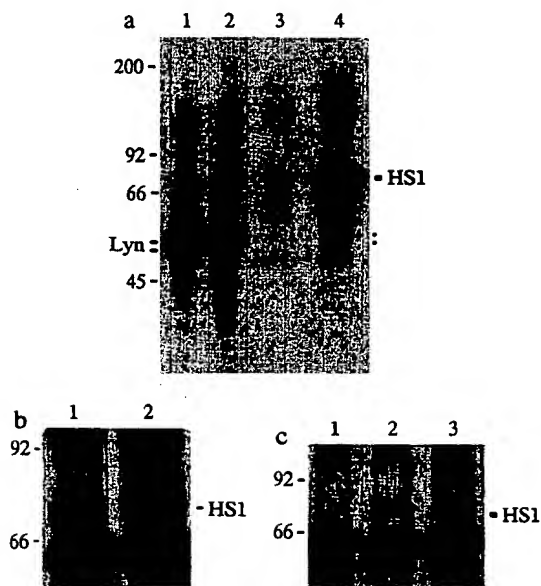
HS1 immunoprecipitates. The mobility of the 75-kDa phosphoprotein in the HS1 immunoprecipitate, which was most likely phosphorylated p75^{HS1}, was the same as that of the 75-kDa phosphoprotein in the Lyn immunoprecipitate of stimulated cells (Fig. 3a, lanes 2–4). Interestingly, the level of phosphorylation of the 75-kDa protein in the HS1 immunoprecipitate was greatly increased 1 min after mIgM crosslinking (Fig. 3a, lanes 3 and 4). The amounts of immunoprecipitated Lyn and HS1 were confirmed not to be affected by the stimulation (Fig. 2a; ref. 8). Since the phosphorylations of both 75-kDa proteins are resistant to 1 M KOH treatment and since p75^{HS1} has no intrinsic kinase activity (20), these data indicate that the apparent activity of p75^{HS1}-associated protein-tyrosine kinase(s) is up-regulated by mIgM crosslinking and suggest that p75^{HS1} is associated with Lyn by stimulation. The presence of 53/56-kDa phosphoprotein in the HS1 precipitate after the crosslinking also supports this notion (Fig. 3a, lane 4).

To demonstrate that Lyn associates with p75^{HS1} during mIgM crosslinking, we evaluated the presence of p75^{HS1} in Lyn immunoprecipitates. The amount of p75^{HS1} in the Lyn immunoprecipitate was up-regulated >4-fold by mIgM crosslinking for 1 min (Fig. 3b), indicating that mIgM crosslinking can induce stable association of Lyn with p75^{HS1}. Thus, p75^{HS1} may be an important substrate of Lyn

FIG. 3.   Association of p75^{HS1} with Lyn by mIgM crosslinking. (a) Lysates were prepared from unstimulated cells (lanes 1 and 3) or cells stimulated for 1 min (lanes 2 and 4) as described in Fig. 2. The Lyn-9 (lanes 1 and 2) and anti-p75^{HS1} (lanes 3 and 4) immunoprecipitates from the lysates of 1 × 10^7 and 4 × 10^5 Daudi cells, respectively, were subjected to *in vitro* phosphorylation. During the procedure, autophosphorylation of p53/56^{lyn} reached a plateau. The phosphorylated proteins were subjected to SDS/8.5% PAGE and treatment with 1 M KOH at 65°C for 90 min, followed by autoradiography. Positions and sizes (kDa) of standard protein markers are indicated at left. Positions of p53/56^{lyn} and p75^{HS1} are indicated, and those of p53 and p56 (see text) are indicated by tiny filled squares at right. (b) Lysates were prepared from 1 × 10^7 cells that were unstimulated (lane 1) or stimulated for 1 min (lane 2) as described in Fig. 2. The Lyn-9 immunoprecipitates from the lysates were tested for p75^{HS1} by immunoblotting. (c) Lysates were prepared from 5 × 10^6 cells unstimulated (lane 1) or stimulated for 1 min (lanes 2 and 3) as described in Fig. 2 and were incubated with glutathione-agarose coated with GST–Lyn/SH2 (lanes 1 and 2) or GST–PTP1C/SH2 (lane 3). The slurry was washed and tested for p75^{HS1} by immunoblotting.

kinase upon B-cell antigen receptor-mediated signaling. As p75^{HS1} has no SH2 motif, which preferentially associates with phosphotyrosine-containing peptides, the SH2 motif of Lyn may interact with tyrosine-phosphorylated p75^{HS1} (13, 14, 22). To examine this possibility, SH2 domain(s) of Lyn or PTP1C, a protein-tyrosine-phosphatase with two SH2 domains (25), was bacterially produced as fusion protein with GST and purified by binding to glutathione-agarose. The GST fusion protein was incubated with lysate of anti-IgM-stimulated or unstimulated cells, and then the amount of p75^{HS1} bound to the fusion protein was evaluated. The amount of p75^{HS1} bound to GST–Lyn/SH2 was up-regulated >6-fold by mIgM crosslinking for 1 min (Fig. 3c, lanes 1 and 2). In addition, p75^{HS1} was not detected in GST–PTP1C/SH2-bound proteins of anti-IgM-stimulated cells (Fig. 3c, lane 3). These data indicate that p75^{HS1} was preferentially associated with the SH2 domain of Lyn kinase in B-cell antigen receptor-mediated signaling. However, these data do not exclude a possible association of p75^{HS1} with non-SH2 domains of Lyn. Two other Src-like kinases, p55^{blk} and p59^{fyn}, have also been reported to be constituents of the B-cell antigen receptor complex and to be activated in receptor-mediated signaling (9). Since SH2 domains of Lyn, Fyn, and Blk differ, these mIg-associated kinases may interact with p75^{HS1} with different preferences.

Implications. Accumulating data suggest that Src-like kinases are intracytoplasmic signaling molecules of a number of cell surface receptors of hematopoietic cells. For instance, Lyn is also suggested to be a signaling molecule of the high-affinity receptor for Fc$_\epsilon$ (26). Components of about 70–80 kDa were also detected by *in vitro* phosphorylation of a Lyn immunoprecipitate after receptor-mediated activation (26). As the HS1 gene is expressed specifically in hematopoietic cells, p75^{HS1} may play a crucial role by interacting with Src-like kinases in various signaling systems of hematopoietic cells. In addition, we previously showed (8) that p53/p56^{lyn} was also rapidly associated with a 70-kDa phosphotyrosine-containing protein after mIgM crosslinking. Therefore, tests for a possible interactions of this unidentified 70-kDa protein with p75^{HS1} and p53/56^{lyn} or other protein-tyrosine kinases upon signaling in hematopoietic cells seem necessary.

Wu *et al.* (27) have recently cloned cDNA for p80/85, which is tyrosine-phosphorylated in chicken embryo cells transformed by p60^{src}. They showed that the p80/85 has six copies of a 37-amino acid repeating motif in its N-terminal region, each of which shows high homology (about 70%) to the three repeating motifs of p75^{HS1}, and also has an SH3 motif at the C terminus. p80/85 was reported to be a cytoskeletal protein and was detected exclusively in the cytosolic fraction of the cells (27). Therefore, we examined the subcellular localization of p75^{HS1} by similar fractionation of unstimulated Daudi cells. We found that p75^{HS1} was mainly localized in the membrane and cytosolic fractions of the cells (Fig. 4). However, a small fraction of p75^{HS1} was also detected in the nuclear fraction, as reported previously (20). Its localization in membranes is consistent with the notion that Lyn kinase, which is also localized in the membrane fraction (28), interacts with p75^{HS1}. The difference between the localizations of p75^{HS1} and p80/85 may reflect the fact that these components show low homology (about 20% amino acid sequence identity) except in their N-terminal regions including the repeating motif (about 70% identity) and in their C-terminal SH3 motif (about 70% identity) (20, 27). Neither the E1A-like structure nor the amphipathic region of p75^{HS1} is found in p80/85 (20, 27). The differences in their subcellular localizations and predicted structures suggest that their biochemical and biological functions also differ. Internal repeating motifs such as ankyrin and knob-and-hole motifs could be a common feature of membrane, cytoskeletal

Immunology: Yamanashi *et al.*

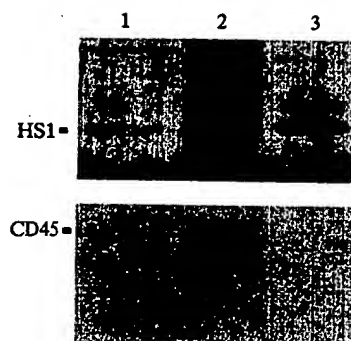*Proc. Natl. Acad. Sci. USA* 90 (1993)   3635

1   2   3

HS1▪

CD45▪

FIG. 4. Subcellular localization of p75^{HS1}. Growing Daudi cells were subjected to subcellular fractionation. Samples of nuclear (lane 1), membrane (lane 2), and cytoplasmic (lane 3) fractions from 2 × 10^5, 1 × 10^5, and 1 × 10^5 cells, respectively, were tested for p75^{HS1} by immunoblotting. The same samples were also tested for CD45 with monoclonal antibody NU-Lpan.

and transcriptional proteins involved in cell cycle control and differentiation (10, 11, 29–31). The 37-amino acid repeating motif may be shared by proteins possessing a variety of functions and localizations.

The physiological role of the SH3 motif is not known (13, 14). However, the helix–turn–helix motif, the amphipathic structure, and the characteristic distribution of ionic residues in p75^{HS1} suggest that p75^{HS1} functions as a DNA-binding protein in hematopoietic cells. If this is the case, p75^{HS1} could transduce some signals from protein-tyrosine kinase(s) to certain genetic loci upon B-cell antigen receptor-mediated signaling. Alternatively, p75^{HS1} may regulate other cytoplasmic or cytoskeletal signaling molecule(s) upon signaling. Studies on the precise localization of p75^{HS1} before and after mIg crosslinking are important to obtain further information on its function.

1. Reth, M., Hombach, J., Wienands, J., Campbell, K. S., Chien, N., Justment, L. B. & Cambier, J. C. (1991) *Immunol. Today* 12, 196–201.
2. Ales-Martinez, J. E., Cuende, E., Martinez-A., C., Parkhouse, R. M. E., Pezzi, L. & Scott, D. W. (1991) *Immunol. Today* 12, 201–205.
3. Campbell, K. S., Hager, J. H., Friedrich, R. J. & Cambier, J. C. (1991) *Proc. Natl. Acad. Sci. USA* 88, 3982–3986.
4. Cooper, J. A. (1990) in *Peptides and Protein Phosphorylation*, eds. Kemp, B. E. & Alewood, P. F. (CRC, Boca Raton, FL), pp. 85–113.
5. Semba, K. & Toyoshima, K. (1990) in *Genes and Cancer*, eds. Sikora, K. & Carney, D. (Wiley, Chichester, U.K.), pp. 73–83.
6. Yamanashi, Y., Kakiuchi, T., Mizuguchi, J., Yamamoto, T. & Toyoshima, K. (1991) *Science* 251, 192–194.
7. Yamanashi, Y., Miyasaka, M., Takeuchi, M., Dusko, I., Mizuguchi, J. & Yamamoto, T. (1991) *Cell Regul.* 2, 979–987.
8. Yamanashi, Y., Fukui, Y., Wongsasant, B., Kinoshita, Y., Ichimori, Y., Toyoshima, K. & Yamamoto, T. (1992) *Proc. Natl. Acad. Sci. USA* 89, 1118–1122.
9. Burkhardt, A. L., Brunswick, M., Bolen, J. B. & Mond, J. J. (1991) *Proc. Natl. Acad. Sci. USA* 88, 7410–7414.
10. Taniguchi, T., Kobayashi, T., Kondo, J., Takahashi, K., Nakamura, H., Suzuki, J., Nagai, K., Yamada, T., Nakamura, S. & Yamamura, T. (1991) *J. Biol. Chem.* 266, 15790–15796.
11. Hutchcroft, J. E., Harrison, M. L. & Geahlen, R. L. (1992) *J. Biol. Chem.* 267, 8613–8619.
12. Campbell, M.-A. & Sefton, B. M. (1992) *Mol. Cell. Biol.* 12, 2315–2321.
13. Cantley, L. C., Auger, K. R., Carpenter, C., Duckworth, B., Graziani, A., Kapeller, R. & Soltoff, S. (1991) *Cell* 64, 280–302.
14. Koch, C. A., Anderson, D., Moran, M. F., Ellis, C. & Pawson, T. (1991) *Science* 252, 668–674.
15. Carter, R. H., Park, D. J., Rhee, S. G. & Fearon, D. T. (1991) *Proc. Natl. Acad. Sci. USA* 88, 2745–2749.
16. Gold, M. R., Chan, V. W.-F., Turck, C. W. & DeFranco, A. L. (1992) *J. Immunol.* 148, 2012–2022.
17. Coggeshall, K. M., McHugh, J. C. & Altman, A. (1992) *Proc. Natl. Acad. Sci. USA* 89, 5660–5664.
18. Hempel, W. M., Schatzman, R. C. & DeFranco, A. L. (1992) *J. Immunol.* 148, 3021–3027.
19. Yamori, T., Iizuka, Y., Takayama, Y., Nishiya, S., Iwashita, S., Yamazaki, A., Takatori, T. & Tsuruo, T. (1991) *Cancer Res.* 51, 5859–5865.
20. Kitamura, D., Kaneko, H., Miyagoe, Y., Ariyasu, T. & Watanabe, T. (1989) *Nucleic Acids Res.* 17, 9367–9379.
21. Breitman, T. R., Selonick, S. E. & Collins, S. J. (1980) *Proc. Natl. Acad. Sci. USA* 76, 2936–2940.
22. Nada, S., Okada, M., MacAuley, A., Cooper, J. A. & Nakagawa, H. (1991) *Nature (London)* 351, 69–72.
23. Yamanashi, Y., Fukushige, S., Semba, K., Sukegawa, J., Miyajima, N., Matsubara, K.-I., Yamamoto, T. & Toyoshima, K. (1987) *Mol. Cell. Biol.* 7, 237–243.
24. Shen, S.-H., Bastien, L., Posner, B. I. & Chretien, P. (1991) *Nature (London)* 352, 736–739.
25. Smith, D. B. & Johnson, K. S. (1988) *Gene* 67, 31–40.
26. Eiseman, E. & Bolen, J. B. (1992) *Nature (London)* 355, 78–80.
27. Wu, H., Reynolds, A. B., Kanner, S. B., Vines, R. R. & Parsons, J. T. (1991) *Mol. Cell. Biol.* 11, 5113–5124.
28. Yamanashi, Y., Mori, S., Yoshida, M., Kishimoto, T., Inoue, K., Yamamoto, T. & Toyoshima, K. (1989) *Proc. Natl. Acad. Sci. USA* 86, 6538–6542.
29. Lux, S. E., John, K. M. & Bennett, V. (1990) *Nature (London)* 344, 36–42.
30. Hirano, T., Kinoshita, N., Morikawa, K. & Yanagida, M. (1990) *Cell* 60, 319–328.
31. Sikorski, R. S., Boguski, M. S., Goebl, M. & Hieter, P. (1990) *Cell* 60, 307–317.

Engineering the Substrate Specificity of the Abl Tyrosine Kinase*

Jeffrey H. Till, Perry M. Chan, and W. Todd Miller‡

From the Department of Physiology and Biophysics, School of Medicine, State University of New York, Stony Brook, New York 11794-8661

c-Abl is a non-receptor tyrosine kinase that is involved in a variety of signaling pathways. Activated forms of c-Abl are associated with some forms of human leukemia. Presently, no high resolution structure of the tyrosine kinase domain of Abl is available. We have developed a structural homology model of the catalytic domain of Abl based on the crystal structure of the insulin receptor tyrosine kinase. Using this model as a guide, we selected residues near the active site predicted to play a role in peptide/protein substrate recognition. We expressed and purified 15 mutant forms of Abl with single amino acid substitutions at these positions and tested their peptide substrate specificity. We report here the identification of seven residues involved in recognition of the P−1, P+1, and P+3 positions of bound peptide substrate. Mutations in these residues cause distinct changes in substrate specificity. The results suggest features of Abl substrate recognition that may be relevant to related tyrosine kinases.

The c-*abl* proto-oncogene encodes a multidomain non-receptor tyrosine kinase that is expressed ubiquitously in human tissues (reviewed in Refs. 1–4). Mutant forms of c-*abl* are found in patients with Philadelphia chromosome-positive chronic myelogenous leukemia and acute lymphocytic leukemia (1–4). In these diseases, a chromosomal translocation event produces a chimeric oncogene consisting of 5'-sequences of *bcr* fused to *abl*. The BCR-Abl fusion protein has elevated tyrosine kinase activity relative to c-Abl, and the tyrosine kinase activity of the BCR-Abl fusion protein is necessary for disease progression. Similarly, tyrosine kinase activity is necessary for transformation of fibroblasts or hematopoietic cells by BCR-Abl (5, 6).

In addition to its tyrosine kinase catalytic domain, c-Abl has a short amino-terminal unique domain followed by SH3 and SH2 domains (1–4). This domain organization is found in many non-receptor tyrosine kinases. Abl also possesses a large carboxyl-terminal region that includes a DNA-binding domain, an F-actin-binding domain, a nuclear localization signal, and a proline-rich region implicated in mediating protein-protein interactions. Studies aimed at understanding the normal physiological role of c-Abl have shown the enzyme to be involved in signal transduction, cytoskeletal rearrangement, RNA polymerase II activation, DNA repair, and cell cycle control (1–4). c-Abl has been shown to physically associate with at least seven unique proteins, including p53 and the nuclear Rb protein (4). Mice with targeted disruptions in the c-*abl* gene have high neonatal mortality rates and are more susceptible to infection,

suggesting a role for c-*abl* in B-lymphocyte development (7).

At least eight *in vivo* substrates for Abl have been identified (4). The amino acid sequences surrounding the phosphorylation sites for two of these proteins, RNA polymerase II (8) and c-Crk (9), have been described. These sequences do not share a common primary sequence motif, suggesting that Abl may have a broad range of substrate specificity. Studies using synthetic peptides have been used to examine the substrate specificity of Abl and to define any primary sequence determinants for substrate recognition (10, 11). These studies suggest that, although Abl does not have an absolute consensus sequence for phosphorylation, the best *in vitro* peptide substrates for Abl contain the sequence Ile-Tyr-Ala-Xaa-Pro, where Xaa is any amino acid. These studies indicate that the P−1 (Ile) and the P+3 (Pro) positions are most important for substrate recognition.

The molecular basis of peptide/protein substrate recognition for tyrosine kinases is not well understood. Presently, a single high resolution crystal structure of a tyrosine kinase in complex with peptide substrate is available: the tyrosine kinase domain of the insulin receptor (IRK)[1] complexed with a peptide substrate (12). This structure reveals interactions between enzyme and substrate that govern substrate specificity. Two adjacent hydrophobic pockets on the surface of the C-terminal lobe of IRK accommodate Met side chains C-terminal to the phosphorylated tyrosine on the peptide substrate. The crystal structure of the activated IRK-peptide complex provides a structural basis for understanding the primary signaling specificity of IRK and serves as a general model for tyrosine kinase substrate recognition.

In this paper, we have developed a molecular homology model of the kinase catalytic domain of Abl (Abl-CAT) to help identify amino acids that may be important in substrate recognition. A similar approach was used to propose a molecular model of the Bruton tyrosine kinase and to provide a structural basis for understanding mutations in this enzyme associated with the disease X-linked agammaglobulinemia (13). Our molecular homology model is based on the crystal structure of the ternary complex of IRK with peptide substrate and AMP-PNP bound (12). Using the model as a guide, we have targeted seven residues in Abl-CAT for amino acid substitutions to examine effects on substrate specificity. Site-directed mutants of Abl-CAT were engineered and tested with a series of peptide substrates to monitor changes in specificity. Kinetic analyses of these mutants with the peptide substrates show distinct changes in substrate preferences.

EXPERIMENTAL PROCEDURES

Homology Model—Amino acids 362–625 of v-Abl were used to generate primary sequence alignments using the CLUSTALW alignment algorithm (14) and were imported into Swiss-PDB Viewer (15). The

[1] The abbreviations used are: IRK, insulin receptor tyrosine kinase domain; Abl-CAT, Abl catalytic domain; AMP-PNP, 5'-adenylylimidodiphosphate; Nle, norleucine.

primary model of the Abl catalytic domain was prepared using the spatial coordinates of α-carbons from the crystal structure of the ternary form of IRK with peptide substrate and AMP-PNP bound (12). Gaps in the sequence alignment were ligated manually, minimizing large steric clashes. Energy minimization and loop insertions were carried out using the Swiss-Model automated modeling system (16). Additional rounds of energy minimization were carried out using Sculpt for Power Macintosh (17). The stereochemical quality of the model was checked using PROCHECK Version 3.3 (18), which reports no distorted main-chain bonds, five distorted main-chain angles, and no distorted planar groups. The distorted main-chain angles were outside of the predicted substrate-binding region and do not interfere with our interpretation of the model. Solvent-accessible surface area was calculated and visualized using Web Lab Viewer (Molecular Simulations Inc.) with a 1.4-Å probe. Figs. 1A and 2 were prepared using Strata Studio Pro (Strata Inc., St. George, UT).

Mutagenesis, Expression, and Purification—Our experiments were carried out on the isolated catalytic domain of v-Abl, expressed in *Escherichia coli* as described previously (19). The sequence numbering used is from the gag-Abl fusion protein of the Abelson murine leukemia virus (20). Mutagenesis of the Abl catalytic domain was carried out using a QuikChange mutagenesis kit (Stratagene). Mutagenesis primers complementary to wild-type template were designed with single, double, or triple nucleotide substitutions. The DNA sequences encoding the entire catalytic domains of the mutants were confirmed by DNA sequencing on an ABI373 automated DNA sequencer. Wild-type and mutant proteins were expressed as glutathione S-transferase fusion proteins in *E. coli* strain NB42 and purified using glutathione-agarose (19). All proteins expressed to similar levels, were of the expected size, and purified to >98% homogeneity.

Peptides—Synthetic peptides were prepared by solid-phase synthesis using standard Fmoc (*N*-(9-fluorenyl)methoxycarbonyl) chemistry on an Applied Biosystems automated 431A peptide synthesizer. Peptides were purified using semi-preparative reversed-phase high performance liquid chromatography. Matrix-assisted laser desorption ionization time-of-flight mass spectrometry was used to confirm the identity of the final products.

Kinase Assays—Tyrosine kinase activity assays were carried out using two methods. In both cases, the intact glutathione S-transferase-Abl fusion proteins were used; we showed previously that the specific activity and substrate specificity of glutathione S-transferase-Abl are similar to those of full-length Abl and that velocity *versus* [enzyme] plots are linear over the concentrations used here (19). For initial comparisons of several substrates, phosphocellulose binding assays were used to measure incorporation of [^{32}P]ATP into peptide substrates (19, 21). These reactions were carried out in triplicate at saturating concentrations of ATP (250 μM) and Mg^{2+} (10 mM). The reactions were carried out in volumes of 25 μl, using peptide concentrations of 50 μM or 1.5 mM and 1 μg of enzyme. Picomoles of phosphate incorporated into peptides were measured after 20 min as described (19).

A continuous spectrophotometric assay (22) was used to measure initial rates of phosphorylation and to determine kinetic constants for some peptides. Reactions were carried out in volumes of 100 μl using 5 μg of purified enzyme. Saturating concentrations of ATP (500 μM) and Mg^{2+} (10 mM) were used, and peptide concentrations ranged from 50 μM to 2 mM. Data were sampled every 30 s to determine rates of phosphorylation. Initial rates (<10% of the reaction) were measured in triplicate. The initial rate values were averaged, and V_{max} and K_m were determined by fitting to the hyperbolic velocity *versus* [substrate] curves using the program MacCurve Fit. For some combinations of peptides and mutants, initial experiments established that their K_m values were in the millimolar range (>2 mM). In addition, we observed that high concentrations of these peptides were inhibitory. Thus, concentrations over 2 mM were not employed, and we were unable to determine K_m values accurately using initial rate kinetics. For these peptides, the complete time courses for phosphorylation were measured using peptide concentrations less than K_m. In these cases, we analyzed the data graphically as described (23) to determine V_{max}/K_m.

RESULTS

Homology Model—The overall topology of the Abl structural homology model reflects the typical bilobal structure shared by all eukaryotic protein kinases (24) with a five-stranded β-sheet and a single α-helix in the amino-terminal lobe, responsible for MgATP binding, and a highly helical carboxyl-terminal lobe (Fig. 1). Based on results for other protein kinases, the C-terminal lobe is predicted to make most of the contacts with

peptide/protein substrates. The total root mean square deviation of the polypeptide backbone between the Abl model and the IRK structure is 1.8 Å. The crystal structure of the activated insulin receptor catalytic domain with peptide bound (12) served as a model for the orientation and structure a peptide may adopt in the Abl active site. Comparison of the C-terminal peptide-binding domains of IRK and Abl indicated that the greatest differences are in the regions responsible for binding the P+3 amino acid side chain. The P−1 region differs only slightly from that of IRK. The activation loop (amino acids 500–521; see Fig. 1) is extremely flexible when examined using molecular mechanics (Sculpt, Interactive Simulations, Inc.), and the structure of the loop in our model is one of many possible conformations. Additionally, the structure of IRK used for our model is multiply phosphorylated on the activation loop (12). Abl contains a single tyrosine within the activation loop, Tyr-513, which is phosphorylated *in vivo* and *in vitro* and is believed to be involved in enzyme activation (25, 26). Although we believe that our model represents the activated form of Abl, the activation loop tyrosine is modeled in its unphosphorylated state.
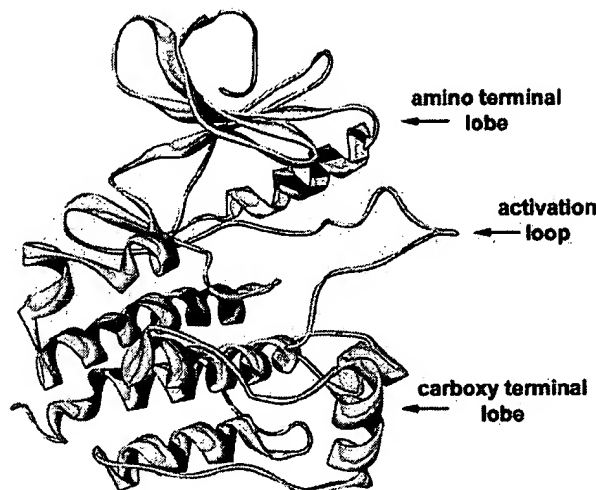
Design of Peptide Substrates—Previous studies of the *in vitro* substrate specificity of Abl have been carried out in this laboratory and by others (for review, see Ref. 27). We designed two groups of peptide substrates to examine any changes in specificity at the P−1 and P+1/P+3 positions for engineered mutant forms of Abl (Table I). (Amino acids in peptide substrates are designated by their position relative to the phosphorylated tyrosine. For example, in the sequence Ile-**Tyr**-Ala-Ser-Pro, Ile is at the P−1 position, Ala is at the P+1 position, and Pro is at the P+3 position.) Peptides used to examine P+1 and P+3 specificity share the sequence Ser-Arg-Gly-Asp-Tyr-Xaa$_1$-Thr-Xaa$_2$-Gln-Ile-Gly, where either Xaa$_1$ or Xaa$_2$ is varied. These peptides are based on a peptide sequence derived from a phosphorylation site of insulin receptor substrate-1 used previously in our laboratory to examine the substrate specificity of wild-type Abl at the P+1, P+2, and P+3 positions (19). In these earlier studies, we found that amino acids at the P+2 position do not strongly influence substrate recognition. Moreover, in the ternary structure of IRK, specificity in peptide binding is achieved through interactions with the P+1 and P+3 residues (12). For these reasons, we did not examine the effects of residue changes at the P+2 position in this study.

We chose to use a different series of peptides to examine P−1 specificity (Table I). This is because, in the context of the insulin receptor substrate-1 peptides, we did not observe a strong dependence on the amino acid at the P−1 position for Abl phosphorylation.[2] Peptides designed to examine specificity at the P−1 position share the sequence Leu-Ile-Glu-Asp-Ala-Xaa-Tyr-Ala-Ala-Arg-Gly, where Xaa is varied. This sequence is based on the autophosphorylation site of Src and has been previously used in our laboratory to examine P−1 specificity in wild-type Abl (11). Amino acids for the substituted position were chosen to explore the effect of size, charge, and hydrophobic character. Because the two groups of peptides are dissimilar in sequence, we did not attempt to draw conclusions about the relative importance of P−1 *versus* P+1/P+3 recognition for each mutant.

Mutations That Affect P+3 Peptide Recognition—Experiments with synthetic peptides and peptide libraries have demonstrated that Abl prefers proline at the P+3 residue of a substrate. In the crystal structure of IRK, Leu-1219 is part of a binding pocket that surrounds the P+3 methionine side chain

---

[2] D. A. Hinds, W. T. Miller, and S. E. Shoelson, unpublished observations.

A

amino terminal
←— lobe

activation
←— loop

carboxy terminal
←— lobe

FIG. 1. *A*, ribbon diagram of the Abl tyrosine kinase catalytic domain molecular homology model. *B*, sequence alignment of the v-Abl and human insulin receptor (IRK) tyrosine kinase catalytic domains. The sequence shown for Abl is the portion modeled in *A*. This portion of Abl is the same as the region expressed in *E. coli* for the mutagenesis experiments. Numbering for Abl is from the gag-Abl fusion protein sequence (20). Residues mutated in this study are *shaded*. *Asterisks* indicate positions that are identical in Abl and insulin receptor kinases; *colons* show positions with conservative substitutions.

B

```
abl  ------DKWEMERTDITMKHKLGGGQYGEVYEG----VWKKYSLT-VAVKTLKEDT--ME 399
irk  SSVFVPDEWEVSREKITLLRELGQGSFGMVYEGNARDIIKGEAETRVAVKTVNESASLRE 1040
     *:**:   *   **:  ::** *  :* ****    : *  : * ****:: *:   *

abl  VEEFLKEAAVMKEIKHPNLVQLLGVCTREPPFYIITEFMTYGNLLDYLR------ECN-- 451
irk  RIEFLNEASVMKGFTCHHVVRLLGVVSKGQPTLVVMELMAHGDLKSYLRSLRPEAENNPG 1100
     ***:**:*** :  ::*:**** ::  *  :: *:*::*:*  **      * *

abl  RQEVSAVVLLYMATQISSAMEYLEKKNFIHRDLAARNCLVGENHLVKVADFGLSRLMTGD 511
irk  RPPPTLQEMIQMAAEIADGMAYLNAKKFVHRDLAARNCMVAHDFTVKIGDFGMTRDIYET 1160
     *   :   :: **::*:  * **: *:*:**********:*  : **: ***::* :

abl  TYTAHAG-AKFPIKWTAPESLAYNKFSIKSDVWAFGVLLWEIATYGMSPYPGIDLSQVYE 570
irk  DYYRKGGKGLLPVRWMAPESLKDGVFTTSSDMWSFGVVLWEITSLAEQPYQGLSNEQVLK 1220
     * : *  :*::* ***** *: **:*:***:****:: :** *: ** :

abl  LLEKDYRMERPEGCPEKVYELMRACWQWNPSDRPSFAEI--------HQAF-ETMFQESS 621
irk  FVMDGGYLDQPDNCPERVTDLMRMCWQFNPKMRPTFLEIVNLLKDDLHPSFPEVSFFHSE 1280
     :: :::*: ***:* :*** ***:** **:* ** * :* * *: *

abl  ISDE 625
irk  ENK- 1283
```

of the peptide substrate (12). In the Abl homology model, the residue homologous to Leu-1219 is Tyr-569. Tyr-569 is partially solvent-exposed in our model and could adopt the same role as Leu-1219 in IRK (Fig. 2). Three separate mutant forms of Abl-CAT were engineered with amino acid substitutions at Tyr-569: Y569L, Y569A, and Y569W. Alanine was chosen as a substitute for Tyr-569 to examine the effects of minimizing the amino acid side chain length. In c-Src, the residue corresponding to Tyr-569 is a leucine (28), and the specificity of c-Src at the P+3 position differs from that of Abl (10). For this reason, we chose to introduce leucine as a substitute for Tyr-569. We also mutated Tyr-569 to Trp because the Abl homology model suggests that a large side chain at this position might cause the putative P+3 substrate-binding pocket to be too narrow to accommodate amino acids with large side chains such as proline.

Initial screens of Abl mutants were carried out using peptide concentrations of 1.5 mM and measuring [^{32}P]ATP incorporation after 20 min to assess any changes in substrate phosphorylation (Fig. 3). Experiments using low (50 μM) peptide concentrations showed no changes in the rank order of specificity compared with those using higher peptide concentrations (data not shown). These initial activity measurements indicated that the Y569W and Y569L mutants had an altered specificity (Fig. 3); in particular, recognition of Pro at the P+3 position was

greatly reduced. These changes in specificity were characterized further by more detailed kinetic analyses (Table II). The kinetic measurements show that the Y569W mutant phosphorylated the P+1$_{Ala}$/P+3$_{Met}$ peptide best, with a V_{max}/K_m value of 5.6. The P+1$_{Met}$/P+3$_{Pro}$ peptide, the best for the wild type with a V_{max}/K_m value of 10.7, was phosphorylated less efficiently by this mutant, with a V_{max}/K_m value of 1.3 (Table II). The phosphorylation of other peptides by the Y569W mutant was similar to the wild type (Fig. 3 and Table II). The difference in specificity observed in the Y569W mutant therefore arises from a decrease in V_{max}/K_m for the P+3$_{Pro}$ peptide specifically rather than an overall decrease in the phosphorylation of all peptides. Kinetic measurements also showed a decrease in the phosphorylation of the P+1$_{Met}$/P+3$_{Pro}$ peptide by Y569L, with a V_{max}/K_m value of 4.4 (wild-type V_{max}/K_m = 10.7) (Table II). The Y569A mutant did not display any changes in phosphorylation of the peptides tested compared with wild-type Abl (Fig. 3), and we did not carry out kinetic analysis of this mutant.

Mutations That Affect P+1 Peptide Recognition—Two residues in Abl-CAT, Phe-521 and Ile-523, were identified as residues that might contribute to P+1 substrate specificity (Fig. 2). Ile-523 was chosen based on the homology model. A solvent-accessible surface representation suggests that Ile-523 is partially solvent-exposed and forms the edge of a groove into which a substrate amino acid side chain may fit. Two substitutions

Engineering the Substrate Specificity of Abl

TABLE I

Amino acid sequences and designations of peptides used in this study

P-1 peptide variants	Designation
Lys-Lys-Leu-Ile-Glu-Asp-Ala-**Glu**-Tyr-Ala-Ala-Arg-Gly	$P-1_{Glu}$
Lys-Lys-Leu-Ile-Glu-Asp-Ala-**Ile**-Tyr-Ala-Ala-Arg-Gly	$P-1_{Ile}$
Lys-Lys-Leu-Ile-Glu-Asp-Ala-**Leu**-Tyr-Ala-Ala-Arg-Gly	$P-1_{Leu}$
Lys-Lys-Leu-Ile-Glu-Asp-Ala-**His**-Tyr-Ala-Ala-Arg-Gly	$P-1_{His}$
Lys-Lys-Leu-Ile-Glu-Asp-Ala-**Ala**-Tyr-Ala-Ala-Arg-Gly	$P-1_{Ala}$
Lys-Lys-Leu-Ile-Glu-Asp-Ala-**Lys**-Tyr-Ala-Ala-Arg-Gly	$P-1_{Lys}$
Lys-Lys-Leu-Ile-Glu-Asp-Ala-**Gln**-Tyr-Ala-Ala-Arg-Gly	$P-1_{Gln}$

P+1 and P+3 peptide variants	Designation
Lys-Lys-Ser-Arg-Gly-Asp-Tyr-**Met**-Thr-**Met**-Gln-Ile-Gly	$P+1_{Met}/P+3_{Met}$
Lys-Lys-Ser-Arg-Gly-Asp-Tyr-**Ile**-Thr-Met-Gln-Ile-Gly	$P+1_{Ile}/P+3_{Met}$
Lys-Lys-Ser-Arg-Gly-Asp-Tyr-**Nle**-Thr-Met-Gln-Ile-Gly	$P+1_{Nle}/P+3_{Met}$
Lys-Lys-Ser-Arg-Gly-Asp-Tyr-**Ala**-Thr-Met-Gln-Ile-Gly	$P+1_{Ala}/P+3_{Met}$
Lys-Lys-Ser-Arg-Gly-Asp-Tyr-**Glu**-Thr-Met-Gln-Ile-Gly	$P+1_{Glu}/P+3_{Met}$
Lys-Lys-Ser-Arg-Gly-Asp-Tyr-Met-Thr-**Pro**-Gln-Ile-Gly	$P+1_{Met}/P+3_{Pro}$
Lys-Lys-Ser-Arg-Gly-Asp-Tyr-Met-Thr-**Thr**-Gln-Ile-Gly	$P+1_{Met}/P+3_{Thr}$
Lys-Lys-Ser-Arg-Gly-Asp-Tyr-Met-Thr-**Ala**-Gln-Ile-Gly	$P+1_{Met}/P+3_{Ala}$
Lys-Lys-Ser-Arg-Gly-Asp-Tyr-Met-Thr-**Glu**-Gln-Ile-Gly	$P+1_{Met}/P+3_{Glu}$

were made for Ile-523: I523V and I523A. These amino acid substitutions were chosen to examine the effect of shortening the side chain on accommodating P+1 residues. Phe-521 was selected to test the possibility that residues near the activation loop contribute to specificity; based on homology to other protein kinases, the activation loop in Abl is predicted to span residues 500–521. We examined the effects of smaller (F521A) and larger (F521W) side chains at this position. Initial measurements of activity were used to assess changes in specificity (Fig. 4) using a panel of peptides that vary at the P+1 position. Initial rate measurements were used to characterize the changes in specificity shown in the I523V and F521A mutants (Table III). The I523A and F521W mutants did not display any changes in specificity and were indistinguishable from wild-type enzyme in our initial comparisons (Fig. 4). For this reason, we did not pursue kinetic characterization of these mutants.

The specificity of the I523V mutant shows a change at the P+1 position. Phosphorylation of the $P+1_{Ala}/P+3_{Met}$ peptide by the wild type (V_{max}/K_m = 6.3) and I523V (V_{max}/K_m = 10.0) was comparable (Table III). However, the I523V mutant phosphorylated the $P+1_{Ile}/P+3_{Met}$ peptide ~3.5 times better than the wild type (Table III). Initial rate measurements on the F521A mutant showed generally higher V_{max}/K_m values for the $P+1_{Ala}/P+3_{Met}$, $P+1_{Nle}/P+3_{Met}$, and $P+1_{Ile}/P+3_{Met}$ peptides when compared with wild-type values (Table III). Like wild-type enzyme, the F521A mutant still phosphorylated the $P+1_{Ala}/P+3_{Met}$ peptide best, with V_{max}/K_m = 13.0, compared with the wild type, which has a V_{max}/K_m value of 6.3 for the same peptide.

Mutations That Affect P-1 Peptide Recognition—Isoleucine at the P-1 position is a strong determinant for substrate recognition in wild-type Abl (10, 11). We produced Abl mutants with amino acid substitutions at residues predicted to be near the P-1-binding region of the enzyme. Abl-CAT residue Leu-444 was chosen as a target for mutagenesis based the role of the corresponding residue in IRK, Lys-1085. In IRK, Lys-1085 extends from the αD helix and makes a water-mediated hydrogen bond with the P-1 residue (Asp) of the substrate peptide (12). In our model, Leu-444 extends from the structurally homologous helix and is partially solvent-exposed. We chose to change Leu-444 to lysine to examine the possibility of a change in substrate specificity to that of IRK (which prefers Glu at P-1) (10). An L444E mutation was made to examine the possibility that introduction of an acidic residue at this position may favor the binding of a basic amino acid at the P-1 position of peptide substrate. The L444K and L444E mutants retained the overall preference for Ile at the P-1 position, although they

differed from the wild type in phosphorylation of other substrates (Fig. 5 and Table IV). The L444K mutant has V_{max}/K_m values of 8.0 for the $P-1_{His}$ peptide and 21.0 for the $P-1_{Ile}$ peptide, whereas wild-type Abl has V_{max}/K_m values of 6.8 for $P-1_{His}$ and 12.3 for $P-1_{Ile}$ (Table IV). Thus, L444K shows enhanced recognition of $P-1_{Ile}$ relative to wild-type Abl. The L444E mutant demonstrated a specificity different from that of L444K. The V_{max}/K_m values for the L444E mutant are 14.5 for $P-1_{His}$ and 18.9 for $P-1_{Ile}$ (Table IV); thus, there is a selective increase in $P-1_{His}$ recognition relative to the wild type. Both L444K and L444E have lower V_{max}/K_m values for $P-1_{Glu}$ than wild-type Abl. Wild-type enzyme has a V_{max}/K_m value of 1.3 for $P-1_{Glu}$. The L444K mutant has a V_{max}/K_m value of 0.5 for $P-1_{Glu}$, and the L444E mutant has a V_{max}/K_m value of 0.07, a 19-fold reduction (Table IV).

Abl-CAT residues Gly-556 and Ser-558 were chosen because these residues are solvent-accessible in the homology model, in close proximity to Leu-444 (Fig. 2). We produced G556A, G556V, S558A, and S558N mutants. The G556A and S558A mutants were indistinguishable from the wild type in our initial screens (Fig. 5). The G556V mutant, however, has a reduced preference for Ile at the P-1 position and an increased preference for Leu at the P-1 position. For wild-type enzyme, the V_{max}/K_m value for $P-1_{Ile}$ is 12.3. For the G556V mutant, the V_{max}/K_m value for $P-1_{Ile}$ is 4.2 (Table IV). The S558N mutant showed subtle changes in specificity. The V_{max}/K_m value for $P-1_{Ile}$, 12.0, is similar to the value of 12.3 for wild-type Abl, and the V_{max}/K_m value of this mutant for $P-1_{His}$, 5.4, is close to the value of 6.8 for wild-type Abl (Table IV). The V_{max}/K_m value of this mutant for $P-1_{Glu}$, 0.08, is substantially lower than the corresponding value of 1.3 for wild-type Abl phosphorylating $P-1_{Glu}$ (Table IV).

We also chose to mutate Trp-525 of Abl based on our modeling studies. To identify residues in Abl that may make contacts with the P-1 side chain, we used the activated IRK structure to model Ile (in place of Asp) at the P-1 position of the peptide substrate. The indole of Trp-1175 of IRK packs against the side chain of one energetically favorable rotamer of the modeled Ile. In our Abl model, the residue homologous to Trp-1175, Trp-525, lies at the bottom of the putative P-1-binding pocket (Fig. 2). Trp at this position is conserved in protein-tyrosine kinases (28). We substituted the bulky residues Phe and His for Trp-525 to minimize perturbations in the structure. The W525F and W525H mutants preferred the $P-1_{Ile}$ peptide overall and showed modest changes toward other substrates. For example, the enzymes showed different abilities to phosphorylate the $P-1_{His}$ and $P-1_{Glu}$ peptides (Table IV). W525H had a de-
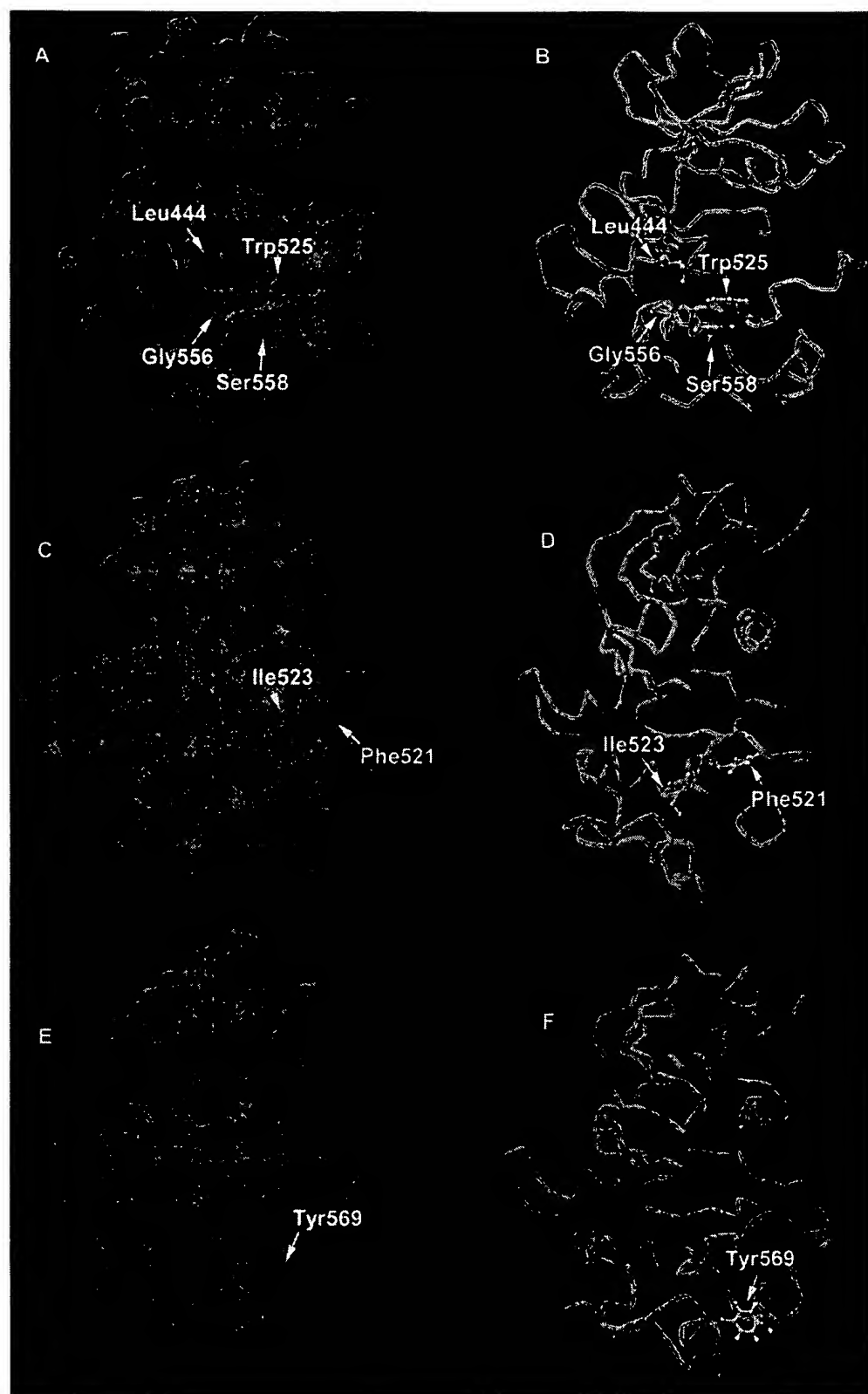
FIG. 2. **Three pairs of models showing amino acids targeted for mutagenesis.** *A* and *B* show residues involved in P−1 substrate specificity. *C* and *D* show residues involved in P+1 specificity. *E* and *F* show the residue involved in P+3 specificity. *A*, *C*, and *E*, molecular surface representations of the Abl homology model showing residues targeted for mutagenesis in *red-orange*. *B*, *D*, and *F*, tube schematic of the Abl homology model showing residues targeted for mutagenesis in *ball and stick* representation.

creased selectivity for P−1$_{His}$ and an increased selectivity for P−1$_{Glu}$ relative to wild-type Abl (Table IV). These results suggest that Trp-525 of Abl is in the vicinity of the P−1 position of bound substrate, although it appears not to play a dominant role in substrate selection.

Indirect Effects—We examined the possibility that mutations designed to affect recognition of one position in the substrate might have effects at other positions as well. Mutants

FIG. 3. **Initial comparisons of wild-type and mutant forms of Abl (Y569W, Y569L, and Y569A) with P+1/P+3 peptide variants.** Wild-type Abl and the three mutant forms of Abl were tested with a panel of eight peptides. The incorporation of [^{32}P]phosphate into peptides was determined after a 20-min reaction using the phosphocellulose paper assay.
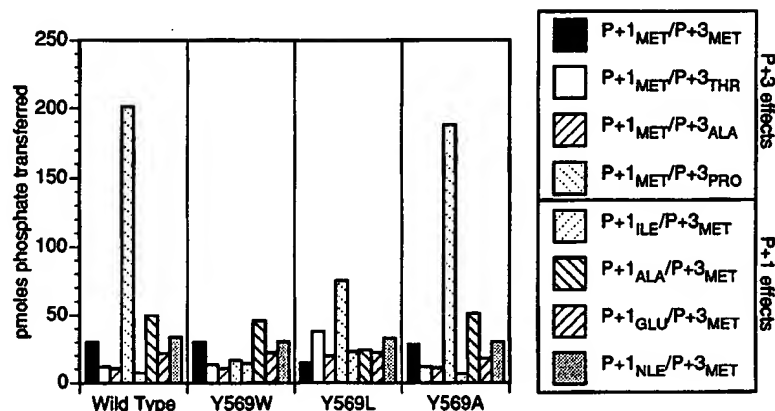
TABLE II

Kinetic measurements for wild-type Abl and two mutant forms of Abl (Y569W and Y569L)

Enzyme/peptide combinations were chosen based on initial comparisons of enzymatic activity toward P+1/P+3 peptides (Fig. 3). Kinetic constants for those enzyme/peptide combinations with significant changes from the wild type are shown. To compare phosphorylation of a particular peptide by mutant versus wild type, the V_{max}/K_m value for the mutant was divided by the value for the wild type. This ratio is given in the last column.

Enzyme	V_{max}	K_m	V_{max}/K_m	V_{max}/K_m ratio
	nmol / min / mg	*mM*		
Wild type				
P+1$_{Met}$/P+3$_{Pro}$	7.5 ± 0.9	0.7 ± 0.2	10.7	1.0
P+1$_{Met}$/P+3$_{Thr}$	2.3 ± 0.5	1.8 ± 0.6	1.3	1.0
P+1$_{Ala}$/P+3$_{Met}$	2.5 ± 0.3	0.4 ± 0.1	6.3	1.0
P+1$_{Nle}$/P+3$_{Met}$	3.4 ± 0.4	0.5 ± 0.2	6.8	1.0
Y569L				
P+1$_{Met}$/P+3$_{Pro}$	4.4 ± 0.4	1.0 ± 0.4	4.4	0.4
P+1$_{Met}$/P+3$_{Thr}$	2.0 ± 0.2	0.9 ± 0.1	2.2	1.7
P+1$_{Ala}$/P+3$_{Met}$	1.9 ± 0.2	0.8 ± 0.2	2.4	0.4
P+1$_{Nle}$/P+3$_{Met}$	3.6 ± 0.4	0.5 ± 0.1	7.2	1.1
Y569W				
P+1$_{Met}$/P+3$_{Pro}$	2.5 ± 0.3	1.9 ± 0.1	1.3	0.1
P+1$_{Ala}$/P+3$_{Met}$	2.8 ± 0.3	0.5 ± 0.1	5.6	0.9

with predicted changes in P+3 recognition were tested with five peptides containing Met, Ile, Ala, Glu, or Nle at the P+1 position (Fig. 3). Whereas the pattern of peptide phosphorylation by Y569W and Y569A closely resembled that of wild-type Abl, Y569L showed some differences from the wild type (Fig. 3). We examined these differences more closely by kinetic analysis of P+1$_{Ala}$/P+3$_{Met}$ and P+1$_{Nle}$/P+3$_{Met}$ (Table II). These measurements showed a decrease in the phosphorylation of P+1$_{Ala}$/P+3$_{Met}$, with V_{max}/K_m = 2.4 (wild-type V_{max}/K_m = 6.3). Thus, in the Y569L mutant, a change in the P+3 region has effects on P+1 recognition as well. We also screened the P+3 mutants with the following peptides varying at P−1: P−1$_{His}$, P−1$_{Glu}$, P−1$_{Gln}$, P−1$_{Ile}$, and P−1$_{Ala}$. These comparisons showed no differences between wild-type Abl and any of the mutants (data not shown).

We tested for indirect effects using the P+1 and P−1 mutants as well. We carried out initial comparisons of the P+1 mutants using four peptides that vary at the P+3 position: P+1$_{Met}$/P+3$_{Met}$, P+1$_{Met}$/P+3$_{Thr}$, P+1$_{Met}$/P+3$_{Ala}$, and P+1$_{Met}$/P+3$_{Pro}$ (Fig. 4). In these experiments, there was no observable difference between the substrate specificities of wild-type Abl and the P+1 mutants toward the peptides varying at P+3 (Fig. 4). Similarly, we observed no differences between the P+1 mutants and the wild type in recognition at the P−1 position (data not shown).

We screened the following four P−1 mutants of Abl for indirect effects: L444K, L444E, S558N, and S558A. We tested the following P+1/P+3 peptides: P+1$_{Met}$/P+3$_{Met}$, P+1$_{Ala}$/P+3$_{Met}$, P+1$_{Glu}$/P+3$_{Met}$, P+1$_{Met}$/P+3$_{Ala}$, and P+1$_{Met}$/P+3$_{Thr}$. All four of the mutants displayed the same rank order of substrate preference as

the wild type in this experiment (P+1$_{Ala}$/P+3$_{Met}$ > P+1$_{Met}$/P+3$_{Met}$ > P+1$_{Glu}$/P+3$_{Met}$ > P+1$_{Met}$/P+3$_{Ala}$ ≈ P+1$_{Met}$/P+3$_{Thr}$) (data not shown). We conclude from these studies on indirect effects that the sites on Abl for recognition of the P−1 and P+1/P+3 positions are distinct. On the other hand, the P+1 and P+3 sites may have some overlap, as at least one mutation (Y569L) had an effect on recognition of both positions.

DISCUSSION

Although Abl is capable of phosphorylating a wide range of peptide and protein substrates, the best peptide substrates for Abl contain the sequence Ile-Tyr-Ala-Xaa-Pro, as shown in peptide library studies (10, 11). Ile at the P−1 position and Pro at the P+3 position are the most important determinants of substrate specificity for Abl. Here, we have identified residues in the catalytic domain of Abl involved in peptide substrate binding and specificity. These residues are located primarily in the C-terminal lobe of the catalytic domain, which has been implicated previously in substrate binding for other protein kinases (12, 24, 27).

The mutant forms of Abl described here fall into three classes with respect to substrate specificity. 1) Two mutants (Y569W and Y569L) have altered substrate specificity. These mutants no longer prefer proline at the P+3 position in peptide substrates. 2) Many of the mutants (*e.g.* I523V, W525H, and L444E) showed no change in the major determinants for substrate recognition, but differed from the wild type in their phosphorylation of other peptide substrates. For example, mutations aimed at altering recognition of the P−1 position resulted in enzymes that still preferred Ile at P−1, but that

FIG. 4. **Initial comparisons of wild-type and mutant forms of Abl (F521A, F521W, I523V, and I523A) with P+1 peptide variants.** Each of the four mutant forms of Abl was tested with the panel of eight peptides. The incorporation of [^{32}P]phosphate into peptides was determined after a 20-min reaction using the phosphocellulose paper assay.
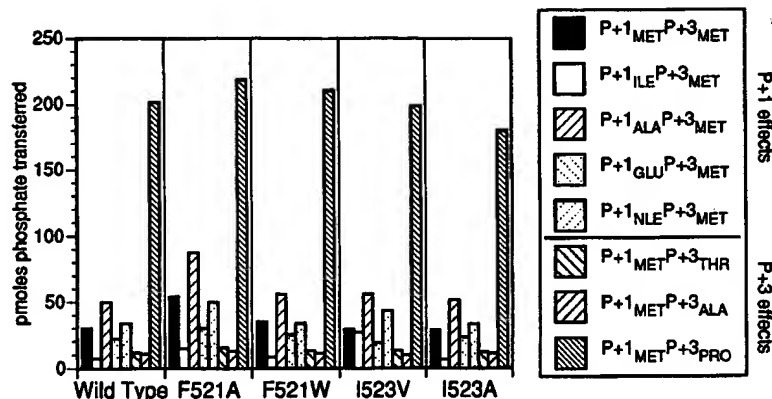
TABLE III
Kinetic measurements for wild-type Abl and two mutant forms of Abl (I523V and F521A)

Enzyme/peptide combinations were chosen based on initial comparisons of enzymatic activity toward all P+1 peptides (Fig. 4). Kinetic constants for those enzyme/peptide combinations with significant changes from the wild type are shown. To compare phosphorylation of a particular peptide by mutant *versus* wild type, the V_{max}/K_m value for the mutant was divided by the value for the wild type. This ratio is given in the last column.

Enzyme	V_{max}	K_m	V_{max}/K_m	V_{max}/K_m ratio
	nmol/min/mg	*mM*		
Wild type				
$P+1_{Ala}/P+3_{Met}$	2.5 ± 0.3	0.4 ± 0.1	6.3	1.0
$P+1_{Nle}/P+3_{Met}$	3.4 ± 0.4	0.5 ± 0.2	6.8	1.0
$P+1_{Ile}/P+3_{Met}$	0.6 ± 0.1	0.5 ± 0.1	1.2	1.0
I523V				
$P+1_{Ala}/P+3_{Met}$	4.8 ± 0.5	0.5 ± 0.1	10.0	1.6
$P+1_{Nle}/P+3_{Met}$	3.3 ± 0.4	0.5 ± 0.1	6.6	1.0
$P+1_{Ile}/P+3_{Met}$	2.1 ± 0.3	0.5 ± 0.1	4.2	3.5
F521A				
$P+1_{Ala}/P+3_{Met}$	5.2 ± 0.5	0.4 ± 0.1	13.0	2.1
$P+1_{Nle}/P+3_{Met}$	3.4 ± 0.4	0.4 ± 0.1	8.5	1.3
$P+1_{Ile}/P+3_{Met}$	2.2 ± 0.2	1.5 ± 0.1	1.5	1.3

diverged from the wild type when screened against peptides containing other amino acids at P−1. In these cases, these residues may not be involved in direct interactions with the P−1 residue of substrate. Instead, because of their vicinity to the P−1 position, they may act indirectly, stabilizing the local structure to interact favorably with Ile at the P−1 position. 3) Some mutants (*e.g.* Y569A, I523A, and G556A) showed no changes in specificity when assayed against a variety of peptide substrates. These mutants were not characterized by kinetic analysis.

The Y569W mutation in Abl has the most dramatic effect on substrate specificity of the mutants we report here. Wild-type Abl phosphorylates a peptide substrate with Pro at the P+3 position best. The Y569W mutant phosphorylates $P+1_{Met}/P+3_{Pro}$ ~10 times less efficiently than does wild-type Abl (Table II). All other amino acid side chains tested at the P+3 position of the substrate were phosphorylated at the same level as in the wild type (Fig. 3). Our structural model suggests that this change in specificity arises from a steric clash between the side chain of Trp-569 in the mutant and the side chain of proline in the substrate. This is not the case with the other peptide substrates tested that have smaller amino acid side chains at the P+3 position. Proline at the P+3 position plays a role in substrate recognition *in vivo* in at least one case: Abl phosphorylates c-Crk at Tyr-221 within the sequence Tyr-Ala-Gln-Pro (9). Phosphorylation by Abl is believed to modulate the protein binding and transforming activity of Crk (29). Preliminary experiments indicate that, in contrast to wild-type Abl, the Y569W mutant has no activity toward Crk *in vitro*.[3]

Mutations predicted to affect substrate recognition at the

P+1 position (I523V) or at the P−1 position (L444K, L444E, G556V, S558N, W525F, and W525H) do so in a more subtle manner. These mutations do not change the overall preference for Ile at P−1 or Ala at P+1; however, we observed effects on specificity when we screened these mutants against peptides containing other residues at P−1 or P+1. For example, the I523V mutant still phosphorylated the $P+1_{Ala}/P+3_{Met}$ peptide best (of the peptides tested), but the V_{max}/K_m value for the $P+1_{Ile}/P+3_{Met}$ peptide was 3.5 times higher in this mutant than in the wild type (Table III). The L444E mutant, while still preferring Ile at the P−1 position, was 2.1 times more efficient at phosphorylating the P−1$_{His}$ peptide than the wild type and 19 times less efficient at phosphorylating the P−1$_{Glu}$ peptide than the wild type (Table IV). There are at least two explanations for these subtle effects on substrate specificity. (i) The residues may not make direct contact with bound substrate, but might instead be involved indirectly in maintaining the three-dimensional structure of Abl to favor certain amino acids in the substrate. (ii) Additionally or alternatively, substrate specificity at P−1 or P+1 may be achieved by a combination of residues, such that single amino acid substitutions do not cause complete alterations in substrate recognition. Indirect effects could explain why, for example, the L444K mutant phosphorylates the P−1$_{Ile}$ peptide better than the wild type and shows a decrease in the phosphorylation of P−1$_{Glu}$ when compared with the wild type (Table IV).

There are residues in the three-dimensional structures of Src family kinases that appear to correspond to residues identified in our study (30, 31). The substrate specificity of Src differs from that of Abl at the P+3 position (10). Src prefers a phenylalanine at the P+3 position in a peptide substrate, whereas Abl prefers proline. The residue homologous to tyrosine 569, a

---

[3] J. H. Till and W. T. Miller, unpublished observations.

FIG. 5. **Initial comparisons of wild-type and mutant forms of Abl (G556V, G556A, L444K, L444E, S558N, S558A, W525H, and W525F) with P−1 peptide variants.** Each of the eight mutant forms of Abl shown here was tested with a panel of five peptides: $P-1_{Ala}$, $P-1_{Gln}$, $P-1_{Ile}$, $P-1_{Glu}$, and $P-1_{His}$. The incorporation of [^{32}P]phosphate into peptides was determined after a 20-min reaction using the phosphocellulose paper assay.
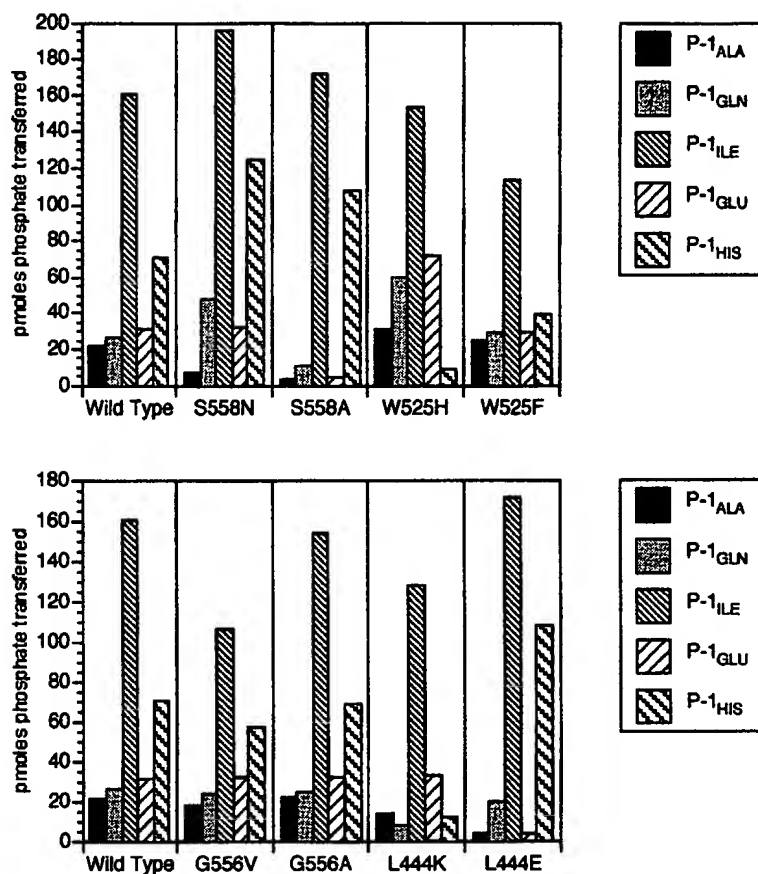
TABLE IV

Kinetic measurements for wild-type Abl and six mutant forms of Abl (L444K, L444E, S558N, G556V, W525H, and W525F)

Enzyme/peptide combinations were chosen based on initial comparisons of enzymatic activity toward all P−1 peptides (Fig. 5). Kinetic constants for those enzyme/peptide combinations with significant changes from the wild type are shown. To compare phosphorylation of a particular peptide by mutant *versus* wild type, the V_{max}/K_m value for the mutant was divided by the value for the wild type. This ratio is given in the last column.

Enzyme	V_{max}	K_m	V_{max}/K_m	V_{max}/K_m ratio
	nmol/min/mg	*mM*		
Wild type				
$P-1_{Ile}$	4.9 ± 0.5	0.4 ± 0.05	12.3	1.0
$P-1_{Glu}$	1.8 ± 0.3	1.4 ± 0.1	1.3	1.0
$P-1_{Leu}$	0.6 ± 0.1	0.8 ± 0.1	0.8	1.0
$P-1_{His}$	4.1 ± 0.4	0.6 ± 0.1	6.8	1.0
L444K				
$P-1_{Ile}$	18.9 ± 3.3	0.9 ± 0.3	21.0	1.7
$P-1_{Glu}$	ND[a]	ND	0.5	0.4
$P-1_{His}$	10.4 ± 1.9	1.3 ± 0.3	8.0	1.2
L444E				
$P-1_{Ile}$	13.2 ± 1.4	0.7 ± 0.1	18.9	1.5
$P-1_{Glu}$	ND	ND	0.07	0.05
$P-1_{His}$	5.8 ± 0.7	0.4 ± 0.1	14.5	2.1
S558N				
$P-1_{Ile}$	3.6 ± 0.4	0.3 ± 0.04	12.0	1.0
$P-1_{Glu}$	ND	ND	0.08	0.06
$P-1_{His}$	1.3 ± 0.1	0.2 ± 0.03	5.4	0.8
G556V				
$P-1_{Ile}$	2.5 ± 0.3	0.6 ± 0.1	4.2	0.3
$P-1_{Leu}$	1.3 ± 0.1	0.7 ± 0.1	1.9	2.3
W525H				
$P-1_{Ile}$	5.1 ± 0.6	0.4 ± 0.04	12.8	1.0
$P-1_{Glu}$	2.3 ± 0.3	0.7 ± 0.1	3.3	2.5
$P-1_{His}$	3.0 ± 0.3	1.5 ± 0.2	2.0	0.3
W525F				
$P-1_{Ile}$	4.5 ± 0.5	0.6 ± 0.1	7.5	0.6
$P-1_{Glu}$	2.0 ± 0.4	1.3 ± 0.2	1.5	1.2
$P-1_{His}$	3.4 ± 0.4	0.5 ± 0.1	6.8	1.0

[a] ND, not determined (see "Experimental Procedures").

residue involved in P+3 specificity in Abl (Fig. 3), is a leucine (Leu-472) in Src. This sequence difference may account for the differences seen in substrate specificity; an L472Y mutant of Src might phosphorylate P+3$_{Pro}$-containing peptides more efficiently. A tryptophan substitution at this position could prevent large side chain amino acids from binding in this region, as we observed for Abl.

The substrate specificities of tyrosine kinase catalytic domains are important in maintaining the fidelity of cellular signal transduction pathways. This is best illustrated in the case of the RET receptor. A naturally occurring mutation in the kinase domain of this receptor changes a methionine residue to a threonine residue in a region homologous to the region of Abl shown here to be involved in substrate recognition of the P+1 residue (32, 33). This change affects the substrate specificity of the enzyme at the P+1 position, changing the preference from methionine at that position in the substrate to alanine (10). This mutant form of the RET receptor is implicated in multiple endocrine neoplasia type 2A (32, 33).

Mutations throughout the Abl protein have been reported previously (4). Many of these mutations affect the regulation of the enzyme *in vivo*. One such mutation, which is sufficient to activate c-Abl enzymatic activity *in vivo*, is found in the catalytic domain. This mutation changes a tyrosine to phenylalanine within the ATP-binding fold of the enzyme (34). Mutations that affect substrate recognition by the catalytic domain, however, have not been reported previously. Our studies on Abl have highlighted seven residues as playing important roles in peptide substrate recognition. We also show that a single amino acid change of Tyr-569 to tryptophan can affect the substrate specificity dramatically. The results raise the possibility of altering tyrosine kinase substrate specificity *in vivo* by protein engineering.

REFERENCES

1. Wang, J. Y. J. (1993) *Curr. Opin. Genet. Dev.* **3**, 35–43
2. Laneuville, P. (1995) *Semin. Immunol.* **7**, 255–266
3. Pendergast, A. M. (1996) *Curr. Opin. Cell Biol.* **8**, 174–181
4. Raitano, A. B., Whang, Y. E., and Sawyers, C. L. (1997) *Biochim. Biophys. Acta* **1333**, F201–F216
5. Lugo, T. G., Pendergast, A. M., Muller, A. J., and Witte, O. N. (1990) *Science* **247**, 1079–1082
6. McLaughlin, J., Chianese, E., and Witte, O. N. (1989) *Mol. Cell. Biol.* **9**, 1866–1874
7. Tybulewicz, V. L., Crawford, C. E., Jackson, P. K., Bronson, R. T., and Mulligan, R. C. (1991) *Cell* **65**, 1153–1163
8. Baskaran, R., Dahmus, M. E., and Wang, J. Y. (1993) *Proc. Natl. Acad. Sci. U. S. A.* **90**, 11167–11171
9. Feller, S. M., Knudsen, B., and Hanafusa, H. (1994) *EMBO J.* **13**, 2341–2351
10. Zhou, S., Carraway, K. L., III, Eck, M. J., Harrison, S. C., Feldman, R. A., Mohammadi, M., Schlessinger, J., Hubbard, S. R., Smith, D. P., Eng, C., Lorenzo, M. J., Ponder, B. A. J., Mayer, B. J., and Cantley, L. C. (1995) *Nature* **373**, 536–539
11. Till, J. H., Annan, R. S., Carr, S. A., and Miller, W. T. (1994) *J. Biol. Chem.* **269**, 7423–7428
12. Hubbard, S. R. (1997) *EMBO J.* **16**, 5572–5581
13. Vihinen, M., Vetrie, D., Maniar, H. S., Ochs, H. D., Zhu, Q., Vorechovsky, I., Webster, A. D., Notarangelo, L. D., Nilsson, L., and Sowadski, J. M. (1994) *Proc. Natl. Acad. Sci. U. S. A.* **91**, 12803–12807
14. Thompson, J. D., Higgins, D. G., and Gibson, T. J. (1994) *Nucleic Acids Res.* **22**, 4673–4680
15. Guex, N., and Peitsch, M. C. (1997) *Electrophoresis* **18**, 2714–2723
16. Peitsch, M. C. (1996) *Biochem. Soc. Trans.* **24**, 274–279
17. Surles, M. C., Richardson, J. S., Richardson, D. C., and Brooks, F. P., Jr. (1994) *Protein Sci.* **3**, 198–210
18. Laskowski, R. A., MacArthur, M. W., Moss, D. S., and Thornton, J. M. (1993) *J. Appl. Crystallogr.* **26**, 283–291
19. Garcia, P., Shoelson, S. E., George, S. T., Hinds, D. A., Goldberg, A. R., and Miller, W. T. (1993) *J. Biol. Chem.* **268**, 25146–25151
20. Reddy, E. P., Smith, M. J., and Srinivasan, A. (1983) *Proc. Natl. Acad. Sci. U. S. A.* **80**, 3623–3627
21. Casnellie, J. E. (1991) *Methods Enzymol.* **200**, 115–120
22. Boerner, R. J., Barker, S. C., and Knight, W. B. (1995) *Biochemistry* **34**, 16419–16423
23. Thomas, N. E., Bramson, H. N., Nairn, A. C., Greengard, P., Fry, D. C., Mildvan, A. S., and Kaiser, E. T. (1987) *Biochemistry* **26**, 4471–4474
24. Taylor, S. S., and Radzio-Andzelm, E. (1994) *Structure* **2**, 345–355
25. Golub, T. R., Goga, A., Barker, G. F., Afar, D. E., McLaughlin, J., Bohlander, S. K., Rowley, J. D., Witte, O. N., and Gilliland, D. G. (1996) *Mol. Cell. Biol.* **16**, 4107–4116
26. Moro, M., Walkenhorst, J., Goga, A., Witte, O. N., and Superti-Furga, G. (1997) *Leukemia (Basingstoke)* **11**, Suppl. 3, 313–315
27. Pinna, L. A., and Ruzzene, M. (1996) *Biochim. Biophys. Acta* **1314**, 191–225
28. Hanks, S. K., Quinn, A. M., and Hunter, T. (1988) *Science* **241**, 42–52
29. Rosen, M. K., Yamazaki, T., Gish, G. D., Kay, C. M., Pawson, T., and Kay, L. E. (1995) *Nature* **374**, 477–479
30. Sicheri, F., Moarefi, I., and Kuriyan, J. (1997) *Nature* **385**, 602–609
31. Xu, W., Harrison, S. C., and Eck, M. J. (1997) *Nature* **385**, 595–602
32. Carlson, K. M., Dou, S., Chi, D., Scavarda, N., Toshima, K., Jackson, C. E., Wells, S. A., Jr., Goodfellow, P. J., and Donis-Keller, H. (1994) *Proc. Natl. Acad. Sci. U. S. A.* **91**, 1579–1583
33. Hofstra, R. M., Landsvater, R. M., Ceccherini, I., Stulp, R. P., Stelwagen, T., Luo, Y., Pasini, B., Hoppener, J. W., van Amstel, H. K., Romeo, G., Lips, C. J. M., and Buys, C. H. C. M. (1994) *Nature* **367**, 375–376
34. Allen, P. B., and Wiedemann, L. M. (1996) *J. Biol. Chem.* **271**, 19585–19591

Phosphorylation of Synthetic Peptides Containing Tyr-Met-X-Met Motifs by Nonreceptor Tyrosine Kinases *in Vitro*[*]

Pilar Garcia‡, Steven E. Shoelson§, Shaji T. George¶‖, Duane A. Hinds‡, Allan R. Goldberg¶‖, and W. Todd Miller‡**

From the ‡Department of Physiology and Biophysics, School of Medicine, State University of New York, Stony Brook, New York 11794, the §Research Division, Joslin Diabetes Center, Department of Medicine, Brigham and Women's Hospital, and Harvard Medical School, Boston, Massachusetts 02215, and ¶Rockefeller University, New York, New York 10021

Several tyrosine phosphorylation sites in the insulin receptor kinase substrate IRS-1 are predicted to be within Tyr-Met-X-Met (YMXM) motifs, and synthetic peptides corresponding to these sequences are excellent substrates for the insulin receptor kinase *in vitro* (Shoelson, S. E., Chatterjee, S., Chaudhuri, M., and White, M. F. (1992) *Proc. Natl. Acad. Sci. U. S. A* **89**, 2027–2031). In this study, YMXM-containing peptides are shown to act as substrates for two members of the nonreceptor subfamily of tyrosine kinases, v-Src and v-Abl (the transforming gene products of Rous sarcoma virus and Abelson murine leukemia virus, respectively). For v-Src, a baculovirus expression system was used which was capable of producing milligram quantities of pure 60-kDa v-Src in *Spodoptera frugiperda* (Sf9) cells. The source of v-Abl was an *Escherichia coli* expression vector that produces a fusion protein of glutathione S-transferase with the *abl* catalytic domain. The synthetic YMXM-containing peptides had among the highest apparent affinities described to date for either tyrosine kinase, with K_m values as low as 97 μM for v-Src and v-Abl. Comparisons with the results obtained with the insulin receptor kinase revealed differences in substrate specificity among the enzymes. In particular, v-Src was more tolerant of substitutions at the Met^{+1} and Met^{+3} positions in the YMXM motif than either v-Abl or the insulin receptor kinase but was more dependent on the presence of a preceding acidic amino acid. For v-Abl, the presence of threonine at any position in the YMXM motif caused a reduction in catalytic efficiency. Phosphorylated YMXM motifs are recognition elements for binding to the src homology 2 domains of phosphatidylinositol 3'-kinase and additional proteins; hence, differences in specificity of tyrosine kinases toward YMXM-containing proteins may have relevance to downstream signaling events.

Tyrosine protein kinases can be divided into two broad categories: the nonreceptor tyrosine kinases and the receptor

tyrosine kinases (1). These two groups share a related catalytic domain of approximately 270 amino acids which also has homology to the catalytic domains of serine/threonine protein kinases (2). The largest subfamily of nonreceptor tyrosine kinases is the src subfamily, whose members are highly homologous to v-Src, the product of the *src* transforming gene from Rous sarcoma virus. Besides shared sequences in the catalytic domains, enzymes in this subfamily exhibit a high degree of conservation in their src homology (SH)[1] 2 and 3 domains, which are thought to regulate intracellular protein-protein interactions (3). To date, relatively few distinctions have been made between receptor and nonreceptor tyrosine kinases with regard to the intrinsic substrate specificities of their catalytic domains. *In vitro* and *in vivo* studies with tyrosine kinases have indicated that the spectrum of substrates recognized by the two groups is largely overlapping (4).

A recently identified determinant for substrate recognition by the insulin receptor tyrosine kinase is the Tyr-Met-X-Met (YMXM) motif. This sequence was identified in the context of potential phosphorylation sites in the IRS-1 protein, an endogenous substrate of the insulin receptor kinase in many cell types (5). The importance of YMXM and YXXM motifs was also inferred from sequence comparisons of receptor tyrosine kinase autophosphorylation sites which bind the phosphatidylinositol 3'-kinase (6). Synthetic peptides based on the YMXM sequences from IRS-1 served as substrates for the insulin receptor kinase *in vitro*, with K_m values in the 24–100 μM range (7). These values for K_m were lower than those reported previously for peptides containing multiple acidic residues N-terminal to tyrosine. The insulin receptor tyrosine kinase was sensitive to amino acid substitutions at the Met^{+1} and Met^{+3} positions in these peptides (relative to the phosphorylated tyrosine), suggesting that those positions play important roles in enzyme-substrate recognition (7).

Recent evidence suggests that phosphorylated YMXM motifs play a role in mediating specific interactions with SH2 domains. In particular, the SH2 domains of the phosphatidylinositol 3'-kinase p85 subunit bind to autophosphorylated YMXM or YXXM motifs in the platelet-derived growth factor receptor (8–10) and colony-stimulating factor 1 receptor (11), as well as in IRS-1 itself (12). The phosphotyrosine residue in the polyoma virus middle T antigen which directs interaction with the p85 subunit, Tyr^{315}, also occurs within a YMXM sequence (13). Moreover, the SH2 domains of phospholipase Cγ1, GTPase-activating protein, and the p85 subunit of the phosphatidylinositol 3'-kinase appear to bind at distinct phosphotyrosine-containing sites (or combinations of sites)

‖ Present address: Innovir Laboratories, 510 E. 73rd St., New York, NY 10021.

** To whom correspondence should be addressed: Dept. of Physiology and Biophysics, Basic Science Tower T-6, School of Medicine, SUNY at Stony Brook, Stony Brook, NY 11794-8661. Tel.: 516-444-3533; Fax: 516-444-3432.

[1] The abbreviations used are: SH, src homology; PAGE, polyacrylamide gel electrophoresis; Nle, norleucine.

within the platelet-derived growth factor receptor (14), indicating that the amino acid sequences surrounding phosphotyrosine are involved in specific interactions with SH2 domains. Crystallographically derived structures of the SH2 domains from v-Src (15) and p56[lck] (16) complexed to phosphotyrosyl peptides, as well as NMR-derived structures of the peptide-free SH2 domains from c-Abl (17) and p85 (18), indicate that binding pockets exist for amino acids that are near the phosphotyrosine residue. Thus, phosphorylation of YM*X*M or Y*XX*M motifs in cellular substrates such as IRS-1 may regulate the binding of SH2-containing downstream signaling proteins.

In this study we compare the *in vitro* specificities of two nonreceptor tyrosine kinases for YM*X*M-containing substrates. We describe a baculovirus-based expression system for active v-Src. We have also expressed (in bacterial cells) a nonreceptor tyrosine kinase from a different subfamily, the v-Abl retroviral oncogene product from Abelson murine leukemia virus. The specificities of these enzymes are compared with that reported previously for the insulin receptor kinase.

EXPERIMENTAL PROCEDURES

Materials—The AcMNPV vector pVL941 was the kind gift of Dr. Max D. Summers (Texas A & M University). The hybridoma-producing monoclonal antibody 327 was kindly provided by Dr. Joan Brugge (University of Pennsylvania), and plasmid pN4 containing the *src* sequence from the Schmidt Ruppin strain of Rous sarcoma virus was a generous gift of Dr. Hidesaburo Hanafusa (Rockefeller University). *Spodoptera frugiperda* (Sf9) cells were obtained from the American Tissue Culture Corporation. The plasmid encoding the glutathione *S*-transferase/*abl* fusion protein was generously provided by Dr. Bruce Mayer (Rockefeller University). Solid phase peptide synthesis was carried out on an Applied Biosystems model 430A synthesizer using a *t*-butoxycarbonyl protection strategy, as described (7). Peptides were purified by preparative high pressure liquid chromatography on a Dynamax-300 Å 12-μm C8 column with a mobile phase composed of acetonitrile in 0.05% trifluoroacetic acid and were characterized by amino acid analysis.

Ex-cell 401 medium was from JRH Biosciences, and antibiotic/antimycotic and fetal bovine serum were from Life Technologies, Inc. Affi-Gel A-15 was purchased from Bio-Rad, and glutathione-agarose was from Molecular Probes, Inc. Phosphocellulose P-81 paper was obtained from Whatman. [γ-³²P]ATP was from Amersham Corp., and Centricon-30 concentrators were purchased from Amicon.

Construction of the Transfer Vector pVL941-src—The pBR322 plasmid pN4 (19) bearing the *src* sequence was digested with the restriction enzymes *Nco*I and *Bgl*I, and the 1,672-base pair fragment was isolated on a gel. The *Nru*I site downstream of the *src* coding sequence had been changed to a *Bgl*II site in this plasmid by linker insertion (19). The recessed ends of this fragment were filled in with deoxynucleotides using the Klenow fragment (20) and cloned into the *Bam*HI site of the baculovirus transfer vector pVL941 and used to transform *Escherichia coli* strain HB101. DNA from bacterial colonies bearing the plasmid with the insert in the correct orientation downstream of the polyhedrin promoter was isolated by the alkaline lysis method and purified twice on a CsCl₂ density gradient. Wild-type AcMNPV DNA was isolated according to the method of Summers and Smith (21).

Transfer of the src Gene into AcMNPV Genome—Transfer of the *src* gene was achieved by cotransfection of pVL941-*src* and AcMNPV DNA into exponentially growing Sf9 cells by the calcium phosphate precipitation technique (23), as modified for insect cells (23, 24). Approximately 2 × 10⁶ Sf9 cells were transfected with 1 μg of AcMNPV DNA and 2 μg of pVL941-*src* DNA. After 6 days the supernatant from the transfection culture (virus titer 1 × 10⁸ plaque-forming units/ml) was serially diluted and used to infect fresh Sf9 cells and overlayed with 1.5% agarose.

Expression of v-Src in Sf9 Cells—Sf9 cells were grown in Ex-cell 401 medium supplemented with 2.5% fetal bovine serum and 1% antibiotic-antimycotic and maintained at 28 °C as described (21). Viral stocks were titered using a plaque assay. Serial dilutions of viral stocks were used to infect exponentially growing Sf9 cells in 60 × 15-mm tissue culture dishes at cell densities of 1.5 × 10⁶ cells/dish. After 1-h incubations, viral supernatant was removed, and the dishes were

overlaid with 1.5% low melting temperature agarose in Ex-cell 401. Occlusion-negative plaques formed after 4–5 days and were visualized by neutral red staining. Two rounds of plaque purification were carried out to obtain pure recombinant virus for large scale infections.

To screen for expression of v-Src by recombinant viruses, viral plaques were used to infect 5 × 10⁵ cells in 24-well microtiter plates. Four days after infection, Sf9 cells were analyzed for v-Src expression by SDS-polyacrylamide gel electrophoresis (SDS-PAGE). Samples of the infected cells (1.5 ml) were harvested, resuspended in Laemmli 2 × SDS/sample buffer (25), boiled, and electrophoresed on 7.5% SDS-PAGE with Coomassie Blue staining. To confirm the presence of active v-Src, an additional sample from the infected cells was collected and resuspended in homogenization buffer (25 mM HEPES (pH 7.5), 5 mM EDTA, 150 mM NaCl, 1% Triton X-100, 5 μg/ml leupeptin, 5 μg/ml aprotinin, 1 mM phenylmethylsulfonyl fluoride). This sample was homogenized in a Potter-Elvhejem homogenizer and analyzed for tyrosine kinase activity using the phosphocellulose binding assay (26) with [Val⁵]angiotensin II as substrate (27) (see below).

For large scale infections of Sf9 cells, 1 liter of exponentially growing cells in a Spinner culture flask (cell density 2 × 10⁶ cells/ml) was centrifuged for 10 min at 1,000 × *g*. The cell pellet was resuspended in 100 ml of medium supplemented with recombinant Ac-MNPV-*src* virus at a multiplicity of infection of 10 and incubated for 1 h. Additional medium (900 ml) was then added, and the culture was incubated for 3 days at 28 °C with constant stirring. The cells were harvested by centrifugation at 1,000 × *g* and stored at −80 °C until ready to be used for protein purification.

Purification of v-Src—Frozen Sf9 cells from a 1-liter infection were resuspended in 100 ml of homogenization buffer (see above) and homogenized in a 150-ml Potter-Elvhejem homogenizer. An additional 100 ml of homogenization buffer was added to this homogenate, and the mixture was stirred for 30 min at 4 °C and then centrifuged for 30 min at 12,000 × *g*.

The supernatant was applied to a 2.5 × 10-cm Affi-Gel 15 column containing immobilized anti-*src* monoclonal antibody 327 (28). The column was constructed by coupling antibody 327 (IgG fraction purified from mouse ascites fluid by Affi-Gel Blue chromatography (29)) to the activated support at 5 mg/ml following the protocol recommended by the manufacturer. The homogenate was loaded onto the column at a flow rate of 2 ml/min, and the flow-through was collected and passed over the column twice more to optimize binding. The column was washed for 8 h with 25 mM HEPES (pH 7.5), 300 mM NaCl, 1% Triton X-100, 0.1% sodium deoxycholate, 5 mM EDTA. The column was eluted with 10 mM glycine-NaOH buffer (pH 10.2) containing 150 mM NaCl, 1% Triton X-100, and 10% glycerol. Five-ml fractions were collected and neutralized immediately with 0.8 ml of 0.5 M Tris-HCl (pH 8). The fractions were analyzed for tyrosine kinase activity using the phosphocellulose paper assay described below with [Val⁵]angiotensin II as substrate. Active fractions were pooled, concentrated by passage over Centriprep-30 concentrators (Amicon), and stored in 40% glycerol at −20 °C; under these conditions v-Src remained active for up to 2 months. These samples were > 95% pure as judged by SDS-PAGE and Coomassie Blue staining.

Expression and Purification of v-Abl Fusion Protein—Expression and purification of the glutathione *S*-transferase fusion protein was performed as described (30). A 50-ml overnight culture of *E. coli* strain NB42 harboring plasmid pGEX-Cat was inoculated into 1 liter of LB broth containing ampicillin (50 μg/ml). The culture was incubated for 2 h at 37 °C, at which time isopropyl 1-thio-β-D-galactopyranoside was added to a final concentration of 0.1 mM. The culture was grown for an additional 3 h at 30 °C and then centrifuged (6,000 rpm for 10 min). The pellet was resuspended in 10 ml of ice-cold lysis buffer (50 mM HEPES (pH 7.4), 100 mM NaCl, 100 mM EDTA, 1% Triton X-100, 10 mM dithiothreitol, 10% glycerol, 1 mM phenylmethylsulfonyl fluoride, 50 μg/ml aprotinin). The cells were lysed by sonication, and the lysate was clarified by centrifugation at 10,000 × *g* for 20 min.

The supernatant was mixed with 5 ml of glutathione-agarose at 4 °C for 30 min. The beads were collected by centrifugation (1,000 rpm, 1 min) and washed four times with 50 mM HEPES (pH 7.4) containing 100 mM EDTA. The beads were then poured into a 1 × 6.4-cm column and washed for 1 column volume with the HEPES buffer and for an additional column volume with 50 mM Tris (pH 8.0). Elution of the glutathione *S*-transferase-*abl* fusion protein was carried out with 50 mM Tris (pH 8.0) containing 10 mM reduced glutathione. One-ml fractions were collected and tested for tyrosine kinase activity using the phosphocellulose paper assay with [Val⁵] angiotensin II as substrate. Active fractions were pooled, concentrated
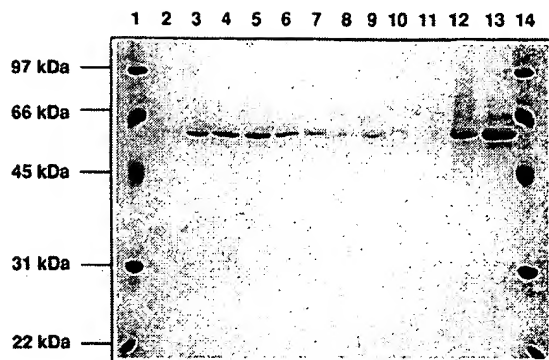
Phosphorylation of Tyr-Met-X-Met Peptides

FIG. 1. **Purification of v-Src from Sf9 cells.** SDS-PAGE analysis is shown of the fractions eluting from the anti-*src* immunoaffinity column. *Lanes 1* and *14*, molecular mass standards; *lanes 2–11*, column fractions from high pH elution; *lane 12*, active v-Src from an earlier preparation; *lane 13*, pooled material from *lanes 2–11*. Protein bands were visualized by Coomassie Blue staining.

using Centricon-30 microconcentrators, and stored in 40% glycerol at −20 °C. The fusion protein was at least 95% pure as judged by SDS-PAGE with Coomassie Blue staining.

Kinetics of Peptide Phosphorylation—Phosphorylation assays were carried out in total volumes of 25 μl at 30 °C. Each reaction contained 50 mM Tris-HCl (pH 7.4), 10 mM MgCl$_2$, 1 mg/ml bovine serum albumin, and 200 μM [γ-^{32}P]ATP (100–500 cpm/pmol), with varying peptide concentrations. Reactions were initiated by the addition of 1 μl of v-Src (0.7 μg) or 2 μl of the glutathione S-transferase-*abl* fusion protein (0.7 μg) and were terminated by the addition of 45 μl of cold 10% trichloroacetic acid. The reaction mixtures were centrifuged for 2 min in an Eppendorf microcentrifuge, and 35 μl of the supernatants was spotted onto 2.1-cm diameter phosphocellulose paper circles, as described (26). The phosphocellulose pads were washed three times with cold 0.5% phosphoric acid and once with acetone, dried, and counted dry in a liquid scintillation counter to measure incorporation of ^{32}P into peptide. The initial rates of reaction (5%) were measured in triplicate, and kinetic constants were determined by weighted nonlinear least squares fit to the hyperbolic velocity *versus* [substrate] plots using the iterative program NFIT (Island Products, Galveston, TX).

RESULTS

Expression and Purification of v-Src—The expression of the Rous sarcoma virus v-*src* gene product for these studies was carried out in Sf9 cells infected with a recombinant baculovirus harboring the v-*src* gene. Maximal expression of v-Src in this system occurred on the 3rd day after infection, at which time the Sf9 cells were still round and excluded trypan blue. The baculovirus expression vector used for these studies produces a mature, 60-kDa form of v-Src which is myristoylated and which localizes to the plasma membrane as demonstrated by immunofluorescence microscopy.[2]

Occlusion-negative viruses were screened for v-Src expression by SDS-PAGE of crude cell lysates from infected cells. Specific expression of a protein of the expected molecular mass (60 kDa) in infected cells was visualized by Coomassie staining (Fig. 1). In addition, crude cell lysates from infected cells were tested for tyrosine kinase activity with the phosphocellulose paper assay (26) using [Val^5]angiotensin II as substrate. These results indicated that the infected Sf9 cells expressed active v-Src (activity $\approx$ 1.5 nmol of phosphate transferred/min/10^6 cells). Baculoviruses expressing v-Src were subjected to two more rounds of plaque purification prior to large scale infection of Sf9 cells.

The purification strategy for v-Src was based on an immunoaffinity column containing anti-*src* antibody 327 (28). The

enzyme was eluted from the column by using a pH 10.2 buffer and was neutralized immediately after elution to pH 8.0. This step was found to be crucial for recovery of active tyrosine kinase. The purified enzyme migrated as a single band with an apparent molecular mass of 60 kDa on SDS-PAGE (Fig. 1). Using the phosphocellulose paper assay, the baculovirus-expressed enzyme exhibited a K_m of 0.9 mM for [Val^5]angiotensin II and a V_{max} of 7.3 nmol/min/mg of enzyme. These values are in good agreement with previously determined values for this substrate using v-Src from Rous sarcoma virus-transformed cells ($K_m = 0.87$ mM; $V_{max} = 6.7$ nmol/min/mg) (27) or expressed in yeast ($K_m = 0.94$ mM; $V_{max} = 10.6$ nmol/min/mg) (31). Neither of these two enzyme preparations involved a denaturing step; hence, the brief exposure of the enzyme to high pH in the present purification does not appear to reduce specific activity significantly.

Phosphorylation of YMXM Peptides by v-Src—Peptides corresponding to the six sequences of YMXM motifs from the insulin receptor kinase substrate IRS-1 were tested for phosphorylation by purified v-Src (Table I). These peptides have recently been shown to serve as excellent *in vitro* substrates for the insulin receptor kinase (7). Additional peptides possessing single amino acid substitutions in the YMXM motif from the Tyr^{987} site of IRS-1 were also tested as substrates for v-Src (Table I). These included peptides containing substitutions for Met^{988} and Met^{990} within the YMXM motif as well as an Asp^{986} → Asn substitution. Finally, a synthetic peptide corresponding to the sequence of the YMXM motif from the polyoma virus middle T antigen was prepared and tested for phosphorylation by v-Src. This protein forms a 1:1 complex with c-Src, the cellular form of v-Src (32), and is phosphorylated *in vivo* at Tyr^{315} within its YMXM motif (13). In each case, if sufficient basic residues were not present within the native sequence for absorption to phosphocellulose paper under the acidic conditions of the assay (26), additional lysine residues were added to the N terminus.

With one exception (the Asp^{986} → Asn analog of the Y987 sequence), all peptides tested served as substrates for the baculovirus-expressed v-Src kinase (Table I). Kinetic measurements were obtained using the phosphocellulose binding assay with [γ-^{32}P]ATP. Experiments were performed at saturating concentrations of ATP (200 μM) and Mg^{2+} (10 mM) to arrive at values of K_m and V_{max} for the peptides. For several of the peptides, these values compare favorably with those of the best peptide substrates for v-Src (4, 33). Values of K_m for the YMXM peptides ranged from 97 to 1,700 μM, and values of V_{max} ranged from 1.0 to 6.1 nmol/min/mg of enzyme. Of the six peptides derived from potential phosphorylation sites in IRS-1, the Y987 peptide was the most efficient ($k_{cat}/K_m = 2.5 \times 10^3$ M^{-1} min^{-1}). This peptide was therefore chosen to examine the effects of substitutions within the YMXM motif.

In the case of the Y987 peptide, the K_m for peptide (300 μM) was not dramatically affected by substitutions at positions corresponding to Met^{988} (Met^{+1}) (Table I). Substitutions of Met^{+1} → Ile and Met^{+1} → norleucine (Nle) increased the K_m for phosphorylation to 390 and 310 μM, respectively, whereas a Met^{+1} → Thr substitution decreased K_m to 250 μM. v-Src was also tolerant to substitutions at the Met^{990} (Met^{+3}) position; the Met^{+3} → Thr peptide gave a slight reduction in K_m compared with the parent Y987 peptide (to 240 μM). Because this substitution caused a significant reduction of phosphorylation by the insulin receptor kinase (the Met^{+3} → Thr peptide was the poorest of all substrates tested for that enzyme (7)), this is a point of contrast between the two enzymes with regard to specificity for the YMXM substrates (see below, under "Discussion").

---

[2] S. George and A. Goldberg, unpublished observations.

TABLE I

Phosphorylation of IRS-1 peptides by v-Src

The synthetic peptides are named according to the position of tyrosine in the sequence of IRS-1. YMXM specificity motifs are underlined, and non-native amino acid substitutions within YMXM motifs are in boldface. Experiments were performed at 50 mM Tris, pH 7.4, at 30 °C using the phosphocellulose paper assay. Reactions were carried out at saturating concentrations of ATP, and kinetic constants (± S.E.) were determined as described under "Experimental Procedures."

Peptide	Sequence	K_m	V_{max}	k_{cat}/K_m
		μM	$nmol/min/mg$	$M^{-1}\,min^{-1}$
YMXM motifs from IRS-1				
Y608	KKHTDDGYMPMSPGVA	1,700 ± 260	1.5 ± 0.2	1.1 × 10²
Y628	RKGNGDGYMPMSPKSV	940 ± 170	4.0 ± 0.3	5.0 × 10²
Y658	KKRVDPNGYMMMSPSGS	630 ± 240	1.0 ± 0.2	1.9 × 10²
Y727	KKKLPATGDYMNMSPVGD	220 ± 50	1.0 ± 0.1	4.1 × 10²
Y939	KKGSEEYMNMDLGPGR	1,300 ± 410	1.9 ± 0.3	1.7 × 10²
Y987	KKSRGDYMTMQIG	300 ± 100	6.1 ± 0.7	2.5 × 10³
Phosphorylation site of polyoma middle T				
Middle T	KKKEEEEEEYMPMEDL	97 ± 37	6.1 ± 1.2	7.4 × 10³
Y987 and modified Y987 sequences				
Y987	KKSRGDYMTMQIG	300 ± 100	6.1 ± 0.7	2.5 × 10³
Y987 (Asp⁹⁸⁶ → Asn)	KKSRGNYMTMQIG	Not phosphorylated		
Y987 (Met⁹⁸⁸ → Ile)	KKSRGDYITMQIG	390 ± 150	1.0 ± 0.2	3.0 × 10²
Y987 (Met⁹⁸⁸ → Thr)	KKSRGDYTTMQIG	250 ± 50	2.5 ± 0.2	1.2 × 10³
Y987 (Met⁹⁸⁸ → Nle)	KKSRGDY-Nle-TMQIG	310 ± 80	4.4 ± 0.3	1.7 × 10³
Y987 (Met⁹⁹⁰ → Thr)	KKSRGDYMTTQIG	240 ± 40	1.6 ± 0.2	8.1 × 10²

The peptide substrate based on the YMXM motif from the polyoma virus middle T antigen was the best substrate for v-Src, with the lowest K_m of the group (97 μM) and, together with the Y987 peptide, the highest V_{max} (6.1 nmol/min/mg). The importance of acidic residues N-terminal to the phosphorylated tyrosine in this and other peptides is indicated by the result that the Asp⁹⁸⁶ → Asn analog of the Y987 peptide was inactive ($K_m > 4$ mM) in our phosphorylation assay (Table I).

Phosphorylation of YMXM Substrates by v-Abl—To determine whether recognition of YMXM-containing peptides is a general property of nonreceptor tyrosine kinases, we studied phosphorylation of these peptides by a fusion protein containing the catalytic domain of v-Abl. In this protein, v-*abl* catalytic sequences (residues Pro²²⁹-Leu⁶⁰⁹) are fused to the C terminus of the 26-kDa glutathione S-transferase, allowing purification of the protein under nondenaturing conditions by absorption to glutathione-agarose, followed by elution with excess reduced glutathione (30). Although a portion of the glutathione S-transferase-*abl* fusion protein was isolated in a soluble form, the majority of the protein was lost as a pellet in the clarifying centrifugation step after the bacterial cells were sonicated. This loss might be because of the insolubility of the expressed protein or coaggregation with bacterial membranes. Because of the low yield of soluble fusion protein (≈ 100 µg/liter of cells), we were unable to carry out the thrombin cleavage reaction (30) (to release the *abl* catalytic domain) in sufficient quantities for kinetic analyses. Consequently, we used the intact glutathione S-transferase-*abl* fusion protein to test for phosphorylation of the YMXM peptide substrates. The kinetic properties of the glutathione S-transferase-*abl* fusion protein toward [Val⁵]angiotensin II were $K_m = 3.0$ mM and $V_{max} = 8.0$ nmol/min/mg (data not shown). These measurements are comparable to those measured previously for the entire v-Abl kinase domain expressed in *E. coli* (34) ($K_m = 3.8$ mM, $V_{max} = 9.2$ nmol/min/mg enzyme), suggesting that the specific activity and substrate specificity of the glutathione S-transferase-*abl* fusion protein is similar to that of full-length v-Abl. However, the specific activity was lower than that reported for a fusion protein containing SV40 small t produced in *E. coli* ($K_m = 3.7$ mM, $V_{max} = 1250$ nmol/min/mg) (35).

The YMXM peptides were substrates for the v-Abl fusion protein (Table II). K_m values for these peptide varied widely, from a low of 97 μM (middle T peptide) to a value too high to measure (Tyr⁹⁸⁷, Met⁹⁸⁸ → Thr variant). The catalytic efficiency (k_{cat}/K_m) of v-Abl for several of the YMXM substrates exceeded that of v-Src, and distinctions between the specificities of the two enzymes were apparent. In terms of k_{cat}/K_m, the Y608 and Y658 peptides were the best substrates of the six IRS-1 motifs for v-Abl, whereas the Y987 and Y628 sequences were superior for v-Src (compare Tables I and II). At the Met⁺¹ position, v-Abl, like v-Src, readily accommodated substitutions of Ile or Nle; unlike v-Src, a Thr⁺¹ substitution completely abolished phosphorylation by v-Abl (Tables I and II). At the Met⁺³ position, substitution with Thr increased K_m by a factor of 5.2 (Table II).

DISCUSSION

One common feature of tyrosine kinase substrates is the presence of negatively charged amino acids in positions proximal to the phosphorylated tyrosine (4, 33). The number and spacing of these residues, however, vary from substrate to substrate, making it difficult to define a "consensus sequence" for tyrosine phosphorylation. Furthermore, receptor and nonreceptor tyrosine kinases have overlapping specificities with regard to synthetic peptide substrates containing acidic residues (4, 33), so these studies have not identified clearly defined recognition motifs for the various tyrosine kinases.

The present study was designed to test the efficacy of the YMXM motif, a determinant for phosphorylation for the insulin receptor kinase *in vivo* and *in vitro*, in reactions with nonreceptor tyrosine kinases. Although it is not known whether the YMXM motifs of IRS-1 are phosphorylated by v-Src or v-Abl, the polyoma virus middle T antigen has been shown to be phosphorylated *in vivo* by Src within its YMXM motif. These results raise the possibility that YMXM motifs may serve as general recognition elements for v-Src. Moreover, interleukin 4 treatment of murine FDC myeloid cells results in association of IRS-1 with the phosphatidylinositol 3'-kinase, presumably through the phosphorylation of IRS-1 by an unidentified nonreceptor tyrosine kinase (22).

A baculovirus-based expression system was chosen for these studies. Expression of active v-Src in the baculovirus system

Peptide	Sequence	K_m	V_{max}	k_{cat}/K_m
		μM	$nmol/min/mg$	$M^{-1} min^{-1}$
YMXM motifs from IRS-1				
Y608	KKHTDDGYMPMSPGVA	160 ± 20	5.2 ± 1.8	1.9×10^3
Y628	RKGNGDGYMPMSPKSV	1,670 ± 200	8.7 ± 2.6	3.0×10^2
Y658	KKRVDPNGYMMMSPSGS	190 ± 20	8.8 ± 2.2	2.7×10^3
Y727	KKKLPATGDYMNMSPVGD	2,000 ± 670	10.1 ± 2.5	3.0×10^2
Y939	KKGSEEYMNMDLGPGR	770 ± 100	1.4 ± 0.1	1.2×10^2
Y987	KKSRGDYMTMQIG	520 ± 170	0.9 ± 0.1	1.0×10^2
Phosphorylation site of polyoma middle T				
Middle T	KKKEEEEEEYMPMEDL	97 ± 29	19.9 ± 3.4	1.2×10^4
Y987 and modified Y987 sequences				
Y987	KKSRGDYMTMQIG	520 ± 170	0.9 ± 0.1	1.0×10^2
Y987 (Asp[986] → Asp)	KKSRGNYMTMQIG	Not phosphorylated		
Y987 (Met[988] → Thr)	KKSRGDYTTMQIG	Not phosphorylated		
Y987 (Met[988] → Ile)	KKSRGDYITMQIG	140 ± 10	3.4 ± 0.7	1.4×10^3
Y987 (Met[988] → Nle)	KKSRGDY-Nle-TMQIG	150 ± 30	1.1 ± 0.1	4.7×10^2
Y987 (Met[990] → Thr)	KKSRGDYMTTQIG	2,700 ± 460	3.3 ± 0.2	7.6×10

occurs at a higher level than that reported in transformed cells (36, 37) or in yeast (31). v-Src expressed in Sf9 cells has been shown previously to associate with and phosphorylate Ras GTPase-activating protein *in vivo* and in cell lysates, arguing that normal specificity is preserved in this system (38). The combination of baculovirus expression and immunoaffinity purification used here has also been applied recently to the study of c-Src (39). In both cases the tyrosine kinases are purified in a native and active form in high yield.

Synthetic peptides containing YMXM motifs were phosphorylated by the v-Src and v-Abl tyrosine kinases (Tables I and II). The range of K_m values determined for v-Src was 97 μM-1.7 mM, with the exception of the Tyr[987] (Asp[986] → Asn) peptide, which was not phosphorylated within the detection limits of our assay. Several of the peptides had K_m values < 440 μM, which is the lowest K_m reported previously for an *in vitro* peptide substrate of v-Src (31). (An exception is Raytide, a peptide supplied by Oncogene Science, Inc. with a K_m of 100 μM for v-Src. However, neither the sequence of this peptide nor the conditions used for the K_m determination are supplied by the manufacturer.) In terms of K_m and k_{cat}/K_m, these YMXM-containing peptides are among the best peptide substrates for v-Src.

Importantly, there were differences in the primary sequence preferences within the YMXM substrates between the insulin receptor kinase, v-Src, and v-Abl. In particular, substitutions at the Met[+1] and Met[+3] positions were less detrimental to catalytic efficiency with v-Src than with the insulin receptor kinase. Whereas a Met[+3] → Thr substitution in the Y987 peptide decreased k_{cat}/K_m for the insulin receptor kinase by ≈ 12-fold (7), this substitution had only a modest effect on K_m and V_{max} for v-Src (Table I). At the Met[+1] position of the Y987 peptide, substitutions of Ile, Thr, or Nle had little effect on K_m for v-Src, whereas substitutions of Ile or Nle increased K_m by 3- and 7-fold, respectively, for the insulin receptor kinase (7). The ability of norleucine to replace methionine at the Met[+1] position may indicate that both kinases prefer an unbranched hydrophobic side chain next to the phosphorylable tyrosine (7). Another point of contrast between the two tyrosine kinases is evident from the result with the Tyr[987] (Asp[986] → Asn) peptide. Although this substitution gave a relatively modest (2.6-fold) reduction in k_{cat}/K_m for the insulin receptor, it reduced phosphorylation by v-Src to below detectable limits. Thus, as seen previously for other peptides (4), the presence of acidic residues N-terminal to tyrosine

appears to be an essential component for recognition of YMXM motifs by v-Src.

To test whether these results were generally applicable to the nonreceptor subfamily of tyrosine kinases, the peptides were also used in phosphorylation assays with a v-Abl fusion protein. Several of these peptides were excellent substrates for the enzyme; the best peptide in the series was the middle T peptide ($k_{cat}/K_m = 1.2 \times 10^4$ M^{-1} min^{-1}). Of the YMXM peptides derived from the sequence of IRS-1, the most efficient substrates for v-Abl (in terms of k_{cat}/K_m) were the Y608 and Y658 substrates. In contrast to v-Src and the insulin receptor kinase, the Y608 and Y658 peptides had higher k_{cat}/K_m values than the Y987 peptide (by 19- and 27-fold, respectively). The Y987 peptide, with Thr at the +2 position, is the poorest of the six YMXM peptides for v-Abl. Threonine at any position in the YMXM motif appears to be a negative determinant for phosphorylation by v-Abl. Substitution of Thr for Met[+3] causes an increase in K_m for both v-Abl (5-fold) and the insulin receptor kinase (10.9-fold). Substitution at the Met[+1] position with Thr causes a reduction in catalytic efficiency to below detectable levels, whereas substitutions with Ile or Nle cause an increase in overall catalytic efficiency.

The insulin receptor kinase exhibited much lower K_m values (24-92 μM) and much higher k_{cat}/K_m values (0.6-2.1 × 10^{4} M^{-1} s^{-1}) for this series of peptides than did v-Src or v-Abl. Peptide substrates have generally been phosphorylated more efficiently by receptor tyrosine kinases than by nonreceptor tyrosine kinases (4, 33), perhaps indicating in the latter case that specificity is governed to a larger extent by the three-dimensional structure of the substrate (31, 40) or by recognition elements that lie outside the immediate sequences surrounding tyrosine.

In conclusion, in addition to being substrates for the insulin receptor kinase, YMXM-containing peptides are recognized by the v-Src and v-Abl nonreceptor tyrosine kinases. Although these enzymes share common recognition motifs in the sequence surrounding the tyrosine phosphoacceptor site, their ability to discriminate among divergent peptide sequences is kinase-specific. YMXM sequences, particularly when preceded by acidic amino acids, may constitute a target site for phosphorylation by nonreceptor tyrosine kinases. The observation that phospho-YMXM sequences differ with regard to their SH2 domain binding specificity indicates that selective phosphorylation of YMXM motifs may play a role in signal transduction.

REFERENCES

1. Hunter, T. (1991) *Methods Enzymol.* **200**, 3–37
2. Hanks, S. K., Quinn, A. M., and Hunter, T. (1988) *Science* **241**, 42–52
3. Koch, C. A., Anderson, D., Moran, M. F., Ellis, C., and Pawson, T. (1991) *Science* **252**, 668–674
4. Geahlen, R. L., and Harrison, M. L. (1990) in *Peptides and Protein Phosphorylation* (Kemp, B., ed) pp. 239–253, CRC Press, Boca Raton, FL
5. Sun, X. J., Rothenberg, P., Kahn, C. R., Backer, J. M., Araki, E., Wilden, P. A., Cahill, D. A., Goldstein, B. J., and White, M. F. (1991) *Nature* **352**, 73–77
6. Cantley, L. C., Auger, K. R., Carpenter, C., Duckworth, B., Graziani, A., Kapeller, R., and Soltoff, S. (1991) *Cell* **64**, 281–302
7. Shoelson, S. E., Chatterjee, S., Chaudhuri, M., and White, M. F. (1992) *Proc. Natl. Acad. Sci. U. S. A.* **89**, 2027–2031
8. McGlade, C. J., Ellis, C., Reedijk, M., Anderson, D., Mbamalu, G., Reith, A. D., Panayotou, G., End, P., Bernstein, A., Kazlauskas, A., Waterfield, M. D., and Pawson, T. (1992) *Mol. Cell. Biol.* **12**, 991–997
9. Escobedo, J. A., Kaplan, D. R., Kavanaugh, W. M., Turck, C. W., and Williams, L. T. (1991) *Mol. Cell. Biol.* **11**, 1125–1132
10. Hu, P., Margolis, B., Skolnik, E. Y., Lammers, R., Ullrich, A., and Schlessinger, J. (1992) *Mol. Cell. Biol.* **12**, 981–990
11. Reedijk, M., Liu, X., van der Geer, P., Letwin, K., Waterfield, M. D., Hunter, T., and Pawson, T. (1992) *EMBO J.* **11**, 1365–1372
12. Backer, J. M., Myers, M. G., Jr., Shoelson, S. E., Chin, D. J., Sun, X.-J., Miralpeix, M., Hu, P., Margolis, B., Skolnik, E. Y., Schlessinger, J., and White, M. (1992) *EMBO J.* **11**, 3469–3479
13. Talmage, D. A., Freund, R., Young, A. T., Dahl, J., Dawe, C. J., and Benjamin, T. L. (1989) *Cell* **59**, 55–65
14. Kashishian, A., Kazlauskas, A., and Cooper, J. (1992) *EMBO J.* **11**, 1373–1382
15. Waksman, G., Shoelson, S. E., Pant, N., Cowburn, D., and Kuriyan, J. (1993) *Cell* **72**, 779–790
16. Eck, M. J., Shoelson, S. E., and Harrison, S. C. (1993) *Nature* **362**, 87–91
17. Overduin, M., Rios, C. B., Mayer, B. J., Baltimore, D., and Cowburn, D. (1992) *Cell* **70**, 697–704
18. Booker, G. W., Breeze, A. L., Downing, A. K., Panayotou, G., Gout, I., Waterfield, M. D., and Campbell, I. D. (1992) *Nature* **358**, 684–687
19. Iba, H., Takeya, T. Cross, F. R., Hanafusa, T., and Hanafusa, H. (1984) *Proc. Natl. Acad. Sci. U. S. A.* **81**, 4424–4428
20. Maniatis, T., Fritsch, E. F., and Sambrook, J. (1982) *Molecular Cloning: A Laboratory Manual*, Cold Spring Harbor Laboratory, Cold Spring Harbor, NY
21. Summers, M. D., and Smith, G. E. (1987) *Tex. Agric. Exp. St. Bull.* **1555**, 1–56
22. Wang, L.-M., Keegan, A. D., Li, W., Lienhard, G. E., Pacini, S., Gutkind, J. S., Myers, M. G., Jr., Sun, X.-J., White, M. F., Aaronson, S. A., Paul, W. E., and Pierce, J. H. (1993) *Proc. Natl. Acad. Sci. U. S. A.* **90**, 4032–4036
23. Barnard, J. P., Summers, M. D., and Smith, G. E. (1980) *Virology* **101**, 286–290
24. Carstens, E. B., Sian, T. T., and Doerfler, W. (1980) *Virology* **101**, 311–314
25. Laemmli, U. K. (1970) *Nature* **227**, 680–685
26. Casnellie, J. E. (1991) *Methods Enzymol.* **200**, 115–120
27. Wong, T. W., and Goldberg, A. (1983) *J. Biol. Chem.* **258**, 1022–1025
28. Lipsich, L. A., Lewis, A. J., and Brugge, J. S. (1983) *J. Virol.* **48**, 352–360
29. Harlow, E., and Lane, D. (1988) *Antibodies: A Laboratory Manual*, pp. 302–305, Cold Spring Harbor Laboratory, Cold Spring Harbor, NY
30. Smith, D. B., and Johnson, K. S. (1988) *Gene (Amst.)* **67**, 31–40
31. Radziejewski, C., Miller, W. T., Mobashery, S., Goldberg, A. R., and Kaiser, E. T. (1989) *Biochemistry* **28**, 9047–9052
32. Courtneidge, S. A., and Smith, A. E. (1983) *Nature* **303**, 435–439
33. Kemp, B. E., and Pearson, R. B. (1991) *Methods Enzymol.* **200**, 121–134
34. Ferguson, B., Pritchard, M. L., Feild, J., Rieman, D., Greig, R. G., Poste, G., and Rosenberg, M. (1985) *J. Biol. Chem.* **260**, 3652–3657
35. Foulkes, J. G., Chow, M., Gorka, C., Frackelton, A. R., Jr., and Baltimore, D. (1985) *J. Biol. Chem.* **260**, 8070–8077
36. Erikson, R. L., Collet, M. S., Erikson, E., and Purchio, A. F. (1979) *Proc. Natl. Acad. Sci. U. S. A.* **76**, 6260–6264
37. Levinson, A. D., Opperman, H., Varmus, H. E., and Bishop, J. M. (1980) *J. Biol. Chem.* **255**, 11973–11980
38. Park, S., Marshall, M. S., Gibbs, J. B., and Jove, R. (1992) *J. Biol. Chem.* **267**, 11612–11618
39. Morgan, D. O., Kaplan, J. M., Bishop, J. M., and Varmus, H. E. (1991) *Methods Enzymol.* **200**, 645–660
40. Tinker, D. A., Krebs, E. G., Feltham, I. C., Attah-Poku, S. K., and Ananthanarayan, V. S. (1988) *J. Biol. Chem.* **263**, 5024–5026

Common *in Vitro* Substrate Specificity and Differential Src Homology 2 Domain Accessibility Displayed by Two Members of the Src Family of Protein-tyrosine Kinases, c-Src and Hck*

Robert J. Sicilia‡, Margaret L. Hibbs§¶, Paul A. Bello§‖, Jeffrey D. Bjorge**, Donald J. Fujita**‡‡, Irene J. Stanley‡, Ashley R. Dunn§, and Heung-Chin Cheng‡§§

*From the ‡Department of Biochemistry and Molecular Biology, University of Melbourne, Parkville, Victoria 3052, Australia, the §Ludwig Institute for Cancer Research, Melbourne Tumour Biology Branch, P. O. Royal Melbourne Hospital, Victoria 3050, Australia, and the **Department of Medical Biochemistry, University of Calgary, Calgary, Alberta T2N 4N1, Canada*

Hck and Src are members of the Src family of protein-tyrosine kinases that carry out distinct and overlapping functions *in vivo* (Lowell, C. A., Niwa, M., Soriano, P., and Varmus, H. E. (1996) *Blood* 87, 1780–1792). In an attempt to understand how Hck and Src can function both independently and in concert, we have compared 1) their *in vitro* substrate specificity and 2) the accessibility of their Src homology 2 (SH2) domain. Using several synthetic peptides, we have demonstrated that Hck and Src recognize similar structural features in the substrate peptides, suggesting that both kinases have the intrinsic ability to carry out overlapping cellular functions by phosphorylating similar cellular proteins *in vivo*. Using a phosphotyrosine-containing peptide that has previously been shown to bind the SH2 domain of Src family kinases with high affinity, we found that although Src could bind to the phosphopeptide, Hck showed no interaction. The inability of Hck to bind the phosphopeptide was not a result of a stable intramolecular interaction between its SH2 domain and C-terminal regulatory phosphotyrosine residue (Tyr-520), as most Hck molecules in the purified Hck preparation were not tyrosine-phosphorylated. In contrast to intact Hck, a recombinant truncation analog of Hck was able to bind the phosphopeptide with an affinity similar to that of the Src SH2 domain, suggesting that conformational constraints are imposed on intact Hck that limit accessibility of its SH2 domain to the phosphopeptide. Furthermore, the difference in SH2 domain accessibility is a potential mechanism that enables Src and Hck to perform their respective unique functions by 1) targeting them to different subcellular compartments, whereupon they phosphorylate different cellular proteins, and/or 2) facilitating direct binding to their cellular substrates.

The Src family of protein-tyrosine kinases, Src, Yes, Lck, Fyn, Lyn, Fgr, Hck, Blk, and Yrk, are nonreceptor tyrosine kinases, a number of which have been shown to be involved in a wide variety of cellular processes, ranging from cell growth and proliferation to neural functions (see Ref. 1 for review). With the exception of a 40–70 residue unique domain, all Src family kinases are highly homologous in structure. The homologous domains include (i) the fatty acid acylation domain, which targets the kinases to the plasma membrane, (ii) the Src homology 2 (SH2)[1] and Src homology 3 (SH3) domains, which facilitate protein-protein interactions, (iii) the kinase domain, and (iv) the C-terminal regulatory domain. A consensus tyrosine residue in the kinase domain can readily undergo autophosphorylation; autophosphorylation of this tyrosine results in autoactivation of the kinase (see ref. 1 for review). In contrast, phosphorylation of a tyrosine in the C-terminal regulatory domain renders the kinase inactive. C-terminal Src kinase (CSK) and/or CSK-related kinases are responsible for phosphorylating the C-terminal regulatory tyrosine. The crystal structures of inactivated Hck and Src reveal that intramolecular interaction between the phosphorylated C-terminal regulatory tyrosine and the SH2 domain contributes to inactivation of the kinases (2, 3).

In addition to stabilizing the inactive conformation of the kinases, the SH2 domain mediates interactions of the Src family kinases with other cellular proteins. The SH2 domain binds to a phosphotyrosine-containing motif in cellular proteins, whereas the SH3 domain binds to proline-rich sequences. Through interactions with other cellular proteins, the kinases can be targeted to specific subcellular compartments, where they have immediate access to their substrate proteins (see Ref. 4 for review). Furthermore, the SH2 and SH3 domains have been shown to mediate binding of Src to some of its substrates, *e.g.* p130^{cas}, Sin, and the focal adhesion kinase (5, 6). For this reason, the accessibility or specificity of the SH2 and SH3 domains of a Src family kinase can influence the subcellular localization of the kinase and hence the subset of cellular proteins available for phosphorylation by the kinase, as well as the direct recognition of substrate proteins.

Sequences of phosphopeptides capable of high affinity binding to the SH2 domain of Src family kinases have been identified using a degenerate combinatorial phosphopeptide library (7). The local structure around Tyr-315 of the hamster polyoma virus middle T antigen was found to contain the pYEEI motif,

[1] The abbreviations used are: PAGE, polyacrylamide gel electrophoresis; SH2, Src homology 2; CSK, C-terminal Src kinase; GST, glutathione *S*-transferase; mAb, monoclonal antibody.

which was shown by combinatorial library studies to be preferred by the SH2 domain of Src family kinases (7). Further studies showed that the synthetic middle T antigen phosphopeptide containing the pYEEI motif (pYEEI peptide) can bind the Src family kinase SH2 domain with high affinity (7, 8).

Previous studies by us (9) and other investigators (10) have shown that the local structures flanking the target tyrosine in substrate proteins and peptides contain structural features recognized by the kinase domain of several Src family members. Thus, short synthetic peptides are useful tools for analyzing the *in vitro* substrate specificities of Src family kinases.

Targeted disruption of the *src* and/or *hck* gene in mice indicates that the two kinases carry out specific and overlapping functions in several cell types, including osteoclasts and macrophages (11–13). In an attempt to elucidate the structural basis accounting for the functional specificity and redundancy of Src and Hck, we have used biochemical approaches to compare their *in vitro* substrate specificity and SH2 domain accessibility. Our results reveal that the kinase domains of both Src and Hck recognize similar structural features in substrate peptides, indicating that both kinases have the potential to carry out overlapping functions by phosphorylating similar cellular proteins. We have also shown that the SH2 domain in intact Src is readily accessible to the pYEEI phosphopeptide, whereas it is inaccessible in intact Hck, supporting the notion that SH2 domain accessibility of the two kinases is regulated by different mechanisms. Because SH2 domain accessibility is one of the factors determining subcellular localizations of the kinases, the different accessibility of the Src and Hck SH2 domains may target them to different subcellular localizations, whereupon they phosphorylate different subsets of cellular proteins, which may contribute in part to the differences in their different cellular functions.

EXPERIMENTAL PROCEDURES

Materials—The Sephadex G25 Fine gel filtration matrix, the FPLC Mono-Q (HR5/5) column, and the Mono-S (HR5/5) column were purchased from Amersham Pharmacia Biotech. Hydroxylapatite and Affi-Gel-15 were from Bio-Rad. The preparative reverse-phase Econosil C_{18} high performance liquid chromatography column was from Alltech (Deerfield, IL), and the analytical Vydac reverse-phase C_{18} high performance liquid chromatography column was from Separation group Inc. Immobilon polyvinylidene fluoride membranes were from Millipore (Bedford, MA). The ECL reagents were from Amersham Pharmacia Biotech. The horseradish peroxidase-linked sheep anti-rabbit IgG and the alkaline phosphatase-linked anti-rabbit IgG were from Silenus Laboratory (Hawthorn, Victoria, Australia). The polyclonal α-hck antibody H1077 was a kind gift of Dr. C. Lowell (University of California, San Francisco, CA) (11). Hybridoma cells producing the monoclonal Src antibody mAb327 were kindly provided by Dr. J. Brugge (20). The monoclonal antiphosphotyrosine antibody (pY69) was purchased from ICN Pharmaceuticals Inc. (Costa Mesa, CA). The polyclonal anti-phosphotyrosine antibody was from Upstate Biotechnology Inc. Recombinant Src was expressed and purified as described by Bjorge *et al.* (20). Less than 5% of purified Src was tyrosine-phosphorylated (20). The recombinant CSK was purified from *Spodoptera frugiperda 9* (Sf9) cells infected with the recombinant baculovirus containing the csk gene, kindly provided by Dr. D. O. Morgan (20).

Construction of the hck Baculovirus Vector and Generation of the Recombinant hck Baculovirus—The full-length *hck* cDNA (21) was subcloned into the *Nhe*I site in pBlueBac II (Invitrogen Corporation, San Diego, CA). Sf9 insect cells (Invitrogen) were co-transfected with wild-type baculoviral DNA and pBB2hck by standard calcium phosphate transfection procedures (22). Recombinant *hck* baculovirus was purified following three rounds of plaque purification by visual screening. The titer of the recombinant *hck* baculovirus was determined, and Western blotting using an anti-*hck* antiserum (12) was used to optimize protein production following infection.

Purification of Hck from Crude Cell Lysates of Sf9 Cells Infected with Recombinant Hck Baculovirus—A large scale (2-liter) culture of Sf9 cells was infected with recombinant Hck baculovirus at a multiplicity of infection of 1.0, and cells were harvested 3 days after infection for
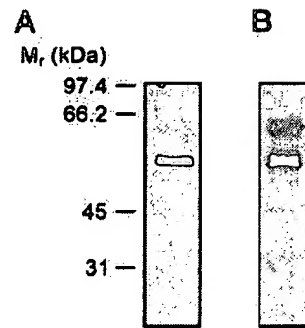
FIG. 1. **Analysis of the purity of the recombinant Hck preparation.** Recombinant Hck from baculovirus-infected Sf9 cells was purified by chromatography on an hydroxylapatite column followed by a Sephacryl-200 gel filtration column. *A*, immunoblot analysis of the purified Hck preparation. *B*, Coomassie Blue-stained SDS gel showing the purity of the final Hck preparation. The SDS-PAGE and immunoblot analyses reveal that the 56- and 59-kDa isoforms are the predominant proteins in the final Hck preparation.

protein purification. All of the extraction and purification procedures were carried out at 4 °C. Cells were pelleted at 1000 × *g* for 5 min, washed once with Grace's serum-free medium, and homogenized in a buffer consisting of 25 mM Hepes, pH 7.0, 5% Nonidet P-40, 1 mM EDTA, 0.1 mg/ml soybean trypsin inhibitor, 0.2 mg/ml benzamidine, 0.1 mg/ml phenymethylsulfonyl fluoride, and 1 mM dithiothreitol. The homogenate was clarified by centrifugation at 100,000 × *g* for 40 min. Recombinant Hck was purified by sequential column chromatography on a Q-Sepharose (Amersham Pharmacia Biotech) anion exchange column and a hydroxylapatite column, followed by a Sephacryl-200 gel filtration column. At pH 7.0, the majority (>95%) of the recombinant Hck was eluted from the Q-Sepharose column when the column was washed with the column buffer. For hydroxylapatite column chromatography, the wash fraction from the Q-Sepharose column was loaded onto the column (length × internal diameter = 80 × 22 mm) pre-equilibrated with column buffer consisting of 25 mM Hepes, pH 7.0, 0.1% Nonidet P-40, 10% glycerol, 0.2 mg/ml benzamidine, 0.1 mg/ml phenylmethylsulfonyl fluoride, and 1 mM dithiothreitol. After the column was washed, bound proteins were eluted with a 200-ml linear gradient of 0–0.3 M potassium phosphate in column buffer (pH 7.0). Hck was monitored by both the protein-tyrosine kinase activity assay using [Lys-19]cdc2(6–20) peptide as the substrate and α-*hck* immunoreactivity. The peak activity fractions from the hydroxylapatite column were pooled, concentrated to 10 ml with an Amicon concentration cell, and then loaded onto a Sephacryl 200 gel filtration column (length × internal diameter = 760 × 22 mm) pre-equilibrated with 0.2 M NaCl in column buffer. The peak Hck activity and immunoreactivity in the eluted column fractions were determined. SDS-PAGE revealed that the 56- and 59-kDa isoforms of Hck are the major proteins in the final preparation after S-200 column chromatography (Fig. 1).

Construction of the Vectors for the Expression of GST-Hck(1–247) and GST-Hck(1–129)—Two polymerase chain reaction products were generated: (i) a 751-base pair DNA fragment encoding residues 1–247 of the 59-kDa isoform of murine Hck (21) was amplified using the full-length *hck* cDNA as a template with primer 1 (5'-G*GAATT*CCTGGGGGGTCGGTCTAGCTGC) and primer 2 (5'-ATC*GAAGCTT*TCATTTCTCCCATGGCTTCTG), and (ii) a 405-base pair DNA fragment encoding residues 1–129 was amplified from the same template with primer 1 and primer 3 (5'- ATC*GAAGCTT*TCAAGCCACATAGTTGCTTGG). In the primer sequences, the restriction sites for *Eco*RI and *Hind*III are in boldface italic and the in-frame stop codons are underlined.

The polymerase chain reactions were carried out in a volume of 100 μl containing 50 ng of template DNA, 67 mM Tris-HCl (pH 8.8 at 25 °C), 16.6 mM $(NH_4)_2SO_4$, 0.45% Triton X-100, 0.2 mg/ml gelatin, 2.5 units of a 16:1 (v/v) mixture of *Taq* polymerase (Biotech) and r*Pfu* polymerase (Stratagene), 2 mM $MgCl_2$, 100 μM dNTPs, and 0.2 μM of each primer. The amplification was performed in a Perkin-Elmer 9600 cycler and consisted of one cycle at 95 °C for 2 min; 25 cycles of 1 min at 94 °C, 1 min at 60 °C, and 1 min at 72 °C; and a final cycle of 7 min at 72 °C.

Site-directed mutagenesis was used to modify the *Escherichia coli* expression vector pGEX2T (AMRAD, Melbourne, Australia). The *Sma*I site in pGEX2T was mutated to a *Hind*III site to allow subcloning of the polymerase chain reaction products. The polymerase chain reaction products from steps (i) and (ii) were digested with *Eco*RI and *Hind*III, purified on a 1% low melting temperature agarose gel (SeaPlaque, FMC

BioProducts, Rockland, ME) and then directionally subcloned into the modified expression vector pGEX2TH to give (i) pGXHck(1–247) and (ii) pGXHck(1–129). Upon expression, GST-Hck(1–247), consisting of the unique, SH3, and SH2 domains, and GST-Hck(1–129), consisting of the unique and SH3 domains of Hck, were obtained.

Purification of the GST Fusion Proteins of Hck Fragments—Both GST-Hck(1–247) and GST-Hck(1–129) bound strongly to glutathione-agarose and could not be released using the high salt/high glutathione buffer (25 mM Hepes, pH 7.0, 0.1% Nonidet P-40, 1 mM EDTA, 50 mM glutathione, 2 M NaCl) (data not shown). For this reason, GST-Hck(1–247) and GST-Hck(1–129) were purified by two sequential steps on a hydroxylapatite column (length × internal diameter = 90 × 12 mm) and an FPLC Mono-S cation exchange column (HR 5/5). The crude cell lysate was loaded onto the hydroxylapatite column pre-equilibrated with Buffer A (25 mM Hepes, pH 7.0, 1 mM EDTA, 1 mM dithiothreitol, 10% glycerol, 0.1% Nonidet P-40, 0.02 mg/ml phenylmethylsulfonyl fluoride, and 0.2 mg/ml benzamidine). After the column was washed with 20 ml of Buffer A, bound proteins were eluted with a 90-ml linear gradient of 0–0.3 M potassium phosphate in Buffer A at a flow rate of 1 ml/min. Peak protein fractions were identified by SDS-PAGE and immunoblot analysis using α-hck (H1077) antibody. The immunoreactive fractions were pooled, dialyzed overnight in 2 liters of Buffer A, and then loaded onto a Mono-S column pre-equilibrated with Buffer A. After being washed with 5 ml of Buffer A, bound proteins were eluted using a 15-ml linear gradient of 0–0.5 M NaCl in Buffer A at a flow rate of 0.5 ml/min. Fractions containing the recombinant proteins were identified using SDS-PAGE and immunoblot analysis.

Although the theoretical molecular mass of GST-Hck(1–247) is ~53 kDa, its mobility on the SDS gel is similar to that of a 55–56-kDa protein (see Fig. 5). The structural basis for its anomalous mobility on SDS gel is not known.

Construction of the GST Fusion Vector and Purification of the GST Fusion Protein of Src(1–258)—Bluescript plasmid (Stratagene) containing the full-length coding region of human Src (20) was digested with NcoI and EcoN1 and then treated with Klenow to create blunt ends. The DNA fragment of 775 nucleotides encoding residues 1–258 of Src was isolated on an agarose gel and ligated into the SmaI site of pGEX-2T vector (Amersham Pharmacia Biotech). The expected orientation and sequence of the resulting expression plasmid was confirmed by restriction enzyme digest and DNA sequencing.

Upon expression, GST-Src(1–258), consisting of the unique, SH3, and SH2 domains of Src, was purified by two sequential steps on a hydroxylapatite column and an FPLC Mono-S cation exchange column under the same conditions as for the purification of GST-Hck(1–247) and GST-Hck(1–129).

Preparation of Synthetic Peptides—Synthetic peptides were synthesized with an Applied Biosystems Model A431 automated peptide synthesizer using N-(9-fluorenyl)methoxycarbonyl-based chemistry. Peptides synthesized included (i) phosphopeptide (pYEEI peptide) derived from the sequence of the hamster polyoma virus middle T antigen THQEEEEPQ(pY)EEIPIYL, and (ii) the substrate peptides. The synthesis and purification of these peptides have been detailed in previous reports (9, 10).

Preparation and Characterization of pYEEI Peptide Immobilized to a Solid Support—Purified pYEEI peptide was covalently coupled to Affi-Gel-15 agarose following the procedures detailed by the manufacturer (Bio-Rad). The degree of coupling of the peptide to Affi-Gel was determined; a coupling density of 3.04 μmol of pYEEI peptide per ml of packed gel was revealed. The immobilized pYEEI peptide (pYEEI-gel) was diluted with the ethanolamine-treated Affi-Gel-15 agarose (control gel) before use.

SH2 Domain Accessibility Assay—The ability of Src, Hck, and the GST fusion proteins GST-Src(1–258), GST-Hck(1–129), and GST-Hck(1–247) to bind pYEEI peptide was assayed by incubating 280 ng of protein at 4 °C for 1 h with 20 μl (equivalent to 0.79 nmol of the immobilized pYEEI peptide) of pYEEI-gel equilibrated in the binding buffer (25 mM Hepes, 1 mM EDTA, 0.2 mg/ml benzamidine, 10% glycerol, 0.1% Nonidet P-40, 0.2 M NaCl, and 1 mM β-mercaptoethanol). The mixture was centrifuged at 10,000 × g for 5 min, and the supernatant containing the unbound enzyme was removed and stored for analysis. The pYEEI-gel was washed with 5 × 1 ml of binding buffer, and the bound proteins were eluted by boiling in 20 μl of SDS-PAGE sample buffer. Bound and unbound proteins were quantified after SDS-PAGE by the procedures described under "Immunoblot Analysis."

Immunoblot Analysis—Immunoblot analysis was performed according to the method of Towbin et al. (23). Briefly, proteins were separated by SDS-PAGE and then transferred to a polyvinylidene difluoride membrane filter. The filter was probed with primary antibody (either α-hck
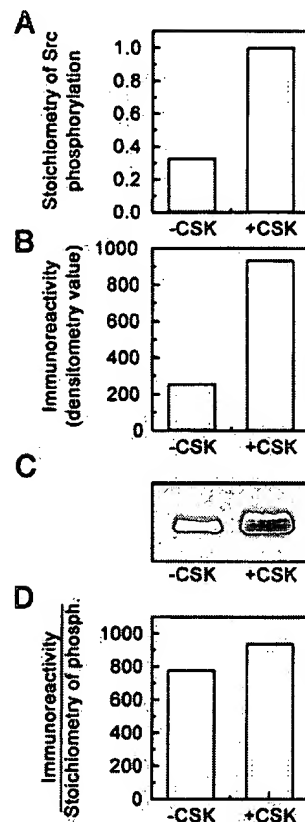

FIG. 2. **Comparison of the immunoreactivity of PY69 monoclonal anti-phosphotyrosine antibody against the autophosphorylation site and the C-terminal regulatory phosphotyrosine of Src.** Src phosphorylated in the presence and absence of CSK (+CSK and −CSK, respectively) was analyzed for stoichiometry of phosphorylation (A) and immunoreactivity with the PY69 antibody (B). The immunoreactivity of the PY69 antibody against the two phosphorylated forms of Src was determined by densitometric scan of the immunoblot shown in C. The ratio of the immunoreactivity and the stoichiometry of phosphorylation is a measure of the relative immunoreactivity of PY69 antibody against pY-419 (−CSK) and pY-530 (+CSK) (D).

polyclonal antibody, the polyclonal anti-phosphotyrosine antibody, α-Src monoclonal antibody (M327), or α-phosphotyrosine (PY69) monoclonal antibody) followed by horseradish peroxidase-conjugated sheep anti-rabbit IgG (for α-hck polyclonal antibody and the polyclonal antiphosphotyrosine antibody) or the horseradish peroxidase-conjugated sheep anti-mouse IgG (for α-Src (M327) and α-phosphotyrosine (PY69) antibodies) and developed using the enhanced chemiluminescence kit following the protocol detailed by the manufacturer. The relative amounts of Src, Hck, GST-Src(1–258), GST-Hck(1–247), and GST-Hck(1–129) were determined by densitometry.

Phosphopeptide Mapping of Autophosphorylated and CSK-phosphorylated Src—Src (18.8 nM) was autophosphorylated by incubation for 10 min at 30 °C in kinase buffer containing 50 μM [γ-^{32}P]ATP in a 16-μl volume. In another reaction, Src was phosphorylated by CSK upon incubation of Src with 188 nM CSK under the same conditions for 30 min (Fig. 2A). The reactions were terminated by addition of 10 μl of 5× SDS sample buffer (26). Phosphorylated Src was separated from CSK and free [γ-^{32}P]ATP by SDS-PAGE. The proteins on the gel were then electrotransferred to nitrocellulose, and the phosphorylated Src was located by autoradiography.

Prior to proteolytic digestion, the nitrocellulose strips corresponding to the phosphorylated Src were excised and processed as described previously (27). For tryptic digestion, the nitrocellulose strips were incubated with 18 μg of TPCK-treated trypsin (Worthington) in 180 μl of 100 mM NH₄HCO₃ (pH 7.9)/acetonitrile (95:5, v/v) at 37 °C for 15 h. After digestion, the supernatant was removed and saved; the nitrocellulose strips were rinsed with 2 × 100 μl of Milli-Q H₂O. The supernatant and the rinse were pooled and lyophilized to dryness. The dry sample was resuspended with 400 μl of Milli-Q H₂O and relyophilized. Finally, the dry samples were resuspended in 10 μl of Milli-Q H₂O

FIG. 3. **Two-dimensional phosphopeptide mapping of the autophosphorylated (−CSK) and CSK-phosphorylated (+CSK) Src.** *A*, phosphopeptide map of the tryptic digest of the autophosphorylated Src. *B*, phosphopeptide map of the tryptic digest of Src inactivated by CSK phosphorylation. *C*, phosphopeptide map of the CSK-phosphorylated Src digested sequentially with trypsin and then chymotrypsin. The polarity of electrophoresis and the orientations of thin layer electrophoresis (TLE) and TLC are shown.
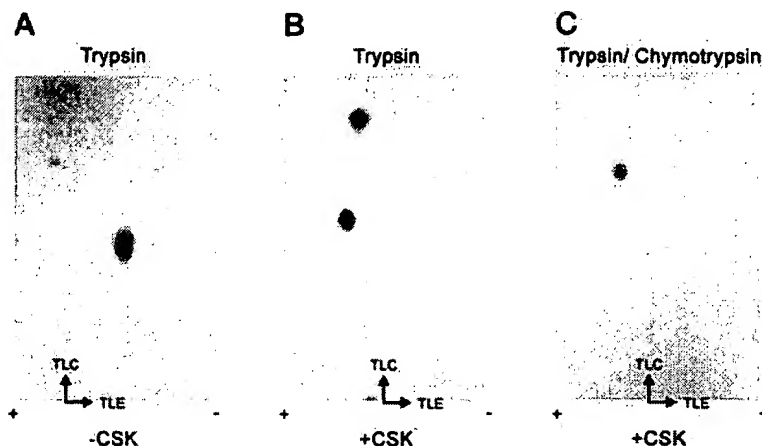
before they were applied onto TLC plates. Separation of the proteolytic fragments was accomplished by (i) thin layer electrophoresis in the first dimension and (ii) TLC in the second dimension, as described previously (24). The radioactive spots on the TLC plates were located by autoradiography. As shown in Fig. 3*A*, the autophosphorylated Src gave a single radioactive tryptic fragment. The fragment is migrating to a location similar to that previously found for the consensus autophosphorylation site of the Src family kinases (Tyr-419 of human Src) (24). Tryptic digestion of the CSK-phosphorylated Src, however, gave at least two radioactive fragments, as indicated by the two spots in Fig. 3*B*). The two fragments were very likely a result of the incomplete tryptic cleavage of the Arg-509-Pro-510 bond close to the C-terminal regulatory domain of Src (25, 28). To further prove that the two radioactive fragments in Fig. 3*B* are derived from the same phosphorylation site, the tryptic digest of CSK-phosphorylated Src was further digested by chymotrypsin overnight under the following conditions: trypsin in the tryptic digest of CSK-phosphorylated Src was inactivated by heating the digest at 100 °C for 10 min. The heat-treated sample was then digested with chymotrypsin (18 μg) in 180 μl of 100 mM NH₄HCO₃ (pH 7.9) at 30 °C for 15 h. After repeated resuspension of the sample in H₂O and lyophilization to remove the NH₄HCO₃, the sample was analyzed by the two-dimensional thin layer electrophoresis-TLC phosphopeptide mapping procedures. As shown in Fig. 3*C*, the tryptic/chymotryptic digest of CSK-phosphorylated Src gave only one major radioactive spot in the map, suggesting that the two radioactive tryptic phosphopeptide fragments were derived from a single phosphorylation site. Thus, the data strongly suggest that Src was autophosphorylated exclusively at Tyr-419, whereas Tyr-530 is the predominant phosphorylation site in CSK-phosphorylated Src.

Characterization of the Immunoreactivity of the Monoclonal (PY69) and the Polyclonal Anti-phosphotyrosine Antibodies against Phosphotyrosines in Different Sequence Contexts—The PY69 anti-phosphotyrosine antibody may bind to phosphotyrosine sequence contexts with differing affinities; therefore, we examined its immunoreactivity against the autophosphorylation site (Tyr-419) and the phosphorylated C-terminal regulatory tyrosine (Tyr-530) of Src. Src was chosen instead of Hck because Hck is a much poorer *in vitro* substrate of CSK (data not shown). In addition, we were unable to obtain enough Hck phosphorylated exclusively at the C-terminal regulatory tyrosine for analysis.

Src was first incubated with ATP in assay buffer in both the presence and the absence of CSK. Under the conditions we used, Src was autophosphorylated at Tyr-419 to a stoichiometry of 0.3 mol PO₃⁻ per mol of enzyme (−CSK) or phosphorylated by CSK at Tyr-530 exclusively to a stoichiometry of 1 mol PO₃⁻ per mol of enzyme (+CSK) (Figs. 2*A* and 3). As expected, the kinase activity of Src was significantly suppressed when it was phosphorylated at Tyr-530, because its activity was less than 15% of that of the autophosphorylated Src (data not shown).

Both autophosphorylated Src and CSK-phosphorylated Src cross-reacted with the PY69 anti-phosphotyrosine antibody (Fig. 2, *B* and *C*). The ratio of immunoreactivity (as measured by densitometry and expressed in instrument units of density) to stoichiometry of Src autophosphorylated at Tyr-416 (250/0.32 = 781) and that of Src phosphorylated at Tyr-530 (920/0.98 = 938) revealed no significant difference in the immunoreactivities of PY69 antibody against the two phosphorylation sites (Fig. 2*D*). Because the sequences around the autophosphorylation site in the kinase domain of Src (Tyr-416) and Hck (Tyr-409)

are identical and the sequences around the C-terminal regulatory tyrosine of Src (Tyr-530) and Hck (Tyr-520) are highly homologous (25), it is likely that the PY69 antibody would display similar immunoreactivities against the phosphorylated Tyr-409 and Tyr-520 of Hck.

The polyclonal anti-phosphotyrosine antibody (Upstate Biotechnology) was also used to analyze the phosphorylation level of Hck. According to the manufacturer's specifications, this antibody was raised against three immunogens, including phosphotyrosine, phosphorylated synthetic peptides derived from the autophosphorylation site, and the C-terminal regulatory phosphorylation site of Src conjugated to a carrier protein. Immunological analysis reveals that the antibody can recognize phosphotyrosine in different sequence contexts. Thus, the polyclonal anti-phosphotyrosine antibody was expected to recognize the phosphorylated form of both Tyr-409 and Tyr-520 of Hck.

Protein Kinase Assay—The protein-tyrosine kinase activity of Hck in hydroxylapatite and S-200 gel filtration column fractions was determined by measuring incorporation of PO₃⁻ from [γ-³²P]ATP into [Lys-19]cdc2(6–20). Routine enzyme assays were carried out at 30 °C in a 50-μl volume of kinase buffer (20 mM Tris-HCl, pH 7, 10 mM MgCl₂, 1 mM MnCl₂, 83 μM Na₃VO₄) with 100 μM ATP (specific radioactivity, 300–400 cpm/pmol) and 300 μM [Lys-19]cdc(6–20). The reactions were allowed to proceed for 6–15 min before they were terminated by the addition of 20 μl of 50% acetic acid. A 30-μl aliquot was spotted onto a phosphocellulose paper square, which was subsequently washed six times in 0.3% H₃PO₄, washed once with acetone, and then dried. Radioactivity in the dried paper square was monitored by Cerenkov counting. Under the conditions used, only the initial rates of phosphorylation of the peptides by the kinases were measured.

For kinetic analyses, Src and Hck were autophosphorylated to a stoichiometry of approximately 1 mol of PO₃⁻ per mol of kinase prior to the routine kinase activity assay. For the autophosphorylation reaction, Src (100 nM) or Hck (152 nM) was incubated with 100 μM ATP and the kinase buffer in a final volume of 50 μl for 60 min at 30 °C. An aliquot of the autophosphorylation reaction mixture containing 0.3–1.02 pmol of Hck or 0.2 pmol of Src was then taken out to determine kinase activity. The kinase activity assays were carried out at 30 °C in a 50-μl volume containing the kinase buffer, 50 μM ATP (specific radioactivity, 300–400 cpm/pmol), 6–20.3 nM Hck, or 4 nM Src and varying concentration of substrate peptides. The reactions were allowed to proceed for 20–40 min before they were terminated by the addition of 20 μl of 50% acetic acid. A 30-μl aliquot was spotted onto a phosphocellulose paper square, which was subsequently processed as described in the first paragraph of this section.

The ability of CSK to inactivate Src by phosphorylating its C-terminal regulatory tyrosine was assayed by comparing the kinase activity of the autophosphorylated Src and the CSK-phosphorylated Src. The methodology has been described in detail in our previous studies (20, 25).

RESULTS

Comparison of the in Vitro Peptide Substrate Specificity of Hck and Src—Because little is known about the identities of the cellular proteins phosphorylated by Src and Hck *in vivo*, we compared the *in vitro* substrate specificities of the two kinases using a series of short synthetic substrate peptides. The ration-

TABLE I
Kinetic parameters of phosphorylation of peptide substrates by c-Src and Hck

The unit of V_{max} is μmol of PO_3-incorporated/min/mg of enzyme. The target tyrosine residue is marked by an asterisk. The substituted amino acid residues in the analogs of cdc2(6–20) peptide and src-optima peptide are underlined.

Peptide substrate	Sequence	c-Src			Hck		
		K_m	V_{max}	V_{max}/K_m	K_m	V_{max}	V_{max}/K_m
		mM			*mM*		
Src-autophosphorylation site peptide	★ ADFGLARLIEDNEYTARG	1.67	0.25	0.15	0.45	0.06	0.13
Src-optimal peptide	★ AEEEIYGEFEAKKKK	0.033	2.3	69.1	0.14	7.5	53.6
[Ala-5,Ala-9] Src-optimal peptide	★ AEEEAYGEAEAKKKK	0.77	0.08	0.11	1.0	0.25	0.25
Abl-optimal peptide	★ AEVIYAAPFAKKKK	0.45	0.6	1.32	0.41	0.6	1.47
cdc2(6–20)	★ KVEKIGEGTYGVVYK	0.25	1.67	6.68	0.17	1.8	10.6
[Lys-19]cdc2(6–20)	★ KVEKIGEGTYGVVKK	0.25	1.25	5.0	0.25	1.25	5.0
[Val-12,Ser-14,Lys-19]cdc2(6–20)	★ KVEKIGVGSYGVVKK	2.5	0.42	0.168	1.1	0.11	0.1

ale behind our choice of peptides was as follows. The Src autophosphorylation site peptide is derived from the autophosphorylation site in the Src kinase domain and is known to be an *in vitro* substrate of the Src family kinases. The cdc2(6–20) peptide has previously been shown to be a specific substrate of several Src family kinases, including Src, Lyn, Lck, and Fyn (9). [Lys-19]cdc2(6–20) and [Val-12,Ser-14,Lys-19]cdc2(6–20), which are substitution analogs of cdc2(6–20), have been used to define the substrate specificity determinants of Src family kinases. We have previously demonstrated that replacement of Glu-12 and Thr-14 in cdc2(6–20) by valine and serine, respectively, adversely affects the ability of Src to phosphorylate the peptide analogs, whereas replacement of Tyr-19 by lysine had no detrimental effect (9). The Src-optimal peptide and abl-optimal peptide were discovered by Songyang *et al.* (10) and shown to carry all the essential structural determinants for efficient phosphorylation by Src and Abl tyrosine kinase. The peptide library study by Songyang *et al.* (10) also revealed that the hydrophobic Ile-5 and Phe-9 at the pY-1 and pY+3 positions in the Src-optimal peptide are the two most crucial structural determinants recognized by Src. We therefore prepared the analog [Ala-5,Ala-9]Src-optimal peptide with the two critical hydrophobic residues replaced by the less hydrophobic alanine residue and examined the effect of the substitution on the efficiency of phosphorylation of the peptide by both kinases.

Of the peptides used, [Val-12,Ser-14,Lys-19]cdc2(6–20), [Ala-5,Ala-9]Src-optimal peptide, and Src autophosphorylation site peptides were very poor substrates (Table I). [Lys-19]cdc2(6–20) and cdc2(6–20), however, were phosphorylated by the kinases with catalytic efficiencies (V_{max}/K_m) 30–50-fold higher than that of Src autophosphorylation site peptide. Similar to Src, Hck phosphorylated the abl-optimal peptide with an efficiency much lower than that of Src-optimal peptide. The Src-optimal peptide was the best substrate for Src and Hck because it was phosphorylated by both kinases at efficiencies that were about 400-fold higher than that of the Src autophosphorylation site peptide. Furthermore, Src and Hck required the presence of Ile-5 and Phe-9 in Src-optimal peptide and Glu-12 and Thr-14 in cdc2(6–20) as crucial substrate specificity determinants, because their substitution dramatically reduced the efficiency of peptide phosphorylation by both kinases (Table I).

In summary, both Src and Hck exhibited strikingly similar patterns of preference for the substrate peptides, suggesting that the catalytic domains of both kinases recognize similar structural features around the phosphorylation sites of the peptides. More importantly, the results imply that Src and Hck have the intrinsic ability to phosphorylate similar cellular proteins *in vivo*.

Comparison of the Ability of Hck and Src to Bind the Immobilized pYEEI Peptide—The ability of a cellular protein to be phosphorylated *in vivo* by a specific member of the Src family is most likely determined by (i) the presence of specific determinants in the cellular protein that are recognized by the catalytic domain, (ii) the ability of the cellular protein to co-localize with the kinase in the same subcellular compartment, and/or (iii) the ability of the cellular proteins to bind to the SH2, SH3, or unique domain of the kinase. Because of the importance of the SH2 domain in determining the subcellular localization and substrate specificities of Src family kinases, we studied the functional properties of the SH2 domains of Src and Hck.

The pYEEI peptide has previously been demonstrated to bind the SH2 domains of several Src family kinases (Src, Lyn, and Lck) with high affinity (7, 8, 24); we therefore used the pYEEI peptide immobilized to agarose as the ligand to study the binding specificity and accessibility of the SH2 domain of Src and Hck. As shown in Fig. 4, at kinase concentrations ranging from 20 to 80 nM, Src displays significant binding to the immobilized pYEEI peptide. In contrast, no detectable binding of Hck to the phosphopeptide was found under similar conditions. There are three possible reasons for the inability of the recombinant Hck to bind the phosphopeptide: (i) the C-terminal regulatory tyrosine of the recombinant Hck is phosphorylated, and interaction between this phosphorylated tyrosine and the SH2 domain renders the SH2 domain inaccessible to the exogenous pYEEI peptide (2, 3); (ii) the structure of the SH2 domain of Hck differs from that of Src in such a way that they display different binding specificities and different affinity toward the pYEEI peptide; or (iii) the native structure of Hck imposes conformational constraints that limit the accessibility of its SH2 domain. In the following experiments, we showed that the inability of Hck to bind pYEEI peptide is most likely due to the presence of conformational constraints within Hck that limit its SH2 domain accessibility.

Determination of the Level of Tyrosine Phosphorylation of the Purified Recombinant Hck—To ascertain whether the inability of Hck to bind the pYEEI peptide is a result of interaction between its SH2 domain and the phosphorylated C-terminal regulatory tyrosine, we determined the level of tyrosine phosphorylation of the purified recombinant Hck. Hck was autophosphorylated *in vitro* to a stoichiometry of approximately 1 mol PO_3^- per mol of Hck (data not shown), and the relative
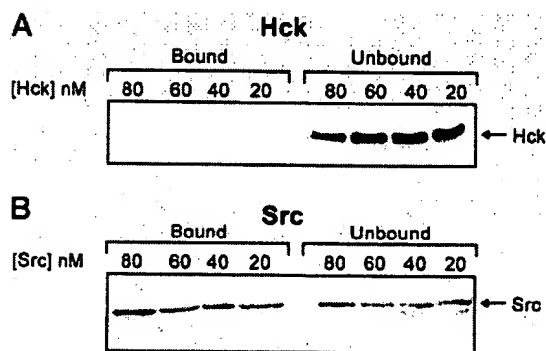
A Hck

Bound   Unbound

[Hck] nM 80 60 40 20 | 80 60 40 20

← Hck

B Src

Bound   Unbound

[Src] nM 80 60 40 20 | 80 60 40 20

← Src

FIG. 4. **SH2 domain accessibility of Hck and Src.** The indicated concentrations of Hck (A) and Src (B) were incubated with immobilized pYEEI peptide. Material bound to the pYEEI-gel (*Bound*) or remaining in the supernatant (*Unbound*) was visualized by SDS-PAGE followed by immunoblot analysis using either the anti-Hck or anti-Src antibody. Although the concentration of immobilized pYEEI peptide used in the binding assay was 15.9 μM, the agarose beads to which the phosphopeptide was attached may impose steric hindrance and hence render some of the phosphopeptide inaccessible to the SH2 domain of the kinases. For this reason, a significant portion of Src was not bound to the immobilized phosphopeptide even though the K_d of the Src-SH2 domain-pYEEI peptide complex was determined to be in the nanomolar range

levels of its tyrosine phosphorylation before and after autophosphorylation were determined by immunoblot analysis with the monoclonal anti-phosphotyrosine antibody (PY69 mAb) and polyclonal anti-phosphotyrosine antibody. As shown in Fig. 5, weak anti-phosphotyrosine immunoreactivity was detected before autophosphorylation, whereas the autophosphorylated Hck reacted very strongly with both the polyclonal and monoclonal (PY69) anti-phosphotyrosine antibodies. Densitometric analysis of the immunoblot revealed that the anti-phosphotyrosine immunoreactivity of Hck prior to autophosphorylation is less than 5% of that of the autophosphorylated Hck. Because the PY69 antibody displays no difference in its ability to recognize the autophosphorylation site and the C-terminal regulatory phosphotyrosine (Fig. 2) and because the polyclonal antiphosphotyrosine antibody can recognize phosphotyrosines in different sequence contexts (see under "Experimental Procedures"), our results strongly suggest that almost all of the potential tyrosine phosphorylation sites, including the C-terminal regulatory tyrosine and the consensus autophosphorylation site, were not phosphorylated in the purified Hck preparation. Thus, the lack of binding of pYEEI peptide by Hck is not a consequence of occupancy of the SH2 domain by the C-terminal regulatory phosphotyrosine.

Demonstration of Specific Interaction between the SH2 Domain of Hck and the pYEEI Peptide—To confirm that the SH2 domain of Hck can indeed specifically bind the pYEEI peptide, we generated two recombinant fragments of Hck as GST fusion proteins and examined their ability to bind the immobilized pYEEI peptide. One of the fragments, GST-Hck(1–247), contains the unique, SH3, and SH2 domains of Hck, whereas the other fragment, GST-Hck(1–129), contains the unique and SH3 domains only. Upon incubation of each sample with the immobilized pYEEI peptide (0.79 nmol), only GST-Hck(1–247) could bind the phosphopeptide (Fig. 6). Because the SH2 domain is present in GST-Hck(1–247) but not in GST-Hck(1–129), our results indicate that the binding of GST-Hck(1–247) to the pYEEI-gel was mediated by the SH2 domain. Upon preincubation of GST-Hck(1–247) with various competitor peptides prior to incubation with the immobilized pYEEI peptide, only the free pYEEI peptide was capable of effectively competing with GST-Hck(1–247) for the immobilized pYEEI peptide, indicating that the binding of GST-Hck(1–247) to pYEEI was specific
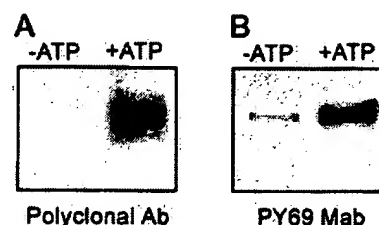

A -ATP +ATP   **B** -ATP +ATP

Polyclonal Ab   PY69 Mab

FIG. 5. **The tyrosine phosphorylation status of purified recombinant Hck before and after autophosphorylation.** Purified recombinant Hck was autophosphorylated to a stoichiometry of 1 mol of $PO_3{}^-$ incorporated per mol of kinase. Samples containing equal amounts of protein either before (−ATP) or after (+ATP) autophosphorylation were subjected to immunoblot analysis using either the polyclonal anti-phosphotyrosine antibody (A) or the monoclonal anti-phosphotyrosine antibody (PY69 mAb) (B). Densitometric analysis of the autoradiograms revealed that the level of phosphotyrosine before autophosphorylation (−ATP) was <5% of that after autophosphorylation (+ATP).
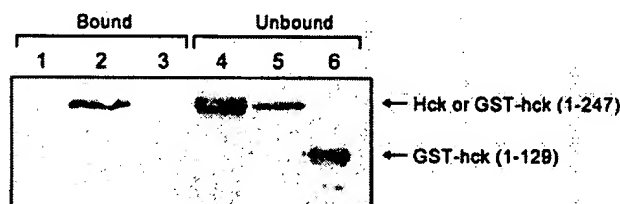

Bound   Unbound

1   2   3 | 4   5   6

← Hck or GST-hck (1-247)

← GST-hck (1-129)

FIG. 6. **Binding of intact Hck, GST-Hck(1–247), and GST-Hck(1–129) to the immobilized pYEEI peptide.** Equivalent amounts (280 ng) of Hck (*lanes 1* and *4*), GST-Hck(1–247) (*lanes 2* and *5*), and GST-Hck(1–129) (*lanes 3* and *6*) were incubated with immobilized pYEEI peptide. Material bound to the pYEEI peptide (*Bound, lanes 1–3*) or remaining in the supernatant (*Unbound, lanes 4–6*) was visualized by SDS-PAGE followed by immunoblot analysis using the anti-Hck antibody.

(data not shown).

In addition to the conformational constraints limiting SH2 domain accessibility in Hck, differences in affinities of the SH2 domains of Src and Hck for the pYEEI peptide could also contribute to the different degree of binding of Src and Hck to the immobilized phosphopeptide. As shown in Fig. 7, when the relative efficiencies of binding of GST-Src(1–258) and GST-Hck(1–247) to the pYEEI peptide were compared, similar amounts of the two GST fusion proteins were found to bind to the phosphopeptide at every phosphopeptide concentration used in the binding study, suggesting that the SH2 domain of Src and Hck, when present in constructs containing only unique, SH3, and SH2 domains, displays similar affinity toward the pYEEI peptide.

Taken together, our data unequivocally demonstrate that the SH2 domain of Hck has the intrinsic ability to bind the pYEEI peptide with an affinity similar to that of the Src SH2 domain. The inability of intact Hck to bind pYEEI peptide is very likely due to the presence of conformational constraints limiting the accessibility of the SH2 domain in the native structure of Hck.

DISCUSSION

In the present study, we have shown that Hck and Src display similar *in vitro* peptide substrate specificity. This builds on the previous studies (9, 10) that show that several Src family kinases recognize similar structural features in synthetic peptides and thus share common substrate specificity determinants. Taken together, these studies suggest that the catalytic domains of Src family kinases recognize similar features in the local structures around the phosphorylation sites in substrate proteins. Because most cellular functions of a kinase are determined by the cellular proteins that they phos-
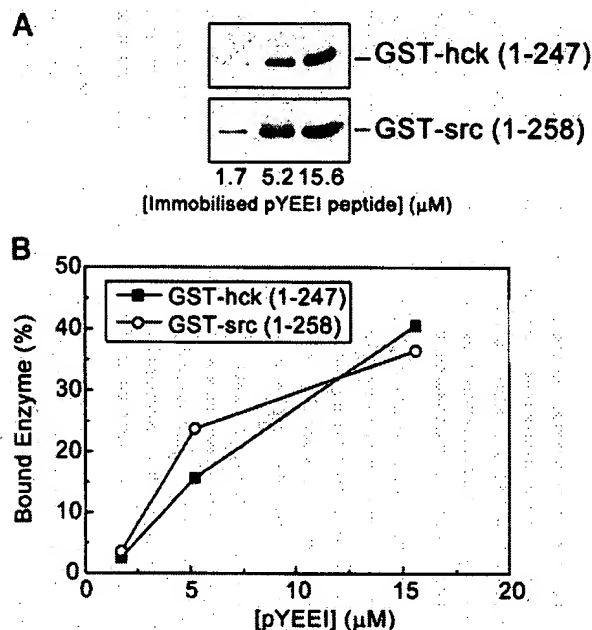
Functional Specificity and Redundancy of Src and Hck

A

GST-hck (1-247)

GST-src (1-258)

1.7 5.2 15.6
[Immobilised pYEEI peptide] (µM)

B

FIG. 7. **Comparison of the relative pYEEI peptide binding affinities of the SH2 domain of Hck and Src.** *A,* immunoblots of GST-Src(1-258) and GST-Hck(1-247) bound to varying concentrations (1.7, 5.2, and 15.6 µM) of the immobilized pYEEI peptide. *B,* the fraction of total GST-Src(1-258) or GST-Hck(1-247) bound to the pYEEI peptide at varying concentrations of the immobilized phosphopeptide. The amounts of Hck and Src GST fusion polypeptides bound to the pYEEI peptide were determined by densitometric comparison of the signals of the bound proteins with those of the protein standards in the immunoblots.

phorylate *in vivo,* our results support the notion that Src and Hck, when co-expressed in the same cells, have the intrinsic ability to carry out redundant cellular functions by phosphorylating similar cellular protein substrates. This idea is supported by studies in which Src family kinases have been disrupted in mice. The milder than expected phenotype associated with mice deficient in Src family kinases suggests that many cellular functions normally performed by the disrupted Src family member(s) are compensated for by other Src family members co-expressed in the same cells (11–19). Despite an inferred degree of functional overlap among the Src family kinases *in vivo,* mice homozygous for a mutation in one Src family gene exhibit some unique developmental and functional defects. For examples, Fcγ-receptor-independent phagocytosis is perturbed in Hck-deficient macrophages (16), and bone resorption by osteoclasts is impaired in *src⁻/⁻* mice (13, 19). This suggests that the roles of Hck and Src in phagocytosis by macrophages and bone formation, respectively, cannot be substituted by other co-expressed Src family members. Thus, in addition to cooperating with other Src family kinases to provide the signals necessary for many cellular functions, each of the kinases also performs unique functions *in vivo.*

How might each Src family member carry out its own unique functions if the catalytic domain of all Src family kinases recognizes similar structural features in cellular protein substrates? Because the cellular protein substrates are differentially distributed in various subcellular compartments, src family kinases co-expressed in the same cells can phosphorylate different cellular proteins if they are targeted to different subcellular compartments (see Ref. 4 for review). Furthermore, the SH2, SH3, and perhaps the unique domains can directly interact with the cellular substrates and hence determine the substrate specificity of the kinases. For example, phosphorylation of focal adhesion kinase by Src requires direct interaction

of the SH3 domain of Src with the [368]RALPSIPKL[376] motif of focal adhesion kinase as well as interaction of the SH2 domain of Src and the phosphorylated Tyr-397 of focal adhesion kinase (5); phosphorylation of the cellular protein Sin by Src requires interaction of a Pro-X-X-Pro containing motif of Sin with the SH3 domain of Src (6). For these reasons, the differential SH2 domain accessibility exhibited by Src and Hck is a potential mechanism of targeting the two kinases to different subcellular compartments, thereby allowing them to carry out different functions by phosphorylating the cellular protein substrates in their immediate vicinity. Taken together, our data suggest that the similar *in vitro* peptide substrate specificity of the catalytic domains of Src family kinases may account for the functional redundancy of the kinases *in vivo* and the difference in accessibility of their SH2 domains may contribute to their functional specificity. To further substantiate this notion, future studies should focus on identification of common and specific *in vivo* cellular protein substrates of the kinases and demonstration of targeting of Src and Hck to different subcellular compartments or binding to different cellular proteins as a consequence of the differential SH2 domain accessibility displayed by both kinases.

Our study also suggests the presence of conformational constraints limiting the SH2 domain accessibility of intact Hck even if its C-terminal regulatory tyrosine is not phosphorylated. Elucidation of the structural basis of these conformational constraints is essential for our understanding of the regulatory properties of Hck. The fact that deletion of the kinase domain and the C-terminal regulatory domain renders the SH2 domain in GST-Hck(1-247) accessible to the pYEEI peptide is consistent with the notion that only the intact form of Hck can impose these conformational constraints. In contrast to our observation that intact Src and Hck display different SH2 domain accessibility, Xu *et al.* (2) and Sicheri *et al.* (3) reported that the crystal structures of the inactive conformation of Hck and Src, which lack the unique and fatty acid acylation domains, are virtually identical. It is therefore reasonable to propose that the unique and/or fatty acid acylation domains confer differences in SH2 domain accessibility of the two kinases. Future studies should test this hypothesis by comparing the SH2 domain accessibility of intact Hck and the truncated form of Hck without the fatty acid acylation and the unique domains. Alternatively, Src and Hck may exhibit a difference in the ability of the C-terminal tail to move away from the SH2 domain after dephosphorylation. Src may have a rather flexible C terminus that can move away from the SH2 domain after dephosphorylation, thereby allowing binding to the pYEEI peptide resin. In contrast, Hck may have a more rigid C terminus that, even upon dephosphorylation, does not allow it to fully move away from the SH2 domain, thereby limiting the accessibility of the SH2 domain to the pYEEI resin.

REFERENCES

1. Courtneidge, S. A. (1994) *Protein Kinases* (Woodgett, J. R., ed) pp. 212–230, IRL Press, Oxford
2. Xu, W., Harrison, S. C., and Eck, M. J. (1997) *Nature* **385,** 595–601
3. Sicheri, F., Moarefi, I., and Kuriyan, J., (1997) *Nature* **385,** 602–609
4. Pawson, T. (1995) *Nature* **373,** 573–579
5. Thomas, J. W. Ellis, B., Boerner, R. J., Knight, W. B., White, G. C., II, and Shaller, M. D. (1998) *J. Biol. Chem.* **273,** 577–583
6. Alexandropoulos, K., and Baltimore, D. (1996) *Genes Dev.* **10,** 1341–1355

7. Songyang, Z., Shoelson, S. E., Chaudhuri, M., Gish, G., Pawson, T., Haser, W. G., King, F., Roberts, T., Rotnofsky, S., Lechleider, R. J., Neel, B. G., Birge, R. B., Farado, J. E., Chou, M. M., Hanafusa, H., Shaffhauser, B., and Cantley, L. C. (1993) *Cell* **72**, 767–778

8. Waksman, G., Kominos, D., Robertson, S. C., Pant, N., Baltimore, D., Birge, R. B., Cowburn, D., Hanafusa, H., Majer, B. J., Overduin, M., Resh, M. D., Rios, C. B., Silverman, L., and Kuriyan, J. (1992) *Nature* **358**, 646–653

9. Cheng, H.-C., Nishio, H., Hatase, O., Ralph, S., and Wang, J. H. (1992) *J. Biol. Chem.* **267**, 9248–9256

10. Songyang, Z., Carraway, K. L., Eck, M. J., Harrison, S. C., Feldman, R. A., Mohammadi, M., Schlessinger, J., Hubbard, S. R., Smith, D. P., Eng, C., Lorenzo, M. J., Ponder, B. A. J., Mayer, B. J., and Cantley, L. C. (1995) *Nature* **373**, 536–539

11. Varmus, H. E., and Lowell, C. A. (1994) *Blood* **83**, 5–9

12. Lowell, C. A., Niwa, M., Soriano, P., and Varmus, H. E. (1996) *Blood* **87**, 1780–1792

13. Soriano, P., Montgomery, C., Geske, R., and Bradley, A. (1991) *Cell* **64**, 693–702

14. Hibbs, M. L., Tarlinton, D. M., Armes, J., Grail, D., Hodgson, G., Maglitto, R., Stacker, S. A., and Dunn, A. R. (1995) *Cell* **83**, 301–311

15. Grant, S. G., O'Dell, T. J., Karl, K. A., Stein, P. L., Soriano, P., and Kandel, E. R. (1992) *Science* **258**, 1903–1910

16. Lowell, C. A., Soriano, P., and Varmus, H. E. (1994) *Genes Dev.* **8**, 387–398

17. Molina, T. J., Kishiara, K., Siderovski, D. P., van Ewijk, W., Narendran, A., Timms, E., Wakeham, A., Paige, C. J., Hartmann, K. U., Veillette, A., Davidson, D., and Mak, T. W. (1992) *Nature* **357**, 161–164

18. Stein, P. L., Vogel, H., and Soriano, P. (1994) *Genes Dev.* **8**, 1999–2007

19. Lowe, C., Yoneda, T., Boyce, B. F., Chen, H., Mundy, G. R., and Soriano, P. (1993) *Proc. Natl. Acad. Sci. U. S. A.* **90**, 4485–4489

20. Bjorge, J. D., Bellagamba, C., Cheng, H.-C., Tanaka, A., Wang, J. H., and Fujita, D. J. (1995) *J. Biol. Chem.* **270**, 24222–24228

21. Holtzman, D. A., Cook, W. D., and Dunn, A. R. (1987) *Proc. Natl. Acad. Sci. U. S. A.* **84**, 8325–8329

22. Graham, F. L., and van der Eb, A. J. (1973) *Virology* **52**, 456–467

23. Towbin, H., Stadhelin, T., and Gordon, J. (1979) *Proc. Natl. Acad. Sci. U. S. A.* **76**, 4350–4354

24. Sotirellis, N., Johnson, T. M., Hibbs, M. L., Stanley, I. J., Stanley, E., Dunn, A. S., and Cheng, H.-C. (1995) *J. Biol. Chem.* **270**, 29773–29780

25. Cheng, H.-C., Bjorge, J. D., Aebersold, R., Fujita, D., and Wang, J. H. (1996) *Biochemistry* **35**, 11874–11887

26. Laemmli, U. K. (1970) *Nature* **227**, 680–685

27. Aebersold, R. (1989) in *A Practical Guide to Protein and Peptide Purification for Microsequencing* (Matsudaira, P. T., ed) pp. 73–86, Academic Press, San Diego, CA

28. Allen, G. (1981) in *Sequencing of Proteins and Peptides, Laboratory Techniques in Biochemistry and Molecular Biology* (Work, T. S., and Burdon, R. H., eds) pp. 53–54, Elsevier/North-Holland Biomedical Press, Amsterdam

tide into the desired Ru⁴⁴-labelled DNA fragments 10a–e and 11a–d. Purification and isolation on reversed-phase (Vydac C₄) was achieved with a linear gradient 10→(30–40)% MeCN in aq. 0.05M triethylammonium acetate buffer (pH 7) over 40 min and led to the diastereoisomerically and enantiomerically pure isomer.

Enzymatic Digestion and Base Analysis. The 3'-5' degradation of 10c was carried out by time dependent enzymatic digestion with snake venom phosphodiesterase (SVP. 5'-exonuclease) in H₂O without the addition of salts and buffer. 1 µl of SVP (1 mg/0.5 ml) was diluted with 5 µl of H₂O. To 25 µl of 10c in H₂O 1 µl of the enzyme soln. was added at 0° and incubated. Samples of 1 µl were taken every min and added to 1 µl of matrix soln. (2,4-dihydroxyacetophenone and ammonium tartrate in MeCN/H₂O 1:1) directly to the MALDI sample plate. The samples were measured directly after drying (25 kV).

REFERENCES

[1] a) W. Bannwarth, D. Schmidt, R. L. Stallard, C. Hornung, R. Knorr, F. Müller, *Helv. Chim. Acta* 1989, 71, 2085; b) W. Bannwarth, D. Schmidt, *Tetrahedron Lett.* 1989, 30, 1513; c) W. Bannwarth, W. Pfleiderer, F. Müller, *Helv. Chim. Acta* 1991, 74, 1991; d) W. Bannwarth, F. Müller, *ibid.* 1991, 74, 2000.
[2] a) Y. Jenkins, I. K. Barton, *J. Am. Chem. Soc.* 1992, 114, 8736; b) C. J. Murphy, M. R. Arkin, Y. Jenkins, N. D. Ghatlia, S. H. Bossmann, N. J. Turro, I. K. Barton, *Science* 1993, 262, 1025; c) E. D. A. Stemp, M. R. Arkin, I. K. Barton, *J. Am. Chem. Soc.* 1995, 117, 2375; d) M. R. Arkin, E. D. A. Stemp, R. E. Holmlin, I. K. Barton, A. Hörmann, E. J. C. Olson, P. F. Barbara, *Science* 1996, 273, 475; e) M. R. Arkin, E. D. A. Stemp, C. Turro, N. J. Turro, I. K. Barton, *J. Am. Chem. Soc.* 1996, 118, 2267; f) D. B. Hall, R. E. Holmlin, I. K. Barton, *Nature (London)* 1996, 382, 731.
[3] a) M. D. Purugganan, C. V. Kumar, N. J. Turro, I. K. Barton, *Science* 1988, 241, 1645; b) T. J. Meade, J. F. Kayyem, *Angew. Chem.* 1995, 107, 358; c) R. E. Holmlin, E. D. A. Stemp, I. K. Barton, *J. Am. Chem. Soc.* 1996, 118, 5236.
[4] a) B. Giese, X. Beyrich-Graf, P. Erdmann, M. Petretta, U. Schwitter, *Chem. Biol.* 1995, 2, 367; b) B. Giese, J. Burger, T. W. Kang, C. Kesselheim, T. Wittmer, *J. Am. Chem. Soc.* 1992, 114, 1322; c) B. Giese, P. Imwinkelried, M. Petretta, *Synlett* 1994, 12, 1003; d) A. Marx, P. Erdmann, M. Senn, S. Körner, T. Jungo, M. Petretta, P. Imwinkelried, A. Dussy, K. I. Kulicke, L. Macko, M. Zehnder, B. Giese, *Helv. Chim. Acta* 1996, 79, 1980.
[5] a) C. Turro, S. H. Bossmann, Y. Jenkins, I. K. Barton, N. J. Turro, *J. Am. Chem. Soc.* 1995, 117, 9026; b) R. M. Hartshorn, I. K. Barton, *ibid.* 1992, 114, 5919; c) C. Hiort, P. Lincoln, B. Nordén, *ibid.* 1993, 115, 3448.
[6] B. C. Long, I. K. Barton, *Acc. Chem. Res.* 1990, 23, 271; b) G. M. Blackburn, M. J. Gait, in 'Nucleic Acids in Chemistry and Biology', Oxford University Press, Oxford, 1992, pp. 310–327; c) I. Haq, P. Lincoln, D. Suh, B. Nordén, B. Z. Chowdhry, J. B. Chaires, *J. Am. Chem. Soc.* 1995, 117, 4788.
[7] a) G. F. Smith, F. W. Cagle, *J. Org. Chem.* 1947, 12, 781; b) R. Amouyal, A. Homsi, J.-C. Chambron, J.-P. Sauvage, *J. Chem. Soc. Dalton Trans.* 1990, 1841.
[8] a) J. D. Entwistle, R. A. W. Johnstone, T. J. Povall, *J. Chem. Soc., Perkin Trans. I* 1975, 1300; b) E. A. Braude, R. P. Linstead, K. R. H. Woolridge, *J. Chem. Soc.* 1954, 3586.
[9] a) G. F. Strouse, P. A. Anderson, J. R. Schoonover, T. J. Meyer, F. R. Keene, *Inorg. Chem.* 1992, 31, 3004; b) T. J. Rutherford, D. A. Reitsma, F. R. Keene, *J. Chem. Soc. Dalton Trans.* 1994, 3659.
[10] a) D. S. C. Black, G. B. Deacon, N. C. Thomas, *Aust. J. Chem.* 1982, 35, 2445; b) M. J. Cleare, W. P. Griffith, *J. Chem. Soc. (A)* 1969, 372.
[11] J. E. Dickeson, L. A. Summers, *Aust. J. Chem.* 1970, 23, 1023.
[12] a) P. J. Garegg, T. Regberg, J. Stawinski, R. Strömberg, *Chem. Scr.* 1985, 25, 280; b) B. C. Fröhler, M. D. Matteucci, *Tetrahedron Lett.* 1986, 27, 469.
[13] W. Saenger, in 'Principles of Nucleic Acid Structure', Ed. C. R. Cantor, Springer-Verlag, New York, 1985, p. 143.
[14] U. Fiedr, W. Zürcher, M. Schär, H. B. Moser, *Nucleic Acids Res.* 1993, 21, 3191.
[15] V. I. Minkin, M. Legrand, M. J. Rougier, in 'Stereochemistry', Ed. H. B. Kagan, G. Thieme Verlag, Stuttgart, 1977.
[16] W. C. Johnson, in 'Circular Dichroism: Principles and Applications', Eds. K. Nakanishi, N. Berova, and R. W. Woody, VCH, Weinheim, 1994, p. 523.
[17] J.-P. Lecomte, A. Kirsch-DeMesmaeker, M. Demeunynck, J. Lhomme, *J. Chem. Soc., Faraday Trans.* 1993, 89, 3261.
[18] G. Gobi, K. Okamoto, T. Okuyani, J. Imada, *Chem. Pharm. Bull.* 1985, 33, 4422.

50. Synthesis of Modified Tripeptides and Tetrapeptides as Potential Bisubstrate Inhibitors of the Epidermal Growth Factor Receptor Protein Tyrosine Kinase

by Gérard Rossé and Urs Séquin*

Institut für Organische Chemie der Universität Basel, St. Johanns-Ring 19, CH-4056 Basel

and Helmut Mett, Pascal Furet, Peter Traxler, and Heinz Fretz*

Pharmaceuticals Division, Cancer/Bone Metabolism Research Department, Ciba-Geigy Ltd., CH-4002 Basel

(9.XII.96)

The synthesis of a series of bisubstrate inhibitors of the epidermal growth factor receptor protein kinase (EGF-R PTK) consisting of small peptides linked covalently to adenosine *via* appropriate triphosphate substitutes is described. Boc-Glu(O'Bu)-Tyr-Leu-OBzl (5) and Aз-Glu(O'Bu)-Tyr-Leu-Arg(Pmc)-NH₂ (8: Pmc = 2,2,5,7,8-pentamethylchroman-6-sulfonyl) were prepared by standard peptide chemistry. (*Scheme 1*), then modified at the OH group of tyrosine either with adipic anhydride or with 4-(chlorosulfonyl)benzoic acid, 4-(chlorosulfonyl)-2-hydroxybenzoic acid, or benzene-1,4-disulfonyldichloride (*Scheme 2*), and finally coupled with the 5'-OH group of 2',3'-O-isopropylideneadenosine (*Scheme 3*). In addition, N⁶-(benzyloxy)carbonyl]-2',3'-O-isopropylideneadenosine 5'-(hydrogencarbonate) (26), an ATP substitute, was coupled with the morpholide of 5(*Scheme 4*). Removal of the protecting groups gave the bisubstrate-type inhibitors 23, 24, and 28. The compounds synthesized were tested as inhibitors of the EGF-R PTK. The most active bisubstrate analog 23, 24, composed of the tripeptide sequence H-Glu-Tyr-Leu-OBzl, the 2-hydroxy-4-sulfonylbenzoyl moiety, and adenosine; it showed an IC₅₀ value of 33 µM.

Introduction. – The proliferation of cells is controlled by complex signal transduction pathways. Regulatory extracellular signals are transduced across the cell membrane by transmembrane receptors and carried to the nucleus through complex reaction cascades, where they stimulate cellular functions. The phosphorylation of proteins on tyrosine residues by protein tyrosine kinases (PTKs) is of prime importance in such transduction pathways [1]. Many studies have established that enhanced activity of PTKs has been implicated in certain human malignant and nonmalignant proliferative diseases (*e.g.* cancer, psoriasis, restenosis, *etc.*) [2].

The receptor tyrosine kinases (RTKs) have intrinsic PTK activity and participate in transmembrane signaling [3]. These receptors are involved in the control of cellular differentiation programs and cell growth. The epidermal growth factor receptor (EGF-R) is a well-characterized member of the large PTK family. It consists of an extracellular binding domain connected trough a transmembrane domain to an intracellular domain which contains a protein tyrosine kinase region and a C-terminal tail [1] [4–8]. Binding of the epidermal growth factor (EGF) or the transforming growth factor α (TGF-α) to the EGF-R [4] [8] induces a conformational change which leads to receptor dimerization. This dimerization then enables mutual phosphorylation of the intracellular domain of the EGF-R ('autophosphorylation') and increases the enzymat-

ic activity of the EGF-R with respect to phosphorylation of cytoplasmic substrates [9]. Also, overexpression of the EGF-R was shown to be implicated in some types of human cancers (e.g. breast tumors) [1] [10]. Thus, compounds that selectively block the activity of EGF-R and, therefore, the signaling pathways could be potential drugs in the treatment of epithelial diseases. To date, several classes of inhibitors of tyrosine kinases have been synthesized [11–16], but none of these inhibitors take advantage of the peptide/protein substrate specificity. In our study, we report the synthesis and initial testings of series of potential bisubstrate analogs based on small peptides, using the intracellular domain of the EGF-R (EGF-R ICD) as the target.

Concept and Design of Inhibitors. – For the transfer of the γ-phosphate group of ATP to a tyrosine moiety in a substrate molecule, a transition state has been postulated with a pentacoordinated P(γ) atom and with the α- and β-phosphate groups complexed with two bivalent metal ions (usually Mg^{2+} or Mn^{2+}) and Arg^{817} (Fig.). As a guideline for the design of potential inhibitors of the epidermal growth factor receptor tyrosine kinase, we used a molecular model of the kinase domain of EGF-R constructed from crystallographic data of the cAMP-dependent protein kinase [16] [17]. On the basis of this model and our previous work [18–20], we designed series of bisubstrate inhibitors consisting of a tri- or tetrapeptide as the protein substrate substitute, a 4-sulfonylbenzoyl (1), a 2-hydroxy-4-sulfonylbenzoyl (2), a benzene-1,4-disulfonyl (3), or an adipoyl moiety (4) as the triphosphate mimic or spacer, and adenosine. The 4-sulfonylbenzoyl and diarbonyl spacers have already been successfully used in the design of multisubstrate-type inhibitors [18–20]. The sequence Glu-Tyr-Leu¹) used for the tripeptide moiety was derived from a consensus sequence for the phosphorylation site of natural substrates of EGF-R [21], whereas the tetrapeptide sequence Glu-Tyr-Leu-Arg corresponds to the major autophosphorylation site of the EGF-R [8]. Combinations of each of the two peptides with one of the triphosphate mimics/spacers led to series of bisubstrate-type inhibitors of EGF-R. In addition, the synthesis of a phosphotyrosine-containing peptide was investigated as well.

Syntheses. – The protected tripeptide 5 (Scheme 1) was synthesized in solution by a conventional peptide-synthesis method from commercially available Boc-Glu(O'Bu)-OSu and the hydrochloride of H-Tyr-Leu-OBzl. For the preparation of the morpholide 6, the benzyl ester 5 was converted to the corresponding acid by catalytic hydrogenation. The mixed anhydride of the latter was then treated with morpholine.

The protected tetrapeptide amide 8 (Scheme 1) was prepared by a combined solid-phase and solution method. First, the N-acetylated peptide acid 7 was built up by standard Fmoc methodology [22] on 4-(4-(hydroxymethyl)-3-methoxyphenoxy)butyric acid benzhydrylamine (HMPB-BHA) polystyrene resin [23] using N,N'-diisopropylcarbodiimide/1-hydroxy-1H-benzotriazol (DICD/HOBt) activation. Compound 7 was then

¹) Symbols and abbreviations used for amino acids, peptides, and nucleosides are in accordance with IUPAC-IUB recommendations. Additional abbreviations: Boc, (tert-butoxy)carbonyl; Fmoc, (9H-fluoren-9-ylmethoxy)carbonyl; 'Bu, tert-butyl; Bzl, benzyl; Dmtr, 4,4'-dimethoxytriphenylmethyl; Fmoc, (9H-fluoren-9-ylmethoxy)carbonyl; HOBt, 1-hydroxy-1H-benzotriazole; HOSu, N-hydroxysuccinimide; Pmc, 2,2,5,7,8-pentamethylchroman-6-sulfonyl; Z, (benzyloxy)carbonyl; A(>CMe₂) = 2',3'-O-isopropylideneadenosine residue.
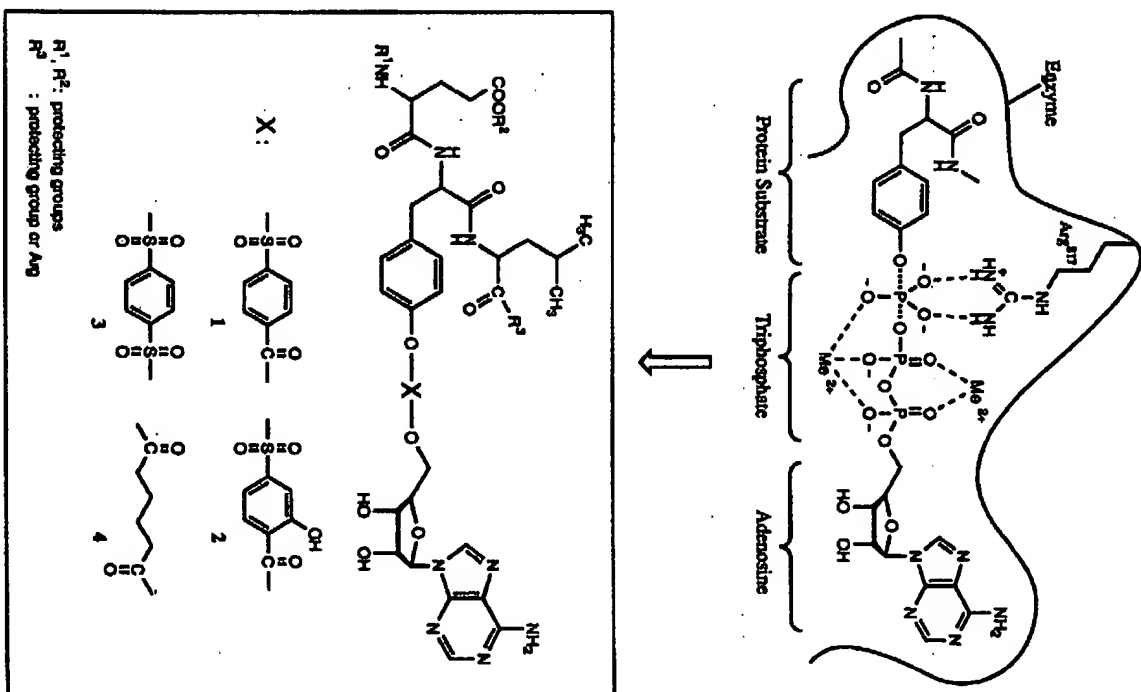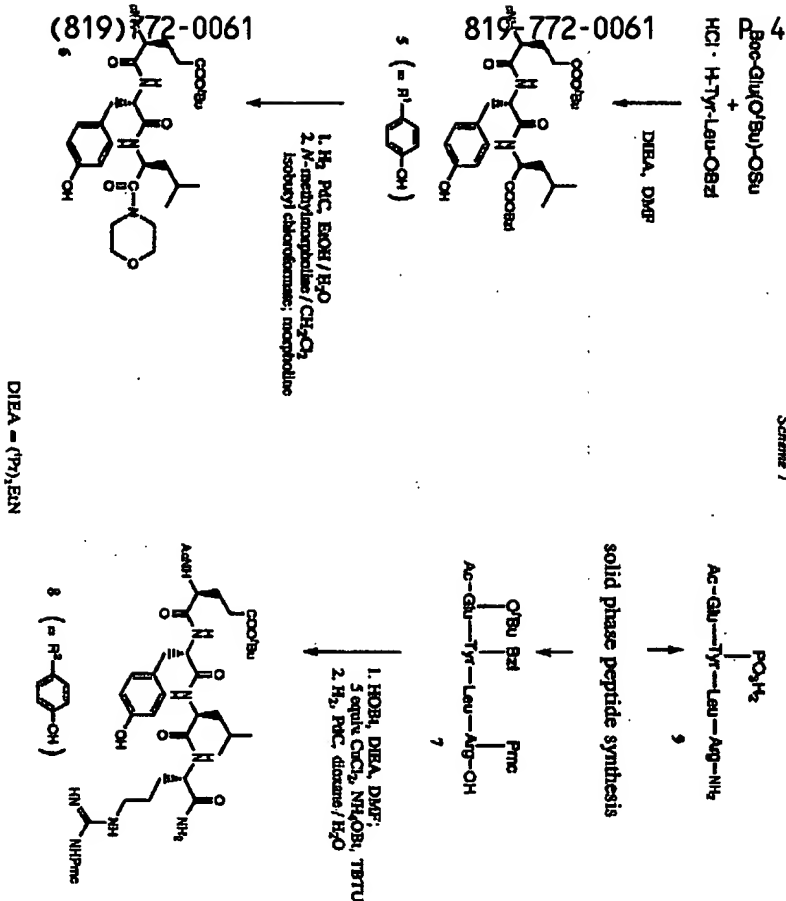
Figure. *Postulated transition state (adapted from [17] [16]) and schematic representation of possible bisubstrate inhibitors*
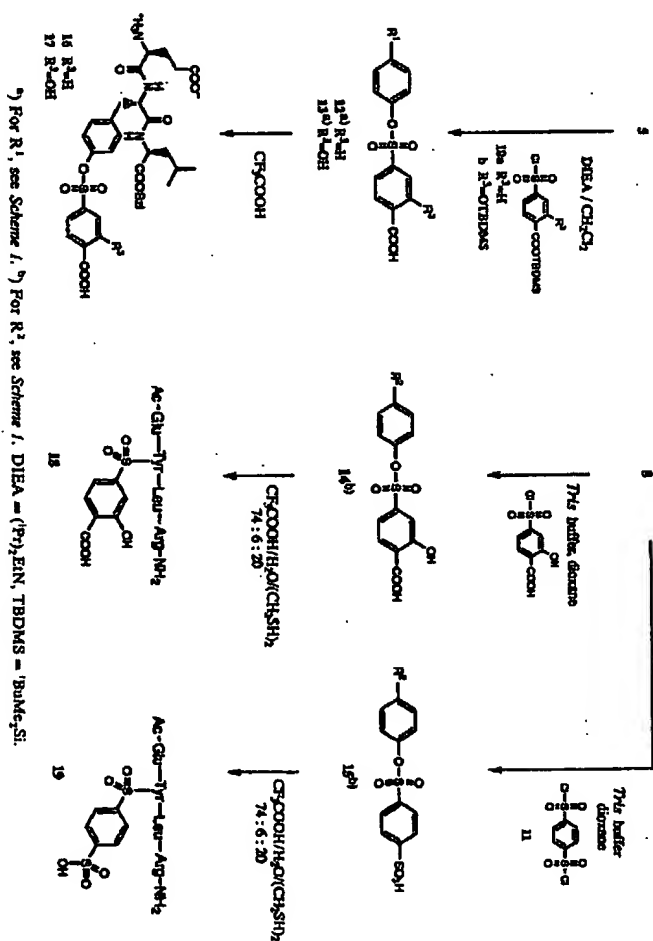
Fmoc-Tyr(PO$_3$H$_2$)-OH (unprotected phosphate group [29] where *N*-[(dimethylamino)-1*H*-1,2,3-triazolo[4,5-*b*]pyridin-1-ylmethylene]-*N*-methylmethanaminium hexafluorophosphate *N*-oxide (HATU) [30] [31] was successfully used as activating agent. The free phosphotetrapeptide amide 9 was obtained after treatment of the resin with CF$_3$COOH/H$_2$O/ethane-1,2-dithiol((CH$_2$SH)$_2$) 74:6:20.

The 4-sulfonylbenzoyl derivatives 12 and 13 as well as 14 and the benzene-1,4-disulfonyl derivative 15(*Scheme 2*) were prepared by reaction of the respective peptides with 4-(chlorosulfonyl)benzoic acid (for compound 12), 4-(chlorosulfonyl)-2-hydroxybenzoic acid (for compounds 13 and 14), or benzene-1,4-disulfonyl dichloride (11) [32] [33] (for compound 15), under modified *Schotten-Baumann* conditions. However, compounds 12 and 13 could be obtained in higher yields when the (chlorosulfonyl)benzoic acids used were first silylated with *N*-methyl-*N*-[(*tert*-butyl)dimethylsilyl]trifluoroacetamide(*tert*-butyl)dimethylsilyl chloride (CF$_3$CON(Me)Si(*t*Bu)Me$_2$/*t*BuMe$_2$SiCl); the (*tert*-butyl)-dimethylsilyl derivatives 10a and 10b thus obtained were then each reacted *in situ* with tripeptide 5 in abs. CH$_2$Cl$_2$ in the presence of (*i*Pr)$_2$EtN. The free peptide-triphosphate analogs 16–19 were obtained after deprotection with CF$_3$COOH or CF$_3$COOH/H$_2$O/(CH$_2$SH)$_2$ 76:4:20 and precipitation from Et$_2$O.

removed from the resin by selective acidolysis of the *C*-terminal ester bond with 1% trifluoroacetic acid (CF$_3$COOH) in CH$_2$Cl$_2$, and was converted to the amide by reaction with the ammonium salt of HOBt (NH$_4$OBt) using TBTU (2-(1*H*-benzotriazol-1-yl)-1,1,3,3-tetramethyluronium tetrafluoroborate)/HOBt [24] as condensing agent in the presence of *Hünig* base (*N,N*-diisopropylethylamine ((*i*Pr)$_2$EtN) and of copper(II) chloride in dimethylformamide (DMF). The use of copper(II) ions eliminates virtually epimerization of a peptide's *C*-terminal residue [25] (*cf.* also [26–28]). The benzyl group was removed selectively by catalytic hydrogenation to yield 8.

The phosphotyrosine-containing peptide amide 9(*Scheme 1*) was prepared by *Fmoc* methodology [22] on 4-(2,4-dimethoxybenzyl-Fmoc-aminomethyl)phenoxyacetamido-MBHA polystyrene (*Rink* amide) resin (MBHA = 4-methylbenzhydrylamine). The synthetic strategy made use of TPTU (2-(2-oxo-1-pyridyl)-1,1,3,3-tetramethyluronium tetrafluoroborate)/HOBt [24] activation throughout, except for chain assembly of

Scheme 1

DIEA = (*i*Pr)$_2$EtN

Scheme 2

^{a}) For R^1, see *Scheme 1*. ^{b}) For R^2, see *Scheme 1*. DIEA = (*i*Pr)$_2$EtN, TBDMS = *t*BuMe$_2$Si.
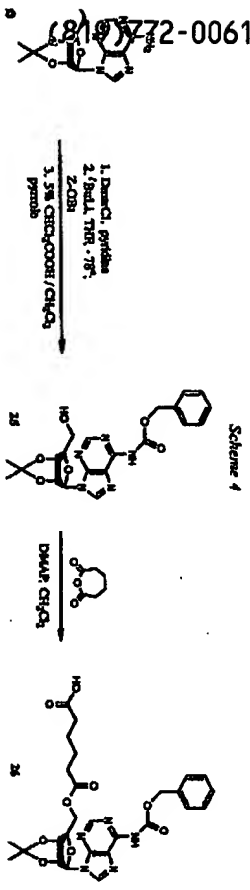
^{a}) For R^1, see *Scheme 1*.

The protected complete transition-state analogs 21 and 22 (*Scheme 3*) were synthesized by reaction of the peptide-triphosphate analogs 12 and 13 with 2',3'-*O*-isopropylideneadenosine (20) using 1,1'-carbonylbis(imidazolium) triflate (CBMIT) [34] as condensing agent. Removal of the protecting groups with CF₃COOH then gave the free compounds 23 and 24, respectively.
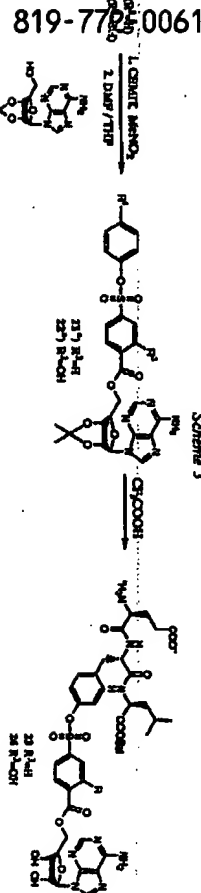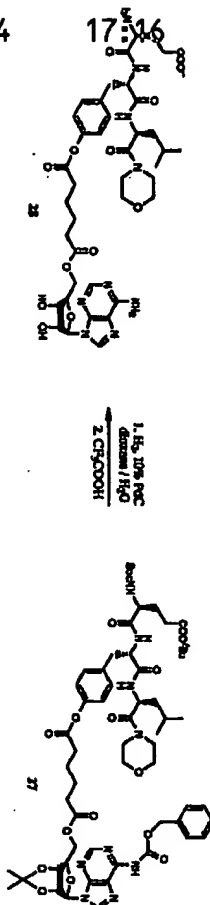

Scheme 3

For the preparation of the protected 5'-adenosyl ester 27 (*Scheme 4*), a different synthetic strategy was applied: the ATP analog 26 was attached to the tripeptide 6. Thus, the *N*⁶-Z-protected derivative 25, which was obtained in a three-step reaction from 20, was reacted with adipic anhydride [35] in the presence of 4-(dimethylamino)pyridine (DMAP) to give 26, which then was converted to the corresponding acyl chloride by the

Scheme 4

DMAP = 4-(dimethylamino)pyridine, DIEA = (ⁱPr)₂EtN

mild 1-chloro-*N*,*N*,2-trimethylprop-1-en-1-amine ('chloroenamine') method [36][37] and subsequently treated *in situ* with 6 to yield 27. The Boc 'Bu, and isopropylidene groups of 27 were removed using first catalytic hydrogenation over Pd/C and then CF₃COOH to yield the free compound 28. All compounds synthesized were characterized by mass and ¹H- and ¹³C-NMR spectra (see *Exper. Part* for selected data).

Results and Discussion. – In our earlier work on EGF-R protein tyrosine kinase inhibitors [18–20], a β-nitrostyrene derivative was used as the tyrosine mimic. Assuming that this nitrostyrene part would indeed interact with the tyrosine binding site of the target enzyme, even better inhibitors might come from a replacement of the nitrostyrene with a short tyrosine-containing peptide. However, it has to be born in mind that tyrosine itself or a tyrosine-containing peptide might interact in a completely different way with the enzyme than the *Michael* acceptor nitrostyrene.

The compounds we synthesized were tested as EGF-R tyrosine kinase inhibitors using the purified recombinant intracellular domain of EGF-R (EGF-R ICD) and angiotensin II as the P-accepting substrate (*Table I*). The results presented here indicate that our combinations of building blocks only led to moderately active inhibitors of the EGF-R tyrosine kinase. The best bisubstrate analog inhibitor in this study is 24, containing the tripeptide H-Glu-Tyr-Leu-OBzl, the 2-hydroxy-4-sulfonylbenzoyl moiety, and adenosine (*IC*₅₀ = 33 μM). The related compound 17, lacking the adenosine, was also found to have a modest inhibitory activity (*IC*₅₀ = 92 μM). The fact that 24 is about three times as active as 17 suggests that the adenosine part indeed adds to the inhibitory activity of the compound.

Table I. *Inhibitory Activities of Compounds 9, 16–19, 23, 24, 28, and 29 against EGF-R ICD*[a]

	9	16	17	18	19	23	24	28	29
*IC*₅₀ [μM][b]	inact.	inact.	92	inact.	inact.	inact.	33	inact.	68[c] [38]

[a]) In addition, the protected intermediates 5, 6, 12–15, 21, 22, and 27 were also tested routinely. With the exception of 13 (*IC*₅₀ = 29 μM), they were inactive.
[b]) Inactive; no inhibitory effect observable at 100 μM.
[c]) Determined with cAMP-dependent protein kinase.

The nature of the spacer part also seems to be of importance. A dramatic decrease in the activity against the EGF-R ICD was observed when the 4-sulfonylbenzoyl group was used as triphosphate substitute instead of the 2-hydroxy-4-sulfonylbenzoyl moiety (23 vs. 24) as was observed earlier for a different series of compounds [18]. The additional OH group may enhance the complexation of bivalent metal ions. Subtle changes in the length of the spacer unit or in the way it is attached to the tyrosine mimic also greatly influence the inhibitory activity as was shown in our earlier reports [19] [20]. In this respect, the adipoyl moiety of 28 is quite a long and flexible spacer, which might be one of the reasons why 28 proved to be inactive.

Elongation of the peptide moiety at the C-terminus with arginine and combination of the resulting tetrapeptide Glu-Tyr-Leu-Arg with the 2-hydroxy-4-sulfonylbenzoyl spacer (*cf.* compound 18) or with a benzene-1,4-disulfonyl moiety (compound 19) also

resulted in inactive compounds. In addition, our experiments established that the phosphotetrapeptide 9 has no inhibitory activity.

The tyrosine-containing peptide moieties that we used in the syntheses of the potential inhibitors described were in addition tested as substrates of the EGF-R tyrosine kinase (data not shown). This enzyme was not able to phosphorylate the tyrosine moiety, probably due to rather weak interactions between the enzyme and these peptides. Nevertheless, the combination 24 of one of these peptide moieties with a spacer and an adenosine derivative led to an inhibitory activity which was in the same range than that reported recently by *Gibson* and coworkers for the adenosine 5′-tetraphosphate heptapeptide 29 (IC_{50} = 68 μM with cAMP-dependent protein kinase) [38]. It is noteworthy that the peptide moiety of 29 was based on the well-known substrate peptide of the cAMP-dependent protein kinase.

29

A possible explanation for the low activity of our compounds might, indeed, be the rather weak or unspecific interactions between the enzyme and the peptide moieties. Also, the influence of polar, charged end groups at the N-terminus, or of the nonpolar morpholides or benzyl esters at the C-terminus of our compounds are hardly predictable in this respect. Optimized peptide sequences with higher affinity to the EGF-R PTK will probably be required if the synthesis of bisubstrate analogs of this type is to lead to compounds showing significant inhibitory activity.

Experimental Part

General. All chemicals were purchased from *Fluka AG, Aldrich, Bachem, Novabiochem,* or *Ciba-Geigy AG* in *purum* or *puriss. p.a.* quality. Solvents used in reactions were distilled and dried or purchased in *abs.* quality. THF was freshly distilled from Na/K. DMF was passed through a column filled with glass wool, neutral, basic, and

acidic Al_2O_3. Glassware was dried with a flame and cooled under Ar. Org. extracts were dried (Na_2SO_4), evaporated on a rotary evaporator (<35°), and dried under high vacuum. TLC: *Merck silica gel 60 F_{254}*, precoated glass plates. Prep. TLC: *Merck silica gel 60 F_{254}*, see precoated 'PSC' glass plates (2 mm). Flash chromatography (FC): procedure of *Still et al.* [39] with H_2O-cooled columns; *Merck silica gel 60*, 40–63 μm. Anal. HPLC (purity control): *Merck Hitachi* gradient HPLC anal. system, *YYDAC* diphenyl reversed-phase column (5 μm, 4.6×150 mm; *Paul Bucher*, Basel): flow rate 1 ml/min; solvents 0.1% CF_3COOH in MeCN (A), 0.1% CF_3COOH in H_2O (B); gradient: within 30 min from 5% B to 100% B; detection at 214 nm; in min. Prep. MPLC: *Büchi* MPLC system with *Knauer* variable-wavelength UV monitor: flow rate 60 ml/min; solvents: 0.1% CF_3COOH in H_2O (A), 0.1% CF_3COOH in MeCN (B). Optical rotation: *Perkin-Elmer* polarimeter model 141. M.p.: *Kofler* hot stage: uncorrected. NMR: *Varian VXR-400* (¹H, 400 MHz; ¹³C, 101 MHz) or *Varian Gemini 300* (¹H, 300 MHz; ¹³C, 75 MHz; ³¹P, 121 MHz); δ in ppm rel. to internal Me_4Si and external 85% aq. H_3PO_4 soln., resp. (= 0 ppm), coupling constants *J* in Hz; multiplicities of ¹³C resonances from APT and H,C-COSY experiments.' means that assignments may be interchanged. FAB-MS: *VG 70-250* or *ZAB-HF*; matrix: 3-nitrobenzyl alcohol (NBA). ³³Cl-PD-MS: *BIO-ION-20* plasma desorption instrument; samples were applied to a nitrocellulose matrix. MALDI-MS: *LDI-1700* mass monitor; matrices: 2,5-dihydroxybenzoic acid (2,5-DHB), 2,6-dihydroxyacetophenone (2,6-DHA), diammonium citrate (DAHC), α-cyano-4-hydroxycinnamic acid (α-CHC).

Boc-Glu(O'Bu)-Tyr-Leu-O-Bzl (5). To a soln. of HCl · H-Tyr-Leu-OBzl (3.46 g, 8.22 mmol) in DMF (30 ml) and ('Pr)$_2$EtN (1.50 ml, 8.22 mmol) in DMF (80 ml), a soln. of Boc-Glu(O'Bu)-OSu (3.31 g, 8.22 mmol) in DMF (50 ml) was added at 5°. After stirring for 23 h at r.t., the solvent was evaporated, the resulting oil dissolved in AcOEt (100 ml), the soln. washed with H_2O, 10% aq. citric acid soln., sat. aq. Na_2CO_3 soln. and brine, dried, and evaporated. FC (CH_2Cl_2/MeOH 98:2, 97:3, 95:5) gave 5 (5.19 g, 94%). Colorless amorphous powder. M.p. 61–63°. $[\alpha]_D^{24}$ = –21.2. $[\alpha]_{365}$ = –67.4 (*c* = 2.03, $CHCl_3$). FAB-MS (NBA): 670(15, $[M+H]^+$), 514(3, $[M–Boc–'Bu]^+$), 337(15), 265(3), 247(3), 222(18), 191(3), 147(3), 136(40), 120(3), 102(20), 91(100, PhCH₂⁺), 77(10, Ph⁺), 57(88, 'Bu⁺).

Boc-Glu(O'Bu)-Tyr-Leu-morpholine (6). A soln. of 5 (3.67 g, 5.48 mmol) in EtOH/H_2O 9:1 (150 ml) was hydrogenated at r.t. (H₂, 1 atm) over 10% Pd/C (1.83 g). After 4 h, the catalyst was filtered off and washed with EtOH/H_2O 9:1, the soln. evaporated, and the resulting solid dried under high vacuum: pure Boc-Glu(O'Bu)-Tyr-Leu-OH (3.16 g, 99.5%). M.p. 95–100°. $[\alpha]_D^{22}$ = –14.5. $[\alpha]_{365}$ = –47.9. (*c* = 2.03, $CHCl_3$). FAB-MS (NBA): 580(6, $[M+H]^+$), 486(6, $[M–Leu]^+$), 337(9), 265(4), 221(3), 191(3), 167(6, Glu⁺), KCl): 618(25, $[M+K]^+$), 580(6, $[M+H]^+$), 486(6, $[M–Leu]^+$), 337(9), 265(4), 221(3), 191(3), 167(6, Glu⁺), 136(36), 120(3), 102(20), 86(18), 77(20), 57(100, 'Bu⁺).

To a soln. of Boc-Glu(O'Bu)-Tyr-Leu-OH (522 mg, 900 μmol) and freshly distilled *N*-methylmorpholine (100 μl, 900 μmol) in abs. CH_2Cl_2 (10 ml), isobutyl chloroformate (120 ml, 918 μmol; freshly distilled under Ar) was added at –15°. After 5 min, freshly distilled morpholine (100 μl, 1.15 μmol) was slowly added at –15°. The mixture was stirred for 25 min at 0° and for 2.5 h at r.t., washed with H_2O, 10% aq citric acid soln., sat. aq. NaHCO₃ soln., and brine, dried, and evaporated. FC (CH_2Cl_2/MeOH 95:5, 9:1) afforded 6 (521 mg, 89%). Colorless amorphous powder. M.p. 97–101°. $[\alpha]_D^{23}$ = –18.1. $[\alpha]_{365}$ = –64.0. (*c* = 2.13, $CHCl_3$). FAB-MS (NBA): 649(21, $[M+H]^+$), 562(3, $[M–morpholine]^+$), 506(3, $[M–morpholine–'Bu]^+$), 450(8), 337(9), 309(3), 293(3), 265(3), 247(3), 232(10), 201(10), 152(3), 136(47), 102(22), 86(88, [morpholine]⁺), 77(12, Ph⁺), 57(100, 'Bu⁺).

(tert-Butyl)dimethylsilyl 4-(Chlorosulfonyl)benzoate (10a). To a soln. of 4-(chlorosulfonyl)benzoic acid (364 mg, 165 mmol) in dry THF (3 ml), $CF_3CON(Me)Si(^tBu)Me_2$, containing 1% of $^tBu)Me_2SiCl$ (767 μl, 3.30 mmol) was added under Ar. The orange mixture was stirred for 20 min and evaporated at 35° under high vacuum. Orange, amorphous solid. M.p. 105–108°.

Boc-Glu(O'Bu)-Tyr[$SO_2C_6H_4(4-COOH)$]-Leu-O-Bzl (12). To a suspension of 5 (790 mg, 1.30 mmol) and molecular sieves (powder 4 Å) in abs. CH_2Cl_2 (6 ml) under Ar, (`Pr)$_2$EtN (225 μl, 1.35 mmol) and a soln. of 10a (474 mg, 1.42 mmol) in abs. CH_2Cl_2 (2 ml) were slowly added at –5°. After stirring for 26 h at r.t. and addition of CH_2Cl_2, the mixture was filtered, washed with H_2O, dried, and evaporated. FC (CH_2Cl_2/MeOH 98:2, 95:5, 90:10) yielded pure 12(445 mg, 45%) and 499 mg (43%) of silyl-protected derivative of 12 as a light-yellow solid.

12: M.p. 125–129°; $[\alpha]_D^{23}$ = –28.8. $[\alpha]_{365}$ = –103.9 (*c* = 1.41, $CHCl_3$). ¹H-NMR (300 MHz, (CD₃)₂SO):
Table 2. ¹³C-NMR (75 MHz, (CD₃)₂SO); 91(100, PhCH₂⁺), 77, (10, Ph⁺), 57(88, 'Bu⁺).
Table 3. FAB-MS (NBA): 834(3, $[M+H]^+$), 742(4), 320(12), 222(7), 202(3), 147(5, Glu⁺), 102(20), 91(100, PhCH₂⁺), 77, (10, Ph⁺), 57(88, 'Bu⁺).
Silyl-protected derivative of 12: M.p. 53–56°. $[\alpha]_D^{23}$ = –18.1, $[\alpha]_{365}$ = –64.0. (*c* = 2.53, $CHCl_3$). FAB-MS (NBA): 968(1, $[M+H]^+$), 434(9), 222(8), 178(6), 136(6), 91(100, PhCH₂⁺), 73(22), 57(68, 'Bu⁺).

Table 2. ^{1}H-NMR Data of Compounds 12, 13, 16–18, 23, 24, and 28[a])

	12	13	16	17	18	23	24	28
Glu:								
H–C(2)[b])	3.74–3.87(m)	3.84–3.88(m)	3.76(br. s)	3.74–3.76(m)	4.13–4.18(m)	[d])	[d])	3.74–3.77(m)
CH$_2$(3)[c])	1.52–1.69(m)	1.51–1.71(m)	1.91–1.94(m)	1.91–1.96(m)	1.43–1.81(m)	1.92–2.10(m)	1.91–1.93(m)	1.93–1.96(m)
CH$_2$(4)	2.10(t, J = 7.5)	2.07–2.10(m)	2.29–2.34(m)	2.28–2.34(m)	2.15(t, J = 7.8)	2.31–2.37(m)	2.29–2.33(m)	2.34–2.39(m)
Boc, ^{t}Bu, Ac	1.36, 1.38(2s)	1.36, 1.39(2s)			1.81(s)			
Tyr:								
H–C(2)[b])	4.32–4.38(m)	4.33–4.36(m)	4.34–4.38(m)	4.32–4.40(m)	4.13–4.18(m)	4.28–4.71(m)	4.35–4.70(m)	4.60–4.65(m)
CH$_2$(3)	2.72(dd, J = 9.5, 13.5);	2.71(dd, J = 9.5, 14);	2.73(dd, J = 9.5, 14.5);	2.72(dd, J = 10, 14);	2.72(dd, J = 9.5, 13.5);	2.74(dd, J = 10, 14);	2.75(dd, J = 9, 13);	2.79(dd, J = 10, 13.5);
	2.91(dd, J = 2.5, 13.5)	2.91(dd, J = 3, 14)	2.94(dd, J = 4, 14.5)	2.94(dd, J = 3.5, 14)	3.03(dd, J = 3.5, 14)	2.95(dd, J = 4, 14)	2.95(dd, J = 3, 13.5)	3.02(dd, J = 3, 14)
H–C(2′,6′)	7.19(d, J = 8)	7.18(d, J = 8.5)	7.26(d, J = 8.5)	7.26(d, J = 8.5)	7.14(d, J = 8.5)	7.26(d, J = 8.5)	7.26(d, J = 8.5)	7.33(d, J = 8.5)
H–C(3′,5′)	6.85(d, J = 8)	6.86(d, J = 8.5)	6.95(d, J = 8.5)	6.96(d, J = 8.5)	6.86(d, J = 8.5)	6.96(d, J = 8.5)	6.97(d, J = 8.5)	7.03(d, J = 8)
Leu:								
H–C(2)[b])	4.51–4.55(m)	4.52–4.58(m)	4.55–4.58(m)	4.51–4.56(m)	4.24–4.27(m)	4.28–4.71(m)	4.35–4.70(m)	4.72–4.77(m)
CH$_2$(3), H–C(4)[c])	1.52–1.69(m)	1.51–1.71(m)	1.52–1.61(m)	1.52–1.61(m)	1.44–1.77(m)	1.54–1.58(m)	1.54–1.61(m)	1.58–1.62(m)
2Me-C(4)	0.83, 0.89(2d, each J = 6)	0.83, 0.89(2d, each J = 6)	0.81, 0.88(2d, each J = 6.5)	0.82, 0.88(2d, each J = 6)	0.82, 0.88(2d, each J = 6.5)	0.82, 0.89(2d, each J = 6)	0.81, 0.88(2d, each J = 6)	0.86, 0.89(2d, each J = 6.5)
PhCH$_2$	5.12(s)	5.13(s)	5.10(s)	5.11(s)		5.10(s)	5.10(s)	[e])
PhCH$_2$	7.31–7.36(m)	7.32–7.36(m)	7.29–7.37(m)	7.30–7.35(m)		7.29–7.35(m)	7.29–7.34(m)	
Arg:								
					4.44–4.48(m)			
					1.44–1.77(m)			
					3.10(q, J = 6)			
Amide resonances:								
NH	6.88(d, J = 9);	6.86[d]);	8.12(br. s);	8.10(br. s);	7.64(t, J = 5.5);	8.10(br. s);	8.05(br. s);	8.51(d, J = 8);
	7.90(d, J = 8);	7.81(d, J = 8.5);	8.60(d, J = 8);	8.59(d, J = 8);	7.82(d, J = 8);	8.60(d, J = 6);	8.60(d, J = 7.5);	8.66(d, J = 8)
	8.51(d, J = 7.5)	8.48(d, J = 7.5)	8.71(d, J = 8)	8.67(d, J = 9)	8.00–8.03(m, 3H)	8.71(d, J = 8)	8.71(d, J = 7.5)	
NH$_2$					7.09(s, 1H);			
					7.31(s, 1H)			

Table 2 (cont.)

	12	13	16	17	18	23	24	28
Spacer:								
H–C(2), H–C(6)	7.81(d, J = 8.5)	6.97–7.00(m)	7.99(d, J = 8.5)	7.18–7.21(m)	7.03–7.05(m)	8.02(d, J = 8.5)	7.38(d, J = 10)	2.34–2.39(m)[f])
H–C(3), H–C(5)	8.14(d, J = 8.5)	7.87(d, J = 8.5)	8.18(d, J = 8.5)	7.87(d, J = 8)	7.89(d, J = 8.5)	8.20(d, J = 8.5)	7.93(d, J = 8.5)	1.58–1.62(m)[g])
CH$_2$(5)								2.52–2.57[d])
Adenosine:								
H–C(1′)						6.01(d, J = 4.5)	5.96(d, J = 5)	5.92(d, J = 5)
H–C(2′)								4.68(t, J = 5)
H–C(3′)								4.27(t, J = 5)
H–C(4′)						4.28–4.71(m)	4.35–4.70(m)	4.09–4.11(m)
CH$_2$(5′)								4.21(dd, J = 6, 12); 4.36(dd, J = 3.5, 12)
H–C(2)						8.60(s)	8.42(s)	8.16(s)
H–C(8)						8.30(s)	8.19(s)	8.32(s)
NH$_2$						[d])	[e])	7.3(s)

[a]) Chemical shifts in ppm rel. to internal SiMe$_4$, measured in (CD$_3$)$_2$SO; coupling constants J in Hz; OH resonances not reported.
[b]) Assignments within the same column may be interchanged.
[c]) Assignments within the same column may be interchanged.
[d]) Resonance observed with difficulty or not observed due to broadening or overlap.
[e]) Morpholine resonances not observed due to overlap.
[f]) CH$_2$(2).
[g]) CH$_2$(3), CH$_2$(4).

Table 3. ^{13}C-NMR Data of Compounds 12, 13, 16–18, 23, 24, and 28[a])

	12	13	16	17	18	23	24	28
Glu:								
C(1)[a])	170.8	170.8	168.2	168.3	169.8	168.3	168.2	168.5
C(2)[b])	53.5	53.6	53.6	53.7	51.8	53.7	53.7	54.1
C(3)	27.2	27.2	26.4	26.4	27.0	26.5	26.4	26.5
C(4)	31.1	31.2	28.8	28.7	30.2	28.8	28.7	28.9
C(5)[b])	171.5	171.8	173.4	173.4	173.1	173.4	171.5	173.5
Boc, ^{t}Bu, Ac	27.6, 28.0	27.7, 28.0			22.4			
Boc, ^{t}Bu, Ac	78.1, 79.5	78.2, 79.5			170.7			
Boc	155.0	155.1						
Tyr:								
C(1)[b])	171.1	171.6	170.7	170.7	171.4	170.7	171.1	170.2
C(2)[b])	52.7	52.5	51.3	51.2	52.0	51.3	52.7	51.4
C(3)	36.9	36.9	38.7	36.2	36.1	36.4	36.1	36.5
C(1')[b])	135.6	135.8	135.8	135.8	137.2[b])	135.8	135.8	135.0
C(2',6')	128.3	130.5[b])	128.6	130.5	130.5	128.7	130.7	130.1
C(3',5')	121.3	121.3	121.6	121.6	121.5	121.7	121.6	121.4
C(4')	147.4	147.6	147.4	147.6	147.6	147.4	147.4	149.4[b])
Leu:								
C(1)[b])	171.9	171.9	171.9	171.9	171.7	172.0	171.9	171.7
C(2)[b])	50.2	50.3	50.4	50.3	53.4	50.4	50.3	46.5
C(3)	40.0	–	40.1	–	40.5	–	40.3	40.6
C(4)	24.0	24.1	24.2	24.2	24.1	24.2	24.1	24.1
2Me–C(4)	21.1, 22.6	21.2, 22.6	21.1, 22.7	21.1, 22.7	21.4, 23.1	21.1, 22.7	21.0, 22.8	21.5, 23.1
PhCH$_2$	65.8	66.0	66.0	66.0		66.0	66.0	41.9, 45.5[c])
PhCH$_2$(o, m, p)	127.7, 127.9, 128.3	127.8, 128.0, 128.3	127.8, 128.0, 128.4	127.8, 128.0, 128.3		127.8, 128.1, 128.4	127.8, 128.0, 128.3	66.3[c])
PhCH$_2$(ipso)	136.8	136.7	137.0	136.9		137.1	137.0	
Arg:								
					173.9			
					52.1			
					29.2			
					24.9			
					40.4			
					156.7			

Table 3 (cont.)

	12	13	16	17	18	23	24	28
Spacer:								
C(1)	135.8[b])	136.6[b])	137.9[b])	138.1	137.0[b])	138.4[b])	138.9[b])	172.6[b])
C(2)	130.7[b])	114.3[b])	130.6[b])	116.2	115.1[b])	130.7[b])	116.6[b])	33.9[b])
C(3)	130.0[b])	164.1	130.6[b])	162.0	163.4	130.5[b])	158.4	23.7
C(4)	135.8[b])	124.8	136.3[b])	122.0	124.2	134.8[b])	119.1	23.7
C(5)	130.0[b])	130.8[b])	130.6[b])	131.5	115.7[b])	130.5[b])	132.1	33.1[b])
C(6)	130.7[b])	115.6[b])	130.6[b])	116.2	131.1	130.7[b])	117.8[b])	169.9[b])
C=O	167.4	169.4	165.8	169.6	169.6	164.2	165.6	
Adenosine:								
C(1')						88.2	88.2	87.8
C(2')						73.2	73.2	72.8
C(3')						70.2	70.2	70.3
C(4')						81.6	81.6	81.5
C(5')						65.5	65.5	63.8
C(2)						147.8	147.8	152.6
C(4)						148.6	148.6	149.1[b])
C(5)						119.0	119.0	119.1
C(6)						158.7	158.7	156.0
C(8)						141.7	141.7	139.7

[a]) Chemical shifts in ppm rel. to internal SiMe$_4$, measured in (CD$_3$)$_2$SO.
[b]) Assignments of similar chemical shifts within the same column may be interchanged.
[c]) Morpholine resonances.

Ac-$Glu(O^tBu)$-$Tyr(SO_3C_6H_4(4$-$SO_2H))$-Leu-$Arg(Pmc)$-NH_2 (19)

30

REFERENCES

[1] A. Ullrich, J. Schlessinger, Cell 1990, 61, 203.
[2] S. A. Aaronson, Science 1991, 254, 1146.
[3] X. Liu, T. Pawson, Recent Prog. Horm. Res. 1994, 49, 149.
[4] G. Carpenter, Ann. Rev. Biochem. 1987, 56, 881.
[5] P. J. Bertics, G. N. Gill, J. Biol. Chem. 1985, 260, 14642.
[6] T. Hunter, J. A. Cooper, Ann. Rev. Biochem. 1985, 54, 897.
[7] J. Schlessinger, Biochemistry 1988, 27, 3119.
[8] Y. Yarden, A. Ullrich, Ann. Rev. Biochem. 1988, 57, 443.
[9] J. Schlessinger, A. Ullrich, Neuron 1992, 9, 383.
[10] L. C. Cantley, K. R. Auger, C. Carpenter, B. Duckworth, A. Graziani, R. Kapeller, S. Soliloff, Cell 1991, 64, 281.
[11] C.-J. Chang, R. L. Geahlen, J. Nat. Prod. 1992, 55, 1529.
[12] P. Workman, V. G. Brunton, D. I. Robins, Semin. Cancer Biol. 1992, 3, 369.
[13] T. R. Burke, Jr., Drugs of the Future 1992, 17, 119.
[14] D. W. Fry, Exp. Opin. Invest. Drugs 1994, 3, 577.
[15] A. Levitzki, A. Gazit, Science 1995, 267, 1782.
[16] P. Traxler, N. Lydon, Drugs of the Future 1995, 20, 1261.
[17] D. R. Knighton, D. L. Cadena, J. Zheng, L. F. Ten Eyck, S. S. Taylor, J. M. Sowadski, G. N. Gill, Proc. Natl. Acad. Sci. U.S.A. 1993, 90, 5001.
[18] P. M. Traxler, O. Wacker, H. L. Bach, J. F. Geisler, W. Kump, T. Meyer, U. Regenass, J. L. Roesel, N. Lydon, J. Med. Chem. 1991, 34, 2328.
[19] S. Peterli, R. Stumpf, M. Schweizer, U. Séquin, H. Mett, P. Traxler, Helv. Chim. Acta 1992, 75, 696.
[20] S. Peterli, D. Hubmann, U. Séquin, H. Mett, P. Traxler, Helv. Chim. Acta 1994, 77, 59.
[21] R. B. Pearson, B. E. Kemp, Methods Enzymol. 1991, 200, 62.
[22] E. Atherton, R. C. Sheppard, in 'Solid Phase Peptide Synthesis - A Practical Approach'. Eds. D. Rickwood and B. D. Hames, IRL Press at Oxford University Press, Oxford, 1989.
[23] B. Riniker, A. Florsheimer, H. Fretz, P. Sieber, B. Kamber, Tetrahedron Lett. 1993, 49, 9307.
[24] R. Knorr, A. Trzeciak, W. Bannwarth, D. Gillessen, Tetrahedron Lett. 1989, 30, 1927.
[25] R. Briand, S. Käusler, G. Rossé, H. Fretz (Ciba-Geigy AG, Basel), unpublished results.
[26] S.-T. Chen, S.-H. Wu, K.-T. Wang, Synthesis 1989, 37.
[27] C. Somlai, G. Szókán, L. Balaspiri, Synthesis 1992, 285.
[28] T. Miyazawa, T. Donkai, T. Yamada, S. Kuwata, Int. J. Pept. Protein Res. 1992, 40, 49.
[29] E. A. Ottinger, L. L. Shekels, D. A. Bernlohr, G. Barany, Biochemistry 1993, 32, 4354.
[30] L. A. Carpino, J. Am. Chem. Soc. 1993, 115, 4397.
[31] L. A. Carpino, A. El-Faham, F. Albericio, Tetrahedron Lett. 1994, 35, 2279.
[32] H. Meerwein, G. Dittmar, R. Göllner, K. Hafner, F. Mensch, O. Steinfort, Chem. Ber. 1957, 6, 841.
[33] B. I. Karavaev, S. P. Starkov, J. Gen. Chem. USSR (Engl. Transl.) 1957, 27, 863.
[34] A. K. Saba, P. Schulz, H. Rapoport, J. Am. Chem. Soc. 1989, 111, 4856.
[35] E. H. Farmer, J. Kracovski, J. Chem. Soc. 1927, 680.
[36] A. Devos, J. Remion, A.-M. Frisque-Hesbain, A. Colens, L. Ghosez, J. Chem. Soc. Chem. Commun. 1979, 1180.
[37] B. Haveaux, A. Dekoker, M. Rens, A. R. Sidani, J. Toye, L. Ghosez, Org. Synth. Coll. 1988, 6, 282.
[38] D. Medzihradszky, S. L. Chen, G. L. Kenyon, B. W. Gibson, J. Am. Chem. Soc. 1994, 116, 9413.
[39] W. C. Still, M. Kahn, A. Mitra, J. Org. Chem. 1978, 43, 2923.
[40] E. McGlynn, M. Becker, H. Mett, S. Reuener, R. Cozens, N. B. Lydon, Eur. J. Biochem. 1992, 207, 265.
[41] E. Kaiser, R. L. Colescott, C. D. Bossinger, P. I. Cook, Anal. Biochem. 1970, 34, 595.

51. Properties and Reactions of Substituted 1,2-Thiazetidine 1,1-Dioxides: Synthesis of N-Substituted 4,4-Dimethyl-1,2-thiazetidin-3-one 1,1-Dioxides, and a New Base-Catalyzed Rearrangement to Thiazolidin-4-one 1,1-Dioxides

by Dietmar Glas[l]), Gerty Rihs[b]), and Hans-Hartwig Otto*

Institute of Pharmaceutical/Medicinal Chemistry, University of Greifswald, Friedrich-Ludwig-Jahn-Str. 17, D-17487 Greifswald

b) Ciba-Geigy; Physik. K-127.626, P.O. Box, CH-4002 Basel

Dedicated to Professor Fritz Eiden, München, on the occasion of his 70th birthday and to Professor Klaus Hartke, Marburg, on the occasion of his 65th birthday

(6.XI.96)

Alkylation of 3-oxo-1,2-thiazetidine 1,1-dioxide 2 yields the N-alkylated 3-oxo-β-sultams 3a–i. Solvolysis with NaOH or NH$_3$ selectively opens the N–S bond forming the sulfonate carboxamides 4 and the sulfonamido-carboxamides 7, respectively. Furthermore, the hitherto unknown compounds of type 5 are prepared, representing a strained four-membered ring with a disarylated, sulfonated N-atom. Depending upon the reaction conditions, 3b–d and 3g are rearranged by base-catalyzed reactions into the substituted 4-oxothiazolidine 1,1-dioxides 9 or 10. Structures are elucidated by spectroscopic methods, established by crystal-structure analyses, and a possible way of formation is proposed. Furthermore, some side reactions and transformations are reported.

Introduction. – The β-lactam ring is the essential moiety of many antibiotics. Penicillins, cephalosporins, and carbapenems exhibit their activity by an attack of the β-lactam to enzymes of the bacterial system [1]. The β-sultam ring – 1,2-thiazetidine 1,1-dioxide – is a highly strained and reactive S-analogue of the β-lactam [2]. Furthermore, both systems are potent synthetic building blocks, and one would expect that reactions known from one system could be adapted for the other one. Examples supporting this idea have already been described [2]. N-Benzyl-β-lactams can be rearranged into pyrrolidinones by bases like lithium diisopropylamide, as described by Durst et al. [3] and extended by Bergmann [4]. All attempts to transfer this rearrangement to parent β-sultams completely failed [5]. Therefore, we decided to study a combination of a β-lactam with a β-sultam structure, which is represented by the 3-oxo-β-sultam 2. Here, we report on synthesis, properties, and our results of the base-catalyzed rearrangement reactions of some N-substituted 3-oxo-4,4-dimethyl-β-sultams 3.

Results. – The N-unsubstituted 3-oxo-β-sultam 2 is available by ring closure from 2-(chlorosulfonyl)-2-methylpropionyl chloride (1), which can be obtained either from isobutyric acid anhydride [6], or from isobutyric acid [7] (Scheme 1). In our hands, the

l) From the thesis of D.G., University of Freiburg, 1993.

NCBI

Pub**M**ed

National Library of Medicine NLM
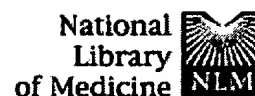
Entrez   PubMed   Nucleotide   Protein   Genome   Structure   OMIM   PMC   Journals   B

Search PubMed ▼ for [   ] Go Clear

Limits   Preview/Index   History   Clipboard   Details

About Entrez

Text Version

Entrez PubMed
Overview
Help | FAQ
Tutorial
New/Noteworthy
E-Utilities

PubMed Services
Journals Database
MeSH Database
Single Citation Matcher
Batch Citation Matcher
Clinical Queries
LinkOut
Cubby

Related Resources
Order Documents
NLM Gateway
TOXNET
Consumer Health
Clinical Alerts
ClinicalTrials.gov
PubMed Central

Privacy Policy

Display Abstract ▼ Show: 20 ▼ Sort ▼ Send to Text

☐ **1:** Bioorg Med Chem Lett. 1999 May 17;9(10):1447-52.   Related Articles, Link

ELSEVIER
FULL-TEXT ARTICLE

Adenosine-5'-carboxylic acid peptidyl derivatives as inhibitors o protein kinases.

Loog M, Uri A, Raidaru G, Jarv J, Ek P.

Institute of Chemical Physics, Tartu University, Estonia.

A new class of protein kinase bisubstrate-analog inhibitors was designed on the basis of adenosine-5'-carboxylic acid derivatives, where a short peptide was attached to the 5'-carbon atom of the adenosine sugar moiety via a linker chain. The potency and selectivity of these inhibitors were adjusted by relevant combination of these structural fragments, resembling the structure of the bisubstrate complex of the peptide phosphorylation reaction.

PMID: 10360754 [PubMed - indexed for MEDLINE]

Identification of Substrate Binding Site of Cyclin-dependent Kinase 5*

Pushkar Sharma, Peter J. Steinbach‡, Monica Sharma, Niranjana D. Amin, Joseph J. Barchi, Jr.§, and Harish C. Pant¶

From the Laboratory of Neurochemistry, NINDS, the ‡Center for Molecular Modeling, Center for Information Technology, and the §Laboratory of Medicinal Chemistry, NCI, National Institutes of Health, Bethesda, Maryland 20892

Cyclin-dependent kinase 5 (CDK5), unlike other CDKs, is active only in neuronal cells where its neuron-specific activator p35 is present. However, it phosphorylates serines/threonines in S/TPXK/R-type motifs like other CDKs. The tail portion of neurofilament-H contains more than 50 KSP repeats, and CDK5 has been shown to phosphorylate S/T specifically only in KS/TPXK motifs, indicating highly specific interactions in substrate recognition. CDKs have been shown to have a high preference for a basic residue (lysine or arginine) as the $n+3$ residue, n being the location in the primary sequence of a phosphoacceptor serine or threonine. Because of the lack of a crystal structure of a CDK-substrate complex, the structural basis for this specific interaction is unknown. We have used site-directed mutagenesis ("charged to alanine") and molecular modeling techniques to probe the recognition interactions for substrate peptide (PKTPKKAKKL) derived from histone H1 docked in the active site of CDK5. The experimental data and computer simulations suggest that Asp^{86} and Asp^{91} are key residues that interact with the lysines at positions $n+2$ and/or $n+3$ of the substrates.

Cyclin-dependent kinases (CDKs)[1] phosphorylate proline-directed serine and threonine residues in peptide/protein substrates. These kinases are active only when bound to their regulatory partners, cyclins. However, maximal kinase activation is achieved only after phosphorylation of these kinases by CDK-activating kinase (1 and references therein). CDK5 is slightly different from other CDKs; it is active only in neuronal cells because of the presence of its cyclin-like neuronal activator p35 and does not seem to require phosphorylation for its catalytic activity (1–3). However, like other CDKs, it phosphorylates S/T in S/TPXK/R motifs unique to the CDK family of kinases (4, 5). The specificity of this interaction is demonstrated by the phosphorylation of the tail portion of high molecular weight neurofilament-H (NF-H) by CDK5. The tail portion of this molecule contains 52 KSP repeats that can be classified as either KSPXK or KSPXXX. CDK5 specifically phosphorylates only KSPXK motifs and does not phosphorylate

any other KSP site (4, 5). Histone H1 is phosphorylated in vitro at a KTPKK motif (6). These studies indicate that the CDKs have high affinity for a basic residue like lysine or arginine at the $n+3$ position of the sequence, where n is the position of the phosphoacceptor serine or threonine. The mechanism of activation of CDK2 by cyclin A was revealed by the crystal structures of CDK2 (7) and its complex with cyclin (8). A recently published structure of a cyclin A-CDK2 complex phosphorylated by CDK-activating kinase demonstrated the structural basis for further activation by phosphorylation (9). However, because of the lack of a crystal structure of a CDK-peptide substrate complex, the highly specific interactions addressed above are not well understood.

Alignment of more than 60 protein kinases (PKs) revealed the minimal catalytic domain to be ~ 260 amino acids; this group exhibited 20–60% sequence homology (10). The crystal structures of the PKs solved to date reveal that the sequence homology and secondary structural elements are conserved at the functionally important sites, such as those involved in ATP binding and catalysis. When these amino acids are used to align the PKs, the major differences occur in the regions coding for loops (10). Despite their homologous sequences and similar global structures, PKs differ surprisingly in the substrate sequences they recognize, indicating highly specific interactions between the active sites of the enzyme and the substrates.

cAMP-dependent protein kinase (PKA) was the first kinase to be crystallized without (11) and with (12) a RRXS/A pseudo substrate peptide (PKI). Consequently, the crystal structure of the PKA·PKI complex has been used as a model kinase-substrate system. The recently published structure of phosphorylase kinase with a peptide substrate further confirms the specificity of these interactions (13). These structures reveal a highly specific network of interactions between the charged residues in the substrate with their oppositely charged partners in the enzyme. The differences in amino acid composition in the catalytic clefts of PKs account for differences in substrate specificity for these kinases (14, 15).

To understand the key interactions involved in this highly specific enzyme-substrate interaction, we have used site-directed mutagenesis, reaction kinetics, and molecular modeling. We constructed a homology model of CDK5 using the CDK2 coordinates from the cyclin-CDK2 crystal structure (9) and docked a peptide derived from histone H1, which is an in vitro substrate for CDK5 and other CDKs (6). Site-directed mutagenesis was used to confirm the interactions suggested by the computer modeling. Further refinement of the model included inter-residue restraints suggested by the enzyme kinetics measurements of the designed CDK5 mutants.

EXPERIMENTAL PROCEDURES

All fine chemicals were purchased from Sigma. The peptide substrates were synthesized by either Research Genetics or QCB Chemi-

[1] The abbreviations used are: CDK(s), cyclin-dependent kinase(s); NF, neurofilament(s); NF-H, high molecular weight NF protein; PK, protein kinase; PKA, cAMP-dependent protein kinase; PKI, cAMP-dependent protein kinase inhibitor; GST, glutathione S-transferase; MC, Monte Carlo; ERK, extracellular signal-regulated kinase.
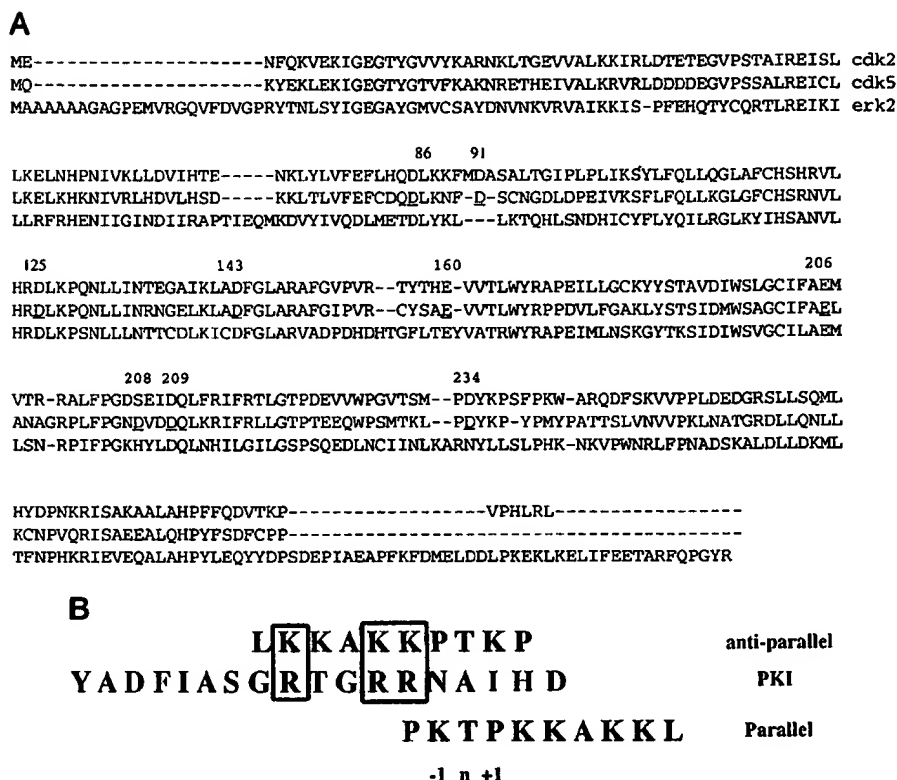
A

```
ME-------------------NFQKVEKIGEGTYGVVYKARNKLTGEVVALKKIRLDTETEGVPSTAIREISL cdk2
MQ-------------------KYEKLEKIGEGTYGTVFKAKNRETHEIVALKRVRLDDDDEGVPSSALREICL cdk5
MAAAAAAGAGPEMVRGQVFDVGPRYTNLSYIGEGAYGMVCSAYDNVNKVRVAIKKIS-PFEHQTYCQRTLREIKI erk2
```

```
                        86    91
LKELNHPNIVKLLDVIHTE-----NKLYLVFEFLHQDLKKFMDASALTGIPLPLIKSYLFQLLQGLAFCHSHRVL
LKELKHKNIVRLHDVLHSD-----KKLTLVFEFCDQDLKNF-D-SCNGDLDPEIVKSFLFQLLKGLGFCHSRNVL
LLRFRHENIIGINDIIRAPTIEQMKDVYIVQDLMETDLYKL---LKTQHLSNDHICYFLYQILRGLKYIHSANVL
```

```
    125          143                160                              206
HRDLKPQNLLINTEGAIKLADFGLARAFGVPVR--TYTHE-VVTLWYRAPEILLGCKYYSTAVDIWSLGCIFAEM
HRDLKPQNLLINRNGELKLADFGLARAFGIPVR--CYSAE-VVTLWYRPPDVLFGAKLYSTSIDMWSAGCIFAEL
HRDLKPSNLLLNTTCDLKICDFGLARVADPDHDHTGPLTEYVATRWYRAPEIMLNSKGYTKSIDIWSVGCILAEM
```

```
    208 209                          234
VTR-RALFPGDSEIDQLFRIFRTLGTPDEVVWPGVTSM--PDYKPSFPKW-ARQDFSKVVPPLDEDGRSLLSQML
ANAGRPLFPGNDVDDQLQKRIFRLLGTPTEEQWPSMTKL--PDYKP-YPMYPATTSLVNVVPKLNATGRDLLQNLL
LSN-RPIFPGKHYLDQLNHILGILGSPSQEDLNCIINLKARNYLLSLPHK-NKVPWNRLFPNADSKALDLLDKML
```

```
HYDPNKRISAKAALAHPFFQDVTKP-----------------VPHLRL-----------------
KCNPVQRISAEEALQHPYFSDFCPP-----------------------------------------
TFNPHKRIEVEQALAHPYLEQYYDPSDEPIAEAPFKFDMELDDLPKEKLKELIFEETARFQPGYR
```

FIG. 1. *Panel A*, sequence alignment and comparison of CDK2, CDK5, and ERK2. The residues mutated in CDK5 are *underlined*. *Panel B*, alignment of H1 peptide in parallel and antiparallel orientations. Thr[3] of H1 and Ala[21] of PKI are the phosphorylation sites. Basic residues that are aligned are *boxed*.

B

```
        L K K A K K P T K P          anti-parallel
YADFIASG R T G R R N A I H D          PKI

               P K T P K K A K K L   Parallel

               -1   n   +1
```

cals. [γ-^{32}P]ATP was purchased from NEN Life Science Products.

Expression and Purification of Proteins—GST-CDK5 in pGEX 2TK was constructed by putting the *Bam*HI fragment of His-tag CDK5 (3) into *Bam*HI-cut pGEX 2TK. GST-p25 in pGEX 4T-2 was constructed by a polymerase chain reaction method using the oligonucleotides 5'-GTC-CGGATCCGCCCAGCCCCCGCCG-3' as a forward primer, 5'-GTGAT-GAATTCTGGATCACCGATC-3' as a reverse primer, and DNA from the His-tag p35 construct as a template (3). The polymerase chain reaction products were digested with *Bam*HI and *Eco*RI, and the resulting fragments were cloned into *Bam*HI-*Eco*RI-cut pGEX 4T-2. The proteins were expressed as described earlier (4, 5). Purification of GST fusion proteins was carried out using glutathione-agarose chromatography by standard procedures (Amersham Pharmacia Biotech) and as described earlier (5). The purity of the proteins was assessed by SDS-polyacrylamide gel electrophoresis and Coomassie Blue staining of the gels. The protein concentration was estimated by densitometric analysis of these gels.

Site-directed Mutagenesis—The "charged to alanine" mutations were made using a commercial kit (Quick Change™, Stratagene). In brief, a pair of complementary primers of 30–40 bases was designed with desired mutations placed in the middle of the sequence. Parental cDNA inserted in pGEX 2TK was amplified using *Pfu* DNA polymerase with these primers for 15 cycles in a DNA thermal cycler (Perkin-Elmer). After digestion of the parental DNA with *Dpn*I, the mutants were transformed into *Escherichia coli* (DH5α strain, Life Technologies, Inc.). The mutations were confirmed by DNA sequencing. The GST fusion mutant proteins were expressed and purified as described above.

Phosphorylation Assay and Enzyme Kinetics—Standard assay mixtures contained 50 mM Tris, pH 7.4, 2.5 mM MgCl₂, 1 mM EGTA, 150–165 ng of wild-type CDK5 or different mutants complexed with a molar excess of p25 (preincubated enzyme preparation), 100 μM [γ-^{32}P]ATP, and 0.1–10 mM peptide substrate in a total volume of 30 μl. Reactions were initiated by adding [γ-^{32}P]ATP and were carried out at 30 °C for 60–80 min. Under these conditions, the rate of phosphorylation was constant for more than 2 h and proportional to the amount of enzyme. Reactions were terminated by adsorption of the assay mixture on phosphocellulose paper P81(Whatman). Phosphopeptide formation was measured by counting the radiolabeled ^{32}P incorporation after several washings of the phosphocellulose paper with 75 mM phosphoric acid. Kinetic constants were derived by fitting the Michaelis-Menten equation to the data using the Kaleidagraph program. Each experiment was done at least twice. Representative kinetic constants are shown in Tables I and II, and the variation in these constants from one experi-

ment to another was typically 10–15%. The apparent peptide affinities are compared on the basis of the K_m and V_{max}/K_m values.

Molecular Modeling—Using the program LOOK (16), CDK5 was aligned to CDK2 (9), and a model of CDK5 was built exploiting its high homology to CDK2 (62% identity). Atoms of CDK5 were assigned coordinates using the SegMod algorithm (16). An ATP molecule and magnesium were docked to CDK5 by copying the corresponding coordinates from the CDK2 complex.

The CDK5 model was then superimposed on the crystal structure of PKA (pdb file 2CPK) by best-fitting only the backbone (N, Cα, C) atoms in the 13-residue "catalytic loops." Of particular interest was the close proximity (1.0 Å separating Cα atoms) of Asp[86] in CDK5 to Glu[127] of PKA. The Glu[127] of PKA forms a salt bridge with Arg[18] of PKI (2cpk), and Arg[18] of PKI corresponds to Lys[6] of the H1 peptide in the antiparallel alignment (Fig. 1B). This structural alignment and subsequent modeling of CDK5 complexed with the H1 peptide were performed with the program CHARMM (17) and an all-atom parameter set (18, 19) running on Hewlett-Packard workstations.

In modeling the CDK5·H1·peptide complex, several approximations were employed. A distance-dependent dielectric ($\epsilon = r$) coefficient was used to screen electrostatic interactions with a potential energy "shifted" to zero at 12 Å. The shifted potential monotonically damps the electrostatic forces for this dielectric model (20). The distance-dependent dielectric is a rather crude approximation to an implicit solvent, but it maintains reasonable hydrogen bond distances.

Entropic effects were ignored, and a limited (non-ergodic) search of conformations was performed. In other words, we did not attempt to solve the *ab initio* docking problem, which would require a more accurate energy function and more exhaustive conformational sampling. Rather, the goal of the modeling was to aid in the choice and interpretation of experiments. Although our electrostatic approximations overly stabilize salt bridges, our intent was to enforce these interactions, not to predict them from first principles. The details of the peptide backbone conformation and side chain packing should not be overinterpreted, but our model can be used to test "lower resolution" hypotheses. For example, we can predict whether the H1 peptide is long enough and flexible enough to interact simultaneously with the ATP and a specific subset of CDK5 residues. Thus, prospective interactions between CDK5 and the peptides identified in early stages of the modeling led us to perform specific mutation experiments. Similarly, the measured enzyme kinetics were incorporated into later stages of modeling through the addition of inter-residue distance restraints favoring specific salt bridges between CDK5 and the H1 peptide.

Multiple families of short Monte Carlo (MC) simulations were run in succession, differing in the moves attempted and the restraints employed. In the latter stages of the modeling, protein residues near the peptide were free to move, but in each MC simulation the CDK5 molecule was held fixed while random rigid body translations and rotations of the entire H1 peptide were explored as well as random rotations of the peptide dihedral angles. Configurations were energy minimized somewhat to relieve bad contacts before applying the Metropolis criterion (21) for accepting conformations at a temperature of 600 K. A subset of torsions was included in the MC move set, but all peptide degrees of freedom were allowed to relax upon minimization. Positional restraints were used to guide the docking of the H1 peptide in a configuration antiparallel to that of PKI binding to PKA. Again, this configuration was investigated because it allows interaction between Asp[86] of CDK5 and Lys[6] of the peptide. In each MC simulation, a restraint was used to keep the gamma oxygen of the peptide Thr[3] close to the third phosphate group of the ATP molecule.

H1 Peptide Docked in the Antiparallel Orientation—The goal of the first family of MC simulations was to dock only the first several residues of the H1 peptide. 100 runs were started with the peptide in an extended conformation near the ATP molecule. Inter-residue distance restraints were used to favor energetically four interactions between a CDK5 residue and a peptide residue: Asp[86] and Lys[6], Asp[86] and Lys[6], Asp[125] and Lys[2], and Asp[143] and Lys[2]. Only 11 ϕ and ψ torsions (excluding proline ϕ angles) of the first seven residues were eligible for rotation during MC moves.

The lowest energy conformation obtained from these simulations was used to initiate the second family of 50 MC runs. The goal here was to guide the peptide toward an orientation like that of PKI bound to PKA. Two additional inter-residue restraints were added: Asp[91] and Lys[6], Glu[193] and Lys[9]. Only the 11 ϕ and ψ angles not involving the first four residues of the peptide were moved by the MC procedure.

Next, MC simulations were performed with both backbone and side chain dihedral angles included in the move set, but the fixed CDK5 molecule resulted in the acceptance of very few moves. Therefore, the protein was made increasingly flexible in the neighborhood of the peptide as follows. First, simulated annealing was employed during which the peptide and all atoms within 5 Å of it were free to move. The system was heated to 600 K in 20 ps and cooled to 100 K over 230 ps and energy minimized. Next, 100 ps of molecular dynamics at 300 K was simulated during which all residues with any atom within 5 Å of the peptide were in motion. The 100 structures saved (1/ps) were energy minimized to a root mean square gradient of 0.01 kcal/mol/Å. Finally, all residues in the lowest energy structure with any atom within 10 Å of the peptide were freed of constraints and energy minimized to a root mean square gradient of 0.001 kcal/mol/Å. The resulting structure is depicted in Fig. 2.

H1 Peptide Docked in the Parallel Orientation—Docking of the H1 peptide in an orientation parallel to that of PKI relative to PKA was also investigated (Fig. 1B). Analogous to the first family of MC runs described above, 40 simulations were performed during which inter-residue restraints were applied between Asp[86] and Lys[2], Asp[143] and Lys[6], and the ATP and Thr[3]. Again, 11 ϕ and ψ torsions of the first seven residues were rotated during MC moves. The lowest energy structure was inspected visually. Aside from Asp[143] and Asp[125], the only acidic residues within reach of the terminus of the peptide were observed to be in two clusters. The first includes Asp[38], Asp[39], Asp[40], Asp[41], and Glu[42]. Based on the cyclin A-CDK2 structure, it seems likely that these residues are buried in the CDK5-p35 complex. The other cluster includes Glu[160], Asp[206], Asp[208], Asp[209], and Asp[234] (9).

RESULTS

Homology Model of CDK5—It is well known that CDKs are not active on their own; they require binding to regulatory cyclins to be activated (1). However, maximal activation is achieved after phosphorylation at Thr/Ser in the T-loop of most CDKs. In the case of CDK2, it is Thr[160] in the cyclin A-CDK2 complex. This complex has been crystallized in both phosphorylated (9) and unphosphorylated (8) forms. These crystal structures help elucidate the mechanism of activation of CDKs. Briefly, the binding of cyclin A to CDK2 causes the T-loop (146–166) to move 21 Å from its position in the CDK2 structure, thereby opening the catalytic cleft, allowing access to the substrate, and orienting ATP in a position that favors phosphotransfer (8, 9). The main regulator of CDK5 is a neuron-specific
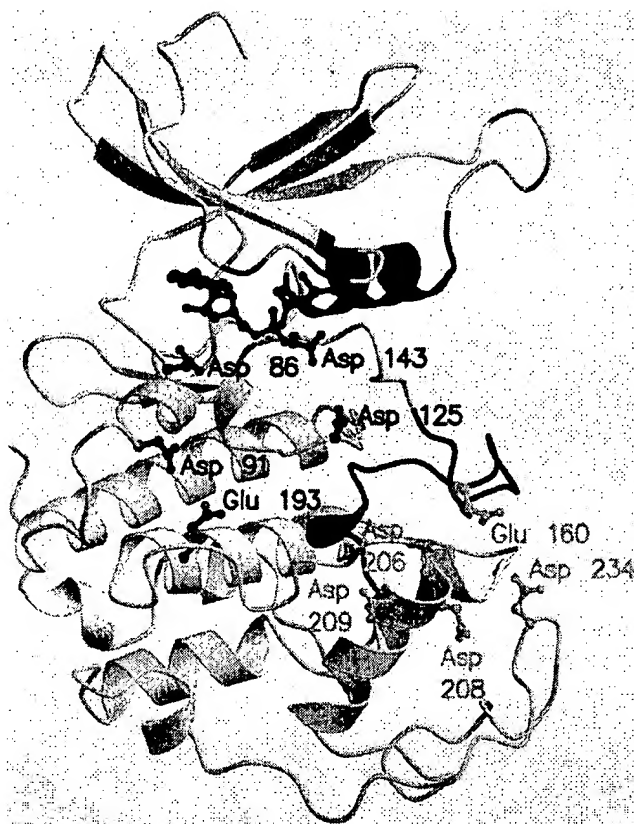

FIG. 2. **Model of CDK5 after H1 peptide (not shown) was docked as described under "Experimental Procedures."** The ATP (*red*) and magnesium ion (*blue*) are shown. Side chains of acidic residues potentially involved with the peptide binding in the antiparallel (*cyan*) and parallel (*yellow*) configuration are represented as *balls* and *sticks*. The PSSALRE helix (Pro[45]–Leu[55]) and the loop (Phe[150]–Asp[170]) analogous to the T-loop of CDK2 are colored *purple*. Glycines 11, 13, and 16 of the glycine-rich motif are colored *green*. This figure was produced using the programs Molscript (30) and Raster 3D (29).

protein p35 or its truncated form p25 (2, 3), accounting for the activity of this enzyme mainly in neurons. p35 does not have any sequence similarity to cyclins. Sequence homology among cyclins is rare; even two structurally similar cyclin motifs typically have very different sequences (22, 23). Recent studies by two groups have suggested that p35 consists of a cyclin-like fold (24, 25); however, unlike the regulators of other CDKs, p35 seems to achieve maximal activation of CDK5. Other CDKs seem to be catalytically active only upon phosphorylation in the T-loop subsequent to cyclin binding (1, 2). A recent crystal structure of cyclin A-CDK2 in this phosphorylated state has revealed that the T-loop moves further away from the catalytic cleft upon phosphorylation at Thr[160] in the T-loop (9). There seems to be no difference in substrate specificity caused by this effect; it only increases the rate of phosphorylation. Therefore, we assume that the active conformation of CDK5 is similar to that of CDK2 in the cyclin A-CDK2 (phosphorylated) complex (9). Thus, we modeled CDK5 in its active form using coordinates from the cyclin A-CDK2 (1jst.pdb) complex using the program LOOK (as described under "Experimental Procedures") taking advantage of the 62% sequence identity and a high sequence homology between these two kinases (Fig. 1A). The CDK5 model exhibits a bilobal structure (Fig. 2), a conformation representative of protein kinases. The small lobe is rich in β-sheets and contains the glycine-rich motif important for ATP binding. The ATP binding site is common to the entire PK family.

The N-lobe of CDK5 also contains the PSSALRE helix, which

TABLE I

Kinetic parameters of CDK5 mutants for peptide substrates

Phosphorylation assays and calculation of kinetic constants were performed as described under "Experimental Procedures." H1, histone peptide (PKTPKKAKKL); NF, neurofilament peptide (VKSPAKEKAK-SPEK).

Mutant	Peptide	K_m	V_{max}
		mM	$pmol\ min^{-1}\ \mu g^{-1}$
Wild type	NF	0.29	
	H1	0.04	0.68
D86A	NF	0.58	
	H1	0.23	0.70
D91A	NF	0.59	
	H1	0.22	0.18
D86A/D91A	H1	0.70	
D206A	H1	0.03	0.30
D209A	H1	0.05	0.35
D234A	H1	0.06	1.09
D143A	H1		0
E160A	H1		0
E193A	H1		0

corresponds to the PSTAIRE helix in CDK2. This helix is another feature found in all CDKs and is important for interaction with cyclins. The PSTAIRE helix rotates by several Å into the catalytic cleft (7- 9) upon cyclin A binding to CDK2. Residues 150–170 in the model of CDK5 are analogous to the T-loop in CDK2. Three conserved residues, Lys^{33}, Glu^{51}, and Asp^{143}, form a catalytic triad that helps orient ATP and facilitate catalysis. These interactions are similar to those found for PKA and other PKs (10). Mutation of Lys^{33} to Ala in case of CDK5 abolishes the kinase activity, implicating the importance of this residue in catalysis since the salt bridge between Lys^{33} and Glu^{51} is broken (3). The bigger C-lobe is predominantly helical but contains loops that are important for interaction with *suc* family proteins (26) and also the T-loop, which is important for the kinase activity as described above. The catalytic site of the enzyme lies between the two lobes, enabling the ATP to transfer phosphate to Ser/Thr residues of the peptide substrate. The residues important for substrate binding have not been identified; but based on the PKA·PKI structure, some residues in the C-lobe have been suggested in substrate binding (9).

Peptides Bound to the Active Site of CDK5—Both of the peptides studied here (H1 and NF-H, Table I) contain at least one S/TPXK motif, which is a consensus sequence for CDK family kinases. The H1 peptide used for docking was derived from histone H1 and contains the TPKK motif, which is the *in vitro* site phosphorylated by CDK5 in histone H1 (6). It is possible that this peptide has a higher affinity because of the presence of 5 lysines (out of 10 residues) that interact with acidic residues in the catalytic cleft and with the ATP. We also used an NF-H-derived peptide for our enzyme kinetics studies with different mutants because NF-H is phosphorylated at similar SPXK motifs by CDKs. We showed recently that CDK5 has a higher affinity for the first KSPXK repeat (X = A) than for the second repeat (X = E) (5), consistent with the work of Beaudette *et al.* (6), who showed that CDK5 prefers X = K or R over X = neutral amino acid. When X =D or E, the peptides make very poor substrates.

It is likely that the substrate in CDK5 or other CDKs binds to a site analogous to that observed in the PKA·PKI complex (12) because CDKs and PKA have similar overall structures and almost superimposable catalytic clefts that include the glycine-rich ATP binding domains and the catalytic base, Lys^{33}. When the peptide substrate sequences are aligned with the PKI sequence in a parallel (conventional) fashion with the Ser/Thr matching the corresponding residue in PKI, none of the lysines of the CDK5 substrate peptides corresponds to any

arginine of PKI (Fig. 1B). However, if the substrate sequences are aligned with PKI in an antiparallel fashion, the $n+3$ lysine of either NF or H1 peptide aligns with the $n-3$ arginine in the RRXS motif of PKI. For the H1 peptide, two other lysines align with PKI arginines in the antiparallel alignment (Fig. 1B).

Effect of Site-directed Mutagenesis of Residues Implicated in Substrate Recognition—Charged to alanine scanning mutagenesis of CDK5, combined with kinetic analyses of the mutant enzymes, was used to investigate interactions involving acidic residues near the ATP binding pocket in our homology model of CDK5. As described above, Asp^{86} and Asp^{91} were implicated in binding to the peptide substrates. Independent mutation of these residues to alanine caused a 2-fold decrease in apparent affinity for the NF peptide (Table I). However, there was no significant difference measured in the K_m for ATP binding to the D86A (K_m = 140 μM) and D91A (K_m = 210 μM) mutants compared with CDK5 (K_m = 160 μM).

For the higher affinity H1 substrate, the decrease in apparent affinity was 5-fold for both CDK5 mutants (Table I). Assuming that the Asp to Ala mutations do not greatly affect the structure of CDK5, it would appear that both Asp^{86} and Asp^{91} form stabilizing interactions with both peptides, arguably salt bridges to one or more lysines. To identify the alleged salt bridge interactions between CDK5 and the H1 substrate, the D86A and D91A mutants were subjected to kinetic analyses with Ala-substituted H1 peptides in which either the $n+2$ or $n+3$ residue (Lys^5 or Lys^6) was replaced by alanine (Table II). We report V_{max}/K_m in Table II to represent the catalytic efficiency of the enzyme. Because, in general V_{max}/K_m decreases as K_m increases, we interpret our results in terms of K_m, which reflects apparent binding affinity.

In H1 peptide binding to wild-type CDK5, the $n+2$ alanine substitution increased K_m by a factor of 5, whereas the $n+3$ alanine substitution increased K_m by a factor of 7 (Table II). These results are in agreement with reports that the presence of non-basic residues in the $n+2$ or $n+3$ position makes for a very poor substrate for CDKs (6, 14).

The K_m values for H1 peptide binding to CDK5 and to the D86A mutant differ by a factor of 5. For the $n+2$ alanine peptide, these K_m values differ by a factor of only 1.5. Thus, the $n+2$ alanine peptide is considerably less sensitive to changes in Asp^{86} than is the H1 peptide, suggesting that Lys^5 of H1 probably interacts with Asp^{86} of CDK5. The weakening of the Lys^5-Asp^{86} interaction was essentially independent of whether it was Lys^5 or Asp^{86} (factor of 5) that was replaced by Ala (Table II).

For the $n+3$ alanine peptide, the K_m values for binding to CDK5 and to D86A differ by a factor of 2.5 compared with the factor of 5 for the H1 peptide. The effects observed for Lys^6 ($n+3$) are less dramatic than those discussed above for Lys^5 ($n+2$). Still, the data suggest that Lys^6 also interacts with Asp^{86}. The proximity of Lys^6 to Lys^5 certainly makes this conclusion plausible.

When Asp^{91} was mutated to Ala, the reduction in apparent H1 affinity was comparable to that resulting from the D86A mutation, implicating Asp^{91} as another residue that interacts favorably with H1. D91A binds both the $n+2$ alanine and $n+3$ alanine peptides very poorly compared with wild type, suggesting that a second interaction has been weakened, *i.e.* that Asp^{91} interacts with an H1 residue other than Lys^5 or Lys^6. The data in Table II suggest that disruption of any one of the interactions between Asp^{86} or Asp^{91} and the peptide substrate results in a reduced apparent affinity but not a complete loss of binding. Multiple interactions stabilize the binding of the substrates to CDK5.

The simultaneous disruption of Asp^{86} and Asp^{91} interactions

TABLE II

Kinetic studies of CDK5 mutants with Ala-substituted H1 peptide

Phosphorylation assays and calculation of kinetic constants were performed as described under "Experimental Procedures." Alanine substitutions in H1 peptide are shown in bold. n represents threonine, the phosphoacceptor residue.

Mutant and peptide substrate		K_m	V_{max}	V_{max}/K_m
		mM	$pmol\ min^{-1}\ \mu g^{-1}$	
Wild type				
H1	PKTPKKAKKL	0.04	0.7	17
H1 $(n+2)$A	PKTPAKAKKL	0.21	1.2	6
H1 $(n+3)$A	PKTPKAAKKL	0.31	0.9	3
H1 $(n+5)$A	PKTPKKAAKL	0.14	0.2	1
H1 $(n+6)$A	PKTPKKAKAL	0.19	0.2	1
D86A				
H1	PKTPKKAKKL	0.23	0.7	3
H1 $(n+2)$A	PKTPAKAKKL	0.33	1.2	4
H1 $(n+3)$A	PKTPKAAKKL	0.77	0.7	1
H1 $(n+5)$A	PKTPKKAAKL	0.45	0.6	1
H1 $(n+6)$A	PKTPKKAKAL	0.55	0.5	1
D91A				
H1	PKTPKKAKKL	0.22	0.2	1
H1 $(n+2)$A	PKTPAKAKKL	0.60	0.1	0.2
H1 $(n+3)$A	PKTPKAAKKL	1.65	0.1	0.1
H1 $(n+5)$A	PKTPKKAAKL	0.11	0.1	1
H1 $(n+6)$A	PKTPKKAKAL	0.14	0.1	1

with the peptide was studied using a CDK5 double mutant (D86A/D91A). Relative to wild-type CDK5, this mutant showed an ~18 fold decrease in apparent affinity (K_m = 0.7 mM) for the H1 peptide, and relative to either D86A or D91A, it showed a 3.5-fold decrease. These results are further evidence that these residues are important for peptide binding.

The modeled complex (Fig. 3) highlights the interactions implicated by the measured enzyme kinetics while suggesting additional interactions that may stabilize the complex. Our model suggests that Asp[91] may interact with Lys[8] and/or Lys[9] of the substrate, which could account for the large K_m values for the binding of the $n+2$ alanine and $n+3$ alanine peptides to D91A. To identify any interactions between Asp[91] and Lys[8] or Lys[9], we measured enzyme kinetics with two additional Ala-substituted H1 peptides, $n+5$ alanine and $n+6$ alanine. The results indicate no increase in K_m for the binding of these peptides to D91A (Table II). In comparison, the binding to wild-type CDK5 and D86A showed a 3–5-fold and 2-fold increase in K_m, respectively. Taken together, the kinetic data for the $n+5$ alanine and $n+6$ alanine peptides support the possibility of interactions between Lys[8] and Lys[9] of the H1 peptide and Asp[91] of CDK5, as was suggested originally by the molecular modeling.

In the model of the H1 peptide bound to CDK5 (Fig. 3), each of the peptide's five lysines interacts with one or more negatively charged groups. Additional salt bridges identified in the model involve the ATP, Asp[143], and Lys[88] (Table III).

Effect of Mutation of Residues Implicated in Substrate Binding in the Parallel Orientation—The crystal structure of the PKA·PKI complex can serve as a template for substrate binding. We modeled the H1 substrate peptide in an orientation comparable to that of PKI bound to PKA (Fig. 1B) with a distance restraint that kept the phosphoacceptor threonine within hydrogen bonding distance of the ATP. It appeared from the modeling (not shown) that the only likely salt bridge partners for Lys[5] and Lys[6] were Asp[143] and Asp[125]. Other acidic residues in the vicinity of the substrate included Asp[206], Asp[208], Asp[209], Asp[234], and Glu[160] (Fig. 2). We mutated each of these six residues (except Asp[208]) to Ala. The D143A and E160A mutants were not active. None of the other three Asp → Ala mutations resulted in a significantly altered K_m value for H1 peptide (Table I). These data strongly support the conclusions based on the D86A and D91A data, namely that the peptide substrate binds in the antiparallel orientation.

DISCUSSION

There is no available crystal structure of a CDK-substrate complex. Thus, the mechanism of this interaction is unknown. Because of the very high specificity of CDKs for the S/TPXK motifs, it is important to probe the mode of binding of these substrates. Although unambiguous interpretation of mutagenesis experiments is difficult, we assume that non-local conformational changes induced by mutations and many-body interactions can be neglected to a first approximation. We therefore interpret our mutagenesis data in terms of pairwise interactions, specifically salt bridges between CDK5 and the peptide substrates.

Based on the crystal structure of the PKA·PKI complex, it has been speculated that some of the acidic residues (*e.g.* Glu[160], Glu[206], Glu[209]) in the C-lobe of CDKs might interact with the essential lysines of the peptide substrate (9). The homology model and mutagenesis of CDK5 have implicated several acidic residues in the binding of peptide substrates: Asp[86], Asp[91], Asp[125], Asp[143], and Glu[193] (Fig. 2A). The consensus sequence for PKA is RRXS/A. Therefore, Lys[5] and Lys[6] of the CDK5 substrates align well with the $n-2$ and $n-3$ arginines in an antiparallel alignment (Fig. 1B). Furthermore, Lys[9] of the H1 peptide corresponds to the $n-6$ arginine.

The parallel alignment of H1 peptide to PKI is not as compelling because no lysines line up with the arginines of PKI (Fig. 1B). Preliminary docking of the peptide in this parallel orientation suggested the possibility of salt bridges involving residues Asp[143], Asp[206], Asp[208], Asp[209], Asp[234], and Glu[160]. These acidic residues have been considered important in substrate binding by other reports (9). We mutated each of them (except Asp[208]) to Ala. There was no significant change in K_m values for peptide interaction with these mutants except for D143A and E160A. For these mutants, there was no kinase activity, and determining the apparent peptide affinity was not possible. Along with Lys[33], Asp[143] orients the ATP in a conformation that facilitates phosphotransfer (7–9). It is thus not surprising that the D143A mutant is inactive. Glu[160] is part of the flexible T-loop, and it may be that the conformation of CDK5 is especially sensitive to mutations in this region (Fig. 2).

The pairwise combinations of the D86A and D91A mutants (each defective in substrate binding) with Ala-substituted peptides suggest that $n+2$ and $n+3$ lysines interact with Asp[86] in

FIG. 3. *Panel A*, modeled binding site of CDK5 with H1 peptide docked. The CDK5 surface is colored according to the electrostatic potential calculated with the program GRASP (31). Regions of negative potential are *red*; positive regions are *blue*. Selected residues of CDK5 visible at the surface are labeled in *white*; selected peptide residues are labeled in *green*. *Panel B*, stereo view of the H1 peptide residues from Lys[5] to Lys[9], as docked to CDK5. Asp[86] (*top*) and Asp[91] (*bottom*) are also shown. Each of the four $N\zeta$–$O\delta$ distances shown (Lys[5]–Asp[86], Lys[6]–Asp[86], Lys[8]–Asp[91], Lys[9]–Asp[91]) is between 2.5 and 2.6 Å.
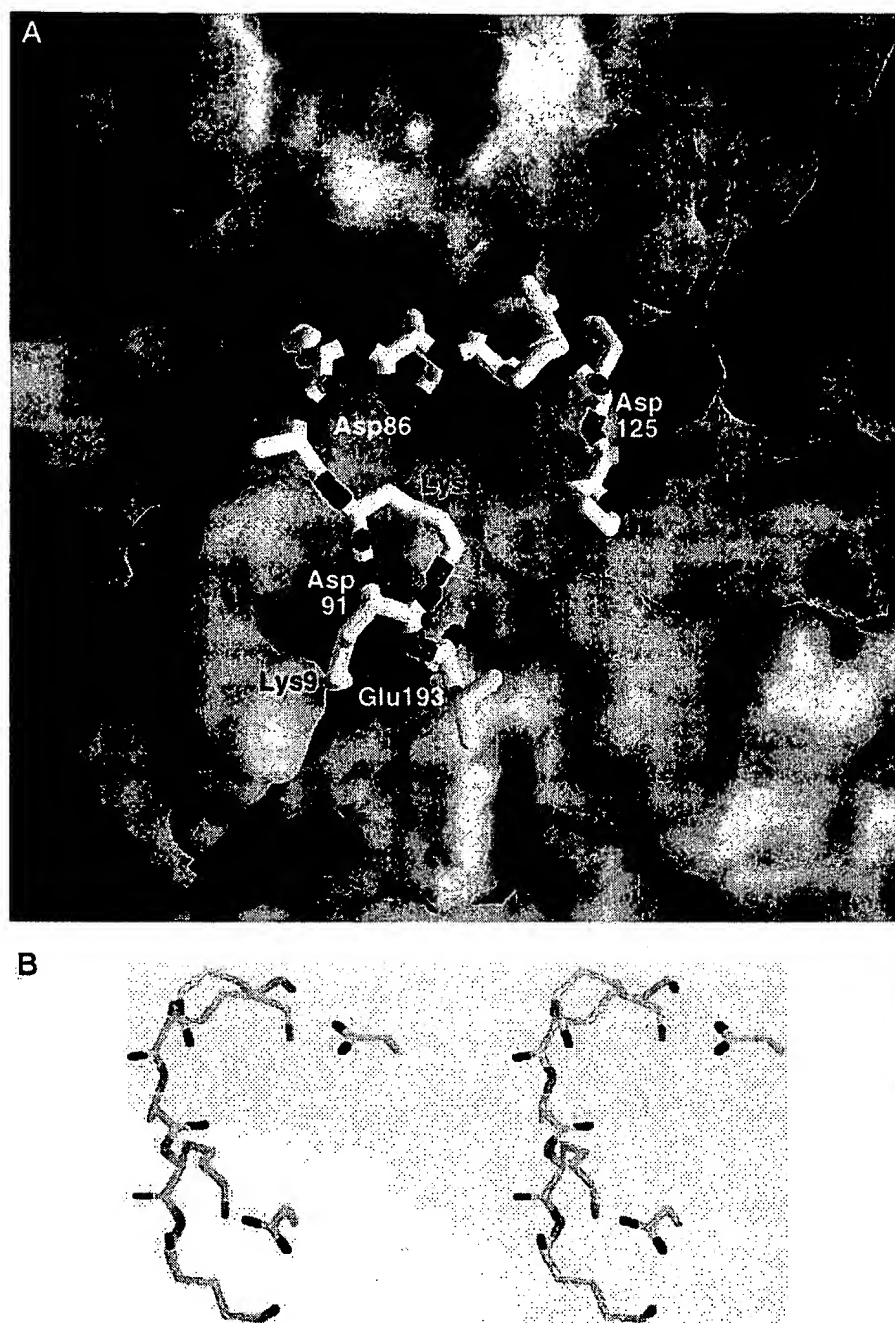
TABLE III

Salt bridges involving H1 peptide in model of peptide docked to CDK5 terminal atoms are OT1 and OT2.

H1 peptide atom	Oppositely charged atoms within 2.5–2.7 Å
Lys[2] $N\zeta$	Asp[143] Oδ1, ATP O3β
Lys[5] $N\zeta$	Asp[86] Oδ2
Lys[6] $N\zeta$	Asp[86] Oδ1
Lys[8] $N\zeta$	Asp[91] Oδ2, H1 Leu[10] OT2
Lys[9] $N\zeta$	Asp[91] Oδ1, H1 Leu[10] OT1
Leu[10] OT2	Lys[88] $N\zeta$

the KTPKK peptide substrate. Presumably, when binding to the D86A mutant, Lys[5] and Lys[6] interact with the ATP or Asp[91]. The first family of MC simulations suggested that Asp[91] is within reach of Lys[8] and Lys[9] when the N_2-terminal half of the peptide is docked to the ATP. Although these lysines are not part of the TPKK consensus CDK motif, the D91A mutant data suggest that a stabilizing interaction outside the TPKK region is present in the native system. Interestingly, in the case of other major proline-directed kinases, extracellular signal-regulated kinases (ERKs), the residue corresponding to Asp[91] is a neutral residue (Fig. 1A). These kinases do not have any known preferences for charged residues following the proline (15). Recently, it was shown that the NF peptide and other related peptides containing $n+3$ as basic residues were very poorly recognized by ERKs (27) compared with the peptides with $n+3$ as nonbasic residues. A proline at the $n+1$ position is a common essential feature in substrates for both CDKs and ERKs. These kinases do not phosphorylate substrates without proline. It is possible that orientation of the serine hydroxyls for hydrogen bonding with ATP requires proline at the $n+1$ position. CDKs seem to require additional interactions with the

substrate lysines at the $n+2$ and $n+3$ positions to stabilize the substrate-enzyme complex. Replacement of Lys[5] or Lys[6] with alanine decreases the apparent affinity for the peptide substrate (Table II). However, when both of these lysines are replaced by a neutral or acidic residue, the peptide is not phosphorylated by CDK5 (27). Our data and model also suggest additional stabilization of the complex by salt bridges involving Lys[8] and Lys[9] of the substrate and Asp[91] of CDK5.

PKA and phosphorylase kinase have been the only two serine/threonine kinases to be crystallized as ternary complexes with ATP and their peptide substrates (12, 13). These two kinases show a high degree of structural similarity in their ternary complexes. Because the cyclin A-CDK2 (phosphorylated) crystal structure differs from PKA and phosphorylase kinase in several ways, it has been speculated that CDKs might have a different catalytic mechanism (10). A recently reported crystal structure of CDK2 complexed with staurosporine, an inhibitor of CDKs and other protein kinases, which binds at the ATP binding pocket, revealed that staurosporine interacts with Asp[86] (28). This interaction suggested that the peptide substrate binding site of CDKs is very close to the ATP pocket, consistent with our observation that mutation of Asp[86] results in a decreased apparent affinity for the peptide. Also, recent work in our laboratory has shown that a pseudo substrate analogue of the NF peptide was surprisingly competitive with ATP.[2] Given the close proximity of the ATP and peptide binding sites, peptide binding at or near Asp[86] could affect ATP binding. Interestingly, in the same study we showed that peptide binding promoted ATP binding.[2] Taken together, these data suggest that a conformational change resulting from peptide binding could trigger events important for catalysis.

Because of the lack of a crystal structure of a CDK-substrate complex, the peptide substrate binding site has not been identified. Therefore, design of specific inhibitors for CDK family kinases has not been possible. Most of the available inhibitors bind in the ATP pocket, which makes them less specific since the ATP pockets of most PKs are structurally very similar. But in the case of CDKs, the interactions with the substrate are very specific; CDKs specifically target SPXK-type motifs. The enzyme kinetics and molecular modeling reported here indicate that the H1 peptide most likely binds to CDK5 in an orientation that is antiparallel to that of PKI bound to PKA. The

binding site implicated by this study should help guide the design of specific inhibitors for CDKs.

REFERENCES

1. Morgan, D. O. (1997) *Annu. Rev. Cell Dev. Biol.* **13**, 261–291
2. Lew, J., Huang, Q. Q., Qi, Z., Winkfein, R. J., Aebersold, R., Hunt, T., and Wang, J. H. (1994) *Nature* **371**, 423–426
3. Tsai, L. H., Delalle, I., Caviness, V. S., Chae, T., and Harlow, E. (1994) *Nature* **371**, 419–423
4. Shetty, K. T., Link, W. T., and Pant, H. C. (1993) *Proc. Natl. Acad. Sci. U. S. A.* **90**, 6844–6848
5. Sharma, P., Barchi, J. J., Huang, X., Amin, N., Jaffe, H., and Pant, H. C. (1998) *Biochemistry* **371**, 419–423
6. Beaudette, K. N., Lew, J., and Wang, J. H. (1993) *J. Biol. Chem.* **268**, 20825–20830
7. De Bondt, H. L., Rosenblatt, J., Jancarik, J., Jones, H. D., Morgan, D. O., and Kim, S. H. (1993) *Nature* **363**, 595–602
8. Jeffery, P. D., Russo, A. A., Polyak, K., Gibbs, E., Hurwitz, J., Massague, J., and Pavletich, N. P. (1995) *Nature* **376**, 313–320
9. Russo, A. A., Jeffrey, P. D., and Pavletich, N. P. (1996) *Nat. Struct. Biol.* **3**, 696–700
10. Johnson, L. N., Noble, M. E., and Owen, D. J. (1996) *Cell* **88**, 149–155
11. Knighton, D. R., Zheng, J., Tenzyck, L. F., Xuong, G. N., Taylor, S. S., and Sowadski, J. M. (1991) *Science* **253**, 407–414
12. Knighton, D. R., Zheng, J., Tenzyck, L. F., Ashport, V. A., Xuong, G. N., Taylor, S. S., and Sowadski, J. M. (1991) *Science* **253**, 414–420
13. Lowe, E. D., Noble, M. E. M., Skamnaki, V. T., Oikonomakos, N. G., Owen, D. J., and Johnson, L. N. (1997) *EMBO J.* **16**, 6646–6658
14. Songyang, Z., Blechner, S., Hoagland, N., Hoekstra, M. F., Piwnica-Worms, H., and Cantley, L. C. (1994) *Curr. Biol.* **4**, 973–982
15. Songyang, Z., Lu, K. P., Kwon, Y. T., Tsai, L. H., Fihol, O., Cochet, C., Brickey, D. A., Soderling, T. R., Bartheson, C., Graves, D. J., DeMaggio, A. J., Hoekstra, M. F., Blenis, J., Hunter, T., and Cantley, L. C. (1996) *Mol. Cell. Biol.* **16**, 6486–6493
16. Levitt, M. (1992) *J. Mol. Biol.* **226**, 507–533
17. Brooks, B. R., Bruccoleri, R. E., Olafson, B. D., States, D. J., Swaminathan, S., and Karplus, M. (1983) *J. Comp. Chem.* **4**, 187–217
18. MacKerell, A. D., Jr., Bashford, D., Bellott, M., Dunbrack, R. L., Jr., Evanseck, J. D., Field, M. J., Fischer, S., Gao, J., Guo, H., Ha, S., Joseph-McCarthy, D., Kuchnir, L., Kuczera, K., Lau, F. T. K., Mattos, C., Michnick, S., Ngo, T., Smith, J. C., Stote, R., Straub, J., Watanabe, M., Wiorkiewicz-Kuczera, J., Yin, D., and Karplus, M. (1998) *J. Phys. Chem. B* **102**, 3586–3616
19. Pavelites, J. J., Bash, P. A., Gao, J., and MacKerell, A. D. A., Jr. (1997) *J. Comp. Chem.* **18**, 221–239
20. Steinbach, P. J., and Brooks, B. R. (1994) *J. Comp. Chem.* **15**, 667–683
21. Metropolis, N., Rosenbluth, A. W., Rosenbluth, M. N., Teller, A. H., and Teller, E. (1953) *J. Chem. Phys.* **21**, 1087–1092
22. Brown, N. R., Noble, M. E., Endicott, J. A., Garman, E. F., Wakatsuki, S., Mitchell, E., Rasmussen, B., Hunt, T., and Johnson, L. N. (1995) *Structure* **3**, 1235–1247
23. Noble, M. E., Endicott, J. A., Brown, N. R., and Johnson, L. N. (1997) *Trends Biol. Sci.* **22**, 482–487
24. Tang, D., Chun, A. C. S., Zhang, M., and Wang, J. H. (1997) *J. Biol. Chem.* **272**, 12318–12327
25. Poon, R. Y. C., Lew, J., and Hunter, T. (1997) *J. Biol. Chem.* **272**, 5703–5708
26. Bourne, Y., Watson, M. H., Hickey, M. J., Holmes, W., Rocque, W., Reed, S. I., and Tainer, J. A. (1996) *Cell* **84**, 863–874
27. Veeranna, Amin, N. D., Ahn, N. G., Jaffe, H., Winters, C. A., Grant, P., and Pant, H. C. (1998) *J. Neurosci.* **18**, 4008–4021
28. Lawrie, A. M., Noble, M. E., Tunnah, P., Brown, N. R., Johnson, L. N., and Endicott, J. A. (1997) *Nat. Struct. Biol.* **4**, 796–801
29. Merritt, E. A., and Bacon, D. J. (1997) *Methods Enzymol.* **277**, 505–524
30. Kraulis, P. J. (1991) *J. Appl. Crystallogr.* **24**, 946–950
31. Nicholls, A., Sharp, K. A., and Honig, B. (1991) *Proteins Struct. Funct. Genet.* **11**, 281–296

---

[2] P. Sharma, N. D. Amir, R. W. Albers, and H. C. Pant, manuscript in preparation.